

Summary Report
**The Phase One I-710 Freeway
Rehabilitation Project: Initial
Design (1999) to Performance after
Five-Plus Years of Traffic (2009)**

Author:
Carl L. Monismith, John T. Harvey, Bor-Wen Tsai,
Fenella Long, and James Signore

Partnered Pavement Research Program (PPRC) Strategic Plan Element 3.1.4: Perform periodic pavement evaluations through 2008 and prepare final summary report containing summaries of laboratory and field test data obtained during the period 1999–2008 and analyses associated with the design, construction, and performance of the pavement sections.

PREPARED FOR:

California Department of Transportation
(Caltrans)
Division of Research and Innovation

PREPARED BY:

University of California
Pavement Research Center
UC Davis and Berkeley



DOCUMENT RETRIEVAL PAGE		Summary Report No: UCPRC-SR-2008-04		
Title: Summary Report: The Phase 1 I-710 Freeway Rehabilitation Project: Initial Design (1999) to Performance after Five Years of Traffic (2009)				
Authors: Carl L. Monismith, John T. Harvey, Bor-Wen Tsai, Fenella Long, and James Signore				
Prepared for: Caltrans Division of Research and Innovation	FHWA No.: CA101891A	Work Submitted: June 24, 2009	Date: February 2009	
Strategic Plan Element No.: 3.1.4	Status: Stage 6 final, approved		Version No: 1	
<p>Abstract: This summary report incorporates into a single document the design, construction, and performance data for the I-710 Freeway Rehabilitation Project in Long Beach, California. Included are the following: summaries of the asphalt mix and structural pavement section designs; construction sequence for a representative 55 hours closure; design and construction experience from post construction interviews with Caltrans and Contractor Staff; pavement performance evaluations in the period November 2003 and January 2009 (five-plus years under traffic), as well as the results of additional analyses and tests on mixes obtained from cores and slabs taken from the pavement after construction. This project is one of the first major freeway rehabilitation projects in the US incorporating 55-hour weekend closures (a total of eight in this instance) for the construction of long-life asphalt pavements. It includes both <i>full-depth asphalt concrete sections</i>, which replaced the existing portland cement concrete (PCC) pavement under the over crossings and at interchanges, and <i>asphalt concrete overlays</i> on cracked-and-seated PCC on the sections between the interchanges and over crossings.</p> <p>Aspects of the project involved a Caltrans, Industry, and University cooperative effort—through the Flexible Pavement Task Group the Long Life Pavement Rehabilitation Strategies (LLPRS) Program—for both design development and construction evaluations. The project utilized asphalt mix and structural pavement section designs based on Strategic Highway Research Program (SHRP) developed technologies, results from the California Accelerated Pavement Testing Program, and innovations in construction specifications and requirements.</p>				
Keywords: I-710 Phase 1 Freeway rehabilitation, fatigue and permanent deformation response, long life M-E pavement design, full-depth asphalt pavement, overlays on cracked-and-seated PCC, CA4PRS				
Proposals for implementation: Lessons learned for future long-life asphalt pavement design and construction projects (Report, Section 6).				
Related documents: See References, Section 9				
Signatures:				
C.L. Monismith First Author	J. T. Harvey Technical Review	D. Spinner Editor	C. L. Monismith Principal Investigator	T. J. Holland Caltrans Contract Manager

DISCLAIMER

The contents of this report reflect the views of the authors who are responsible for the facts and accuracy of the data presented herein. The contents do not necessarily reflect the official views or policies of the State of California or the Federal Highway Administration. This report does not constitute a standard, specification, or regulation.

PROJECT OBJECTIVES

1. Perform periodic tests and field surveys through 2008 (approximately five years of traffic) including: shear and fatigue tests on specimens obtained from field samples; falling weight deflectometer tests approximately annually; and some skid and noise measurements.
2. Prepare final summary report containing the asphalt mix and structural pavement section designs, construction experience; pavement performance during period 2003 to 2008 as well as results of analyses performed from 1999 (start of University of California Pavement Research Center involvement in project) through January 2009.

ACKNOWLEDGMENTS

Many people have contributed to the information contained herein; a few will be acknowledged. Msrs. David Hung and Irwin Guada obtained the fatigue and RSST-CH data for the original mix design and Irwin Guada provided the RSST-CH test data for the field cores obtained following construction. Dr. E.B. Lee, who developed the *CA4PRS* software program, directed the calibration studies during the three of the eight 55-hour weekend closures. Drs. Manuel Bejarano and Bruce Steven obtained, with the assistance of Dynatest staff, the FWD data. Mr. Erdem Coleri conducted some of the analyses of the data to determine the measures of pavement performance described in Section 7. Mr. David Spinner prepared and formatted the manuscript. The efforts of these and other PRC personnel are gratefully acknowledged.

It must be emphasized that completion of this project was made possible by the dedicated efforts of Caltrans Headquarters and District staff and the staff of Excel, the paving contractor.

EXECUTIVE SUMMARY

This summary report incorporates, in a single document, design, construction, and performance data for the I-710 Freeway Rehabilitation Project in Long Beach, California. The report includes summaries of: asphalt mix and structural pavement section designs, construction experience, pavement performance in the period November, 2003 to January 2009 (five-plus years under traffic), as well as the results of additional analyses and tests on mixes obtained from cores and slabs taken from the pavement after construction.

This project is one of the first major freeway rehabilitation projects in the U.S. incorporating 55-hour weekend closures (a total of eight in this instance) for the construction of long-life asphalt pavements. It includes both *full-depth asphalt concrete sections*—which replaced existing portland cement concrete (PCC) pavement under the over crossings and at interchanges—and *asphalt concrete overlays* on cracked-and-sealed PCC on the sections between the interchanges and over crossings.

Aspects of the project involved a Caltrans, Industry, and University cooperative effort through the Flexible Pavement Task Group of the Long Life Pavement Rehabilitation Strategies (LLPRS) Program for the design development and construction evaluations. The project utilized asphalt mix and structural pavement section designs based on technologies developed by the Strategic Highway Research Program (SHRP) and research results from the California Accelerated Pavement Testing Program, as well as innovations in construction specifications and requirements.

More specifically, the information includes: results of the mix and structural section designs based on the SHRP-developed shear and flexural fatigue tests; aspects of the construction specifications unique to the project; representative construction sequence during the 55 hours weekend closures; “lessons learned” from both the design and construction activities associated with the project; measurements of mix characteristics obtained from the as-constructed pavement; and, periodic measurements of pavement performance from the opening to traffic in the summer 2003 to January 2009. The performance measurements include those made with the falling weight deflectometer (FWD) at approximately yearly intervals, as well as some pavement noise and skid measurements.

This summary report is intended to provide a document that Caltrans will have available to assist in the development of future major freeway rehabilitation projects using asphalt-surfaced pavements. Chapters 2 through 8 contain summaries of the various elements of the project, which began with the UCPRC’s involvement with the LLPRS Flexible Pavement Task Group in 1999 and continued through January 2009 when a series of pavement noise measurements were completed.

Chapter 2 contains a brief description of the project site and the rehabilitation alternatives selected. Chapter 3 provides: a summary of the properties of the AR-8000 and PBA-6a* binders and aggregates used; the SHRP-developed methodology used for the designs of the mixes containing the two binders; an evaluation of the rutting resistance of the mixes at an elevated temperature using the Heavy Vehicle Simulator (HVS); and the structural pavement design methodologies using a mechanistic-empirical approach. The section also includes summaries of additional analyses performed during the study concerning the fatigue and permanent deformation behavior of the full-depth pavement section, and an analysis associated with specifications for the fatigue and permanent deformation requirements for the mixes.

Aspects of construction are described in Chapter 4. Included are: a description of a new approach to define performance requirements for the mixes selected for the pavement sections; use of tack coats between multiple lifts of asphalt concrete; and incorporation of more stringent compaction requirements of the asphalt concrete mixes. Chapter 5 provides a brief description of the construction activities, concentrating on the sequence followed for a typical 55-hour weekend closure.

Chapter 6 summarizes the results of interviews conducted by members of the LLPRS Flexible Pavement Task Group separately with Caltrans District 7 Construction staff and contractor staff. “Lessons learned” from these interviews are categorized as “What went well?” and “What didn’t go well?,” and recommendations based on these results are included for minimizing what didn’t go well in future projects of this type.

Chapter 7 summarizes the studies conducted at the conclusion of construction. The analyses of the FWD deflection measurements indicate little change in the stiffness characteristics of the pavement layers; these results corroborate recent pavement assessments performed by Caltrans staff.

Chapter 8 summarizes the various facets of the project, including incorporation of new technology and the results of earlier HVS tests relative to materials design and construction. A total of nine appendices have been included which contain: laboratory test data obtained prior to the start of the contract and from cores and slabs following construction; results of the analyses of the FWD tests; additional analyses of pavement performance, one of which (Appendix I) included use of backcalculated layer stiffnesses with the software program *CalME*; and some analyses for revised specification mix performance parameters incorporated in the Phase 2 Special Provisions.

TABLE OF CONTENTS

Project Objectives	v
Acknowledgments	v
Executive Summary	vii
List of Figures	xi
List of Tables	xv
1 Introduction	1
2 Pavement Site	3
3 Mix and Structural Section Designs	5
3.1 Materials	6
3.2 Mix Evaluations	8
3.2.1 Hveem Stabilometer Tests	9
3.2.2 RSST-CH Tests.....	11
3.2.3 Flexural Fatigue Tests	13
3.3 Mix Designs	14
3.4 Structural Section Designs	17
3.4.1 Full-Depth AC Replacement Pavement Structure.....	17
3.4.2 Subsequent Additional Analyses.....	21
3.4.3 Overlay Structure on Existing Cracked and Seated PCC Pavement	23
4 Construction Considerations	33
5 Construction	37
6 Lessons Learned at Conclusion of Construction, Fall 2003	41
7 Follow-up Investigations	45
7.1 HWD Test Results	45
7.2 Laboratory Tests on Field-Mixed, Field-Compacted Test Specimens.....	51
7.3 Longitudinal Profile, Skid, and Noise Measurements	55
7.4 Performance Analysis of the Phase 1 Rehabilitation Using <i>CalME</i>	58
8 Summary	59
9 References	63
Appendix A: Laboratory Shear and Fatigue Test Data	65
Appendix B: Initial Designs for Full-Depth Structural Sections	67
Appendix C: Analyses for Staged Construction	73
Appendix D: Fatigue Performance Confirmation of I-710 Full-Depth Pavement Structure	77
D.1 Fatigue Performance Confirmation of I-710 Full-Depth Pavement Structure	77
D.1.1 Initial Stiffness Equations and Fatigue Life Equations	77

D.1.2	ELSYM5 Input and Pavement Structure.....	78
D.1.3	Temperature Distribution	79
D.1.4	Traffic.....	82
D.1.5	Fatigue Performance Prediction and Comparison.....	82
Appendix E: Evaluation of Potential Contribution of Unbound Pavement Layers Contributing to Surface Rutting.....		85
E.1	Rutting Performance Confirmation of I-710 Pavement Structures	85
E.1.1	Initial Stiffness Equations	85
E.1.2	ELSYM5 Input and Pavement Structures	86
E.1.3	Temperature Distribution	89
E.1.4	Traffic.....	90
E.1.5	Variation of Subgrade Vertical Compressive Strain	90
E.1.6	Traffic.....	92
E.2	Rutting Performance Estimation	92
Appendix F: Asphalt Concrete Shear and Fatigue Performance Test Requirements.....		101
F.1	Permanent Deformation (Shear Test Requirements)	101
F.1.1	Assumptions.....	101
F.1.2	Normal One-Sample Model	101
F.2	Fatigue Cracking (Fatigue Test Requirements)	102
F.3	<i>S-Plus</i> Analysis	110
F.4	Statistical Simulation	121
F.4.1	Simulation Approach	121
Appendix G: Analysis of Phase 2 Pavement Structure Using Revised Specification Requirements for Fatigue.....		123
G.1	Initial Stiffness Equations and Fatigue Life Equations.....	123
G.1.1	ELSYM5 Input and Pavement Structure.....	124
G.1.2	Temperature Distribution	125
G.1.4	Traffic.....	128
G.2	Fatigue Performance Prediction and Comparison.....	128
G.3	<i>S-Plus</i> log	132
Appendix H: Postconstruction Measurements and Analyses		135
Appendix I: Pavement Analyses of Full-Depth and Overlays on Cracked and Seated PCC Sections Using the <i>CalME</i> Design/Analysis Program		141

LIST OF FIGURES

Figure 2.1: Project location.....	3
Figure 3.1: Framework for mix design: permanent deformation system.....	5
Figure 3.2: Framework for mix analysis/design: fatigue system.....	6
Figure 3.3: Aggregate gradation, semilogarithmic chart.....	8
Figure 3.4: Aggregate gradation, 0.45 grading chart.....	8
Figure 3.5: Permanent shear strain versus stress repetitions in RSST-CH at 50°C; PBA-6a* mix, 4.7 percent binder content.....	12
Figure 3.6: Results of controlled strain fatigue tests at 20°C, 10 Hz frequency.....	13
Figure 3.7: Mix stiffnesses versus temperature; mixes containing AR-8000 and PBA-6a* binders.....	14
Figure 3.8: Repetitions to 5 percent permanent shear strain, N_{supply} , versus binder content; tests at 50°C.....	15
Figure 3.9: Rut depth versus HVS load applications with 40 kN load on dual tires at 50°C.....	16
Figure 3.10: Fatigue analysis procedure.....	19
Figure 3.11: Proposed design, full-depth AC replacement of structure.....	22
Figure 3.12: Pavement systems considered for final design.....	25
Figure 3.13: Pavement and loading configurations used for finite element analyses.....	25
Figure 3.14: Finite element idealization for the pavement system shown in Figure 3.13.....	26
Figure 3.15: Comparison of strains at underside of mix just above the fabric interlayer for three thickness combinations of the PBA-6a* and AR-8000 mixes (1 in. \cong 25 mm).....	28
Figure 3.16: Comparison of bending strains in mix just above PCC joints/cracks for three thickness combinations of the PBA-6a* and AR-8000 mixes (1 in. \cong 25 mm).....	29
Figure 3.17: Comparison of bending strains on underside of the top layer for three thickness combinations of the PBA-6a* and AR-8000 mixes (1 in. \cong 25 mm).....	29
Figure 3.18: Comparison of shear strains in the underside of the mix adjacent to the fabric interlayer for three thickness combinations of PBA-6a* and AR-8000 mixes (1 in. \cong 25 mm).....	30
Figure 3.19: Proposed design for overlay on cracked and seated existing PCC structure.....	31
Figure 5.1: Contractor’s revised staging plan (sequence of 55-hour weekend closures shown in parentheses).....	37
Figure 5.2: Typical CPM schedule for a 55-hour weekend closure (second weekend closure).....	40
Figure 7.1: Deflection testing patterns for crack, seat, and overlay (CSOL) and full-depth asphalt concrete sections.....	45
Figure 7.2: Deflections, Lane 3 Southbound, 2003 to 2008, 19°C.....	46
Figure 7.3: Deflections, Lane 3 Northbound, 2003 to 2008, 19°C.....	47
Figure 7.4: Southbound Lane 3 layer moduli versus time.....	48

Figure 7.5: Northbound Lane 3 layer moduli versus time.	49
Figure 7.6: Weibull curves for the rich bottom AR-8000 mix.	52
Figure 7.7: Field-mixed, field-compacted (FMFC) test data with the lower bounds of the 95 percent confidence bands based on the pooled data contained in Appendix F (Tables F5 and F8 [pooled data]). Field-mixed, field-compacted (FMFC) test data with the lower bounds of the 95 percent confidence bands based on the pooled data contained in Appendix F (Tables F5 and F8 [pooled data]).	53
Figure 7.8: Average core thicknesses for cores obtained in November 2003.	54
Figure 7.9: IRI on northbound (a) and southbound (b) lanes.	55
Figure 7.10: Spectral content at each pavement section.	57
Figure 7.11: Spectral content at OGAC sections, inner and outer lanes.	57
Figure B.1: Structural sections for AR-8000 and composite pavements (6 percent voids in AC layer and 3 percent in “rich bottom” layer).	68
Figure B.2. Structural sections for AR-8000 and composite pavements with increase in air-void contents.	69
Figure B.3. Structural sections for mixes containing asphalt from the California Valley source with increasing air-void contents.	70
Figure B.4. Structural sections for mixes prepared with asphalt from the California Coastal sources with increasing air-void contents.	71
Figure D.1: Pavement structure and <i>ELSYM5</i> input.	78
Figure D.2: Histogram of surface temperatures.	79
Figure D.3: Histogram of temperatures at bottom of AC layer.	79
Figure D.4: Temperature distributions for surface temperature and temperature at bottom of AC layer. .	80
Figure D.5: Histogram of surface temperatures (5:00 A.M. to 7:00 P.M.).	80
Figure D.6: Histogram of temperatures at bottom of AC layer (5:00 A.M. to 7:00 P.M.).	81
Figure D.7: Temperature distributions for surface temperature and temperature at bottom of AC layer (5:00 A.M. to 7:00 P.M.).	81
Figure E.1: <i>ELSYM5</i> input for pavement structure P1.	86
Figure E.2: <i>ELSYM5</i> input for pavement structure P2.	87
Figure E.3: <i>ELSYM5</i> input for pavement structure P3.	88
Figure E.4: The histograms and distribution functions of bottom AC temperatures for various pavement structures (from 5:00 A.M. to 7:00 P.M.).	89
Figure E.5: The histograms and distribution functions of temperature gradients of asphalt concrete layer for various pavement structures (from 5:00 A.M. to 7:00 P.M.).	90
Figure E.6: Variations of subgrade vertical compressive strains versus surface temperatures for various pavement structures with 65 MPa subgrade or/and 130 MPa granular base.	91

Figure E.7: Variations of subgrade vertical compressive strains versus surface temperatures for various pavement structures with 400 MPa granular base and/or 100 MPa subgrade.	91
Figure E.8: Asphalt Institute subgrade strain criteria and cutoff point.	92
Figure F.1: 95% confidence band of PBA-6a* mixes (pooled).	104
Figure F.2: 95% confidence band of AR-8000 mixes with high air-void content.	104
Figure F.3: 95% confidence band of AR-8000 mixes with low air-void content.	105
Figure F.4: 95% confidence band of AR-8000 mixes (pooled).	105
Figure F.5: Comparison of lower bound of 95% confidence band for AR-8000 and PBA-6a* mixes. ..	106
Figure G.1: Pavement structure and <i>ELSYM5</i> input.	124
Figure G.2: Histogram of surface temperatures.	125
Figure G.3: Histogram of temperatures at bottom of AC layer.	126
Figure G.4: Temperature distributions for surface temperature and temperature at bottom of AC layer.	126
Figure G.5: Histogram of surface temperatures (5:00 A.M. to 7:00 P.M.).	127
Figure G.6: Histogram of temperatures at bottom of AC layer (5:00 A.M. to 7:00 P.M.).	127
Figure G.7: Temperature distributions for surface temperature and temperature at bottom of AC layer (5:00 A.M. to 7:00 P.M.).	128

LIST OF TABLES

Table 3.1: Binder Characteristics	7
Table 3.2: Aggregate Characteristics	7
Table 3.3: Summary of Mix Tests	9
Table 3.4: Hveem Stabilometer Test Results	11
Table 3.5: RSST-CH Test Results at 50°C	12
Table 3.6: Material Properties for Pavement Analysis	18
Table 3.7: Fatigue Characteristics of Evaluated Mixes*; 20°C	18
Table 3.8: Comparison of I-710 Phases 1 and 2 Performance Specification Requirements	23
Table 3.9: Material Characteristics	27
Table 4.1: Asphalt Concrete Mixture Performance Requirements [Table 39-3A from Reference (6)].....	34
Table 4.2: Minimum Process Control Requirements [Table 39-4 from Reference (6)]	35
Table 4.3: Minimum Quality Control Requirements [Table 39-9 from Reference (6)].....	36
Table 6.1: Lessons Learned	42
Table 6.2: General Recommendations	43
Table 7.1: Tensile and Vertical Compressive Strains in Full-Depth Sections	50
Table 7.2: RSST-CH on Specimens from Cores Obtained in June 2003 from Northbound Lanes	54
Table 7.3: IRI by Pavement Type and Direction	56
Table 7.4: Sound Intensity Results, dBA	56
Table A.1: RSST-CH Test Data.....	65
Table A.2: Fatigue Test Data	66
Table B.1: Structural Section Designs	67
Table D.1: Regression Equations of Initial Stiffness and Fatigue Life for PBA-6a* and AR-8000.....	77
Table D.2: TCF Calculation.....	82
Table D.3: TCF Calculation (5:00 A.M. to 7:00 P.M.).....	83
Table E.1: Regression Equations of Initial Stiffness and Fatigue Life for PBA-A and AR-8000.....	85
Table E.2: Pavement Structure P1	86
Table E.3: Pavement Structure P2	87
Table E.4: Pavement Structure P3	88
Table E.5: Allowable ESALs for Pavement Structure P1 (Traffic from 5:00 A.M. to 7:00 P.M.).....	94
Table E.6: Allowable ESALs for Pavement Structure P2 (Traffic from 5:00 A.M. to 7:00 P.M.).....	95
Table E.7: Allowable ESALs for Pavement Structure P3 (Traffic from 5:00 A.M. to 7:00 P.M.).....	96
Table E.8: Allowable ESALs for Pavement Structure P1 with 100 MPa Subgrade (Traffic from 5:00 A.M. to 7:00 P.M.).....	97

Table E.9: Allowable ESALs for Pavement Structure P2 with 400 MPa Granular Base and 100 MPa Subgrade (Traffic from 5:00 A.M. to 7:00 P.M.).....	98
Table E.10: Allowable ESALs for Pavement Structure P3 with 400 MPa Granular Base and 100 MPa Subgrade (Traffic from 5:00 A.M. to 7:00 P.M.).....	99
Table F.1: 95% Confidence Interval of Ln(reps to 5% shear strain)	102
Table F.2: Lower and upper bounds of 95% Confidence Bands for Ln(Nf) of PBA-6a* and AR-8000 Mixes	103
Table F.3: Minimum Requirements of Fatigue Life	106
Table F.4: Lower Bounds of 95% Confidence Bands of Ln(Nf) of PBA-6a* and AR-8000 Mixes	107
Table F.5: Fatigue Data of PBA-6a* Mixes (Pooled).....	107
Table F.6: Fatigue Data of AR-8000 Mixes with High Air-Void Content	108
Table F.7: Fatigue Data of AR-8000 Mixes with Low Air-Void Content.....	108
Table F.8: Fatigue Data of AR-8000 Mixes (Pooled).....	109
Table F.9: Simulation Summary	122
Table G.1: Regression Equations of Initial Stiffness and Fatigue Life for PBA-6a* and AR-8000.....	123
Table G.2: TCF Calculation.....	129
Table G.3: TCF Calculation (5:00 A.M. to 7:00 P.M.).....	129
Table H.1: Backcalculated Siffness Moduli Based on 2003-2008 HWD Measurements.....	135
Table H.2: Layered Elastic Stress and Strain Calculations.....	137
Table H.3 Shear Test Results on Specimens Prepared from Pavement Samples	138
Table H.4: Summary of Fatigue Tests of I-710 QC/QA Project (Field-Mixed, Field-Compacted)	139

1 INTRODUCTION

In California, as elsewhere in the United States and overseas, deterioration of aging pavement systems as well as traffic volumes considerably greater than those for which the systems were originally designed, have required new approaches in pavement design/rehabilitation and to construction practices. In 1998, in response to this situation, the California Department of Transportation (Caltrans) embarked on a Long-Life Pavement Rehabilitation Strategies (LLPRS) program to rebuild approximately 2,800 lane-km (1,740 lane mi.) of deteriorated freeways in the 78,000 lane-km (48,400 lane mi.) system of highways under the Department's jurisdiction. The goals of this program include providing pavements with design lives of 30-plus years, require minimal maintenance, and utilize fast-track construction in order to minimize traffic delays and inconvenience to the traveling public.

This summary report assembles in a single document the asphalt mix and structural pavement section designs, accounts of construction experience, and discussions of pavement performance in the period 2003 to 2009 (five-plus years under traffic), as well as the results of additional analyses and tests on mixes obtained from cores and slabs taken from the post construction pavement of the I-710 Freeway Rehabilitation Project in Long Beach, California, one of the first major freeway rehabilitation projects in the US to incorporate 55-hour weekend closures in the construction of long-life asphalt pavements. The project included both *full-depth asphalt concrete sections*—replacing the existing portland cement concrete (PCC) pavement under the over crossings and at interchanges—and *asphalt concrete overlays*, which were placed on cracked and seated PCC on the sections between the interchanges and over crossings

Aspects of the project were a Caltrans, Industry, and University cooperative effort (of the LLPRS Flexible Pavement Task Group)¹ both for design development and construction evaluations. The effort utilized

¹ The sequence of events which led to the activities of the LLRS Flexible Pavement Task Group is as follows: June 1996: Caltrans makes an initial presentation to the California Transportation Commission (CTC) promoting the concept of Long Life Pavements (LLP).

- October 1996: Caltrans meets with the CTC and proposes a “new” long-life rehabilitation strategy.
- January 1997: Caltrans holds a workshop on LLP with the CTC at which Corridors of Economic Significance are identified that total approximately 26,000 lane-km of which 2,600 lane-km (1,600 lane-mi) are selected for the LLP Program (no flexible pavement option was included in the program).
- March 1997: The flexible pavement option is added to the program on the recommendation from the hot-mix asphalt (HMA) Industry.
- June 1997: The Asphalt Pavement Association of California (APACA) forms a Technical Advisory Group to promote inclusion of a flexible pavement option in the LLP rehabilitation strategy (LLPRS).
- February 1998: Caltrans hosts a Transportation Research Board (TRB) Panel/Workshop to examine the LLPRS and focus on the I-710 corridor.
- March 1998: Caltrans and the HMA Industry form a Joint Asphalt Concrete (HMA) Committee to evaluate the possibility of a flexible pavement strategy for LLPRS. Three subcommittees are formed to address issues concerning mix design, structural section design, and constructability. At this time, UC Berkeley is invited to participate.

asphalt mix and structural pavement section designs based on technologies developed by the Strategic Highway Research Program (SHRP) (1,2,3) and results from the California Accelerated Pavement Testing Program CAL/APT] (4,5), as well as innovations in construction specifications and requirements (6,7).

Incorporated in this report are results of the mix and structural sections designs based on the SHRP-developed shear and flexural fatigue tests; aspects of the construction specifications; description of the sequence of construction activities during a typical weekend closure; “lessons learned” from both the design and construction activities associated with the project; measurements of mix characteristics obtained from the as-constructed pavement; and periodic measurements of pavement performance during the five-plus years from November 2003 to January, 2009, a period of approximately five years (completed sections were opened to traffic as early as March 2003). Reconstruction of the traveled way and shoulders was completed during eight 55-hour weekend closures (late March to early June 2003).

This summary report is intended to provide Caltrans with an available document to assist in the development of future major freeway rehabilitation projects using asphalt-surfaced pavements.

2 PAVEMENT SITE

Interstate 710, located in Southern California in Los Angeles County, is a heavily trafficked route that carries traffic into and out of the Port of Long Beach. Prior to its selection as an LLPRS project and its subsequent reconstruction, I-710 had an Average Daily Traffic (ADT) of 155,000 during weekdays, 13 percent of which was trucks. The specific section of I-710 selected by Caltrans District 7 for this project is between the Pacific Coast Highway (SR-1) and Interstate 405 (Figure 2.1). This freeway segment has a total length of about 4.4 km (2.7 mi) with three lanes in each direction (26.3 lane-km [16.1 lane-mi]), and it includes four overpasses.

The original as-designed pavement structural section consisted of 200 mm (8 in.) of portland cement concrete (PCC), 100 mm (4 in.) of cement-treated subbase, 100 mm (4 in.) of aggregate base, and 200 mm (8 in.) of imported subbase material. Having been constructed and opened to traffic in 1952 and without addition of any overlays prior to reconstruction, the pavement was in poor condition when the LLPRS project began.

Two rehabilitation strategies were selected:

1. Where clearance was acceptable, the existing PCC was cracked, sealed and overlaid with asphalt concrete (2.8 km [1.8 mi.] total length); and
2. Under structures where minimum clearance requirements did not allow an overlay, full-depth asphalt concrete sections were utilized with the freeway grade reconstructed² and lowered to provide the required clearance for interstate projects (1.6 km [1 mi.] total length).

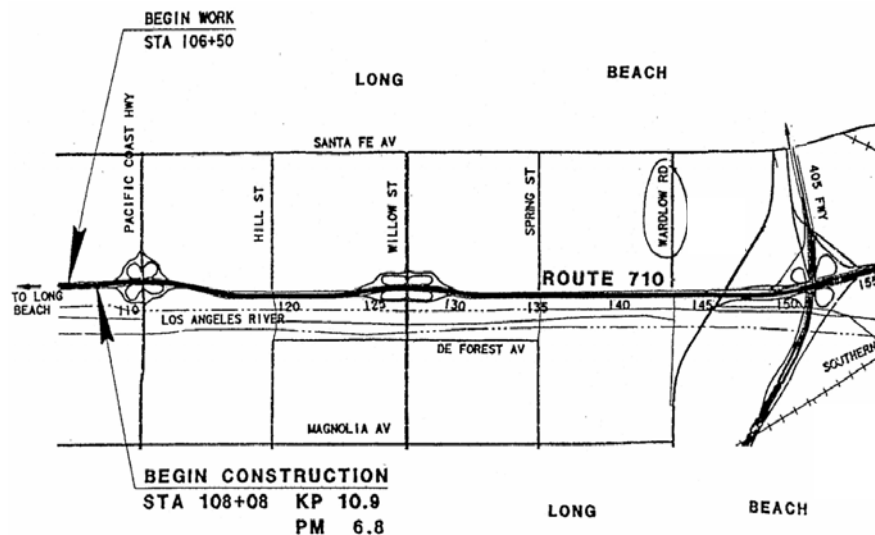


Figure 2.1: Project location.

² The existing concrete, cement-treated base (CTB), and granular subbase, as well as some subgrade were removed to a depth of 625 mm (~25 in.).

3 MIX AND STRUCTURAL SECTION DESIGNS

Strategic Highway Research Program (SHRP) mix evaluation technologies (1,3) augmented by research results from the Caltrans Partnered Pavement Research Center (PPRC) Program,³ (4,5) were used in the development of both the mix and structural pavement section designs. The framework for mix design is illustrated in Figure 3.1 and the mix analysis/design for fatigue is shown in Figure 3.2 (1,3,5). The pavement section has been designed to accommodate 200×10^6 ESALs, the equivalent traffic estimated for a 30-year period by Caltrans District 7 staff.

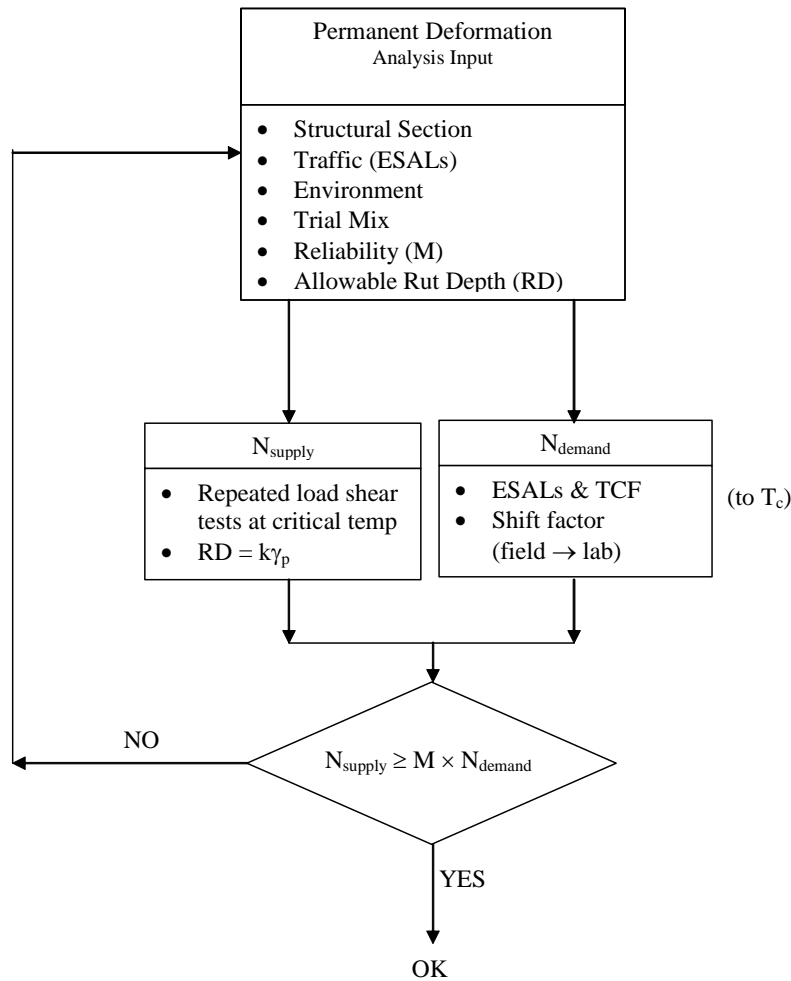


Figure 3.1: Framework for mix design: permanent deformation system.

³ During the period 1994 to 2000, this program was termed the California Accelerated Pavement Testing (CAL/APT) Program.

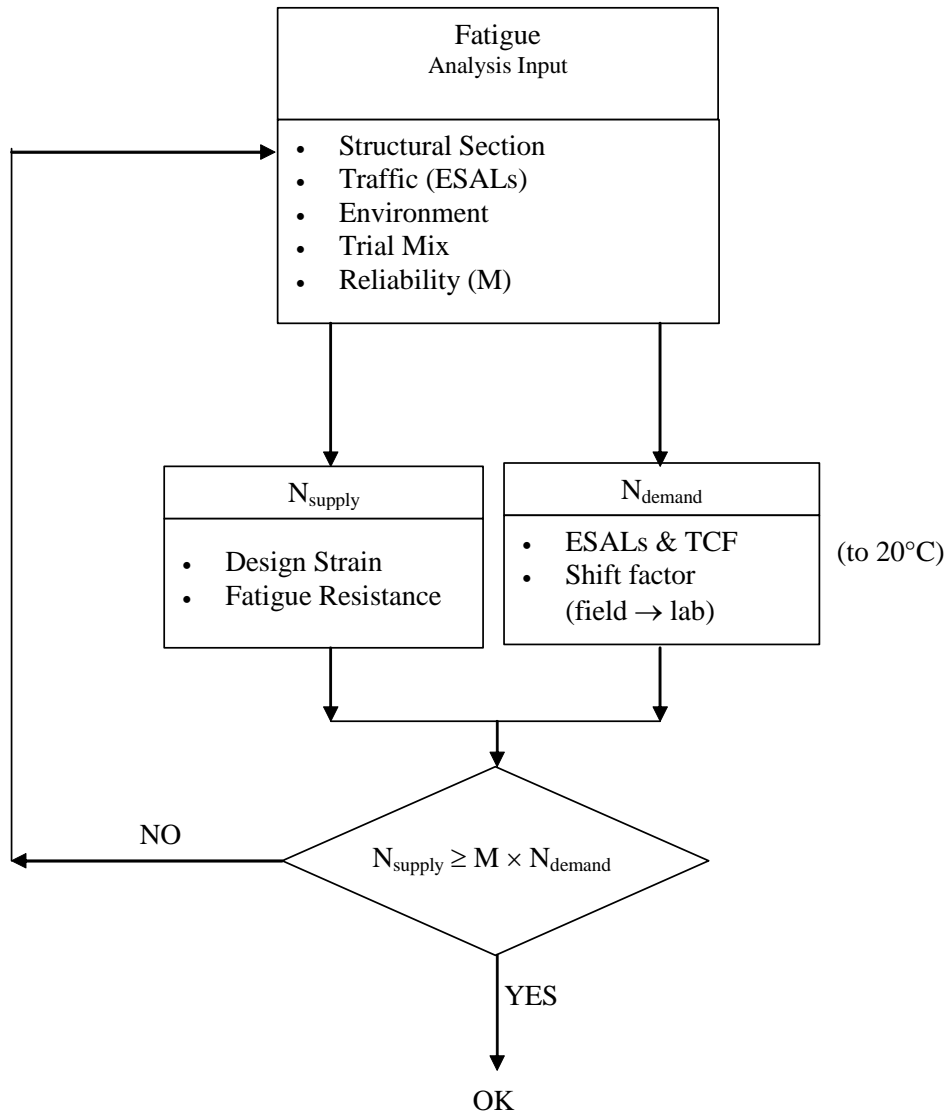


Figure 3.2: Framework for mix analysis/design: fatigue system.

3.1 Materials

Representative asphalt binders used for paving in the Los Angeles Basin were supplied by the Valero Marketing and Supply Company (formerly known as Huntway Refining) and aggregates representative of the Basin were supplied by Vulcan Materials Company (formerly, CAL/MAT). These materials were provided through the Asphalt Pavement Association located in Southern California (APACA).

Two *asphalt binders* were utilized: (1) AR-8000 paving asphalt (AASHTO MP1 designation PG64-16) and (2) polymer-modified asphalt, PBA-6a* (AASHTO MP1 designation PG64-40). (The * refers to the fact that this material contains additional elastomeric components and exceeds the “normal” PBA-6a specification requirements). Available test data for the two binders are summarized in Table 3.1. The

AR-8000 binder would be designated as a Class S binder according to the classification suggested by Heukelom (8).

The *aggregate* was obtained from the Vulcan Materials plant in the San Gabriel River Valley at Azusa, California. Some material characteristics are listed in Table 3.2. The aggregate grading used for mix design is shown in Figure 3.3 and Figure 3.4; the former showing the grading and limits on the conventional semilogarithmic plot and the latter showing the grading on the 0.45 chart (9). The control points and the maximum density line for an aggregate grading with a 19 mm (0.75 in.) nominal maximum size are also shown in Figure 3.4. It will be noted that the grading curve passes through the “restricted” zone.

Table 3.1: Binder Characteristics

Property	AASHTO Method	AR-8000		PBA-6a*	
		Test Result	Spec. ^a	Test Result	Spec. ^b
<i>Tests on Original Asphalt</i>					
Flash Point, C.O.C., °C	T-48	288	230 min	302	232 min
Solubility in TCE (%)	T-44		99 min	99.8+	Report
Absolute Viscosity, 60°C, poise	T-202	2113	–	10000+	2000 min
Kinematic Viscosity, 135°C, cSt	T-201	388	–	673	2000 max
<i>Tests on Residue from RFTO (AASHTO T-240)</i>					
Absolute Viscosity, 60°C, poise	T-202	8322	6000-10000	10000+	5000 min
Kinematic Viscosity, 135°C, cSt	T-201	706	400 min	1187	275 min
Viscosity Ratio: residual/original	–		–	1.8	4.0 max
Mass Loss, percent	T-240		–	0.149	0.6 max
Ductility at 25°C, cm	T-51		750 min	NA	60 min
<i>Tests on PAV Residue (AASHTO PP-1), 100°C</i>					
BBR, Creep Stiffness at –30°C, MPa			–	236	300 max
BBR, m-value at –30°C			–	0.312	0.300 min

a. State of California Department of Transportation, Section 92: Asphalts, *Standard Specifications*, Sacramento, California, July 1999.

b. State of California Department of Transportation, Special Provisions, *Performance Based Asphalt Binder Grades*, 1999.

Table 3.2: Aggregate Characteristics

Fraction	$\frac{3}{4}$ inch (19.0 mm)	$\frac{1}{2}$ inch (12.5 mm)	$\frac{3}{8}$ inch (9.5 mm)	Rock Dust	Spec. Limits
LA Abrasion: Loss at 100 rev. (%)	8.6	11.0	11.0	–	10 max
Loss at 500 rev. (%)	34.2	37.8	37.8	–	45 max
Specific Gravity	2.69	2.67	2.65	2.67	–

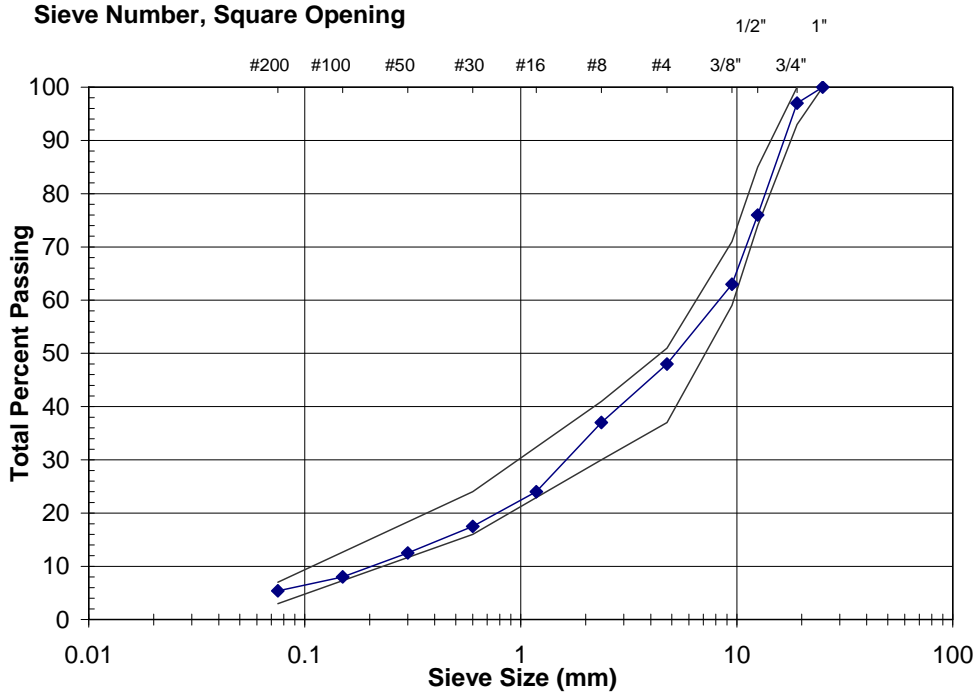


Figure 3.3: Aggregate gradation, semilogarithmic chart.

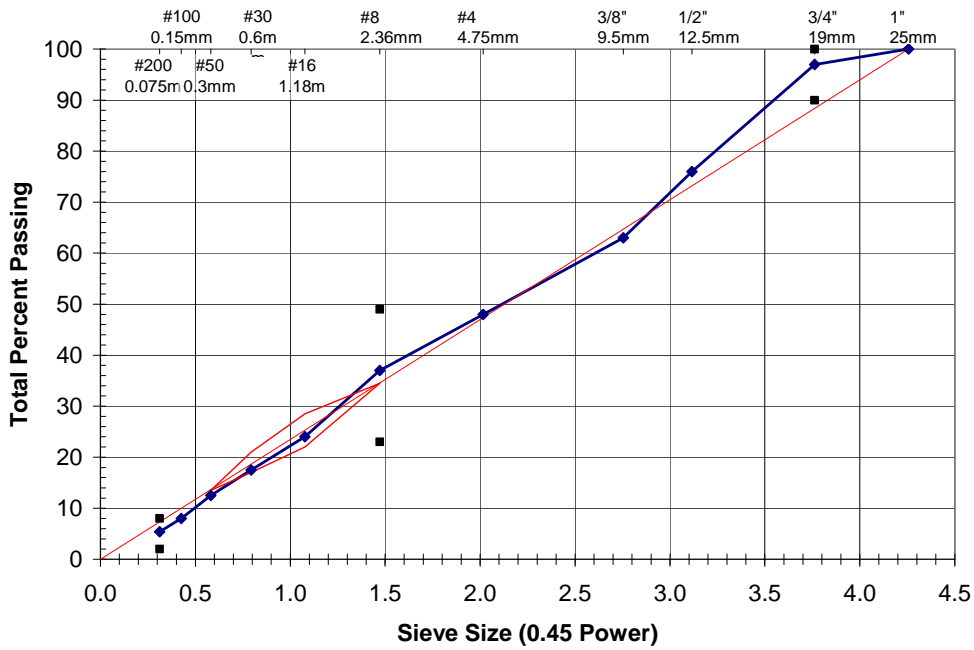


Figure 3.4: Aggregate gradation, 0.45 grading chart.

3.2 Mix Evaluations

A series of mix tests were performed for both mix design and analysis purposes. These included Hveem Stabilometer tests at 60°C (140°F), RSST-CH tests at 50°C (122°F) and 60°C (140°F) (AASHTO T 320), and flexural fatigue tests at 20°C (68°F) (AASHTO T 321). For the mix with the PBA-6a* binder, a

limited number of fatigue tests were also performed at 10°C, 25°C , and 30°C (50°F, 77°F, and 86°F). Table 3.3 contains a summary of the various tests conducted and the intended uses of the resulting data.

Table 3.3: Summary of Mix Tests

Materials: Aggregate Source/Binder	Binder Content(s)*	Test	Purpose(s)
Crushed cold feed/AR-8000	4.2 to 5.7	Hveem Stabilometer	Mix design—preliminary binder content selection
	4.2 to 5.2	Repeated simple shear test at constant height (RSST-CH) at 50°C, 60°C	Mix design—binder content selection
	4.7, 5.2	Controlled strain fatigue test at 20°C	Define relationship between tensile-strain and load repetitions for fatigue cracking analysis and evaluation of “rich-bottom” application.
	5.0	500 and 1,000 tamps in kneading compactor; Hveem Stabilometer	Check behavior after heavy trafficking as represented by 500 and 1,000 tamps in the kneading compactor.
Crushed cold feed/PBA-6a*	4.7 to 5.7	Hveem Stabilometer	Mix design—preliminary binder content selection
	4.2 to 5.2	Repeated simple shear test at constant height (RSST-CH) at 50°C, 60°C	Mix design—binder content selection
	4.7, 5.2	Controlled strain fatigue tests at 20°C; and limited number of additional tests at 10°C, 25°C, and 30°C	Define relationship between tensile-strain and load repetitions for fatigue cracking analysis and evaluation of “rich-bottom” application

*Binder contents by weight of aggregate.

3.2.1 Hveem Stabilometer Tests

The Stabilometer tests were performed at 60° C (140° F) following State of California Test Method 366 (CT 366) (10) using specimens prepared by kneading compaction with the Triaxial Institute Kneading Compactor, State of California Test Method 304 (CT 304). The majority of the Stabilometer tests were performed on mixes containing the AR-8000 asphalt cement to provide a tie-in with data obtained for such mixes produced for in-service pavements in the Los Angeles Basin as well as to provide a guide for selecting the range of binder contents for the simple shear test specimens to be prepared. Results of Stabilometer tests on mixes containing the PBA-6a* binder were used primarily as a guide to select the range of binder contents for mixes to be subjected to simple shear tests.

In addition to the regular compactive effort of the kneading compactor, additional specimens of the AR-8000 mix at the 5.0 percent binder content were subjected to 500 and 1,000 additional tamps. These additional tamps were applied while the specimens were maintained at a temperature of 60°C (140°F). The purpose of this study was to ascertain the change in stability with increased trafficking, which is likely to be representative of the heavy truck traffic on I-710. This procedure was recommended by Vallerga and Zube (11) to evaluate the influence of additional heavy traffic. Vallerga has used the same procedure to evaluate a mix from a heavily trafficked pavement in Dubai that had rutted (12); in addition he has introduced this concept for mixes subjected to the Boeing 747-400 aircraft at San Francisco International Airport (13) and for pavements subjected to “port-packers” at the Port of Oakland. The additional compaction requirement (500 tamps) now is also a part of the Caltrans Desert Specification (14).

Stabilometer test results for the mixes containing the AR-8000 binder at the standard compactive effort (Table 3.4) are in the range 34 to 40. Based on these data, an initial binder content of 5.0 percent was selected for the additional compactive efforts of 500 and 1,000 tamps at 60°C (140°F) to evaluate the effects of heavy traffic mix performance. In Table 3.4 it will be noted that the Stabilometer values are considerably reduced, as are the air-void contents. For the heavy I-710 traffic it likely that the design binder content should be less than 5.0 percent. Accordingly, it was decided to reduce the asphalt content range of 4.2 to 5.2 percent (by weight of aggregate) for the RSST-CH test program on mixes containing the AR-8000 asphalt.

Results of the Stabilometer tests at 60°C (140°F) for the PBA 6a* mix are also summarized in Table 3.4. These values are somewhat lower than those for the mix with the AR-8000 binder. Experience with the Stabilometer testing of other mixes containing modified binders is similar. Note too that the air-void contents of the compacted PBA-6a* mixes are somewhat lower than those for mixes containing the AR-8000 asphalt (Table 3.4).

Table 3.4: Hveem Stabilometer Test Results

Binder Type	Binder Content— Percent (by Weight of Aggregate)	Air-Void Content— Percent	Stabilometer “S” Value	Remarks
AR-8000	4.2	7.0	37	Standard ^a compactive effort
	4.7	5.6	40	Standard compactive effort
	5.2	4.4	35	Standard compactive effort
	5.7	2.5	34	Standard compactive effort
	5.0	1.5	16	150 tamps at 110°C 500 tamps at 60°C
	5.0	0.7	8	150 tamps at 110°C 1,000 tamps at 60°C
PBA-6a*	4.7	3.9	26	Standard compactive effort
	5.2	3.1	35	Standard compactive effort
	5.7	1.7	27	Standard compactive effort

a. Standard compactive effort: 150 tamps; 500 psi compaction pressure; and 110°C (230°F) temperature

3.2.2 RSST-CH Tests

Repeated simple shear tests at constant height (RSST-CH) were performed both at 50°C and 60°C (122°F and 140°F). The temperature of 50°C (122°F) is likely close to the critical temperature (T_c) for the portion of I-710 under investigation. The following includes a summary of the test results for both mixes.

To obtain the test results reported herein, a shear stress of 69 kPa (10 psi) was repeatedly applied with a loading time of 0.1 sec and a time interval between load applications of 0.6 sec. This stress and time of loading have been used for both mix analysis and design, e.g., References (1,15). The tests are normally conducted for 5,000 stress applications or to a permanent shear strain of 5 percent, whichever occurs first. Test specimens, 150 mm (6.0 in.) in diameter and 50 mm (2.0 in.) high, were obtained by coring from slabs compacted by rolling wheel compaction.

A representative relationship between permanent shear strain (γ_p) and the number of load applications (N) is shown in Figure 3.5. Curves, like the one shown in this figure, are adjusted by defining the intercept of γ_p at $N = 0$ and subtracting this value from all measurements of γ_p . An equation of the form:

$$\gamma_p = aN^b \quad (1)$$

is then fit to the data, usually for values of $N \geq 100$ or 1,000 repetitions depending on mix response. In this expression, the coefficients a and b (like those shown in Figure 3.5) result from regression analysis.

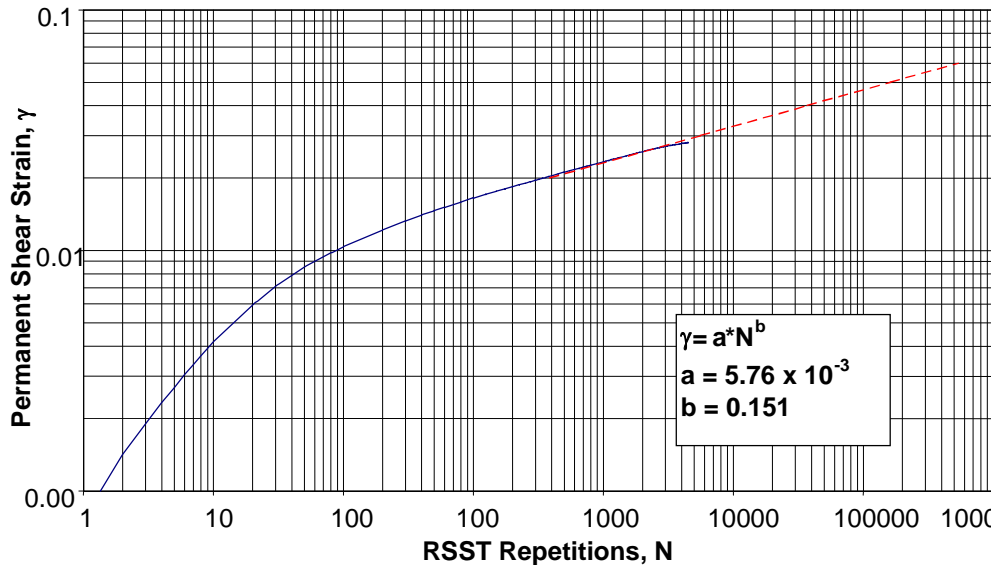


Figure 3.5: Permanent shear strain versus stress repetitions in RSST-CH at 50°C; PBA-6a* mix, 4.7 percent binder content.

Test data for mixes containing the AR-8000 and PBA-6a* binders are summarized in Table 3.5. While tests were performed at both 50°C (122°F) and 60°C (140°F), only the results obtained at 50°C (122°F) were used in selecting design binder contents, as will be seen subsequently. Results of all shear tests performed are contained in Appendix A: Laboratory Shear and Fatigue Test Data.

It is interesting to observe in Table 3.5 that the shear stiffnesses for the PBA-6a* mixes are less than those for mixes containing the AR-8000 binder; yet the resistance to permanent deformation of the PBA-6a* mixes is higher than those for the AR-8000 mixes.

Table 3.5: RSST-CH Test Results at 50°C

Binder Type	Binder Content, Percent (Aggregate Basis)	Average Air-Void Content (Percent)	N at $\gamma_p = 0.05$	G^\dagger , MPa (psi)
AR-8000	4.2	4.8	5.08×10^4	74.3 (10.8×10^3)
	4.7	3.6	1.72×10^5	82.0 (11.9×10^3)
	5.2	3.0	2.42×10^4	63.1 (9.14×10^3)
PBA-6a*	4.2	5.5	2.67×10^5	27.3 (3.96×10^3)
	4.7	3.8	1.23×10^6	32.2 (4.65×10^3)
	5.2	5.1	2.26×10^5	26.2 (3.79×10^3)

[†] G measured at $N = 100$ repetitions.

3.2.3 Flexural Fatigue Tests

Fatigue tests performed on the AR-8000 mix at 20°C (68°F) were conducted in the controlled-strain mode of loading. Load was applied sinusoidally (no stress reversal) using third-point loading at a frequency of 10 Hz (2). Test specimens 63.5 mm (2.5 in.) wide by 50 mm (2 in.) high and approximately 400 mm (16 in.) long were sawed from slabs compacted by rolling wheel compaction. Results of these tests are shown in Figure 3.6 and detailed test data are contained in Appendix A. The tests were performed at two binder contents: 4.7 and 5.2 percent (aggregate basis).

Mix stiffnesses were determined from both the RSST-CH and flexural fatigue tests. While flexural stiffness was measured only at 20°C (68°F), the shear stiffnesses at 50°C (122°F) and 60°C (140°F), as well as the Shell procedure (8,16), were used to obtain the range of stiffness values shown in Figure 3.7.

Results of the RSST-CH tests on the PBA-6a* mixes, also tested over the same range of binder contents as the AR-8000 mixes, are summarized in Table 3.5. In this table it will be noted that the PBA-6a* mixes have larger values of N at a permanent shear strain of 5 percent than the AR-8000 mixes. However, at 50°C (122°F), the shear stiffnesses of these mixes are less than those of the AR-8000 mixes, and Stabilometer values at 60°C (140°F) (see Table 3.4) are also less than those for the AR-8000 mixes.

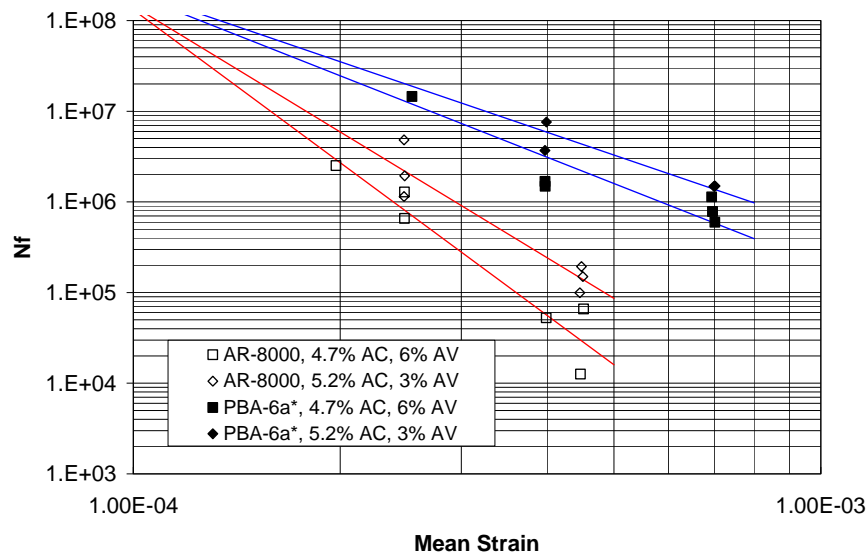


Figure 3.6: Results of controlled strain fatigue tests at 20°C, 10 Hz frequency.

Flexural fatigue test results for the PBA-6a* mixes are also shown in Figure 3.6. As with the AR-8000 mix tests, the tests on PBA-6a* mixes were conducted at binder contents of 4.7 and 5.2 percent (aggregate basis). As seen in Figure 3.6, the mixes containing the PBA-6a* binder exhibit longer fatigue lives than the mixes containing the AR-8000 asphalt cement for the range of strains used.

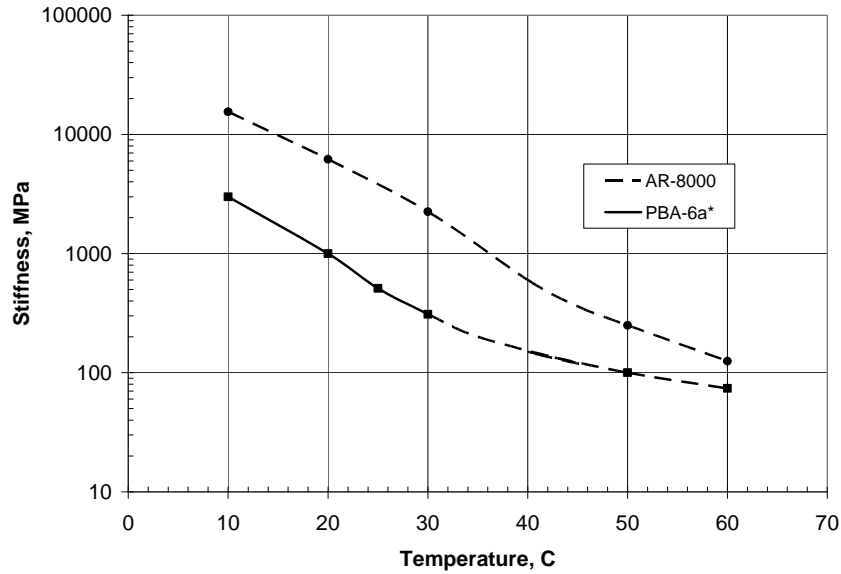


Figure 3.7: Mix stiffnesses versus temperature; mixes containing AR-8000 and PBA-6a* binders.

Mix stiffness data for the PBA-6a* mix are also shown in Figure 3.7. At 20°C (68°F), the stiffness of the AR-8000 mix is approximately six times greater than that of the PBA-6a* mix. At 50°C (122°F), however, the stiffness differs by a factor of 2.5. This difference in the stiffness of the two mixes influenced the thickness design for the full-depth section, as will be seen subsequently. The stiffer material, i.e., the mix containing the AR-8000 binder, was selected for use in a major portion of the structural section.

3.3 Mix Designs

Results of the RSST-CH tests were used to determine the design binder content for the surface course mix. The decision was made to base the mix design on traffic expected during the first five years. While the total traffic for the thirty year period was estimated to be 200×10^6 ESALs, a design value of 30×10^6 ESALs for the five-year period was selected considering both current traffic and different estimates of traffic growth. The framework illustrated in Figure 3.1 was followed.

For the equation shown in Figure 3.1:

$$(N_{\text{supply}}) \geq M \cdot (N_{\text{demand}}) \quad (2)$$

N_{demand} was determined as follows:

$$N_{\text{demand}} = \text{Design ESALs} \cdot \text{TCF} \cdot \text{SF} \quad (3)$$

where:

TCF = temperature conversion factor; estimated to be 0.11 for the site.

SF = shift factor, value of 0.04 was used as developed in Reference (1).

To determine N_{supply} , a reliability multiplier, M , equal to 5 for a reliability level of 95 percent was used based on RSST-CH test variance (I) and an estimate in the variance in $\ln(\text{ESALs})$. For the traffic of 30×10^6 , N_{supply} was estimated to be 660,000 repetitions. Figure 3.8 contains plots of the repetitions at $\gamma_p = 5$ percent ⁴(N_{supply}) versus binder content for both the PBA-6a* and AR-8000 mixes determined from the RSST-CH tests at 50°C.

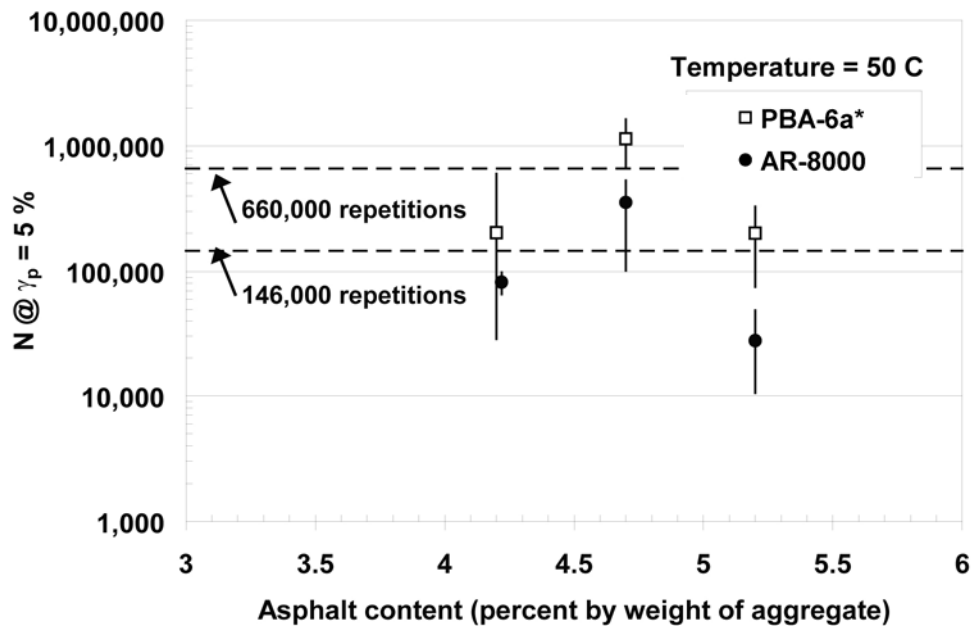


Figure 3.8: Repetitions to 5 percent permanent shear strain, N_{supply} , versus binder content; tests at 50°C.

As seen in Figure 3.8, the PBA-6a* mix satisfies the design estimate of 660,000 repetitions at a binder content of 4.7 percent (by weight of aggregate). Accordingly, the PBA-6a* mix was recommended for use as the surface course.

The AR-8000 mix, because of its higher stiffness characteristics, was selected for use in the remainder of the structural section below the surface course. Thus during construction it was considered likely that the AR-8000 mix would carry some traffic prior to the placing of the PBA-6a* mix. A conservative estimate of the traffic during this period resulted in a value of $N_{\text{supply}} = 146,000$ repetitions. From Figure 3.8, a design binder content of 4.7 percent, the same as that for the PBA-6a* mix, satisfies the traffic requirement and was used as the design value.

⁴ The value of $\gamma_p = 5$ percent is associated with rut depths not to exceed about 12 to 13 mm (0.5 in.) in pavements containing comparatively thick AC layers (1). This value is obtained from the equation shown in Figure 3.1, $RD = k\gamma_p$. When the rut depth (RD) is expressed in inches k has a value of 10; hence the value for $\gamma_p = 0.05$ or 5 percent.

To evaluate the mix design prior to construction, an overlay was constructed on an existing jointed PCC pavement at the Richmond Field Station of the University of California, Berkeley. The overlay consisted of 75 mm (3 in.) of the mix with the PBA-6a* binder over 75 mm (3 in.) of the AR-8000 mix, both at 4.7 percent binder content.

Aggregate representative of the type likely to be used on the project was shipped from Southern California, mixed at a central batch plant operated by Dumbarton Quarry Associates, and placed by O. C. Jones Engineering and Construction. Both layers were compacted to about 6 percent air voids. Arrangements for this operation were made by the APACA and the Northern California Asphalt Producers Association (NCAPA)⁵.

Following construction, a Heavy Vehicle Simulator (HVS) was used to load the PBA-6a* mix with about 10,000 (*one-way*) repetitions per day of a 40 kN (9,000 lb) load on dual tires with a cold inflation tire pressure of 690 kPa (100 psi). The temperature of the pavement was maintained at the critical temperature, 50°C (122°F), at a 50 mm (2 in.) depth.

Results of the accelerated loading on the PBA-6a* mix carried to about 170,000 repetitions (*one-way*) are shown in Figure 3.9. Also shown in the figure are results obtained from an earlier study (17) using both a

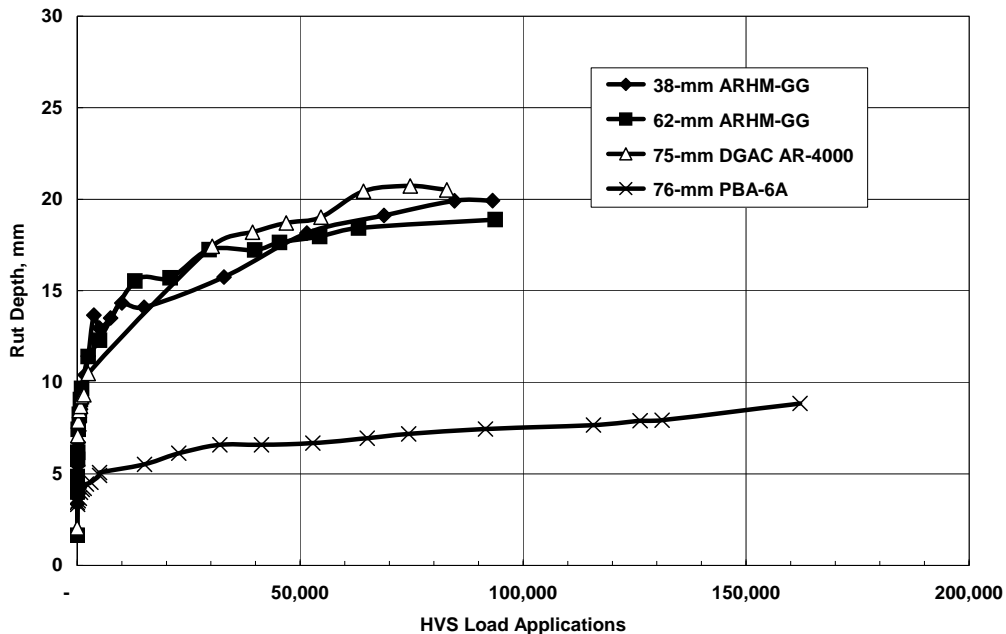


Figure 3.9: Rut depth versus HVS load applications with 40 kN load on dual tires at 50°C.

⁵ This organization now is named the California Asphalt Pavement Association (CAAPA).

dense-graded asphalt concrete with AR-4000 asphalt cement (Stabilometer “S” value = 43) and an asphalt rubber gap-graded hot mix (Stabilometer “S” value = 23). It will be noted that the PBA-6a* mix performed significantly better in terms of rutting than the other two mixes.

3.4 Structural Section Designs

This section briefly summarizes the methodology used to determine the structural pavements for both the full-depth AC replacement structure and the overlay structure on the cracked-and-sealed PCC pavement. More detailed information is included in References (18) and (19).

3.4.1 Full-Depth AC Replacement Pavement Structure

The approach to structural section design for the full-depth AC pavement followed that developed during the Strategic Highway Research Program (SHRP) (2) and was extended for California conditions through the CAL/APT program (4,5). The framework is illustrated in Figure 3.2; essentially the system evaluates the likelihood that the mix in the critical location of the pavement structure will resist fatigue cracking for the anticipated in-situ conditions. For a trial pavement structure, the principal tensile strain, the damage determinant for fatigue, is computed at the underside of the AC layer using layered elastic analysis (20).

To insure that the rutting resulting from permanent deformations in the underlying untreated materials does not contribute significantly to surface rutting, the vertical compressive strain at the subgrade surface is limited (21). This determination is also computed using layered elastic analysis.

While a number of different combinations of materials were evaluated using the methodology noted above⁶, only the analyses associated with the recommended structural section will be described. This section consists of the rut-resistant mix (PBA-6a* binder), the AR-8000 mix with 4.7 percent content, and a “rich-bottom” layer constructed with the AR-8000 binder at 5.2 percent binder content (to permit increased compaction). This layer is placed in the bottom portion of the full-depth section to improve the fatigue resistance of the pavement and should not affect the rutting resistance of the mix near the surface (4).

The elastic characteristics shown in Table 3.6 were used to perform the multilayer analyses to arrive at a suitable thickness to satisfy both fatigue and rutting (based on subgrade strain considerations). Figure 3.10 illustrates the detailed procedure for the thickness to mitigate fatigue cracking.

⁶ Appendix B contains a summary of the sections considered.

The test data shown in Figure 3.6 were used in the fatigue analyses. Equations representing these data are summarized in Table 3.7. With the calculated strain, the corresponding laboratory fatigue life was determined from the appropriate equation of Table 3.7 and denoted N_f .

Table 3.6: Material Properties for Pavement Analysis

Material	Modulus MPa (psi)	Poisson's Ratio	Remarks
Subgrade	83 (12,000)	0.45	"Reasonable" design value; determination from backcalculation, FWD tests
	55 (8,000)	0.45	Lower bound based on backcalculations
AR-8000 mix	6,372 (0.924×10 ⁶)	0.35	20°C, 4.7% binder content, V _{air} = 5.6%
	6,898 (1.0×10 ⁶)	0.35	20°C, 5.2% binder content V _{air} = 3.2%
PBA-6a* mix	1,008 (0.146×10 ⁶)	0.35	20°C, 4.7% binder content, V _{air} = 5.2%
	9,18 (0.133×10 ⁶)	0.35	20°C, 5.2% binder content, V _{air} = 3.3%

Table 3.7: Fatigue Characteristics of Evaluated Mixes*; 20°C

Mix Binder	Binder Content –Percent	Fatigue Equation	Remarks
AR-8000	4.7	$N_f = 5.142 \times 10^{-15} \varepsilon_t^{-5.602}$	$\varepsilon_t > 70 \times 10^{-6}$ mm/mm
	5.2	$N_f = 5.083 \times 10^{-11} \varepsilon_t^{-4.614}$	$\varepsilon_t > 70 \times 10^{-6}$ mm/mm
PBA-6a	4.7	$N_f = 2.229 \times 10^{-4} \varepsilon_t^{-2.989}$	$\varepsilon_t > 70 \times 10^{-6}$ mm/mm
	5.2	$N_f = 9.478 \times 10^{-3} \varepsilon_t^{-2.589}$	$\varepsilon_t > 70 \times 10^{-6}$ mm/mm

*Data presented in Figure 3.6.

To accommodate the 200×10⁶ ESALs, the structural sections resulting from the fatigue analyses for Interstate 710 are relatively thick. Consequently the computed strains were small and it was necessary to extrapolate the laboratory fatigue data. It has been assumed that at strain values of less than 70×10⁻⁶ mm/mm (in./in.) the likelihood of fatigue failure is minimal (22).

The temperature conversion factor (TCF) for the California coastal environment, in which Interstate 710 is situated, is shown in Figure 3.10 (4). It will be noted that the TCF is dependent upon AC thickness.

The fatigue shift factor is given as a function of tensile strain and was calibrated against the Caltrans pavement design procedure (5). Reliability multipliers, M, were calculated for fatigue distress at different levels of reliability. The number of ESALs that the pavement can carry before fatigue was determined by the equation shown in Figure 3.10 (5).

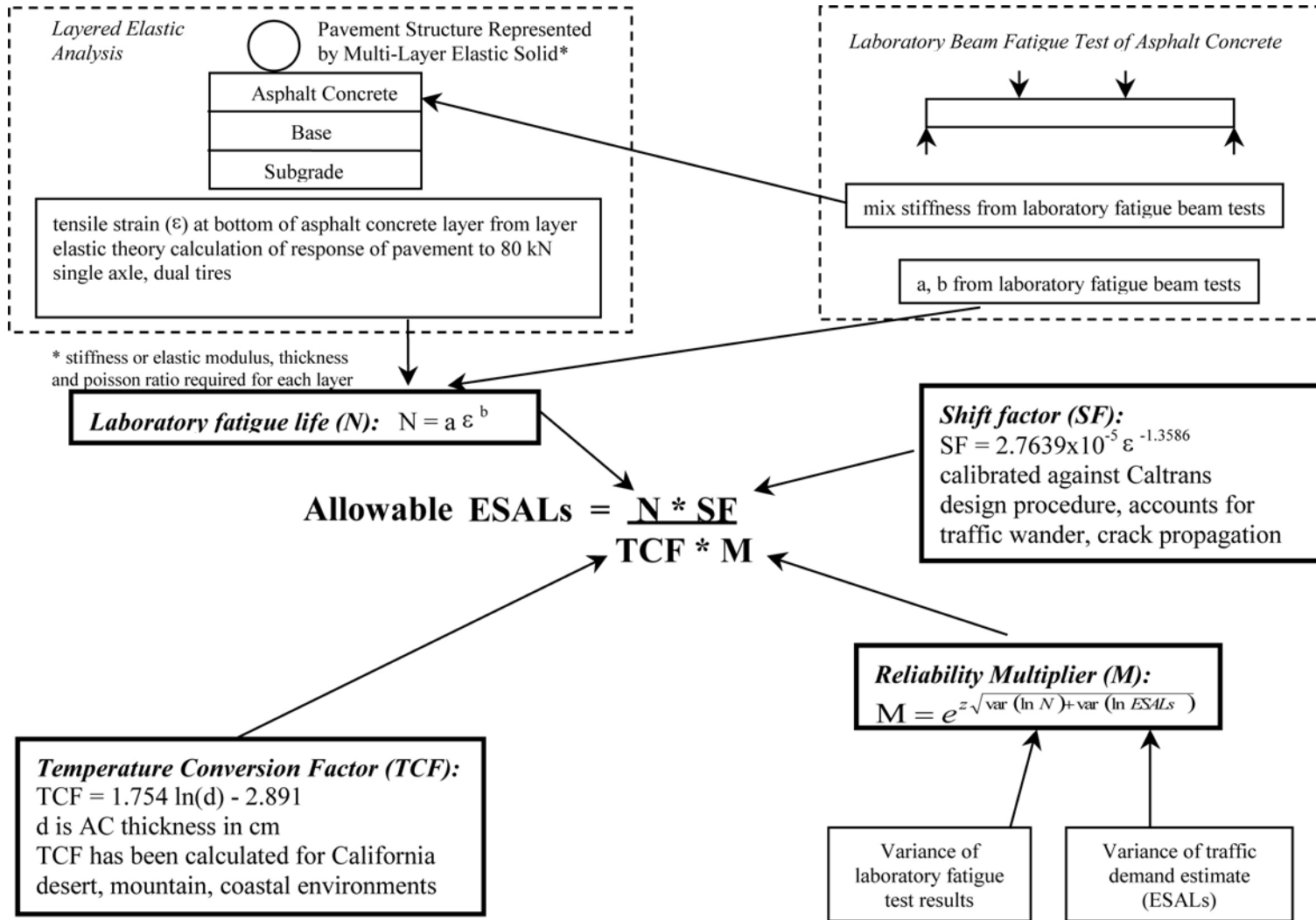


Figure 3.10: Fatigue analysis procedure.

To minimize rutting resulting from permanent deformation in the unbound layers, the Asphalt Institute subgrade strain criteria have been used according to the relationship shown below (21) where ϵ_v is the vertical compressive strain at the top of the subgrade:

$$N = 1.05 \times 10^{-9} \epsilon_v^{-4.484} \quad (4)$$

An iterative procedure was used to determine the minimum thickness of the AC layer to withstand fatigue failure and limit the subgrade strain. The minimum ESALs for the fatigue analyses are 200×10^6 and 50×10^6 to satisfy the subgrade strain requirement.⁷

The recommended structural pavement section resulting from the analyses is shown in Figure 3.11. The PBA-6a* mix is recommended for use only in the upper part of the structure even though its fatigue resistance is higher than mixes containing the AR-8000 mix. To satisfy the subgrade strain criteria a substantially thicker section consisting of all PBA-6a* mix would be required since its stiffness is only about one-sixth that of the AR-8000 mix at 20°C. The 75 mm (3 in.) thickness of the rich bottom layer is based on a limited analysis reported in Reference (4).

It is important to emphasize that the resulting design shown in Figure 3.11 is based on the assumption that the PBA-6a* and AR-8000 mixes (with 4.7 percent binder) will be compacted to an air-void content of 6 percent and the rich-bottom AR-8000 mix (with 5.2 percent binder) to 3 percent. As will be seen subsequently, the construction specifications have been prepared to reflect these compaction requirements.

The design includes a porous friction course using asphalt-rubber placed on the surface of the PBA-6a* mix. This layer, in addition to reducing hydroplaning, splash, spray, and tire noise, will also serve to reduce wear on the PBA-6a* mix. It is intended that this mix will be periodically removed and replaced during the design life of the structure.

In the mix design section, the design binder content of AR-8000 mix (4.7 percent binder content) situated between the PBA-6a* mix and the AR-8000 rich-bottom mix was selected based on its carrying traffic for some period prior to the placing of the PBA-6a* mix and the porous friction course. Because of this phased construction it was necessary to check the adequacy of the structural section for fatigue. Analysis like that described above indicated that the pavement section without the two final courses could carry the

⁷ Equation (4) was developed from an analysis of Caltrans structural section designs (22, 23). At values of 12×10^6 to 40×10^6 ESALs, the computed values for ϵ_v reached a limiting value of about 200×10^{-6} . Equation (4) resulted from a fit to computed values of ϵ_v greater than this level.

traffic without premature damage (18). Appendix C contains these analyses for an intermediate layer (AR-8000 mix [4.7% asphalt content]) 110 mm (4.3 in.) thick, one of the original alternatives considered.

3.4.2 Subsequent Additional Analyses

In this section three additional analyses related to the project are briefly described. The first was an analysis of fatigue performance performed that assumes that the truck traffic is applied between 5:00 A.M. and 7:00 P.M. The second was an analysis of the potential for surface rutting that might result from permanent deformations in the untreated materials (aggregate base and subgrade). The third analysis was an attempt to develop a revised set of shear and fatigue criteria (for succeeding I-710 projects) taking into account test variability in both the flexural fatigue and RSST-CH tests in response to an issue raised in the “Lesson Learned” activity to be discussed subsequently. To check the adequacy of the revised specification relative to fatigue cracking, an additional analysis similar to the first described above was performed.

Fatigue Analysis. The fatigue analysis performed initially (1999) was based on the assumption that traffic was applied uniformly throughout a 24-hour period. At the time of the initial design, there was some indication that the bulk of the truck traffic occurred in the period 5:00 A.M. to 7:00 P.M. Subsequently another analysis was done that assumed that the same daily truck traffic applied uniformly during the shorter 14-hour period. The detailed analysis for this traffic assumption is included in Appendix D. As will be seen in this appendix, the fatigue life was estimated to be about 9.6×10^9 ESALs, more than adequate to accommodate the assumed design traffic.

Permanent Deformation Analyses. A series of analyses were performed to evaluate the contribution of the untreated aggregate base and subgrade to the permanent deformation at the pavement surface. This approach was briefly discussed in Section 3.4.1 and it makes use of the Asphalt Institute subgrade strain criteria (22) modified to recognize the minimal contribution to surface permanent deformation/rutting resulting from additional repetitions beyond about 50×10^6 ESALs. As for the fatigue analyses described above, traffic was concentrated in the 14-hour period between 5:00 A.M. and 7:00 P.M. These results are included in Appendix E. The results shown in Table E.8 suggest that, *as long as these untreated materials are properly compacted*, the section shown in Figure 3.11 should exhibit minimal rutting at the pavement surface based on subgrade strain considerations.

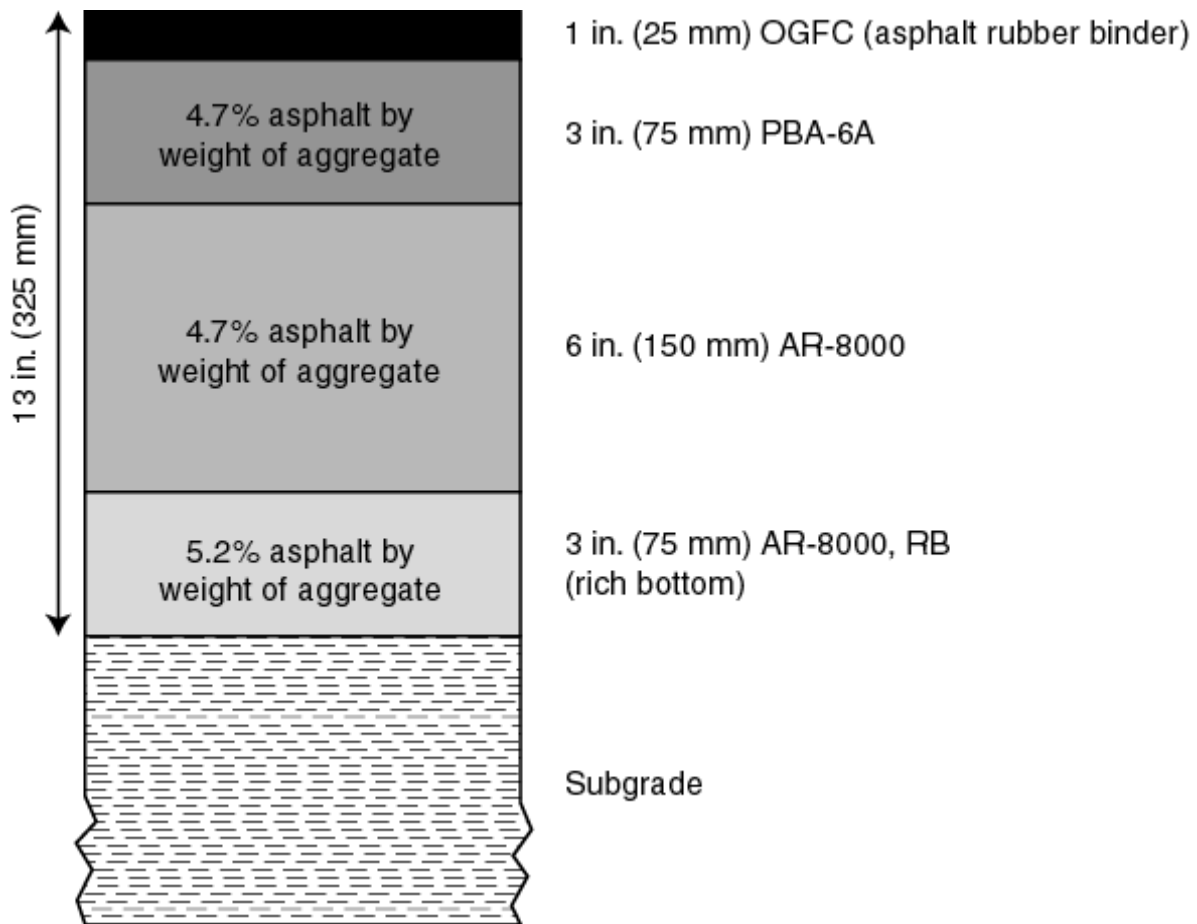


Figure 3.11: Proposed design, full-depth AC replacement of structure.

Revised Asphalt Concrete Performance Requirements, Subsequent Projects. During the course of the project, an issue was raised regarding the specification criteria for the shear and fatigue tests incorporated in the contract requirements. These requirements will be discussed in Chapter 4. At the time the specifications were established, values for the laboratory shear and fatigue test results were selected to coincide with those used for mix design (shear test results) and the structural pavement section designs (fatigue tests). The requirements were based on relatively new tests for which little precision and bias information were available. Thus, prior to the issuance of specifications for the Phase 2 project an analysis was performed to establish requirements for both the shear and fatigue tests for those mixes that the contractor planned to use. The results of this evaluation are included in Appendix F. Table 3.8 provides a comparison between the original specification requirements and recommended values for both shear and fatigue test results for subsequent projects. The repetitions are based on available UCPRC variability test data for both tests. These numbers represent mean values of repetitions for three test specimens that will provide a 95 percent confidence level for the test results.

Table 3.8: Comparison of I-710 Phases 1 and 2 Performance Specification Requirements

Test Type	Mix Type	Phase 1 Requirements (Repetitions)	Phase 2 Requirements (Repetitions)
Shear	AR-8000 mix	132,000 ^e	55,000 ^e
	PBA-6a* mix	660,000 ^e	275,000 ^e
Fatigue	AR-8000 mix	300,000 ^a 15,000,000 ^b	50,000 ^c 2,000,000 ^d
	PBA-6a* mix	7,000,000 ^a 60,000,000 ^b	950,000 ^c 8,000,000 ^d

^a. At a strain of 300×10^{-6} in. per in.; ^b. at a strain of 150×10^{-6} in. per in.; ^c. at a strain of 400×10^{-6} in. per in.;
^d. at a strain of 200×10^{-6} in. per in.; ^e. at a shear strain of 5 percent.

To check whether the minimum fatigue requirements shown above would still provide a satisfactory pavement in terms of fatigue cracking, an analysis included in Appendix G was performed using the Phase 2 requirements. The resulting estimated fatigue life was 4.1×10^9 ESALs, which is about 20 times the design life 200×10^6 ESALs.

3.4.3 Overlay Structure on Existing Cracked and Seated PCC Pavement

Design of the overlay pavement structure required a different approach than that used for the full-depth AC replacement structure (19). In this case, the primary concern was to select an adequate thickness to mitigate the loss in pavement serviceability resulting from *reflection cracking*. Current Caltrans practice for this type of construction has consisted of an asphalt concrete overlay that includes an asphalt-saturated nonwoven fabric interlayer placed on an AC leveling course on the cracked-and-seated concrete. Thicknesses of AC overlays of this type of the order of 125 to 150 mm (5 to 6 in.) have provided service lives of the order of 10 years (10 to 20×10^6 ESALs).

With existing practice as a guide, the same concept was used for the overlay pavement structure. The problem then became one of determining a “reasonable” thickness to sustain 200×10^6 ESALs.

The approach taken was to perform finite element simulations on idealized representations of asphalt concrete overlays of different thicknesses on the existing plain, jointed PCC pavement. The 200-mm (8 in.) thick existing slabs were assumed to be broken and seated prior to placement of the overlay.⁸

Reference (19) contains a detailed discussion of the various alternatives considered and associated analyses. This section discusses only results of the analyses associated with the combination of materials,

⁸ All of the finite element analyses were performed by Dr. Jeffery Simons of Applied Research Associates of Sunnyvale, CA, and formerly with Stanford Research Institute when the contract was initiated.

the PBA-6a*, and AR-8000 mixes, used in the full-depth AC above the rich-bottom layer. This combination is shown in Figure 3.12.

For the analyses, the crack spacing obtained by the pavement cracking procedure was assumed to average about 0.91 m (3.0 ft). A limited study was also done with a joint spacing of 4.57 m (15 ft), the joint spacing used at the time of the original construction.

For design of this type of overlay, the effects of both traffic loading and environmentally-induced stresses must be considered, the latter resulting from length changes caused primarily by temperature changes. By breaking the concrete slabs into smaller sections, the relative movements at the cracks/joints are reduced from temperature changes.

In this case, the effects of temperature-induced deformations/stresses were neglected based on temperature changes estimated to occur at a depth of 229 mm (9.0 in.), the actual depth of the final overlay section. Results of an analysis using the *Integrated Climatic Model (ICM)* (19,24) and the average of 30 years of temperature data for the Los Angeles (Long Beach) area indicated that the temperature change at this depth would be about 3.9°C (7°F) for average summer temperature fluctuations and about 2.8°C (5°F) for average winter conditions.

To analyze the effects of loading, the *NIKE 2D* program (25) was utilized. The pavement configuration selected for calculation is shown in Figure 3.13. Note that three 0.91-m (3.0-ft) sections are included.

The finite element mesh generated is shown in Figure 3.14(a) and contains a total of about 12,000 elements. Figure 3.14(b) shows a close-up of the mesh in the vicinity of the crack. The analyses were run in a plane strain state.

The vertical boundaries on either side of the mesh shown in Figure 3.13 are symmetry boundaries, which implies the geometry is repeated on either side of the mesh in a mirror image. This configuration gives a more realistic representation of the cracked pavement, and is not a conservative assumption since the load is also repeated on either side of the symmetry boundary.

The joint/crack was assumed to be in 2.5 mm (0.1 in.) wide with some load transfer. Utilizing elements representing the crack with a stiffness of either 10 percent or 1 percent of the stiffness modulus of the PCC, traffic loading was applied statically, as shown in Figure 3.13. A contact pressure of 725 kPa (105 psi) and length of tire in contact with the pavement of 254 mm (10 in.) were assumed. A total of 12

different cases were analyzed, including one with a joint spacing of 4.57 m (15.0 ft.)⁹. Only the results of the composite overlay analyses are included.

Table 3.9 summarizes the material properties used in the analyses.

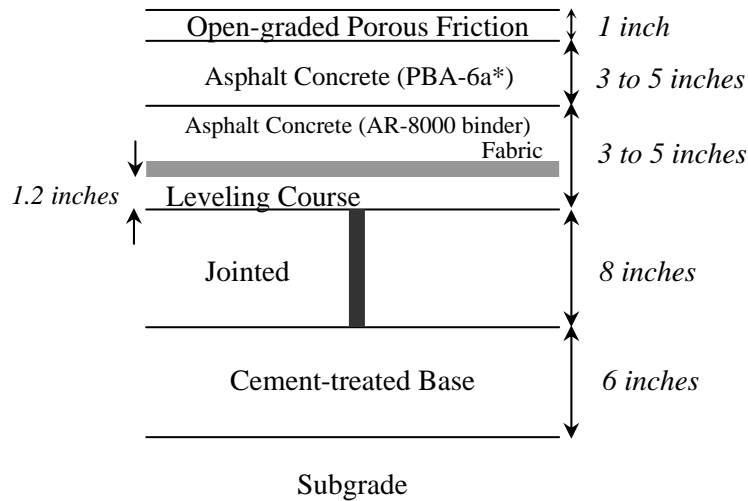


Figure 3.12: Pavement systems considered for final design.

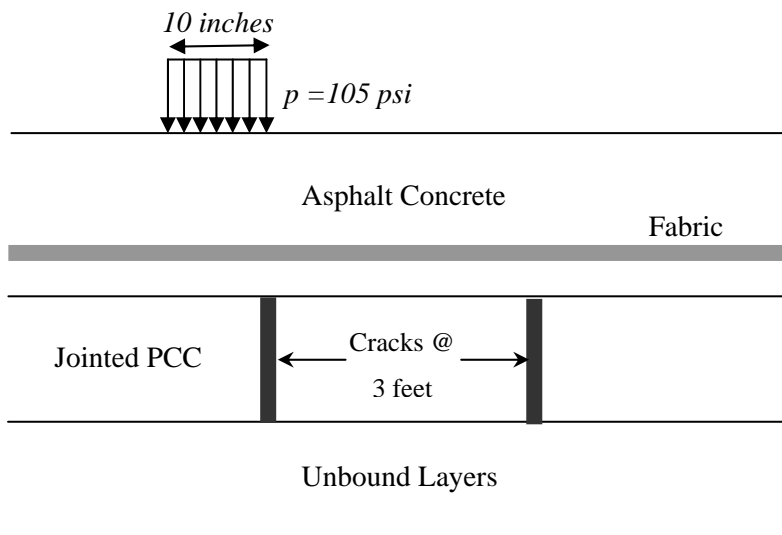
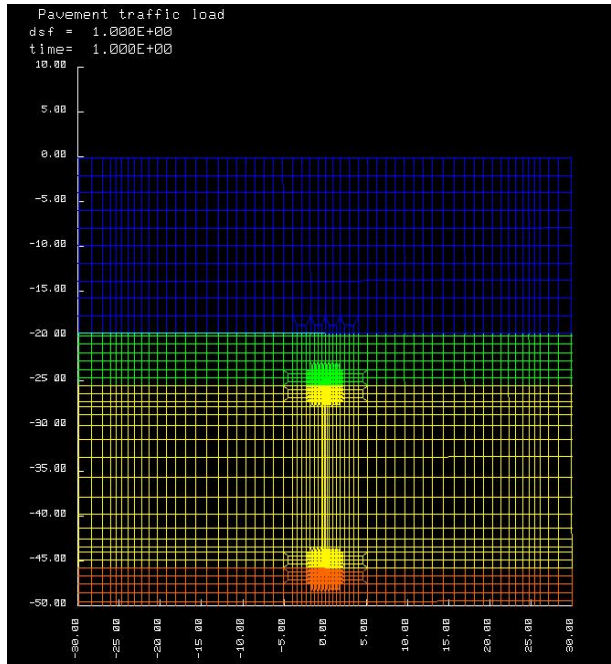
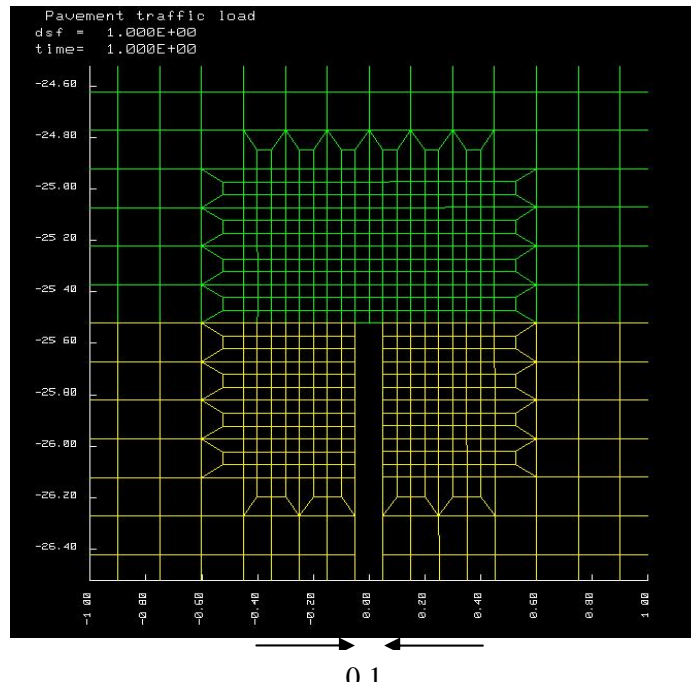


Figure 3.13: Pavement and loading configurations used for finite element analyses.

⁹ The results indicated, for the sections analyzed, that the bending strains in the asphalt concrete just above the fabric interlayer at the joint were about 10 percent less for the 15 ft. vs. the 3 ft. joint spacing.



(a) Close-up of finite element mesh in the vicinity of crack.



(b) Finite element mesh used for Nike 2D analyses; a total of about 12,000 elements.

Figure 3.14: Finite element idealization for the pavement system shown in Figure 3.13.

Table 3.9: Material Characteristics

Layer	Material	Thickness mm (in.)	Young's Modulus MPa ($\times 10^3$ psi)	Poisson's Ratio
1	Open-graded mix	25 (1.0 ^a)	1,030 (150)	0.4
2	Asphalt concrete (PBA-6a* binder)	75-100 (3.0-4.0)	1,030 (150)	0.4
3	Asphalt concrete (AR-8000 binder)	75-125 (3.0-5.0) ^b	6,210 (900)	0.4
4	Fabric	2.5 (0.1)	10 (1.5)	0.45
5	Leveling course (AR-8000 binder)	30.5 (1.2) ^c	6,210 (900)	0.4
6	Jointed PCC	200 (8.0)	27,590 (4000)	0.21
7	CTB	150 (6.0)	138 (20.0)	0.35
8	Subgrade	–	55 (8.0)	0.35

^a. For analysis purposes, considered as a part of AC with PBA-6a* binder (Reference [19]).

^b. Thickness includes leveling course.

^c. Same material as Layer 3.

Figure 3.15 illustrates the variation of tensile strain just above the fabric layer for three thickness combinations. It will be noted that maximum tensile strain is about the same for the three conditions. However, the compressive strain in the 125 mm/100 mm (5 in./4 in.) combinations is less than one-half of that for the 75 mm/75 mm (3 in./3 in.) combinations. For many materials, when the ratio of the minimum strain in compression increases relative to the maximum strain in tension (increased stress reversal), fatigue life is less. That is, as the ratio $R = \frac{\sigma_{\min}}{\sigma_{\max}}$ increases in the negative direction (assuming compression has a negative sign), the fatigue life decreases. Thus the “R” value for the 125 mm/100 mm (5 in./4 in.) combination is less (i.e., less negative) than for either the 75 mm/75 mm (3 in./3in.) or the 75 mm/125 mm (3 in./5 in.) combination; hence its fatigue life is expected to be longer.

Bending strains just above the cracks in the PCC layer are almost the same for the three conditions (see Figure 3.16). Since these strains are larger than those at the underside of the layer adjacent to the fabric, cracking is anticipated at these locations at fewer repetitions than in the mix above the fabric interlayer.

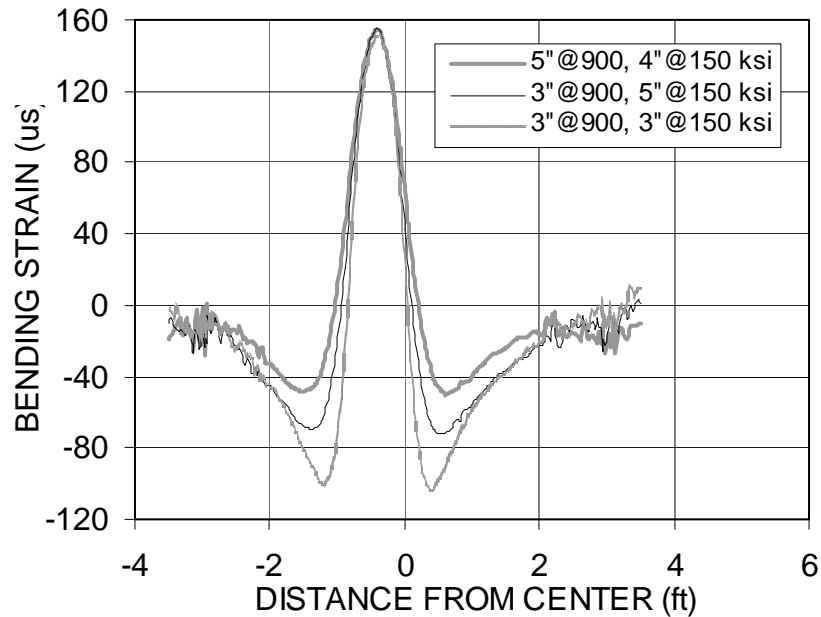


Figure 3.15: Comparison of strains at underside of mix just above the fabric interlayer for three thickness combinations of the PBA-6a* and AR-8000 mixes (1 in. \cong 25 mm).

Figure 3.17 illustrates the initial bending strain distribution at the underside of the top layer (PBA-6a* mix). For the cases examined, the distribution of strain for the 125 mm/100 mm (5 in./4 in.) combination remains compressive while that for the 75 mm/75 mm (3 in./3 in.) exhibits some strain reversal. This suggests that if cracking does progress above the interlayer it is likely to take substantially longer to reach the mix containing the PBA-6a* binder.

Shear strains have also been determined in the mixes at various locations. Figure 3.18 shows the variation of shear strains in the AR-8000 mix just above the interlayer. It will be noted that the magnitude of the maximum shear strain is about the same for the three cases; however, the patterns of distribution are different. The 125 mm/100 mm (5 in./4 in.) combination exhibits smaller secondary peak values than the 75 mm/75 mm (3 in./3 in.) combination. The level of peak shear strain is about 140×10^{-6} mm/mm (in./in.) for the 125 mm/100 mm (5 in./4 in.) combination. In the shear test used to evaluate the permanent deformation characteristics of the mix, the shear strain repeatedly applied was about 850×10^{-6} mm/mm (in./in.) at 50°C (122°F). It is unlikely that the pavement temperature at the depth of the interlayer will reach this temperature. Since the strain determined from this analysis is substantially less than that used in the shear test and would be even lower at a lower temperature it is unlikely that shear deformations contributing to permanent deformation of the mix will result.

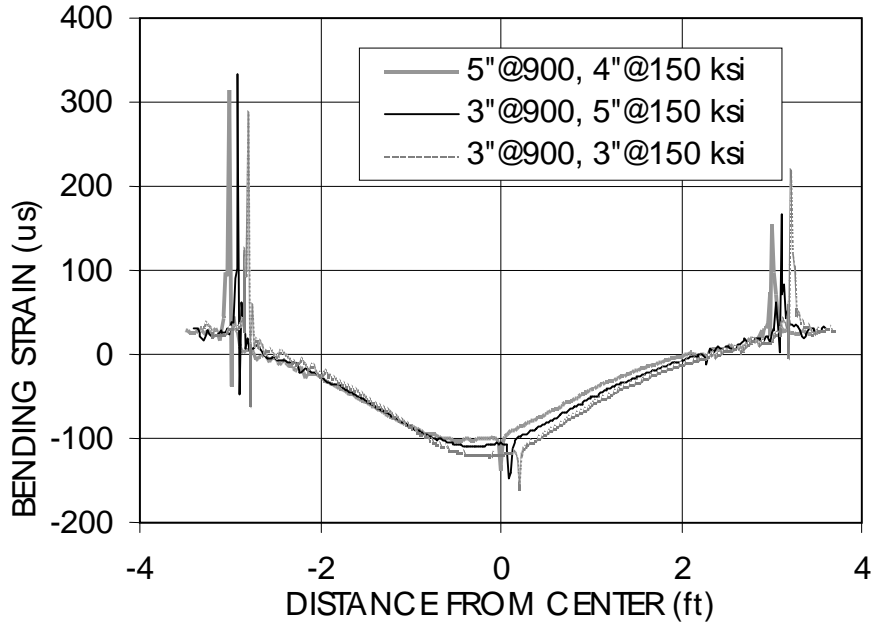


Figure 3.16: Comparison of bending strains in mix just above PCC joints/cracks for three thickness combinations of the PBA-6a* and AR-8000 mixes (1 in. \cong 25 mm).

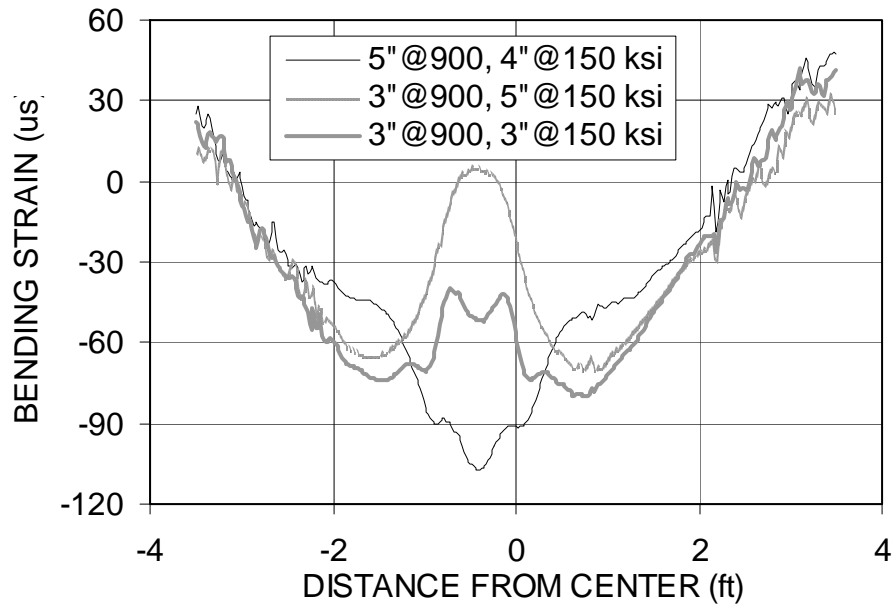


Figure 3.17: Comparison of bending strains on underside of the top layer for three thickness combinations of the PBA-6a* and AR-8000 mixes (1 in. \cong 25 mm).

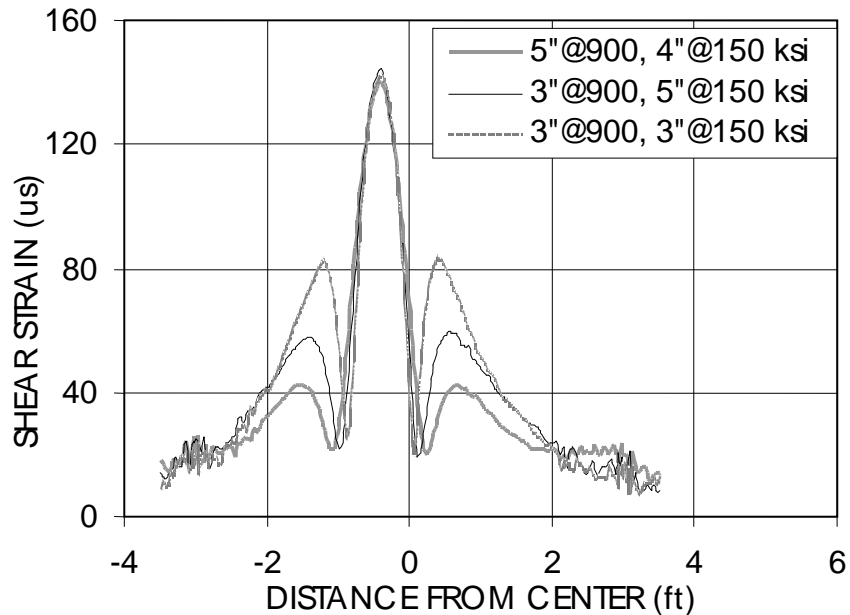


Figure 3.18: Comparison of shear strains in the underside of the mix adjacent to the fabric interlayer for three thickness combinations of PBA-6a* and AR-8000 mixes (1 in. \cong 25 mm).

Shear strains were also determined in: (1) the leveling course adjacent to the PCC; (2) at the bottom of the PBA-6a* layer; and (3) at the top of the PBA-6a* layer (19). Generally the results of these computations show the beneficial effects of the stiffer lower layer in controlling the shear strains in the PBA-6a* mix and suggest that the 125 mm/100 mm (5 in./4 in.) combination is a reasonable thickness combination relative to consideration of permanent deformation in the overlay.

The resulting design, shown in Figure 3.19, consists of: 30.5 mm (1.2 in.) leveling course-DGAC with AR-8000 asphalt content; asphalt-saturated fabric as an interlayer; 96.5 mm (3.8 in.) asphalt concrete course-DGAC with AR-8000 asphalt cement (same mix as leveling course); 75 mm (3 in.) asphalt concrete course-DGAC with PBA-6a* binder; and a 25 mm (1 in.) open-graded asphalt concrete with asphalt rubber binder (RAC-O).

The thickness including the open-graded porous friction course is 75 mm (3 in.) thicker than the current Caltrans design of 125 to 150 mm (5 to 6 in.) (associated with traffic volumes up to 20×10^6 ESALs). This design has the advantage that the 75 mm (3 in.) PBA-6a* mix and the 25 mm (1 in.) open-graded layer can be placed continuously. Moreover, at the junction of the replacement section and the overlay, the thickness of the replacement section will be 432 mm (17 in.) of asphalt mix, since the 200 mm (8 in.) concrete slab will have to be removed. With such a thickness the “bump” which might result at the

juncture of the two pavements should be minimized so long as “proper” compaction is achieved in the asphalt concrete layer.

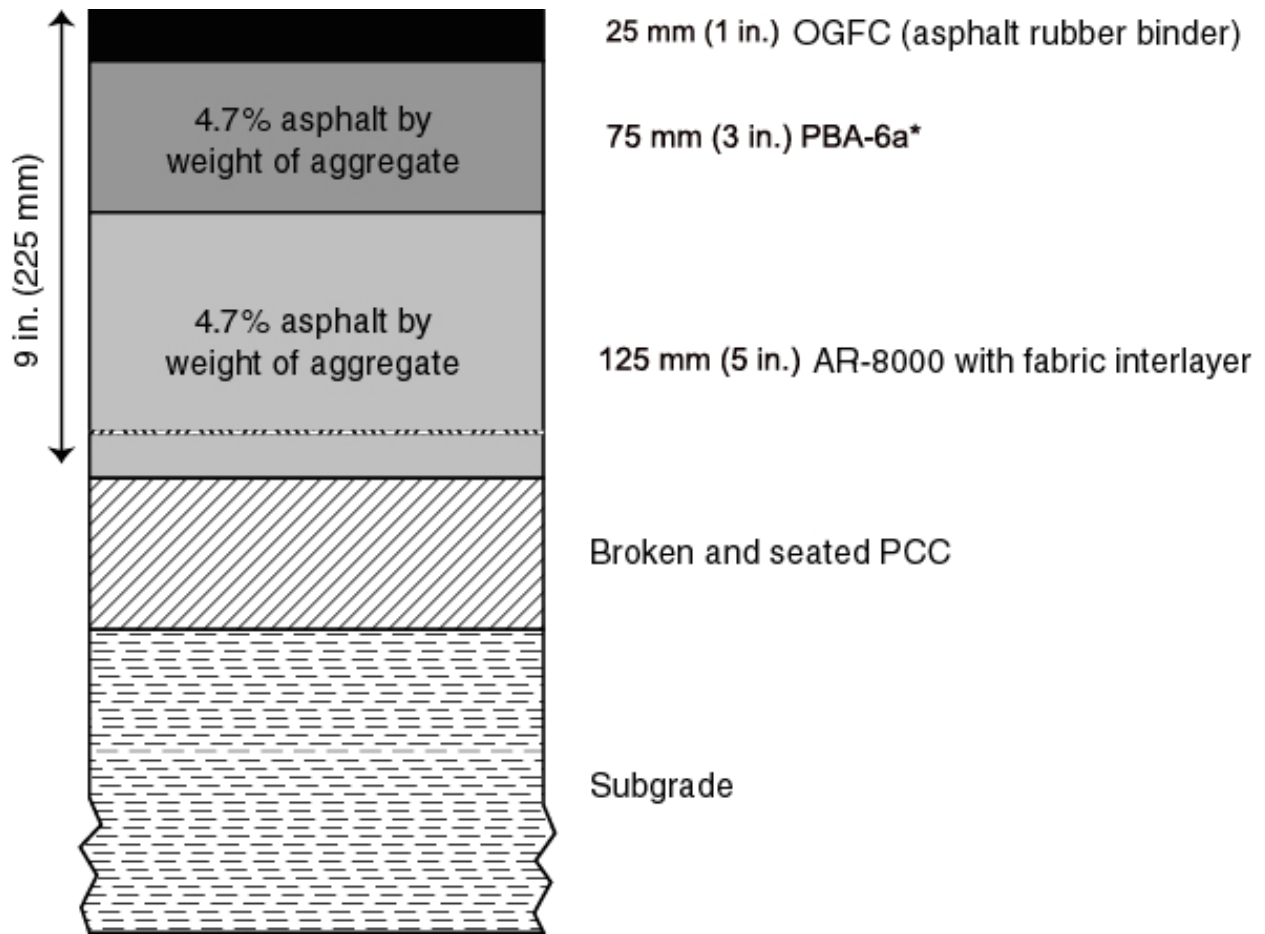


Figure 3.19: Proposed design for overlay on cracked and seated existing PCC structure.

4 CONSTRUCTION CONSIDERATIONS

For these pavements to perform successfully, strict attention to pavement construction was required, including careful control of the mix components, mix compaction, and layer thicknesses. The performance requirements, minimum process control requirements, and minimum quality control requirements excerpted from Reference (6) are included in this discussion.

In a significant departure from Caltrans “Standard” requirements, the specifications included mix design “recommendations” with mix performance requirements. This allowed the contractor to optimize the materials selection process while requiring the specified mix performance characteristics.

Prior to construction, shear and fatigue test data defining mix performance were required to be submitted by the contractor to Caltrans for mix approval. This requirement was incorporated into the project specifications to ensure that the mixes to be used by the contractor met the performance characteristics shown in Table 4.1 (6). These characteristics correspond to those used in the mix and pavement design processes. In addition, prior to construction, materials were required to be submitted to Caltrans for verification of these mix characteristics. (At this time of specification preparation, the shear test was shown as TP7-94; it is now an AASHTO Standard Test, T-320 and the fatigue test is now AASHTO T-321).

Minimum process control requirements are shown in Table 4.2. Compaction and other quality control requirements are summarized in Table 4.3 (6). The mixes containing the PBA-6a* mix and the AR-8000 at a binder content of 4.7 percent were to be compacted to an air-void content of about 6 percent (93 to 97 percent of the theoretical maximum density, ASTM D 2041) whereas compaction requirements for the rich-bottom mix required an air-void content of not more than 3 percent. It should be emphasized that this project, which used ASTM D 2041 as the basis for compaction control, is a departure from the Caltrans procedure in use at the onset of the project (26).

Prior to this project, Caltrans practice did not require a tack coat between lifts for multiple lift construction. The specification stated that the decision to use a tack coat could be made on a case-by-case basis by the Resident Construction Engineer. This practice was changed for the I-710 project, and a tack coat was required between each lift. This change resulted from observations of the performance of HVS test sections as part of the CAL/APT program (17).

During mix production, the contractor was required to provide the minimum process control requirements shown in Table 4.2 (6).

Table 4.1: Asphalt Concrete Mixture Performance Requirements [Table 39-3A from Reference (6)]

Design Parameters		Test Method	Requirement
Permanent Deformation (min.)	PBA-6a* (modified) ²	AASHTO TP-94 modified ¹	660,000 stress repetitions ^{3,4}
	AR-8000 ²	AASHTO TP-94 modified	132,000 stress repetitions ^{3,4}
Fatigue (min.)	PBA-6a* (modified) ^{5,6}	AASHTO TP8-94 modified ¹	7,000,000 repetitions ^{4,8} 60,000,000 repetitions ^{4,9}
	AR-8000 ^{5,7}	AASHTO TP8-94 modified ¹	300,000 repetitions ^{4,8} 15,000,000 repetitions ^{4,9}

Notes to Table 4.1:

1. Included in the testing guide provided upon request.
2. At proposed asphalt binder content and with mix compacted to $3 \pm 0.3\%$ air-void content.
3. In repeated simple shear test at constant height (RSST-CH) at a temperature of 50°C
4. Mean of 3 specimens.
5. At proposed asphalt binder content and with mix compacted to $6 \pm 0.3\%$ air-void content (determined using AASHTO 209 [Method A]).
6. At proposed asphalt binder content, minimum stiffness at 20°C and a 10-Hz load frequency must be equal to or greater than 1,000 MPa (150,000 psi). At proposed asphalt binder content, minimum stiffness at 30°C (86F°) and a 10-Hz loading frequency must be equal to or greater than 300 MPa (45,000 psi).
7. At proposed asphalt binder content and $6 \pm 0.3\%$ laboratory air-void content (determined using AASHTO 209 [Method A]), minimum stiffness at 20°C and a 10-Hz loading frequency must be equal to or greater than 6,200 MPa (900,000 psi). At proposed asphalt binder content plus 0.5 percent and $3 \pm 0.3\%$ laboratory air-void content (determined using AASHTO 209 [Method A]), minimum stiffness at 20°C and a 10-Hz loading frequency must be equal to or greater than 6,800 MPa (990,000 psi).
8. At 300×10^{-6} mm/mm. Results shall be reported for this strain level, but may be obtained by extrapolation. Minimum number of repetitions required prior to extrapolation defined within test procedure.
9. At 150×10^{-6} mm/mm. Results shall be reported for this strain level, but may be obtained by extrapolation. Minimum number of repetitions required prior to extrapolation defined within test procedure.

Table 4.2: Minimum Process Control Requirements [Table 39-4 from Reference (6)]

Quality Characteristic	Action Limit	Test	Minimum Sampling and Testing Frequency	Point of Sampling	Reporting Time Allowance
Sand Equivalent (Min.)	47	CT 217	One sample per 2,000 tonnes	Batch plant from hot bins	24 hours
		See (1)	Not less than one sample per day		
% of Crushed Particles (Min.) Coarse Aggregate	100%	CT 205	Not less than one sample per day	or	24 hours
Fine Aggregate (Passing 4.75 mm, Retained on 2.36 mm)	100%			Drum plant-from cold feed	
Hveem Stabilometer (Min.) PBA-6a* (modified)	TV _{S1} ² TV _{S2} ³	CT 366	Sample at least once per 500 tonnes	Mat behind paver	36 hours
AR-8000	TV _{S3} ² TV _{S4} ³	See (1,3,4,6,7, & 8)	Minimum testing schedule ⁹		
REPORT ONLY					
Hveem Stabilometer (Min.) AR-8000 (rich bottom)	TV _{S5} ² TV _{S6} ³	CT 366	Sample at least once per 500 tonnes	Mat behind paver	36 hours
		See (1, 3, 4, 6, 7, 8)	minimum testing schedule ⁹		
Laboratory Percent Air Voids PBA-6a* (modified)	TV _{AV1}	CT 367	See note 9 for minimum testing schedule	Mat behind paver	36 hours
AR-8000	TV _{AV2}	See notes 1, 4, & 10			
AR-8000 (rich bottom)	TV _{AV3}				

Notes to Table 4.2:

1. Reported value shall be the average of three test results. Samples used for the 3 tests to be averaged shall be from a single split sample.
2. Do not modify CT 304.
3. Perform CT 304, and then apply an additional 500 tamping blows at 3,400 kPa (500 psi) at 60°C (140°F).
4. Sets of three briquettes must be prepared and tested to meet conditions of Notes 3 and 4 separately.
5. Limited reheat for sample preparation to two hours. Do not place sample or briquette in oven for 15-hour cure.
6. Briquettes shall be fabricated from a single, combined sample obtained from at least four locations across the mat behind the paver in conformance with the requirements of California Test 125.
7. If the range of stabilities for the three briquettes is more than 12 points, the samples shall be discarded and new samples shall be obtained before the end of the following shift of paving and tested per Table 39-3B (6).
8. During production start-up evaluation, a correlation factor for cured vs. uncured specimens shall be established in conformance with the requirements of Section 39-10.01A, "Production Start Up Evaluation."
9. Asphalt Concrete will be sampled each 500 tonnes. Each type of asphalt concrete shall be tested each day the first 5 days (or at least per 2,000 tonnes of production) and testing may be decreased to one per each 5,000 tonnes thereafter unless stability falls below the action limit. Samples shall be retained to define limits of problem areas should the stability fall below the action limit. When stability falls below the action limit, testing will be increased to one test for each of the first 2,000 tonnes and may be decreased to one per each 5,000 tonnes thereafter. Each asphalt concrete type being produced and placed shall be sampled and tested at least once per 55-hour window if the quantity is less than 2,000 or 5,000 tonnes as it applies to the interval. The sequence of the first five test results shall not be broken by more than seven days of nonproduction.
10. Use CT 308A for determination of bulk specific gravity and AASHTO T209 (Method A) for maximum theoretical specific gravity.

Table 4.3: Minimum Quality Control Requirements [Table 39-9 from Reference (6)]

Index (i)	Quality Characteristic	Specification Limits	Weighting Factor (w)	Test Method	Minimum Sampling and Testing Frequency	Point of Sampling	
1	Asphalt Content	TV1±0.3%	0.30	CT 379 or CT 382	One sample per 500 tonnes or part thereof Not less than one sample per day	Mat behind paver	
2	Gradation	25.4 mm		CT 202	One sample per 500 tonnes or part thereof Not less than one sample per day	Batch plant – from hot bins or Drum plant – from cold feed	
3		19 mm	TV ±5%				0.01
4		12.5 mm	TV ±5%				0.02
5		9.5 mm	TV ±6%				0.02
6		4.75 mm	TV ±7%				0.02
7		2.36 mm	TV ±5%				0.04
8		600 µm	TV ±4%				0.05
9		300µm	TV ±4%				0.07
9		75 µm	TV ±2%				0.07
10	Percent of Maximum Theoretical Density	PBA-6a* (modified): 93-97% AR-8000: 93-97% AR-8000 (rich bottom): 97-100% AR-8000 (working platform): 91-97%	0.40	CT 375	One sample per 500 tonnes or part thereof Not less than one sample per day	Finished mat after final rolling	
	Maximum Theoretical Density ³ % Air Voids ⁴				CT 308 AASHTO T209 (Method A) AASHTO T269		Mat behind the paver
11	Mix Moisture Content	≤1%		CT 370	One sample for 1000 tonnes but not less than one sample per day	Mat behind the paver	
	Asphalt and Mix Temperature	120°C to 190°C (Asphalt) ≤ 165°C (Mix)			Continuous using an automated recording device	Plant	

Notes to Table 4.3:

1. TV = Target Value from Contractor’s Mix Design Proposal
2. The percent passing the 75µm sieve shall be reported to the first decimal place (tenths).
3. California Test 375, “Density of Asphalt Concrete Using a Nuclear Gage,” modified to use maximum theoretical density in accordance with ASTM D2041 (Rice Method) in lieu of test maximum density as provided in Part 5, “Determining Test Maximum Density.”
4. Report only.
5. Quality characteristics 1 and 10 are defined as critical quality characteristics.

5 CONSTRUCTION

Details of the construction activities associated with the I-710 project are contained in Reference (7). This section briefly summarizes these activities to provide an indication of the approaches followed. Construction was accomplished in six stages. In the first stage, the median was widened and the old metal beam guardrails were replaced with concrete barriers. The second stage included excavating, widening, and paving the outside shoulders up to the existing pavement surface elevation. The remaining four stages involved the main work of rehabilitating the four full-depth asphalt concrete (FDAC) sections under the overpasses and the two AC overlays of the cracked-and-seated PCC (CSOL) sections. In the Caltrans plan, a total of 10 consecutive weekend closures were scheduled for completion of these last four stages.

Encouraged by the incentives (\$100,000 per weekend fewer than 10), the contractor revised the Caltrans staging plan by splitting the freeway into eight segments in order to complete those segments in eight consecutive weekend closures, as shown in Figure 5.1.

During the main rehabilitation work, the contractor was required to adopt a “counterflow traffic” closure strategy. With this strategy, one direction of the freeway is closed for the construction work zone (CWZ), and traffic is then rerouted through crossover areas located at both ends of the CWZ to two lanes in each direction (three traffic lanes plus the shoulder) on the other half of the freeway. The two directions of traffic are separated by a moveable concrete barrier (MCB). During the first four weekend closures, the contractor shut down the southbound side for construction while maintaining two lanes of traffic in each direction on the northbound side. The closure was reversed during the latter four weekend closures. A short (eight-hour) full closure of the entire freeway was used for mobilization and demobilization in each 55-hour weekend closure.

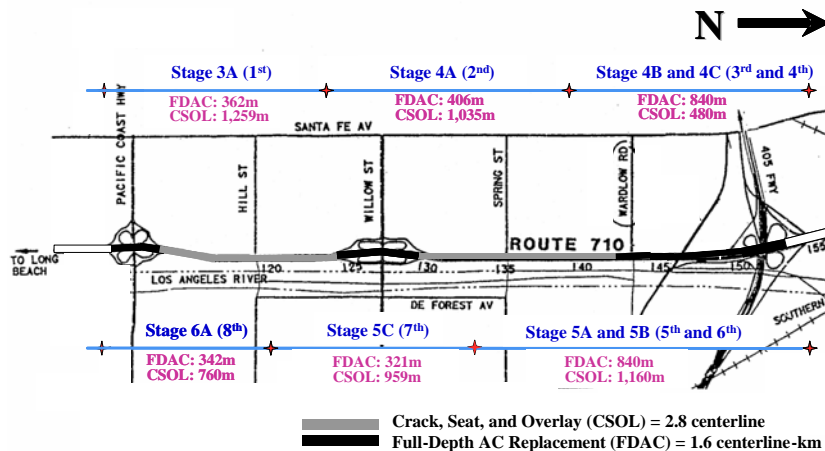


Figure 5.1: Contractor’s revised staging plan (sequence of 55-hour weekend closures shown in parentheses).

The sequence of activities followed for the major CSOL and FDAC construction for a typical 55-hour weekend closure was as follows:

1. Traffic Full Closure
 - Set up CWZ signs and close both directions of the freeway.
 - Remove existing striping and markers on temporary traffic roadbed.
 - Set up MCB and place temporary striping and markers.
 - Open counterflow traffic on the traffic roadbed.
2. CSOL Rehabilitation
 - Crack and seat existing PCC pavement.
 - Place 45 mm (1.8 in.) AR-8000 leveling course.
 - Install pavement-reinforcing fabric.
 - Place 85 mm (3.3 in.) AR-8000 and 75 mm (3 in.) PBA-6a*.
3. FDAC Rehabilitation
 - Fracture (rubblize, or so-called “stomp”) and remove existing PCC pavement.
 - Excavate roadway and cut subgrade.
 - Place 50 mm (2 in.) AR-8000 working platform or 150 mm (6 in.) new aggregate base.
 - Place 75 mm (3 in.) AR-8000 rich bottom, 150 mm (6 in.) AR-8000, and 75-mm (3 in.) PBA-6a*.
4. FDAC Rehabilitation
 - Fracture (rubblize, or so-called “stomp”) and remove existing PCC pavement.
 - Excavate roadway and cut subgrade.
 - Place 50 mm (2 in.) AR-8000 working platform or 150 mm (6 in.) new aggregate base.
 - Place 75 mm (3 in.) AR-8000 rich bottom, 150 mm (6 in.) AR-8000, and 75-mm (3 in.) PBA-6a*.
5. Traffic Opening
 - Place striping and markers on new pavement.
 - Close both directions of the freeway.
 - Remove temporary striping and markers on the traffic roadbed.
 - Relocate MCB to the median, and restore striping and markers.
 - Remove CWZ signs.
 - Reopen both directions of the freeway.

Figure 5.2 shows the contractor’s overall CPM schedule submitted for a typical 55-hour weekend closure. Because of extreme time, space, and resource constraints, many activities were scheduled to be performed concurrently. Large amounts of schedule float were assigned to riskier demolition activities at the FDAC

section. PCC cracking at the CSOL section and PCC fracturing at the FDAC section were scheduled to begin shortly after the full traffic closure was implemented. AC placement was planned to be completed at the CSOL section first and proceed to the FDAC section.

At each weekend closure, median and outside shoulders were completely overlaid and/or replaced with AC, together with three main traffic lanes, in four passes with the paver (pulls), each approximately 4.3 m (14 ft.) wide. An alternating paving sequence was utilized to avoid potential suspension of the paving operation due to AC cooling time. This schedule enabled hot-mix asphalt (HMA) delivery trucks to reach the discharging location without driving on the hot AC, eliminating material pickup by truck tires. On a few occasions the planned schedule did not provide enough time for placing the 75-mm (3 in.) PBA-6a* on the FDAC section; for these circumstances this layer was placed during the following weekend closure. The 25-mm (1 in.) RAC-O was placed during weekday nighttime closures, after completion of all weekend closures.

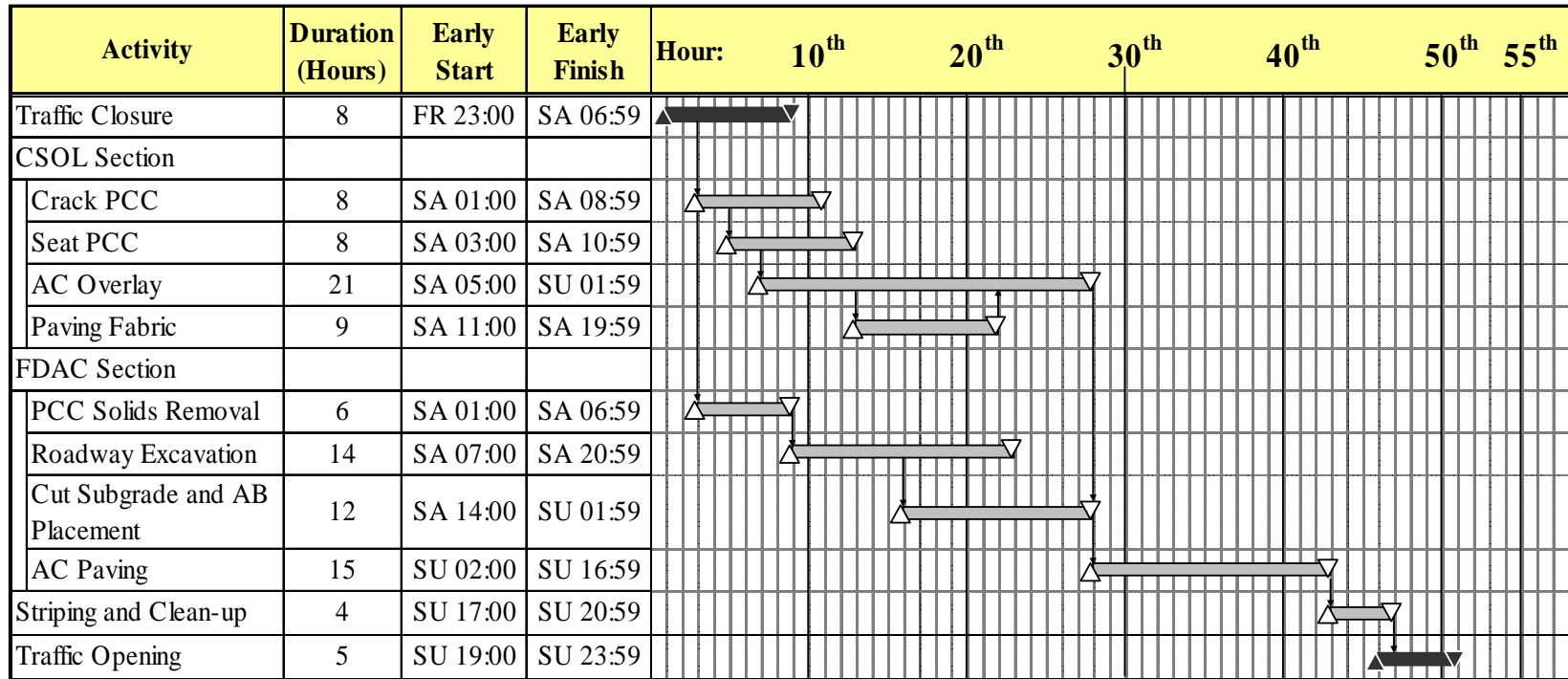


Figure 5.2: Typical CPM schedule for a 55-hour weekend closure (second weekend closure).

6 LESSONS LEARNED AT CONCLUSION OF CONSTRUCTION, FALL 2003

On November 4, 2003, a team consisting of Caltrans (T. Bressette, C. Suszko, W. Farnbach), Industry (J. St. Martin), and University (C.L. Monismith) members of the Flexible LLPRS Task Group, conducted post construction interviews with Caltrans staff for one-half day (morning) and Contractor and Materials Suppliers for one-half day (afternoon). The purpose of the interviews was to ascertain what went well with the project and what aspects should be considered for improvement on future projects of this type.

The following provides a brief summary of the results of the interviews, which included considerations of *design*, *construction*, and *traffic monitoring* as well as *other factors*. The results are presented in tabular form in terms of what went well and what required improvement (didn't go well) (Table 6.1). Responses from both Caltrans and Contractor staff are noted. As will be seen in this table, in some instances both groups noted the same point while other issues were noted either by Caltrans or Contractor staff.

A summary of general recommendations resulting from the interviews is listed in Table 6.2. All of these should be useful in planning for future projects of this type.

Relative to the construction planning, a software program called *CA4PRS*, developed by UCPRC staff with support of Caltrans, WSDOT, MNDOT, and TXDOT (27), assisted both the Caltrans staff and the Contractor in planning for the construction operations described in the previous section. The program was further calibrated by monitoring three of the eight weekend closures, and is now available for use on future projects.

Associated with this program is a traffic simulation program for assessing the impact of the closure on traffic operations in the network surrounding the project. Monitoring of traffic during the three weekend closures in which the *CA4PRS* program was being calibrated also permitted further refinements in this program (7).

Table 6.1: Lessons Learned

DESIGN		
What went well?	Caltrans	Contractor
1. Full-depth design utilized allowed construction completion within 55-hour closure.	X	
2. Structural section on cracked and seated PCC worked well.	X	
What didn't go well?		
1. Mix design verification by contractor using shear and fatigue tests.	X	X
2. Lack of exploratory testing in digout areas for FDAC sections prior to actual construction.	X	X
3. Insufficient thickness for AC working platform in sand subgrade (first weekend closure).	X	X
4. Different interpretations for the definition of the leveling course in the CSOL section.	X	X
5. Difference between as-designed and as-constructed existing pavement sections in the digout areas.		X
CONSTRUCTION		
What went well?	Caltrans	Contractor
1. Long-life pavement construction generally went well.	X	X
2. Contingency plan worked well (except for first weekend closure).	X	X
3. Different mixes presented no difficulties* * (RAC-O construction at night presented some difficulties in attaining required degree of compaction)	X	X
What didn't go well?		
1. Some mix segregation.	X	
2. Compaction problems with AC in confined areas (particularly in median due to narrow width).	X	X
3. QC/QA—dealing with large quantities of materials in short time frame.	X	X
4. Selection of AC target stability values (See Table 4.2)	X	
5. Subgrade preparation in digout area for first weekend	X	X
6. Timeliness of QA results.		X
7. Timeliness of subgrade compaction check by Caltrans personnel in digout areas.		X
8. Construction of RAC-O layer.	X	X
TRAFFIC MONITORING PLAN (TMP)		
What went well?	Caltrans	Contractor
1. TMP worked well, no major accidents; very little congestion.	X	X

Table 6.1 (continued)

What didn't go well?	Caltrans	Contractor
1. Insufficient clearance in lane next to moveable barrier. A few instances occurred in which vehicles hit barrier causing it to impinge a lane in opposite direction.	X	
2. Location of crossovers (contractor would have preferred to select these; believed that construction productivity could have been improved).		X
OTHER FACTORS		
What went well?	Caltrans	Contractor
1. Union concessions—permitted use of construction personnel from other contractors for 55-hour closures since added staff required for contingencies.		X
What didn't go well?	Caltrans	Contractor
1. Maintenance of existing pavement (already in poor condition) during winter shutdown—better planning required.	X	X
2. Pavement profile requirements too stringent.		X
3. Insufficient information on location of existing utilities, etc. under existing pavement in digout areas.		X

Table 6.2: General Recommendations

Recommendation/Action	Caltrans	Contractor
1. Mandatory attendance at pre-bid conference by prospective bidders.	X	X
2. Prequalification of contractors for this type of project	X	
3. 55-hour closure satisfactory for this type of rehabilitation.	X	X
4. Reasonable incentive/disincentive for reduced or extra number of weekend closures (in this case, less than or greater than 10); actual amount: \$100,000.	X	
5. Larger incentive required (contractor suggested \$150,000 to \$200,000 versus \$100,000 used for project).		X
6. Human resources were “stretched”; recommended number of weekend closures in succession of 3 to a maximum of 5 with 1 or 2 weekends in between.	X	X
7. Contractor should select closure locations.		X
8. RAC-O construction of the open-graded friction course should be done during 55-hour closure rather than at night.		X
9. Meteorologists important for contractor for weather forecasting for 55-hour closures.		X
10. Contingency planning extremely important, in this case, aggregate supply for working platform was locally available.		X

In addition to the “lessons learned” discussed in Table 6.1, two additional points should be noted. The first is the matter of “partnering.” In this instance, new technology (SHRP-developed) was used for mix evaluation. Had there been partnering on a technical level at the outset of the project between Caltrans staff, the Contractor, and members of the LLPRS Flexible Pavement Task Group, Item 1 of “What didn’t go well?” in the Design portion of Table 6.1 might have been minimized. Thus an important conclusion from this experience is that technical “partnering” at the outset of a project of this type is mandatory.

The second point is related to the matter of the establishment of criteria like those shown in Table 4.1. These criteria required the performance of new tests for which there is little precision and bias information. Thus, when establishing new criteria of this type, consideration must be given to requirements based on the best available statistical information related to the test procedures utilized. Such information would also assist in mitigating the problem referred to in the previous paragraph. This was done for Stage 2; as seen in Appendix F.

7 FOLLOW-UP INVESTIGATIONS

In order to track the performance of the pavement sections, a plan for heavy weight deflectometer (HWD) testing was instituted. Testing was carried out at approximately yearly intervals for a period of five years. Other postconstruction activities have included in-situ sampling from a few sections of the pavement for specimens to perform beam fatigue and RSST-CH tests for comparison with initial design test results. (Results of these tests are included in Appendix H.) In addition, ride quality was measured on two occasions: April 2006 and January 2009. The January 2009 measurements were conducted on both the Phase 1 Rehabilitation and the section from I-405 to I-10. Skid measurements were also performed in February 2006.

Results of the HWD tests and their interpretations are summarized in this section. In addition, results of the RSST-CH shear and flexural fatigue testing are summarized and compared to the initial mix test results described earlier in Section 3. Also included is a summary of ride quality, as measured by International Roughness Index (IRI). Skid measurements were conducted in both directions; a brief summary of the test results is included.

7.1 HWD Test Results

The schedule for the HWD tests throughout the five-plus years after construction was as follows: (1) November 2003; (2) September 2004; (3) September 2005; (4) December 2005, northbound; February 2006, southbound; (5) September 2007, Lanes 2 and 3 only; and (6) September 2008. The schematic for testing all three lanes is shown in Figure 7.1

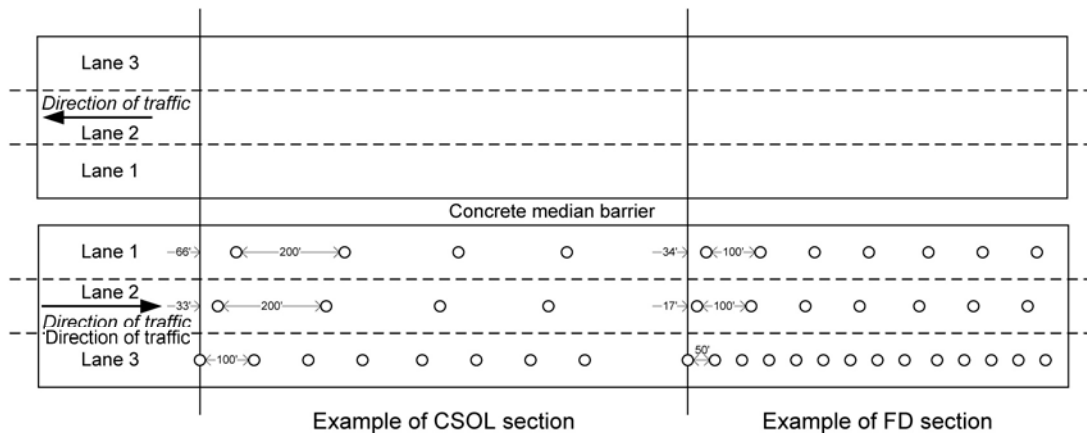


Figure 7.1: Deflection testing patterns for crack, seat, and overlay (CSOL) and full-depth asphalt concrete sections.

The layout of the project (Figure 2.1) and the sequence of construction (Figure 5.1) were used to establish the HWD test sections, labeled 1 through 5, beginning at the Pacific Coast Highway (PCH). Section numbers increase in the northbound direction (i.e., to the I-405 Freeway). Sections 1, 3, and 5 are the full-

depth HMA sections, and Sections 2 and 4 are the HMA overlay pavements on the cracked-and-sealed PCC. This resulted in a total of 10 sections, five northbound and five southbound.

HWD tests were conducted in the outer wheelpath of each of the lanes (except for the September 2007 test program). Testing was normally accomplished between the hours of 9 P.M. and 7 A.M. Three load level were applied at each point; target values were 40, 80, and 120 kN (9, 18 and 27 kips). Measured deflections and backcalculated moduli have been used to illustrate pavement response over the five years of trafficking. The backcalculation program used to determine the stiffness moduli of the individual layers in each of the sections is termed *CalBack*, which was developed by Dr. Per Ullidtz of Dynatest, Inc. (a UCPRC research partner in the Caltrans-supported program).

Deflections from the 120-kN load measured in Lane 3 in both the south- and north-bound directions are shown in Figure 7.2 and Figure 7.3, respectively for the five-year period.

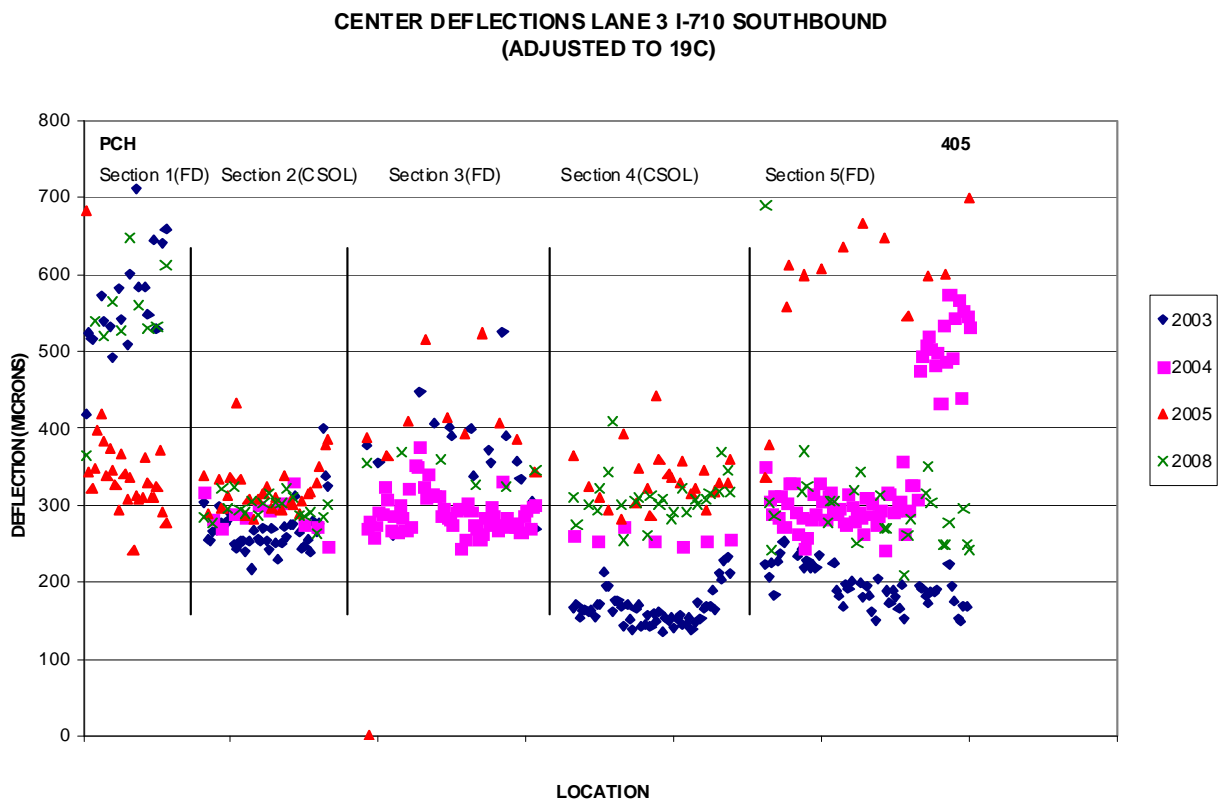


Figure 7.2: Deflections, Lane 3 Southbound, 2003 to 2008, 19°C.

It will be noted that deflections are highest in Section 1 southbound, the first section constructed. The 6-in. granular base and engineering fabric were not used although they had been called for to insure that the rich bottom AC layer would have a good working platform to achieve the requisite degree of compaction.

Instead, a layer of AC approximately 2 in. thick was placed directly on the sand subgrade, but it was not sufficient to permit proper compaction of the rich bottom layer.

**CENTER DEFLECTIONS LANE 3 I-710 NORTHBOUND
(ADJUSTED TO 19C)**

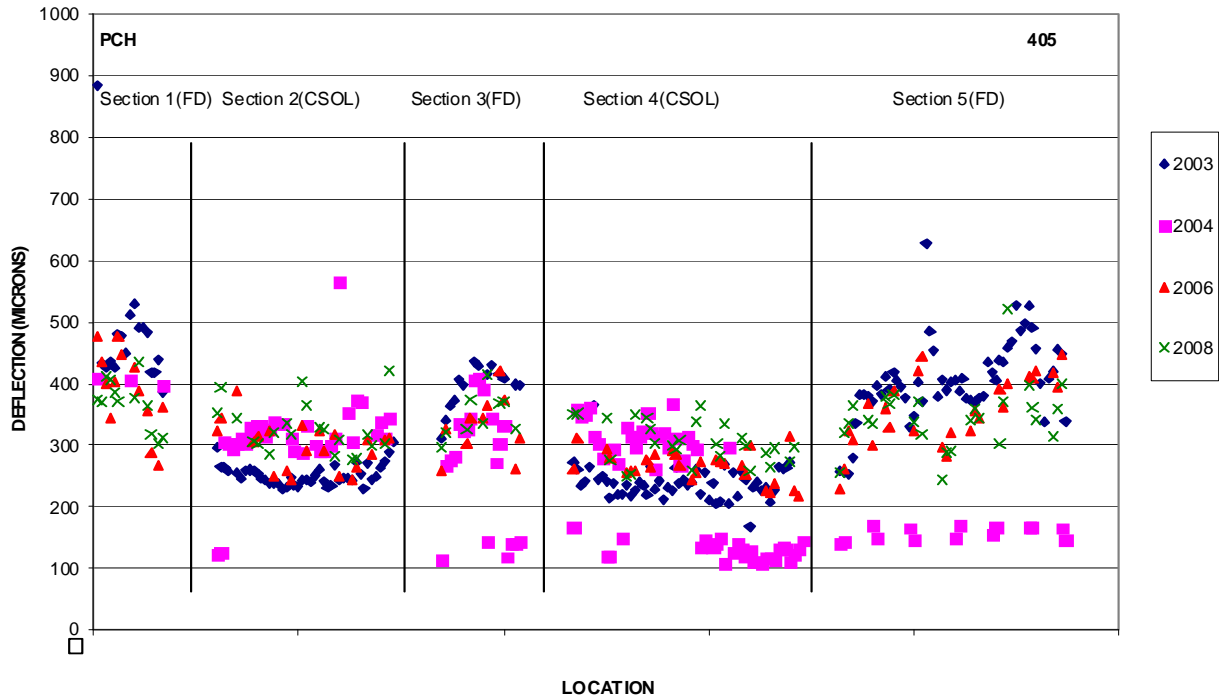


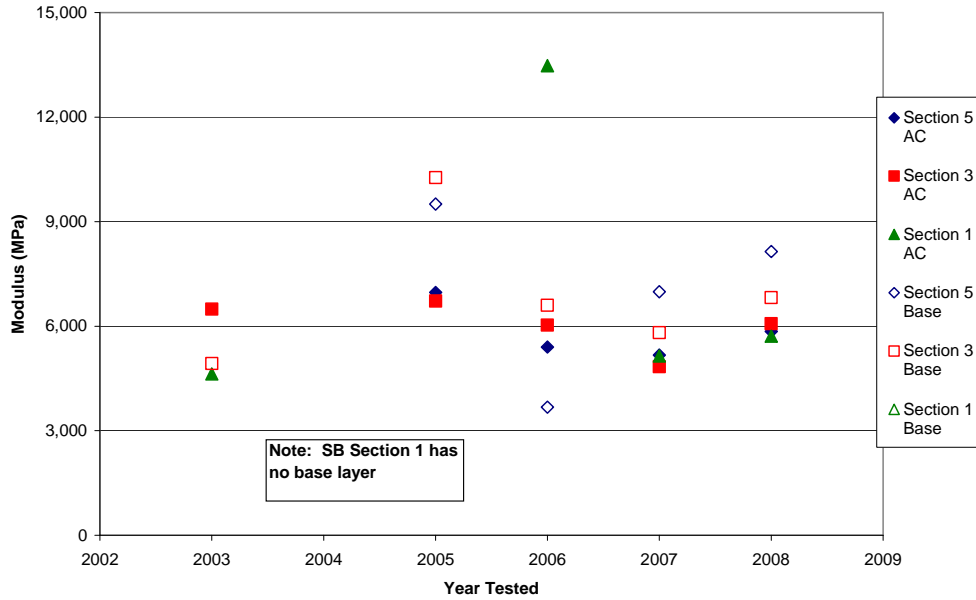
Figure 7.3: Deflections, Lane 3 Northbound, 2003 to 2008, 19°C.

In both figures it will be noted that deflections in the cracked-and-sealed sections are less than those in the full-depth AC sections. It will also be noted that the deflections measured in 2008 are in the same range as those measured in earlier years. Comparisons of the deflections for the corresponding north- and southbound sections, other than Section 1 southbound, are observed to be similar.

A summary of deflections for Lane 1 in both northbound and southbound directions is included in Appendix H. While deflections were measured in Lane 2, these data have not been plotted; however the raw data are available in the UCPRC database maintained at the UCPRC Berkeley Offices located at the Richmond Field Station.

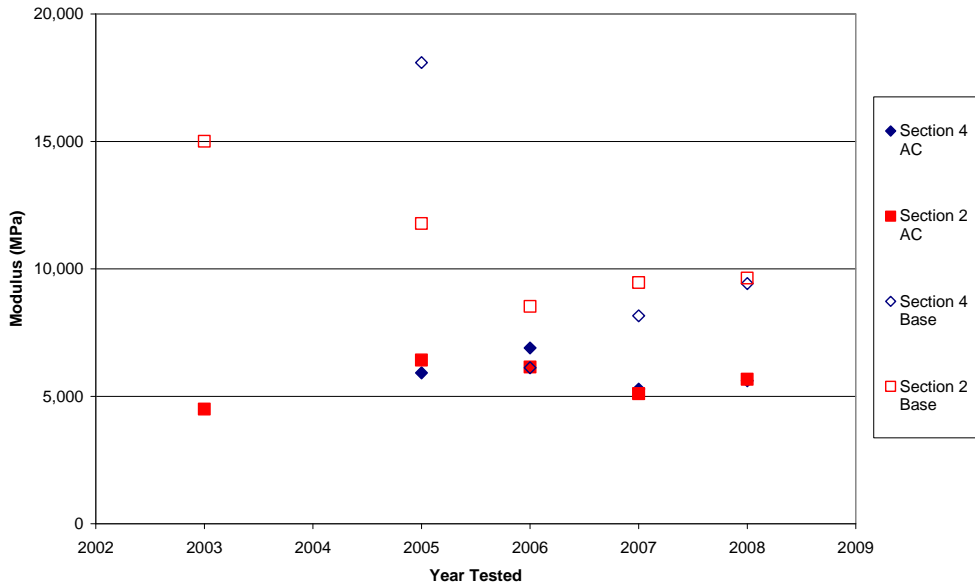
A comparison of the deflections for the 40, 80, and 120 kN loads indicated a linear relationship between load and deflection. Accordingly the measured deflections for the 120kN load were used for the backcalculation of layer moduli. Results of these moduli calculations for each yearly set of measurements are included in Appendix H. Computed moduli based on the 2008 deflection data for AC and base for Lane 3 southbound and northbound are shown in Figure 7.4 and Figure 7.5.

I-710 Southbound Lane 3 Full Depth Sections - Layer Moduli with Time



a. Full-depth sections

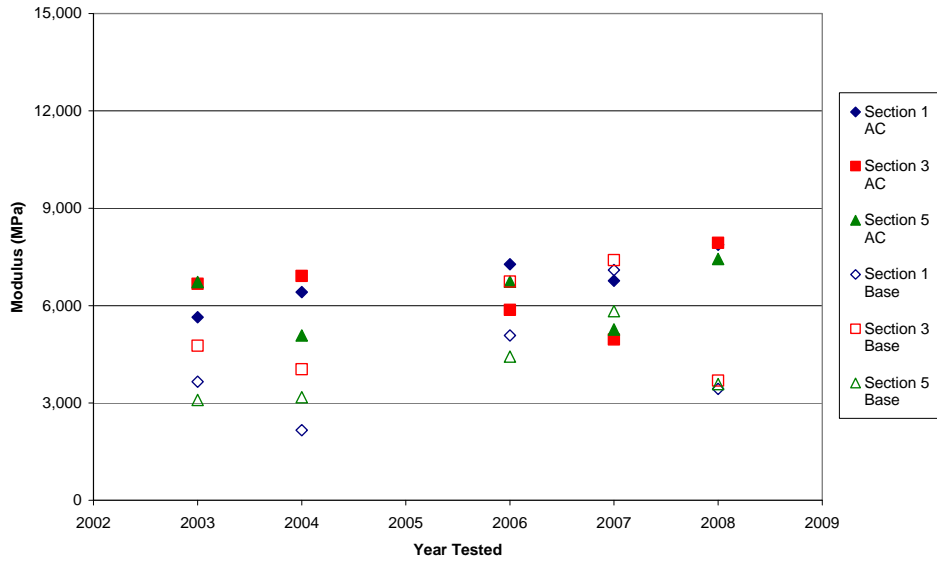
I-710 Southbound Lane 3 CSOL Sections - Layer Moduli with Time



b. Crack, seat, and overlay sections

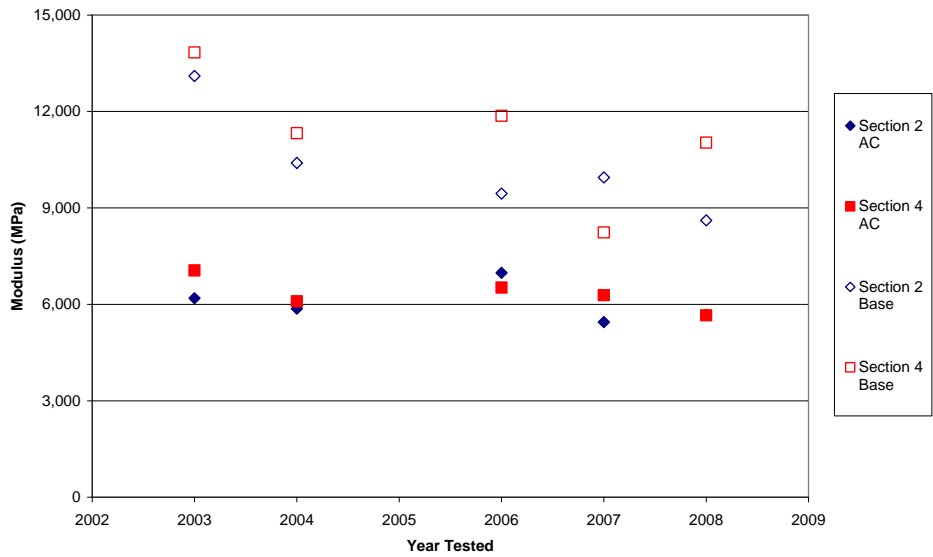
Figure 7.4: Southbound Lane 3 layer moduli versus time.

I-710 Northbound Lane 3 Full Depth Sections - Layer Moduli with Time



a. Full-depth sections

I-710 Northbound Lane 3 CSOL Sections - Layer Moduli with Time



b. Crack, seat and overlay sections

Figure 7.5: Northbound Lane 3 layer moduli versus time.

It can be seen in Figure 7.4 and Figure 7.5 that the back-calculated moduli for the AC layers are reasonably uniform in both the southbound and northbound directions. For the three full-depth sections, the computed moduli average is approximately 7,500 MPa northbound and 6,000 MPa southbound. For the four (two in each direction) crack, seat, and overlay sections the computed moduli average about 5,600 MPa. This difference in stiffness between the moduli of the crack, seat and overlay and full-depth sections is reasonable. Referring to Figure 3.7, it will be noted that the flexural stiffness of the PBA-6a* mix is about one-sixth of the stiffness AR-8000 mix. The full-depth sections have 9 in. of the AR-8000 mix and 3 in. of the PBA-6a* mix, whereas the crack, seat, and overlay sections have 5 in. of the AR-8000 mix and 3 in. of the PBA-6a* mix. The difference in stiffnesses between the northbound and southbound full-depth sections could result, in part, from the backcalculation procedure.

Computed subgrade stiffness moduli range from 100 to 150 MPa as seen in Appendix H1. The aggregate base for the full-depth sections consisted of crushed concrete. Computed stiffness moduli were in the range 3,000 to 7,000 MPa. These values are larger than normally associated with untreated aggregate base suggesting some cementing in this material.¹⁰

To estimate the pavement performance of Lane 3, both northbound and southbound, for the full-depth sections, multilayer elastic analyses were performed. Backcalculated layer moduli for the 2008 HWD tests summarized in Appendix H, Table H1 were used. Results of these analyses are included in Appendix H, Table H2. Selected measures of performance parameters from this appendix are summarized in Table 7.1.

Table 7.1: Tensile and Vertical Compressive Strains in Full-Depth Sections

Section	Northbound		Southbound	
	Tensile strain, $\epsilon_t \times 10^{-6}$	Vertical compressive subgrade strain, $e_v \times 10^{-6}$	Tensile strain, $\epsilon_t \times 10^{-6}$	Vertical compressive subgrade strain, $e_v \times 10^{-6}$
1	18	80	49	151
3	17	78	11	82
5	16	72	8.4	73

It will be noted that the strains are low, suggesting little damage from fatigue cracking and minimal contributions to permanent deformation from the untreated components of the full-depth sections in these sections at this time. However, the results in Table 7.1 do illustrate a difference between southbound

¹⁰ At the time of this report a separate analysis to examine this phenomenon in more detail is underway and will be reported in a separate technical memorandum.

Section 1 and the five other full-depth sections because of the absence of the untreated aggregate base in this section.

7.2 Laboratory Tests on Field-Mixed, Field-Compacted Test Specimens

Following construction, cores and slabs were obtained from the pavement at various locations. A few cores were taken from Lanes 1 and 3 in June 2003 near the end of construction of the last section, Stage 6A (Figure 5.1). These cores were obtained in the traffic lanes in the northbound direction near Stations 131-133, (CSOL section). Subsequently, additional cores were obtained from shoulder areas and a traffic lane in November 2003. These included cores from the northbound median shoulder (near Station 111) and northbound right shoulder (near Stations 127 and 151); also from southbound Lane 1 (near Station 111). In January 2005 slabs were obtained from the outside shoulder areas in the full-depth section under Willow St. These slabs were used to obtain flexural fatigue test specimens. Results of the fatigue tests on these specimens, included in Appendix H, Table H4, are discussed below.

To arrive at the fatigue lives shown in Appendix H, Table H4, three stage Weibull distributions were used to interpret the test data. The Weibull plots for the tests on the rich bottom AR-8000 mix (AR-8000RB) are shown in Figure 7.6. Appendix F contains an analysis that was developed to establish minimum specification requirements for the fatigue and shear laboratory test data. For the fatigue test data, bounds in terms of numbers of repetitions were established for the 95 percent confidence levels. Figures 7.7a, b, and c contain plots of the fatigue test data for the three mix types (AR-8000RB, AR-8000, and PBA-6a*) together with the curve showing the lower bound of the 95 percent confidence level for repetitions.

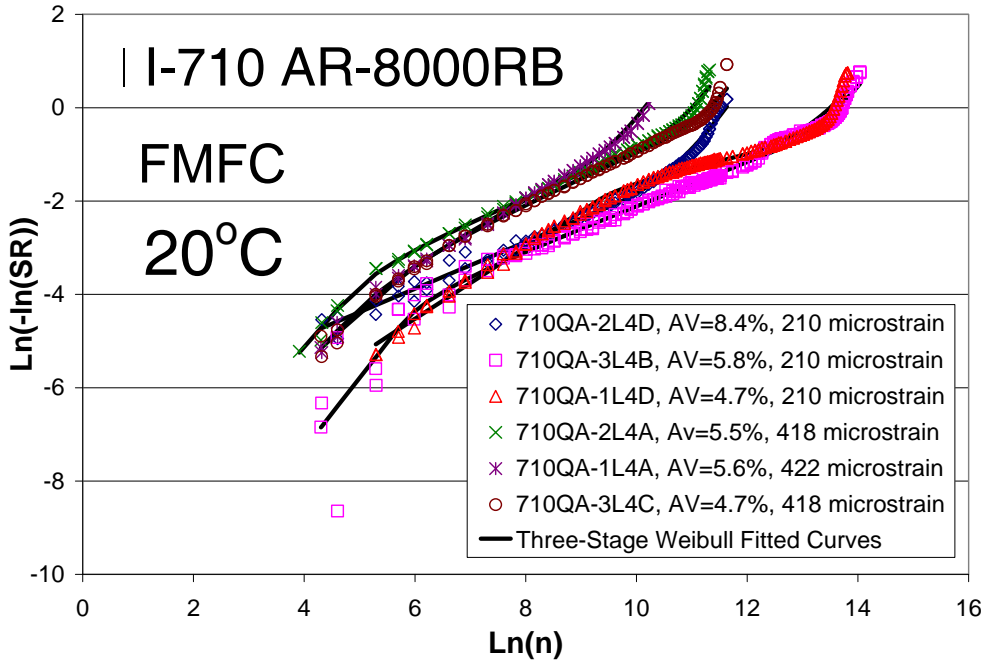
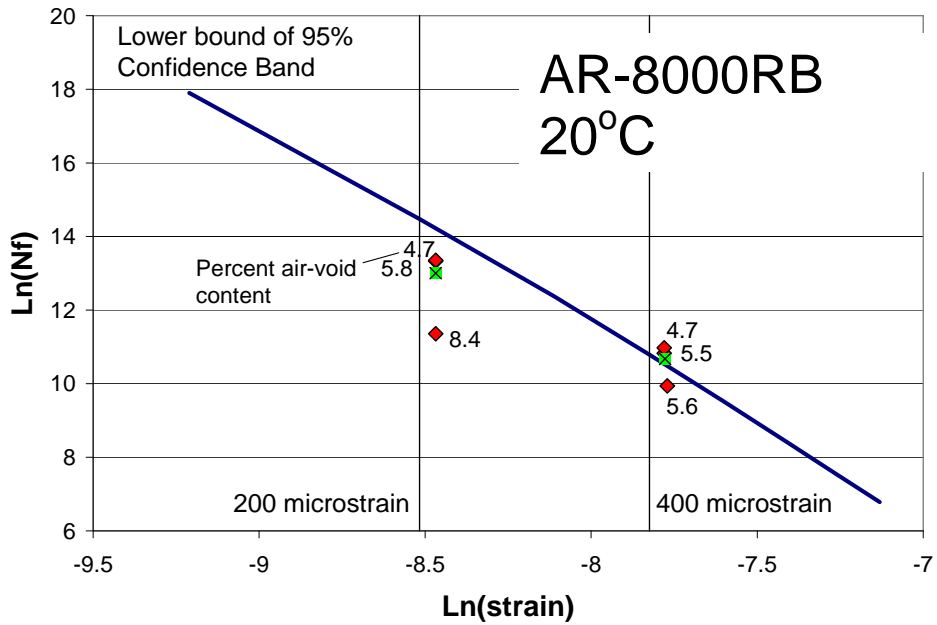
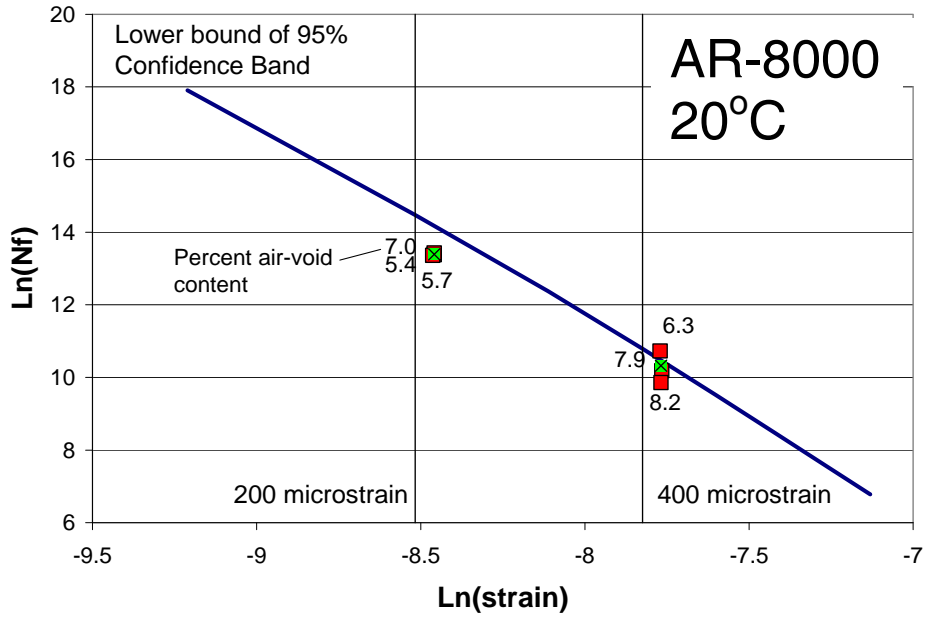


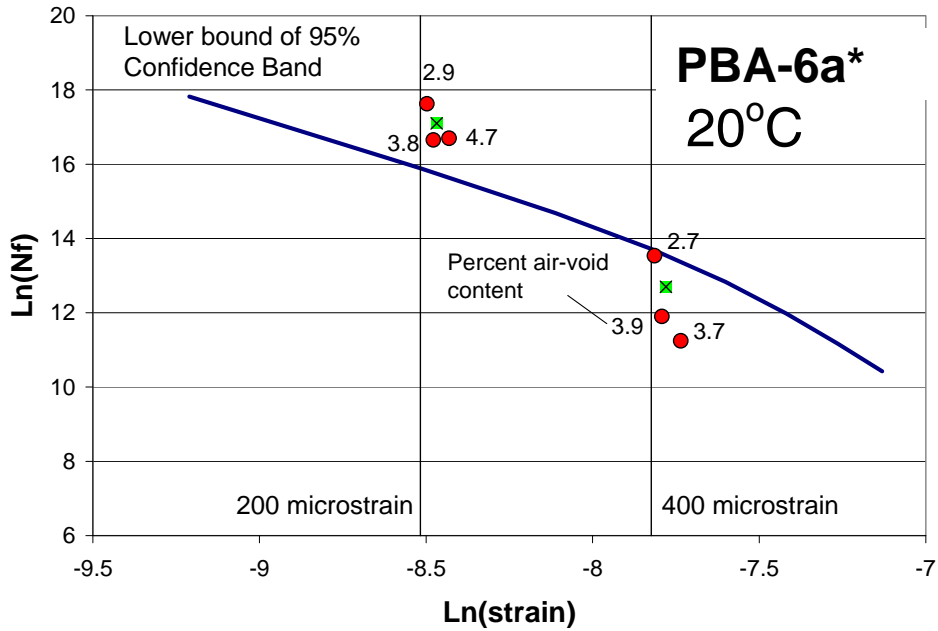
Figure 7.6: Weibull curves for the rich bottom AR-8000 mix.



a. AR-8000RB mix



b. AR-8000 mix



c. PBA-6a* mix

Figure 7.7: Field-mixed, field-compacted (FMFC) test data with the lower bounds of the 95 percent confidence bands based on the pooled data contained in Appendix F (Tables F5 and F8 [pooled data]). Field-mixed, field-compacted (FMFC) test data with the lower bounds of the 95 percent confidence bands based on the pooled data contained in Appendix F (Tables F5 and F8 [pooled data]).

Average air-void contents for the three mixes are 5.8 percent for the AR-8000RB mix, 6.8 percent for the AR-8000 mix, and 3.6 percent for the PBA-6a* mix. It will be noted that the mix compaction requirements for the AR-8000RB mix (3 percent maximum) are not met. Since this material was sampled from the shoulder section it may not have received the same compaction effort as the material in Lanes 1, 2, and 3.

Thickness measurements were obtained for the cores obtained in the November 2003 samples. Average thicknesses are shown in Figure 7.8. The measured data are included in the UCPRC database.

The layers appear fairly uniform in thickness. From top to bottom the layers are: RAC-O mix (Pull 1); PBA-6a* mix (Pull 2); AR-8000 mix (Pulls 3 and 4); and, AR-8000RB mix (Pull 5); the measured values correspond reasonably well to the design thicknesses.

RSST-CH tests were performed on specimens from cores taken in June 2003 from the northbound traffic lanes in the area between Stations 131 and 133. These are shown in Table 7.2.

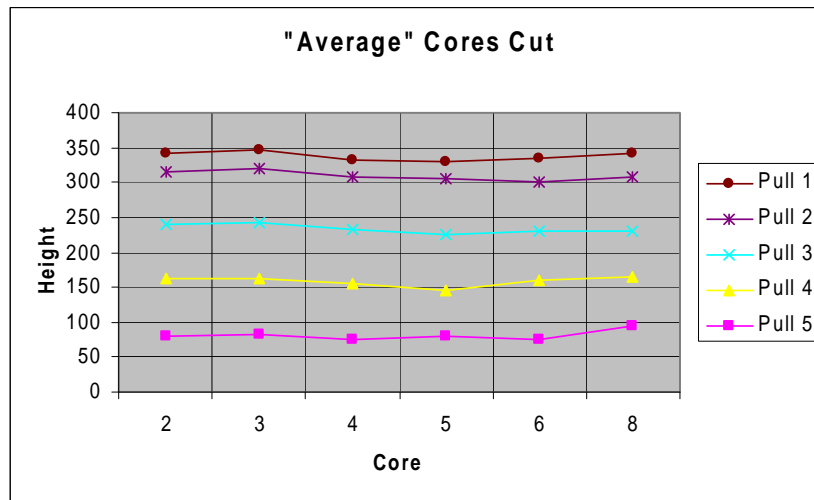


Figure 7.8: Average core thicknesses for cores obtained in November 2003.

Table 7.2: RSST-CH on Specimens from Cores Obtained in June 2003 from Northbound Lanes

Station	Mix Type	Core Number	Air-Void Content, percent	Repetitions to 5% Shear Strain	Shear Stiffness G* (MPa)
133	DGAC AR 8000	1B	5.8	51,600	127.3
		2B	2.7	430,000	110.5
		3B	4.2	107,000	128.4
		average		190,000	—
133	DGAC PBA 6a*	2A	5.5	75,400	31.5
3A		3.3	1,324,000	60.8	
131		5A	2.0	126,000	40.9
—		average		480,000	—

Appendix H, Table H.3 contains more detailed information on the shear test results.

7.3 Longitudinal Profile, Skid, and Noise Measurements

Longitudinal profile measurements were made in 2006 and 2009 and IRI values were determined. Skid measurements were obtained by Caltrans in 2006. Noise measurements were obtained in 2006 and 2008.

The longitudinal profile measurements in January 2009 were conducted by the UCPRC throughout the length of the I-710 freeway from the Pacific Coast Highway (SR 1) to the I-10 (Santa Monica) freeway, a distance of approximately 20 miles. Results of these measurements in terms of the International Roughness Index (IRI, in. per mi.) are shown in 7.9. The first approximately 2.7 miles are the rehabilitated section discussed herein with the asphalt rubber open-graded AC (RAC-O and now termed RHMA-O) wearing course while the remainder is predominantly jointed portland cement concrete. Table 7.3 provides overall average results by pavement type, lane, and direction.

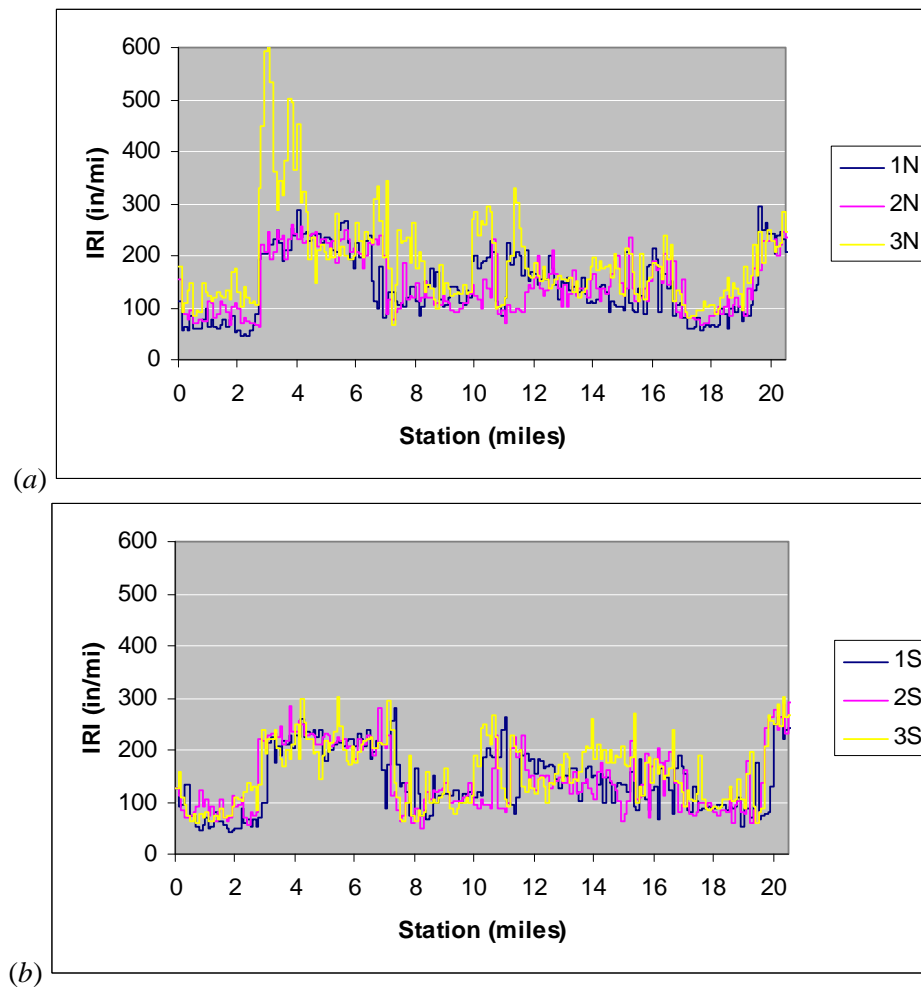


Figure 7.9: IRI on northbound (a) and southbound (b) lanes.

Table 7.3: IRI by Pavement Type and Direction

Pavement Type	Overall IRI	Station (mi.)	IRI (in./mi.)		
			Lane	Northbound	Southbound
RHMA-O	89	0.00 – 2.76	1	70	69
			2	90	86
			3	126	91
			average	96	82
PCC	163	2.76 – 20.5	1	155	151
			2	154	153
			3	199	166
			average	170	157

Skid measurements were performed by Caltrans in February 2006 using its skid test equipment. A summary of these skid data for the I-710 freeway from the Pacific Coast Highway to the I-10 freeway are included in the UCPRC database. The data for the Phase 1 rehabilitation have been summarized and an average skid number, SN₄₀, has been determined for each direction. The average values are: northbound, 47 (126 values), range 38 to 54; and, southbound, 49 (97 values), range 43 to 57.

Noise measurements were obtained in April 2006 and April 2008. These measurements were made by the UCPRC staff using a UCPRC vehicle equipped with an on-board sound intensity (OBSI) measuring device. These measurements were made as a part of another Caltrans/University of California Pavement Research Center (UCPRC) study concerned with pavement noise. Two sections of the I-710 freeway were included: One was in the Phase 1 rehabilitated pavement with the RAC-O pavement (two locations northbound, Post Miles 8.1 and 8.6; two locations southbound, Post Miles 8.7 and 7.9). The other was located in the PCC section north of the I-45 interchange (two locations northbound, Post Miles 11.4 and 16.2; two locations southbound, Post Miles 15.9 and 11.2). Results of these measurements made in April 2006 are summarized in Table 7.4.

Table 7.4: Sound Intensity Results, dBA

By Pavement Type				By Site & Lane		
Pavement Type	Average	Inner Lane	Outer Lane	Site	Inner Lane	Outer Lane
RAC-O	102.9	102.7	103.0	1	101.8	101.5
				2	103.2	103.2
				3	102.8	103.6
				4	103.1	103.8
PCC	107.2	107.1	107.3	5	107.1	106.2
				6	106.5	107.5
				7	106.7	107.9
				8	107.9	107.6

Spectral content for both pavement types are shown in Figure 7.10. It will be noted that above 800 KHz the PCC pavements exhibit higher sound intensity readings than the RHMA-G surfaces.

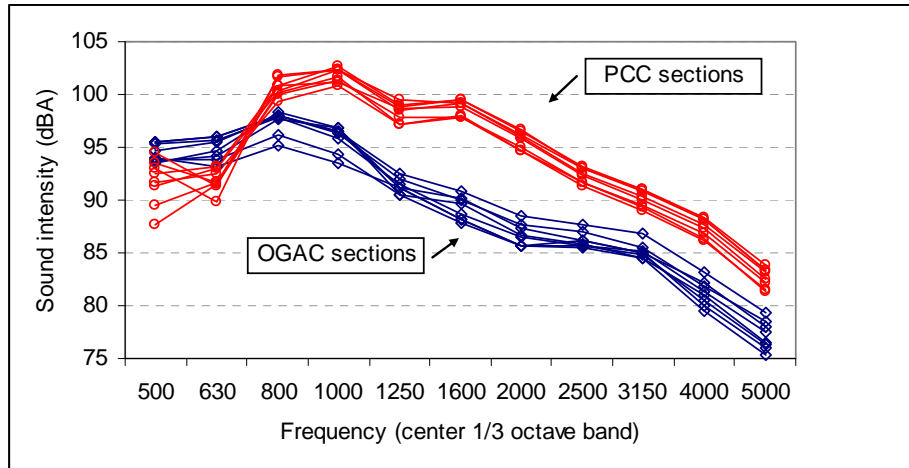


Figure 7.10: Spectral content at each pavement section.

Some differences in spectral content exist between the RHMA-O sections as seen in Figure 7.11. Sites 1 and 4 are the full-depth sections while Sites 2 and 3 are overlays on the cracked-and-seated PCC.

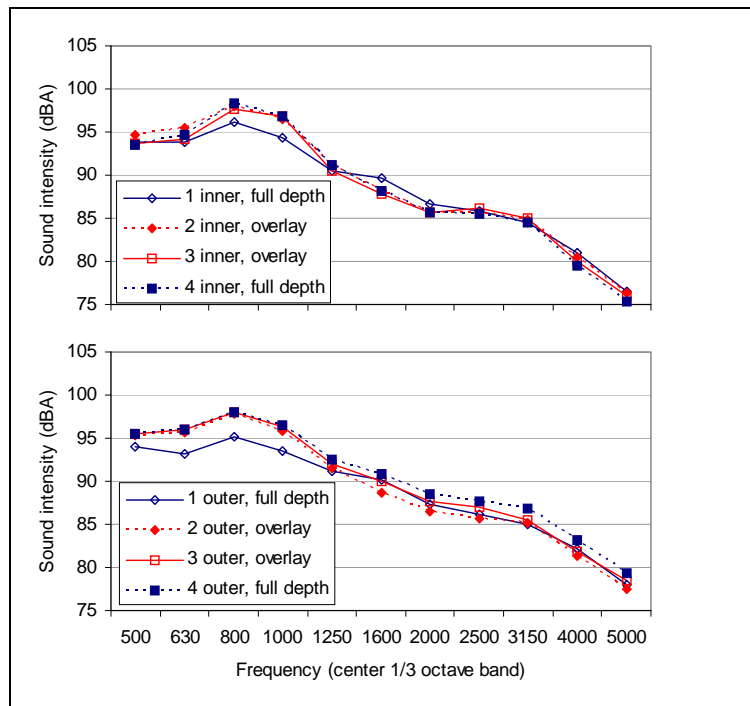


Figure 7.11: Spectral content at OGAC sections, inner and outer lanes.

7.4 Performance Analysis of the Phase 1 Rehabilitation Using *CalME*

In December 2008 an analysis was performed by Dr. R. Wu using the *CalME* design methodology under development for Caltrans. Dr. Wu's analysis, in summary form, is included in Appendix I. As will be seen in this appendix, based on the analyses using the backcalculated data included in Section 7.2, the section should sustain the 200 million ESALs for which both the full-depth and crack, seat, and overlay sections were designed.

8 SUMMARY

The I-710 Project provided an opportunity to implement approaches for asphalt concrete mix design and structural pavement design developed by UCPRC Staff during the Strategic Highway Research Program (SHRP).

The selected pavement section for the full-depth AC replacement structure consists of: (1) a rut-resistant surface course using a mix containing a 100 percent crushed aggregate and PBA-6a* modified binder for both rutting resistance and improved durability characteristics; (2) an asphalt concrete base course containing an AR-8000 asphalt that provides good stiffness characteristics for the structural section; (3) the same mix with 0.5 percent more asphalt—and termed a “rich-bottom mix”—to provide improved fatigue resistance in the lower part of the structural section; and, (4) an open-graded asphalt rubber porous friction course to provide splash, spray, and hydroplaning resistance and noise reduction as well as to serve as a protective layer for the PBA-6a* mix. It is anticipated that this surface course will be replaced during the design life of the structure.

The structural section thickness was selected using a procedure developed during the SHRP investigation and calibrated to California conditions using the HVS.

Mix designs for both the PBA-6a* and AR-8000 mixes were performed using the SHRP-developed simple shear test. The PBA-6a* mix was subjected to approximately 170,000 repetitions with the HVS at a pavement temperature controlled at 50°C (122°F) at a depth of 50 mm (2 in.). Results of the test suggest that the PBA-6a* mix should satisfactorily carry the anticipated traffic without excessive deformations.

The pavement structures for the cracked-and-sealed portion of the freeway followed Caltrans practice in that they consist of a leveling course placed on the PCC pavement, followed by the application of an asphalt-saturated fabric serving as a membrane interlayer and additional asphalt concrete and the porous friction course. Since the anticipated traffic is significantly greater than that on which current thicknesses are based (i.e., 200×10^6 versus approximately 20×10^6 ESALs), finite-element analyses were conducted for a range in the AC thicknesses. Based on these analyses, the overall thickness of the overlay was increased from about 150 mm (6 in.) to 225 mm (9 in.). The mixes used are the same as those for the full-depth AC replacement structure resulting in continuity of the mixes throughout the project.

Successful performance of the pavement structures requires strict attention to pavement construction, including careful control of the mix components during production and the degree of densification during compaction. Results of the QC/QA testing (not included herein) indicate that this objective was achieved.

The “lessons learned” from this project provide worthwhile information for both agency and contractor staff interested in this type of construction. The technique of “partnering” is extremely important to achieve the highest quality possible in the finished pavement structures.

High quality of the constructed pavement is essential to achieve performance for the longer time periods associated with this type of pavement rehabilitation.

The constructability software program *CA4PRS* served as a useful tool to both the Caltrans and Contractor staff in achieving the necessary goals associated with the 55-hour weekend closure. In this regard, it is interesting to note that the program can provide an indication of the maximum length of full-depth AC that can be placed in digout areas in the 55-hour closure. For this project, the maximum AC thickness for a three-lane freeway for a 300 m (1,000 ft.) length would be about 300 mm (20 in.), paving only in the traveled way. Similarly, for a four-lane freeway, the maximum thickness for the same length would be about 380 mm (15 in.)

Following completion of construction in June 2003, a five-year program was established to evaluate the performance of the pavement. This program included HWD measurements at approximately yearly intervals through fall 2008. In addition, some cores and slabs were obtained to assess in-situ mix behavior using performance tests that were used to establish mix designs and the thickness of both the full depth and overlays on the cracked-and-sealed PCC. Longitudinal profile measurements were made in January 2009 on both the rehabilitated sections (Pacific Coast Highway to I-405) and the remaining section (I-405 to I-10). Noise measurements using OBSI equipment were made in 2006 and 2008.

Moduli of the pavement layers were estimated and performance measures were calculated based on the HWD measurements. The same parameters as used for the original design suggest that the pavement sections are performing as expected. Visual condition surveys conducted in November 2008 indicated some areas of surface distress in the RAC-O surface course. However the satisfactory performance of the pavement to date was corroborated by Mr. Rob Marsh (Caltrans HQ Maintenance) in an e-mail to Dr. John Harvey in early February 2009. The excerpt from that e-mail stated:

In speaking with Leo Mahserelli (Division of Pavement Management, Regional Level) [concerning the 710 LL HMA pavement, it's clear that there is no widespread deterioration which would constitute a failure for the project. D7 Maintenance Engineering South Region Engineer, Shay Banduk, sent his assessment and photographs of localized distress, small patches, isolated ravelling and some mechanical damage/gouges but no deterioration which would spell pavement failure. The rehabilitation of the ramps throughout the project were deleted from the project (costs?) and they do look worn, rough and crack sealed/damaged.

However, with no record of exceptional workload or work expenditures from this pavement, and visual inspection by our very experienced pavement reviewer as well as the Region engineer, it would seem to be a case of mistaken reporting of a pavement failure.

The objective evaluation of pavement condition since construction is our PCS which, as I stated Thursday, reported only light raveling (it is 8 years old) and good to fair IRI numbers.

From the results reported herein thus far, considering the strains determined from the backcalculation procedure as well the condition surveys, the information would appear to validate the approach adopted by the LLPRS Flexible Pavement Task Group for this project.

In conclusion, it must be emphasized that the process used to arrive at the designs as well as the construction requirements was a “partnered” effort between Caltrans, the Asphalt Industry in California, and academia through UC Berkeley. This partnering provided an excellent opportunity to successfully implement new ideas and research results on this challenging project in which some traditional approaches were insufficient. It is hoped that such partnership can continue in the future.

9 REFERENCES

1. Sousa, J. B., J. A. Deacon, S. Weissman, J. T. Harvey, C. L. Monismith, R. B. Leahy, G. Paulsen, and J. S. Coplantz, *Permanent Deformation Response of Asphalt-Aggregate Mixes*, Report No. SHRP-A-415, Strategic Highway Research Program, National Research Council, Washington, D. C., 1994.
2. Tayebali, A. A., et al. *Fatigue Response of Asphalt-Aggregate Mixes*. Report no. SHRP-A-404. Strategic Highway Research Program, National Research Council, Washington, D. C., 1994, 309 pp.
3. Deacon, J. A., J. S. Coplantz, A. A. Tayebali, and C. L. Monismith. "Temperature Considerations in Asphalt Aggregate Mixture Analysis and Design." *Research Record 1454*. Transportation Research Board, Washington, D. C., 1994, pp. 97-112.
4. Harvey, J. T., J. A. Deacon, B. W. Tsai, C. L. Monismith. *Fatigue Performance of Asphalt Concrete Mixes and Its Relationship to Asphalt Concrete Pavement Performance in California*. University of California, Berkeley, Institute of Transportation Studies, Asphalt Research Program, CAL/APT Program, 1995, 188 pp.
5. Harvey, J. T., J. A. Deacon, A. A. Tayebali, R. B. Leahy, C. L. Monismith. "A Reliability-Based Mix Design and Analysis System for Mitigating Fatigue Distress," *Proceedings, Vol. 1., Eighth International Conference on Asphalt Pavements*, Seattle, August 1997, pp. 301-324.
6. California Department of Transportation. "Special Provisions for Construction on State Highway in Los Angeles County in Long Beach from Route 1 to Route 405/710 Separation," District 08, Route 710, Contract No. 07-1384U.4, October 2000.
7. Lee, E.B., H. Lee, and J. T. Harvey. *Fast-Track Urban Freeway Rehabilitation with 55-hour Weekend Closures: I-710 Long Beach Case Study*. Report to California Department of Transportation (Caltrans) and NAPA, Pavement Research Center, University of California Berkeley and David, December 2003, 25 pp.
8. Heukelom, W. "An Improved Method of Characterizing Asphaltic Bitumens With the Aid of Their Mechanical Properties," *Proceedings*, Association of Asphalt Paving Technologists, Vol. 42, 1973, pp. 67-98.
9. The Asphalt Institute. *Superpave Mix Design*. SP-2, Lexington, KY, 1996.
10. State of California Department of Transportation, "California Test Method Nos. 302, 304, 305, 306, 307, 308, 366, 367," *Materials Manual*, Vol. II, Sacramento, California, latest edition.
11. Vallerga, B. A. and E. Zube. "An Investigation of Design Methods for Asphaltic Paving Mixtures," *Proceedings*, ASTM Vol. 53, 1953, pp. 1079-1102
12. Vallerga, B. A., A. A. Tayebali, and C. L. Monismith. "Early Rutting of Asphalt Concrete Pavement Under Heavy Axle Loads in Hot Desert Environment: Case History," *Transportation Research Record No. 1473*, Transportation Research Board, Washington, D.C., 1995, pp. 25-34.
13. Monismith, C. L., J. T. Harvey, I. Guada, F. Long, and B. A. Vallerga, *Asphalt Mix Studies San Francisco International Airport*, Pavement Research Center, University of California, Berkeley, June 1999

14. Desert Mix: Specification No.: XE “39-010_A09-16-99” 39-010 (Dist_8)-09-01.doc, Caltrans District 8.
15. Harvey, J. T., B. A. Vallerga, and C. L. Monismith. “Mix Design Methodology for a Warrantied Pavement: Case Study,” *Transportation Research Record No. 1492*, Transportation Research Board, Washington, D.C., 1995, pp. 184-192.
16. Shell International Petroleum Company Ltd. *Shell Pavement Design Manual*. London, 1978.
17. Harvey, J. T., J. Roesler, N. F. Coetzee, and C. L. Monismith. *Caltrans Accelerated Pavement Test Program, Summary Report Six Year Period: 1994-2000*. Prepared for California Department of Transportation, Pavement Research Center, University of California, Berkeley, June 2000. 112pp.
18. Monismith, C. L. and F. Long. “Mix Design Analysis and Structural Design for Interstate Route 710.” *Technical Memorandum No. TM-UCB-PRC-99-2*, prepared for Long Life Pavement Task Force. June 1999.
19. Monismith, C. L. and F. Long. “Overlay Design for Cracked and Seated Portland Cement Concrete (PCC) Pavement—Interstate Route 710,” *Technical Memorandum No. TM-UCB-PRC-99-3*, prepared for Long Life Pavement Task Force. September 1999, 33 pp
20. Wardle, L., *Program CIRCLY, User’s Manual*, Revision 1, Geomechanics Computer Program Number 2, Division of Applied Geomechanics, Commonwealth Scientific and Industrial Research Organization, Melbourne, Australia, 1976.
21. The Asphalt Institute. *Research and Development of the Asphalt Institute’s Thickness Design Manual (MS-1), Ninth Edition*. Research Report No. 82-2. College Park, MD. 1982, 204 pp.
22. Monismith, C. L., and D. B. McLean. “Structural Design Considerations.” *Proceedings*, Association of Asphalt Paving Technologists, Vol. 41, 1972, pp. 258–314.
23. Santucci, L. E. “Thickness Design Procedure for Asphalt and Emulsified Asphalt Mixes.” *Proceedings*, Fourth International Conference of the Structural Design of Asphalt Pavements, University of Michigan, August 1977, Vol. 1, pp.424–456.
24. Larson, G. and B. Dempsey. *ICM Software. Enhanced Integrated Climatic Model Version 2.0 (ICM)*. Urbana, Illinois: University of Illinois, 1997.
25. Hallquist, J. O. *NIKE 2D, An Implicit Finite-Deformation, Finite-Element Code for Analyzing the Static and Dynamic Response of Two-Dimensional Solids*. Department of Energy, Lawrence Livermore Laboratory, Livermore, CA. 1979. iv, 104 p. (For sale by the National Technical Information Service, Springfield, VA.)
26. California Department of Transportation. *Standard Specifications*. Sacramento, California. July 1999.
27. Lee, E. B., and C.W. Ibbs. *A Computer Simulation Model: Construction Analysis for Highway Rehabilitation Strategies (CA4PRS)*. *Journal of Construction Engineering and Management*, ASCE, Vol. 131, No. 4, 2005, pp. 449–458.

APPENDIX A: LABORATORY SHEAR AND FATIGUE TEST DATA

Table A.1: RSST-CH Test Data

Binder Type	Binder Content – percent (by weight of aggregate)	Test Temperatures						
		50°C (122°F)			60°C (140°F)			
		Air-void content – percent	N at $\gamma_p = 0.05$	G ^a MPa (psi)	Air-void content – percent	N at $\gamma_p = 0.05$	G ^a MPa (psi)	
AR-8000	4.2	4.8	3.48×10^4	76.9 (11.2×10^3)	5.0	4.00×10^3	39.6 (5.7×10^3)	
		4.7	6.67×10^4	71.7 (10.4×10^3)	4.8	3.06×10^3	35.2 (5.10×10^3)	
		–	–	–	4.4	11.8×10^3	34.9 (5.06×10^3)	
	4.7	4.8	1.50×10^5	90.7 (13.2×10^3)	–	–	–	
		3.4	0.89×10^5	71.0 (10.3×10^3)	4.5	2.82×10^4	43.9 (6.37×10^3)	
		2.5	2.78×10^5	84.4 (12.2×10^3)	3.3	1.41×10^4	37.5 (5.44×10^3)	
	5.2	2.7	1.78×10^4	73.1 (10.6×10^3)	2.9	1.58×10^3	34.3 (4.97×10^3)	
		2.9	1.06×10^4	57.8 (8.38×10^3)	3.2	6.31×10^3	37.4 (5.42×10^3)	
		3.4	4.43×10^4	58.3 (8.45×10^3)	–	–	–	
	PBA-6a*	4.2	4.9	0.93×10^5	31.0 (4.50×10^3)	4.4	6.14×10^4	26.9 (3.90×10^3)
			5.7	6.76×10^5	26.5 (3.84×10^3)	5.0	9.34×10^4	25.0 (3.63×10^3)
			6.0	1.17×10^5	26.7 (3.87×10^3)	5.1	4.98×10^4	27.0 (3.92×10^3)
6.3			2.06×10^5	25.0 (3.63×10^3)	6.2	7.00×10^4	20.9 (3.03×10^3)	
4.7		3.5	1.70×10^6	35.5 (5.12×10^3)	2.0	0.58×10^5	23.2 (3.36×10^3)	
		4.0	0.76×10^6	28.8 (4.18×10^3)	3.9	1.27×10^5	26.0 (3.77×10^3)	
5.2		2.4	3.06×10^5	25.1 (3.64×10^3)	4.1	0.63×10^5	23.6 (3.42×10^3)	
		4.2	3.80×10^5	24.8 (3.60×10^3)	4.5	4.10×10^5	28.8 (4.18×10^3)	
		6.7	1.38×10^5	25.7 (3.73×10^3)	–	–	–	
		6.9	0.78×10^5	29.0 (4.20×10^3)	–	–	–	

a. Air-void contents were determined using AASHTO T209 Method which uses parafilm rather than paraffin.

b. Measured at N = 100 repetitions.

Table A.2: Fatigue Test Data

Specimen	Binder	AV (%)	AC(%)	Temp. (C)	Test Strain	S0 (MPa)	Nf
P47F21CA	PBA6A	5.50	4.7	20.0	0.000254	1098	14546777
P47F13CA	PBA6A	5.67	4.7	20.0	0.000397	1405	1680627
P47F22CA	PBA6A	5.06	4.7	20.0	0.000397	813	1487722
P47F22CB	PBA6A	5.00	4.7	20.0	0.000694	721	1139038
P47F13CB	PBA6A	5.28	4.7	20.0	0.000696	1242	783517
P47F21CB	PBA6A	4.40	4.7	20.0	0.000701	770	595154
P52F21CA	PBA6A	2.87	5.2	20.0	0.000444	1117	22327512
P52F33CA	PBA6A	3.90	5.2	20.0	0.000399	1117	7615056
P52F32CB	PBA6A	3.43	5.2	20.0	0.000397	700	3695276
P52F33CB	PBA6A	3.60	5.2	20.0	0.000702	979	1499999
P52F32CA	PBA6A	2.87	5.2	20.0	0.000699	677	1486866
P47F32CA	PBA6A	6.50	4.7	9.7	0.000697	2903	284073
P47F31CA	PBA6A	5.12	4.7	9.7	0.000692	2835	669308
P47F33CA	PBA6A	5.06	4.7	9.8	0.000397	3269	21452327
P47F34CA	PBA6A	6.37	4.7	9.6	0.000399	2998	93151851
P47F35CB	PBA6A	6.61	4.7	24.4	0.000694	572	1008582
P47F33CB	PBA6A	5.18	4.7	24.7	0.000708	503	2873044
P47F36CA	PBA6A	5.80	4.7	25.4	0.000401	482	10527626
P47F31CB	PBA6A	5.33	4.7	30.0	0.000699	290	6337225
P47F32CB	PBA6A	6.27	4.7	29.9	0.000397	383	9691270
P47F34CB	PBA6A	5.79	4.7	30.0	0.000396	255	17196672
C47F2A	AR8000	5.99	4.7	20.0	0.000197	6684	2514516
C47F1A	AR8000	6.73	4.7	20.0	0.000248	6085	1286696
C47F2B	AR8000	5.35	4.7	20.0	0.000248	7279	656618
C47F3B	AR8000	4.95	4.7	20.0	0.000452	6072	65950
C47F3A	AR8000	4.50	4.7	20.0	0.000399	6660	52631
C47F1B	AR8000	6.14	4.7	20.0	0.000447	5451	12600
C52F1A	AR8000	3.60	5.2	20.0	0.000248	6319	4823471
C52F2A	AR8000	3.20	5.2	20.0	0.000248	7091	1939332
C52F3A	AR8000	3.00	5.2	20.0	0.000248	7933	1148394
C52F2B	AR8000	3.40	5.2	20.0	0.000449	6358	193685
C52F3B	AR8000	3.00	5.2	20.0	0.000451	5897	149999
C52F1B	AR8000	2.70	5.2	20.0	0.000446	7789	99549
AR11B	AR8000	3.14	4.7	19.7	0.000196	11841	334771000
AR17B	AR8000	3.04	4.7	20.0	0.000197	6310	3.47818E+011
AR27A	AR8000	2.98	4.7	20.0	0.000395	9327	120287
AR11A	AR8000	3.07	4.7	20.0	0.000395	10586	264833
AR15A	AR8000	2.96	4.7	20.1	0.000665	5734	26977
AR25A	AR8000	3.12	4.7	19.8	0.000426	9015	92847
AR12A	AR8000	2.96	4.7	20.2	0.000600	8489	13406
AR15B	AR8000	3.14	4.7	19.9	0.000193	9813	1707024000
AR32A	AR8000	3.71	4.7	19.9	0.000196	9993	3949978
AR31B	AR8000	3.37	4.7	20.1	0.000197	11545	3178281
AR05B	AR8000	3.64	4.7	20.2	0.000396	10770	22156
AR07A	AR8000	3.16	4.7	20.2	0.000394	10790	117543
AR24B	AR8000	3.87	4.7	20.6	0.000588	10643	14134
AR07B	AR8000	3.29	4.7	20.8	0.000583	10320	3619
AR20A	AR8000	3.67	4.7	20.5	0.000787	8861	5215
AR08B	AR8000	3.73	4.7	20.6	0.000786	9729	2706
AR49A	AR8000	3.79	4.7	29.6	0.000199	6268	36545630
AR06A	AR8000	3.72	4.7	29.5	0.000198	5829	331328500
AR25B	AR8000	3.19	4.7	29.5	0.000400	6032	301603
AR23A	AR8000	4.07	4.7	29.6	0.000398	5442	127997
AR26A	AR8000	4.10	4.7	29.6	0.000599	5190	56633
AR14A	AR8000	3.26	4.7	29.6	0.000598	4981	19435
AR04A	AR8000	3.28	4.7	29.4	0.000796	4315	5238
AR09A	AR8000	3.42	4.7	29.4	0.000798	4961	14616

APPENDIX B: INITIAL DESIGNS FOR FULL-DEPTH STRUCTURAL SECTIONS

Table B.1: Structural Section Designs

Total Pavement Thickness (mm)			Subgrade Modulus = 83 MPa (12,000 psi)			Subgrade Modulus = 55 MPa (8,000 psi)		
			Fatigue 200 million	Subgrade Strain 50 million	Critical Thickness	Fatigue 200 million	Subgrade Strain 50 million	Critical Thickness
COASTAL AR-4000	3" Rich bottom	6 %, 3 % *	260 (10.2")	315 (12.4")	315 (12.4")	280 (11.0")	345 (13.6")	345 (13.6")
		8 %, 5 %	310 (12.2")	355 (14.0")	355 (14.0")	335 (13.2")	385 (15.2")	385 (15.2")
	No Rich Bottom	6% 8%	345 (13.6") 405 (15.9")	345 (13.6") 385 (15.2")	345 (13.6") 405 (15.9")	365 (14.4") 430 (16.9")	375 (14.8") 420 (16.5")	375 (14.8") 430 (16.9")
VALLEY AR-4000	3" Rich bottom	6 %, 3 %	335 (13.2")	190 (7.5")	335 (13.2")	350 (13.8")	205 (8.1")	350 (13.8")
		8 %, 5 %	380 (15.0")	200 (7.9")	380 (15.0")	395 (15.6")	220 (8.7")	395 (15.6")
	No Rich Bottom	6% 8%	395 (15.6") 445 (17.5")	195 (7.7") 210 (8.3")	395 (15.6") 445 (17.5")	410 (16.1") 465 (18.3")	215 (8.5") 230 (9.1")	410 (16.1") 465 (18.3")
AR-8000	3" Rich bottom	6 %, 3 %	195 (7.7")	215 (8.5")	215 (8.5")	210 (8.3")	235 (9.3")	235 (9.3")
		8 %, 5 %	230 (9.1")	-	230 (9.1")	245 (9.6")	-	245 (9.6")
	No Rich Bottom	6% 8%	205 (8.1") 235 (9.3")	220 (8.7")	220 (8.7") 235 (9.3")	215 (8.5") 245 (9.6")	240 (9.4")	240 (9.4") 245 (9.6")
COMPOSITE	3" PBA-6A Surface, 3" Rich bottom	6 %, 3 %	240 (9.4")	260 (10.2")	260 (10.2")	250 (9.8")	280 (11.0")	280 (11.0")
		8 %, 5 %	270 (10.6")	-	270 (10.6")	285 (11.2")	-	285 (11.2")
	5" PBA-6A Surface, 3" Rich bottom	6 %, 3 % 8 %, 5 %	255 (10.0") 290 (11.4")	280 (11.0") -	280 (11.0") 290 (11.4")	270 (10.6") 280 (11.0")	305 (12.0") -	305 (12.0") 305 (12.0")
ASPHALT INSTITUTE	3" Rich bottom	4 %, 7%, 2 % ** 4 %, 7%, 2 %	370 (14.6")	-	370 (14.6")	400 (15.7")	-	400 (15.7")
		No Rich Bottom	4%, 7% 4%, 7%	510 (20.1")	-	510 (20.1")	535 (21.0")	-

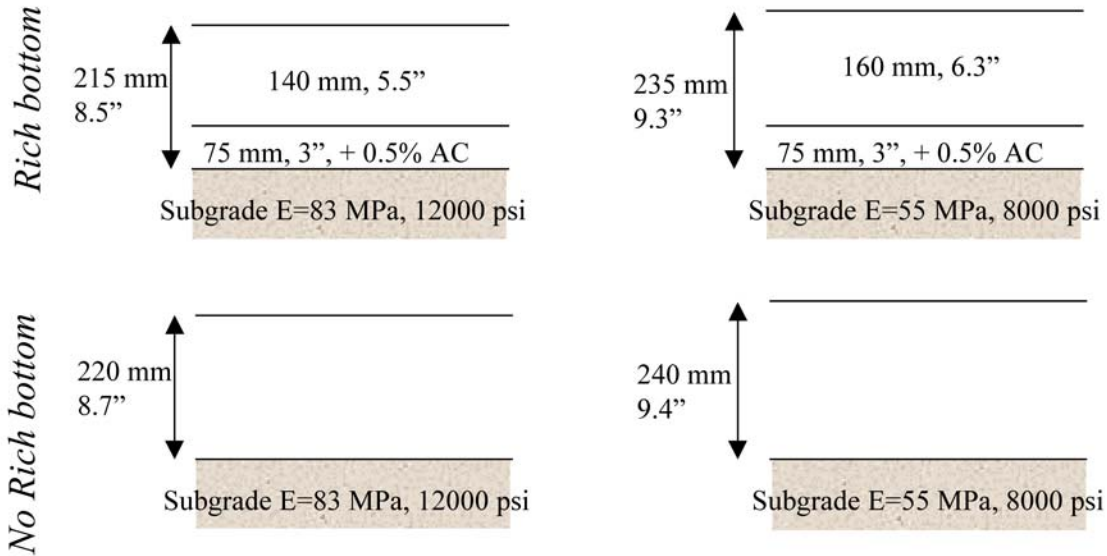
Notes:

* % voids in AC layer, % voids in Rich bottom layer

** Asphalt Institute designs have a 2 inch top layer (4% voids) and a middle layer (7% voids). The rich bottom layer, where applicable, has 2 % voids.

Thickness given is total pavement thickness

AR-8000



Composite

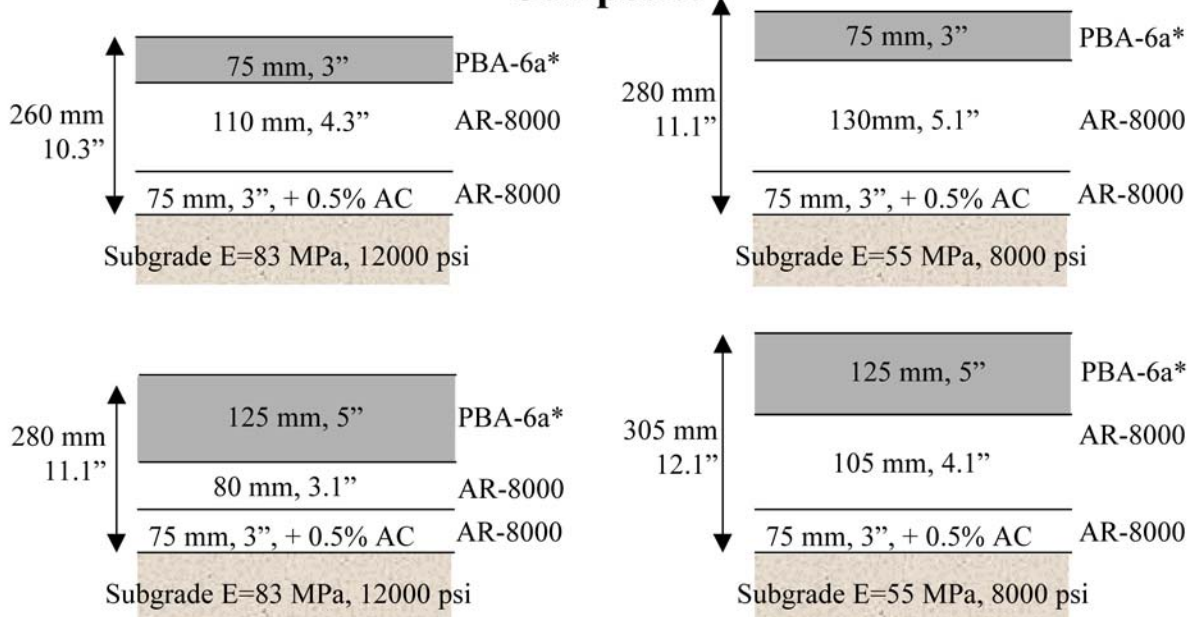


Figure B.1: Structural sections for AR-8000 and composite pavements (6 percent voids in AC layer and 3 percent in "rich bottom" layer).

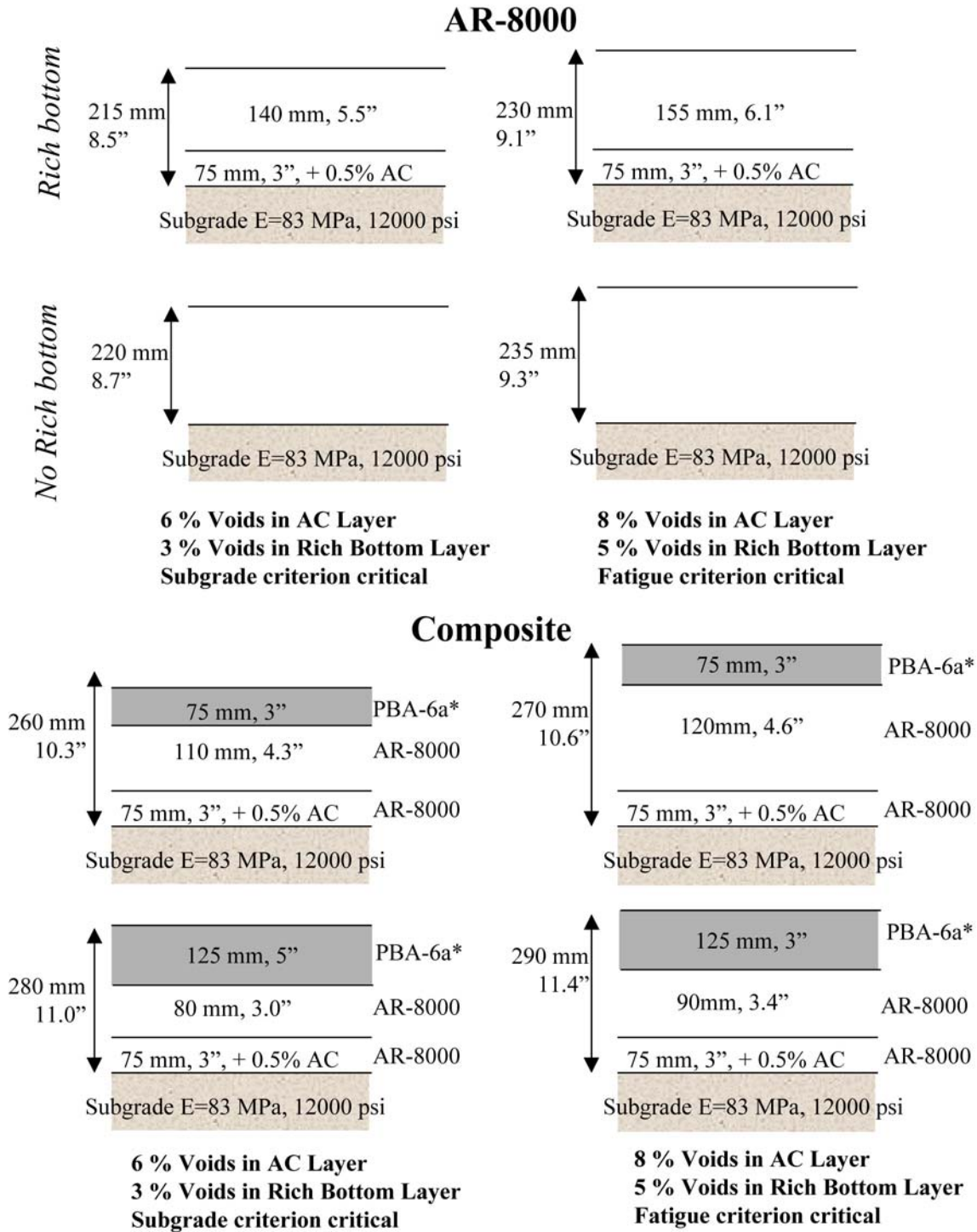


Figure B.2. Structural sections for AR-8000 and composite pavements with increase in air-void contents.

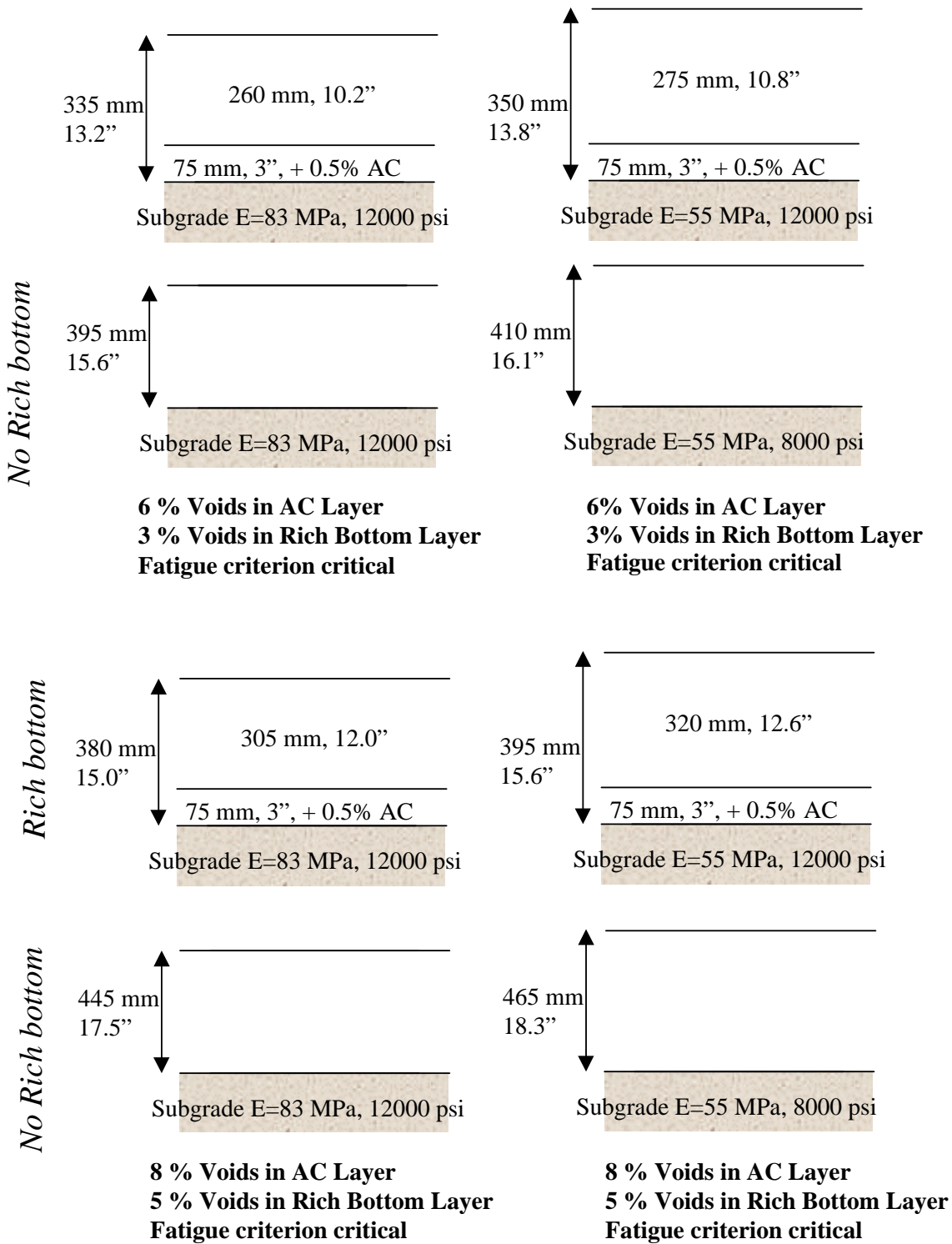


Figure B.3. Structural sections for mixes containing asphalt from the California Valley source with increasing air-void contents.

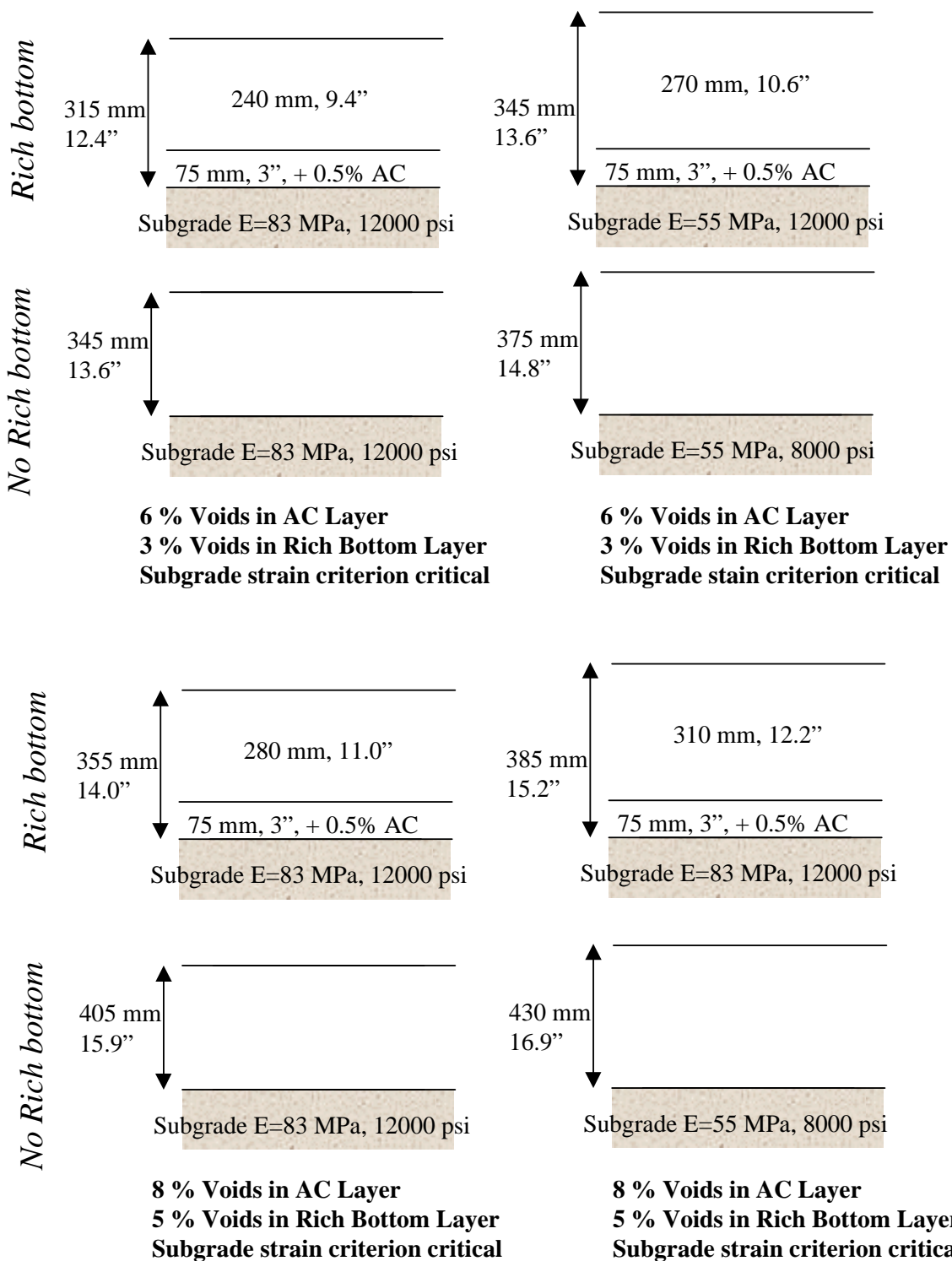


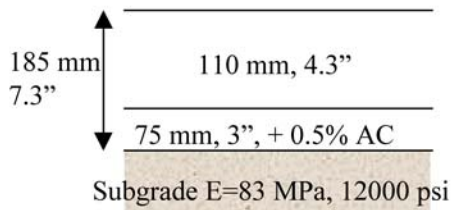
Figure B.4. Structural sections for mixes prepared with asphalt from the California Coastal sources with increasing air-void contents.

APPENDIX C: ANALYSES FOR STAGED CONSTRUCTION

Staged Construction

**Assume: 3" PBA surface layer placed 1 year after initial construction
(For 1 design alternative)**

In First Year



**6 % Voids in AC Layer
3 % Voids in Rich Bottom Layer
Fatigue criterion critical**

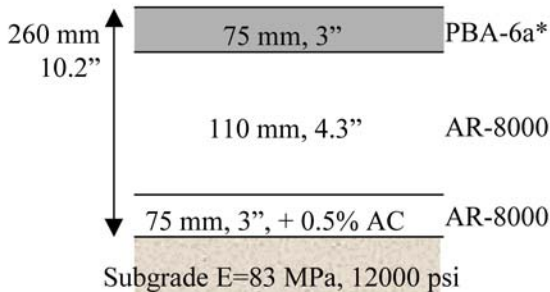
Traffic:

**6.667 million ESALs in first year
 $n_1 = 6.667$ million ESALs**

For this pavement:

**Fatigue Life $N_1 = 137$ million ESALs
Subgrade Strain, $N_1 = 18$ million ESALs**

Remaining Years



**6% Voids in PBA-6a* Layer
6 % Voids in AC Layer
3 % Voids in Rich Bottom Layer
Fatigue criterion critical**

Traffic:

**Fatigue:
(200-6.67) million ESALs in remaining years
 $n_2 = 193.33$ million ESALs
Subgrade
(50-6.67) million ESALs in remaining years
 $n_2 = 43.33$ million ESALs**

For this pavement:

**Fatigue Life $N_2 = 414$ million ESALs
Subgrade Strain, $N_2 = 51.8$ million ESALs**

Calculations

$$\frac{n_1}{N_1} + \frac{n_2}{N_2} \leq 1$$

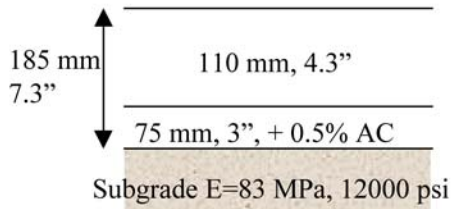
Fatigue: $\frac{6.67}{137} + \frac{193.33}{414} = 0.516 \leq 1$

Subgrade: $\frac{6.67}{18} + \frac{43.33}{51.8} = 1.21 \geq 1$

Staged Construction

Assume: 3" PBA surface layer placed 6 months after initial construc
(For 1 design alternative)

In Six Months



6 % Voids in AC Layer
3 % Voids in Rich Bottom Layer
Fatigue criterion critical

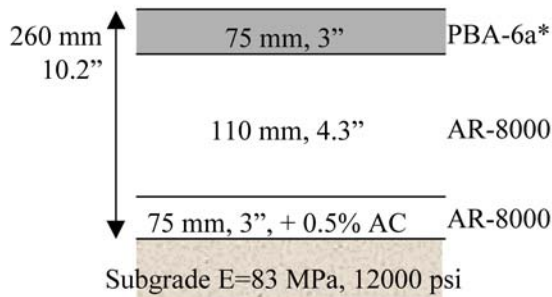
Traffic:

3.333 million ESALs in first year
 $n_1 = 3.333$ million ESALs

For this pavement:

Fatigue Life $N_1 = 137$ million ESALs
Subgrade Strain, $N_1 = 18$ million ESALs

Remaining Years



6% Voids in PBA-6a* Layer
6 % Voids in AC Layer
3 % Voids in Rich Bottom Layer
Fatigue criterion critical

Traffic:

Fatigue:
(200-3.33) million ESALs in remaining years
 $n_2 = 196.667$ million ESALs
Subgrade
(50-3.33) million ESALs in remaining years
 $n_2 = 46.667$ million ESALs

For this pavement:

Fatigue Life $N_2 = 414$ million ESALs
Subgrade Strain, $N_2 = 51.8$ million ESALs

Calculations

$$\frac{n_1}{N_1} + \frac{n_2}{N_2} \leq 1$$

Fatigue: $\frac{3.33}{137} + \frac{196.67}{414} = 0.499 \leq 1$

Subgrade: $\frac{3.33}{18} + \frac{46.67}{51.8} = 1.085 \geq 1$

The question of staged construction was raised prior to the final selection of the design structured section. Accordingly one of the thinner section alternatives was selected for the analysis. As has been shown, the potential for fatigue cracking was minimal. However, the section had been subjected to traffic for one year. The potential for rutting from the subgrade existed. If no fatigue cracking was indicated, any permanent deformation could be taken care of at the time the surface layer was placed; hence the statement included Section 3.4.1 regarding staged construction.

APPENDIX D: FATIGUE PERFORMANCE CONFIRMATION OF I-710 FULL-DEPTH PAVEMENT STRUCTURE

D.1 Fatigue Performance Confirmation of I-710 Full-Depth Pavement Structure

D.1.1 Initial Stiffness Equations and Fatigue Life Equations

Table D.1 lists the regression equations of initial stiffness and fatigue for PBA-6a* and AR-8000 respectively. The data to obtain the regression equations are listed in Appendix A: Laboratory Shear and Fatigue Test Data. The associated residual plots are listed in Appendix B: Initial Designs for Full-Depth Structural Sections.

Table D.1: Regression Equations of Initial Stiffness and Fatigue Life for PBA-6a* and AR-8000

PBA-6a*	
$E(\ln stif) = 9.1116 - 0.1137 Temp$ <small>(0.1493) (0.0071)</small>	$R^2 = 0.93$
$E(\ln nf) = -6.5326 - 0.3505 AV + 0.2053 Temp - 2.4436 \ln stn$ <small>(2.7207) (0.1382) (0.0355) (0.3561)</small>	$R^2 = 0.87$
AR-8000	
$E(\ln stif) = 14.6459 - 0.1708 AV - 0.8032 AC - 0.0549 Temp$ <small>(0.6701) (0.0235) (0.1221) (0.0058)</small>	$R^2 = 0.82$
$E(\ln nf) = -36.5184 - 0.6470 AV - 6.5315 \ln stn$ <small>(4.0492) (0.2553) (0.5242)</small>	$R^2 = 0.83$

Where,

$\ln stif$ is the natural logarithm of initial stiffness (MPa),

$\ln nf$ is the natural logarithm of fatigue life,

$\ln stn$ is the natural logarithm of tensile strain level,

AV is the percent air-void content,

AC is the percent asphalt content, and

$Temp$ is the temperature in °C.

Notice that the stiffness of

PBA-6a* depends only on the temperature.

D.1.2 ELSYM5 Input and Pavement Structure

Figure D.1 illustrates the I-710 full-depth pavement structure and the associated loading configuration. The tires of a dual-tire configuration were used at a 720 kPa (~104 psi) inflation pressure. The traffic loading on the pavement structure is 40 kN (~9 kips) on the dual tires.

The pavement structure consists of a four-layer system as follows:

Layer	Thickness (mm)	Stiffness (MPa)	Poisson Ratio	AC (%)	AV (%)
PBA-6a*	76 (3")	Varied	0.35	5.0	6.0
AR-8000	152 (6")	Varied	0.35	4.7	
AR-8000 (Rich bottom)	76 (3")	Varied	0.35	5.2	3.0
Subgrade		65 (9427 psi)	0.45		

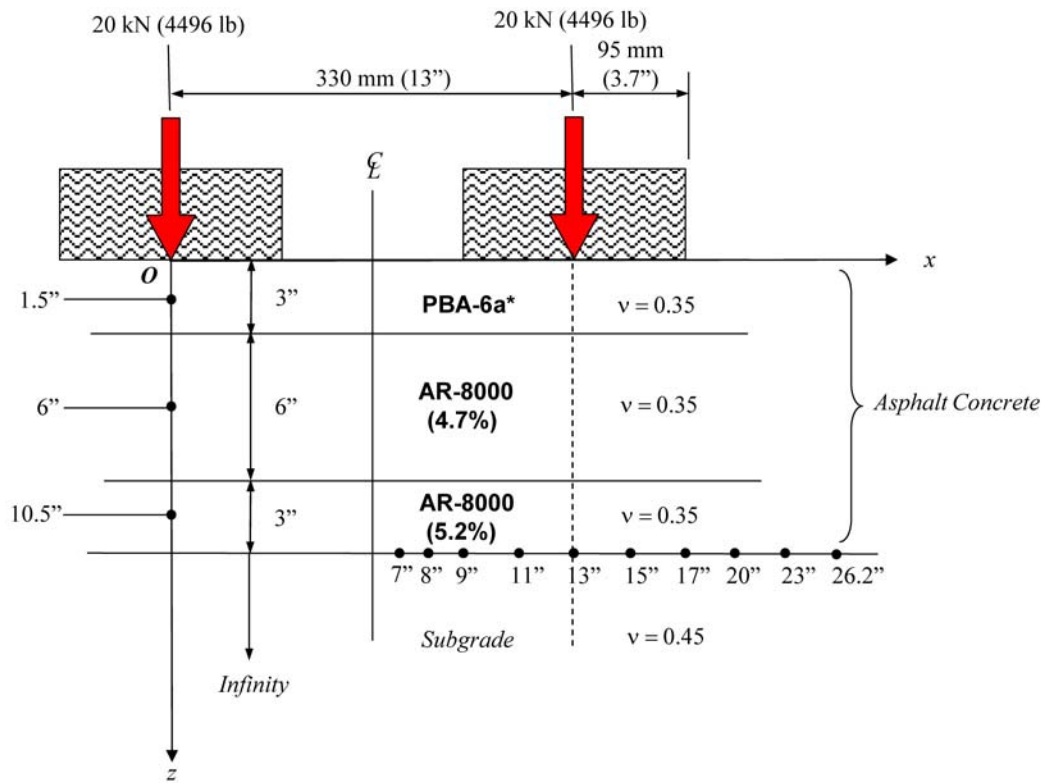


Figure D.1: Pavement structure and ELSYM5 input.

The tensile strains were calculated at depth of 305 mm (~12 in.) and at 10 positions along the x-axis as shown in Figure D.1. The maximum tensile strain (near the 7 in. location) was selected for the calculation of temperature equivalency factor (TEF) and temperature conversion factor (TCF).

D.1.3 Temperature Distribution

The temperature data used in this calculation is based on the temperature data of Long Beach, California, which is embedded in the *EICM* program. The pavement temperature profiles, temperature gradients, and temperatures at bottom of asphalt concrete were calculated using *EICM* program in an hourly base from 09/01/1996 to 01/31/2001. Temperature gradient is defined as $g\left(\frac{^{\circ}C}{in.}\right) = \frac{T_s(^{\circ}C) - T_b(^{\circ}C)}{12"}$, where T_s is the surface temperature and T_b the temperature at bottom of asphalt concrete. Figure D.2 and Figure D.3 display the temperature histograms for surface temperatures and temperatures at the bottom of AC layer respectively. Figure D.4 plots the corresponding temperature distribution curves. The distributions of temperatures extracted from 5:00 A.M. to 7:00 P.M. are also plotted in Figure D.5 through Figure D.7.

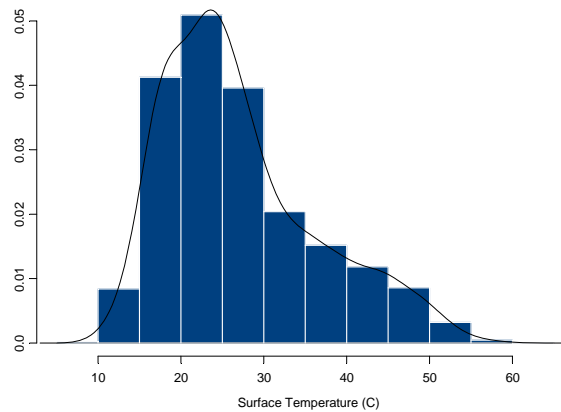


Figure D.2: Histogram of surface temperatures.

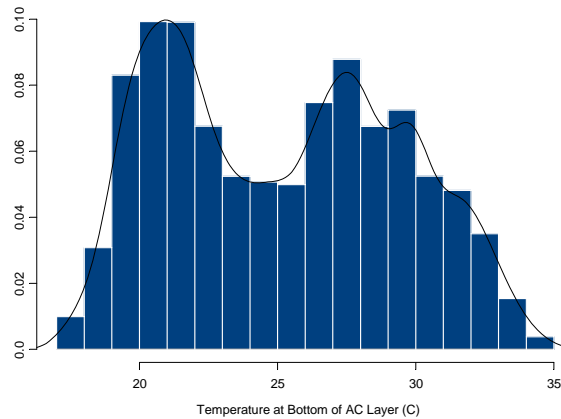


Figure D.3: Histogram of temperatures at bottom of AC layer.

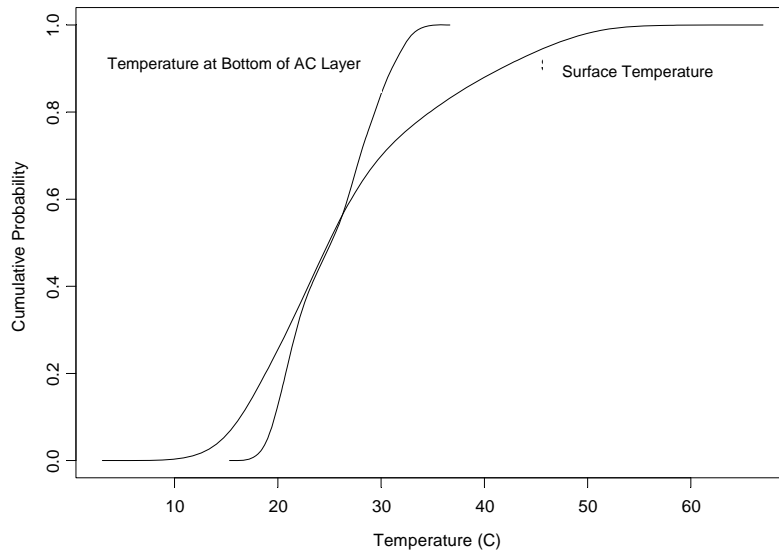


Figure D.4: Temperature distributions for surface temperature and temperature at bottom of AC layer.

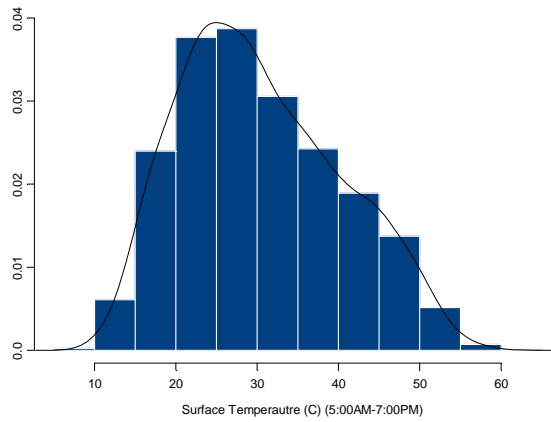


Figure D.5: Histogram of surface temperatures (5:00 A.M. to 7:00 P.M.).

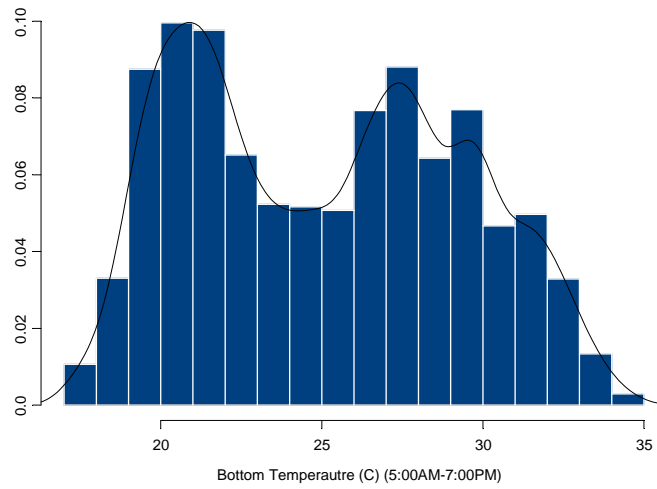


Figure D.6: Histogram of temperatures at bottom of AC layer (5:00 A.M. to 7:00 P.M.).

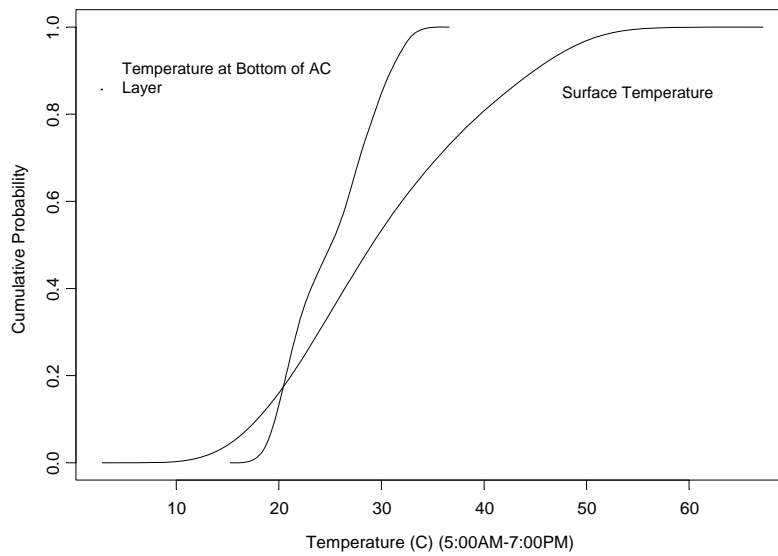


Figure D.7: Temperature distributions for surface temperature and temperature at bottom of AC layer (5:00 A.M. to 7:00 P.M.).

D.1.4 Traffic

A couple of assumptions are postulated in the calculation:

1. It is assumed that no wander traffic was applied onto the specified full-depth pavement structure.
2. The trafficking was applied only from 5:00 A.M. to 7:00 P.M.

D.1.5 Fatigue Performance Prediction and Comparison

TCF Calculation

The calculation of the temperature conversion factor is as follows:

1. Obtain the laboratory fatigue life and initial stiffness equations.
2. Run *ELSYM5* to obtain the maximum tensile strain and then calculate the fatigue life.

3. Calculate $TEF_i = \frac{Nf @ T_{ref} = 20C}{Nf @ T_i}$.

4. $TCF = \sum_i^n f_i \cdot TEF_i$

Table D.2 lists the TCF calculation for temperatures at bottom of AC layer and Table D.3 presents the temperatures extracted from 5:00 A.M. to 7:00 P.M.

Table D.2: TCF Calculation

Temperature (°C), T_b	Temperature Frequency, f_i	Temperature Equivalency Factor, TEF_i	$f_i \cdot TEF_i$
17.5	0.027563	0.546362	0.015059
20.0	0.215566	1.000000	0.215566
22.5	0.182243	1.986708	0.362064
25.0	0.130941	4.849383	0.634985
27.5	0.199086	10.569098	2.104155
30.0	0.150341	21.525919	3.236228
32.5	0.087156	41.661305	3.631051
35.0	0.007104	63.592132	0.451742
TCF			10.65085

Table D.3: TCF Calculation (5:00 A.M. to 7:00 P.M.)

Temperature (°C), T_b	Temperature Frequency, f_i	Temperature Equivalency Factor, TEF_i	$f_i \cdot TEF_i$
17.5	0.030254	0.547092	0.016552
20.0	0.220335	1.000000	0.220335
22.5	0.178467	2.044977	0.364960
25.0	0.133209	5.282466	0.703674
27.5	0.200331	11.680794	2.340021
30.0	0.148088	25.176337	3.728325
32.5	0.084067	49.027394	4.121584
35.0	0.005249	71.047033	0.372927
TCF			11.86838

SF Calculation

The formulation for the shift factor calculation is $SF = 2.7639 \times 10^{-5} \cdot \varepsilon^{-1.3586}$, where ε is the tensile strain. In this calculation, the tensile strain occurred at bottom of AC layer at 20°C while subjected to a zero temperature gradient is 67 microstrain. Thus, the shift factor is 12.94843.

M Calculation

The formulation of reliability multiplier M for a reliability level of 90 percent is shown in the following,

$$M = \exp(1.28\sqrt{0.22 + \text{Var}(\ln Nf)})$$

The regression analysis of *S-Plus* for the fatigue life of AR-8000 is shown in the following,

	Value	Std. Error	t value	Pr(> t)
(Intercept)	-36.5184	4.0492	-9.0186	0.0000
av	-0.6470	0.2553	-2.5339	0.0164
log(stn)	-6.5315	0.5242	-12.4595	0.0000

Residual standard error: 1.414 on 32 degrees of freedom

Multiple R-Squared: 0.8291

Notice that the residual standard error is 1.414.

Let $x'_0 = (x_{00}, x_{01}, \dots, x_{0k})$ represent a set of values of the covariates in the regression equation, where $x_{00} = 1$ if an intercept is present. In this calculation, $x'_0 = (1, AV, \ln stn) = (1, 3.0, \ln(0.000067))$. Then,

the predicted value of y , i.e., $\ln Nf$, at the point x_0 is $\hat{y}_0 = x_0' b$. Hence, the variance $Var(\hat{y}_0) = Var(\ln Nf) = \sigma^2 [x_0' (X'X)^{-1} x_0]$, where X is the design matrix and σ^2 the variance that is square of the residual standard error of the regression equation, in this case, $\sigma^2 = 1.999396$. Finally, we have $Var(\ln Nf) = 0.999529$.

Then, by substituting the value into the formulation, we have,

$$M = \exp(1.28\sqrt{0.22 + Var(\ln Nf)}) = 4.110454$$

Fatigue Performance Calculation

The allowable ESAL for this pavement design can be calculated according the formulation, $ESAL_{allowable} = \frac{Nf_{Lab} \cdot SF}{TCF \cdot M}$, where the Nf_{Lab} is the laboratory fatigue life of AR-8000 (Rich Bottom) at 20°C with the tensile strain 0.000067. The allowable ESAL calculated is then approximately 9.62×10^9 .

$$\begin{aligned} ESAL_{allowable} &= \frac{Nf_{Lab} \cdot SF}{TCF \cdot M} \\ &= \frac{36248265390 \cdot 12.94843}{11.86838 \cdot 4.110454} \\ &= 9,621,064,069 \\ &\cong 9.62 \times 10^9 \end{aligned}$$

APPENDIX E: EVALUATION OF POTENTIAL CONTRIBUTION OF UNBOUND PAVEMENT LAYERS CONTRIBUTING TO SURFACE RUTTING

E.1 Rutting Performance Confirmation of I-710 Pavement Structures

E.1.1 Initial Stiffness Equations

Table E.1 lists the regression equations of initial stiffness for PBA-6a* and AR-8000 respectively. The data used to obtain the regression equations are listed in Appendix A. The associated residual plots are listed in Appendix B: Initial Designs for Full-Depth Structural Sections.

Table E.1: Regression Equations of Initial Stiffness and Fatigue Life for PBA-A and AR-8000

PBA-6a*	
$E(\ln stif) = 9.1116 - 0.1137 Temp$ <div style="display: flex; justify-content: space-around; font-size: small;"> (0.1493) (0.0071) </div>	$R^2 = 0.93$
AR-8000	
$E(\ln stif) = 14.6459 - 0.1708 AV - 0.8032 AC - 0.0549 Temp$ <div style="display: flex; justify-content: space-around; font-size: small;"> (0.6701) (0.0235) (0.1221) (0.0058) </div>	$R^2 = 0.82$

Where,

$\ln stif$ is the natural logarithm of initial stiffness (MPa),

AV is the percent air-void content,

AC is the percent asphalt content, and

$Temp$ is the temperature in °C.

Notice that the stiffness of PBA-6a* depends only on the temperature.

E.1.2 ELSYM5 Input and Pavement Structures

The loading configuration and the detailed pavement structure information are listed in Table E.2 through Table E.4 and schematically plotted in Table E.1 through Figure E.3 for various pavement structures. The tires of a dual-tire configuration were used at a 720 kPa (~104 psi) inflation pressure. The traffic loading on the pavement structure is 40 kN (~9 kips) on the dual tires.

The pavement structures are listed and schematically plotted as follows:

Table E.2: Pavement Structure P1

Layer	Thickness (mm)	Stiffness (MPa)	Poisson Ratio	AC (%)	AV (%)
PBA-6a*	76 (3")	Varied	0.35	5.0	6.0
AR-8000	152 (6")	Varied	0.35	4.7	
AR-8000 (Rich Bottom)	76 (3")	Varied	0.35	5.2	3.0
Subgrade		65 (9427 psi) or 100 (14503 psi)	0.45		

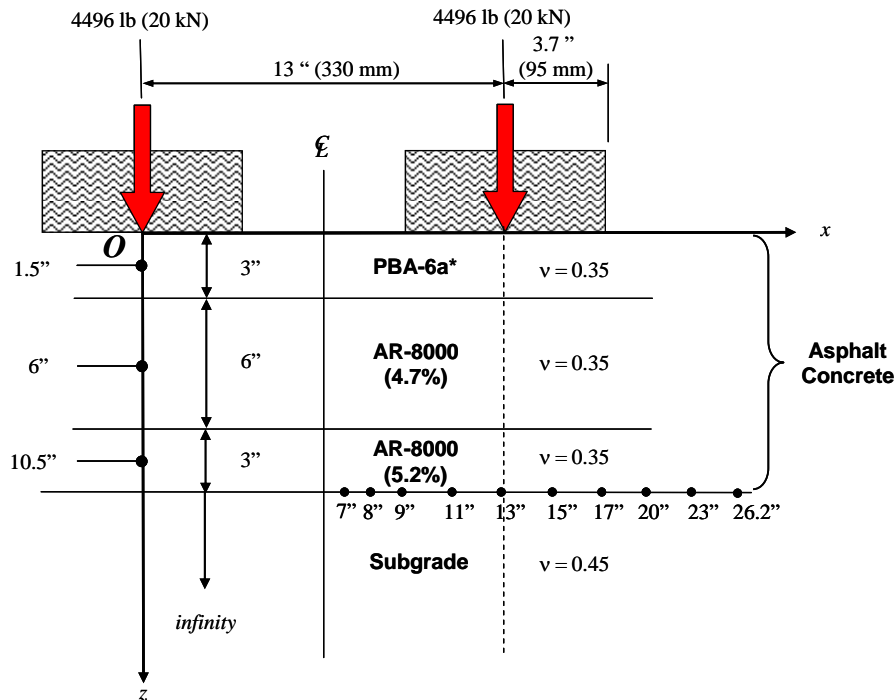


Figure E.1: ELSYM5 input for pavement structure P1.

Table E.3: Pavement Structure P2

Layer	Thickness (mm)	Stiffness (MPa)	Poisson Ratio	AC (%)	AV (%)
PBA-6a*	76 (3")	Varied	0.35	5.0	6.0
AR-8000	152 (6")	Varied	0.35	4.7	6.0
AR-8000 (Rich Bottom)	76 (3")	Varied	0.35	5.2	3.0
Granular Base	152 (6")	130 (18,854 psi) or 400 (58,012 psi)	0.35		
Subgrade		65 (9,427 psi) or 100 (14,503 psi)	0.45		

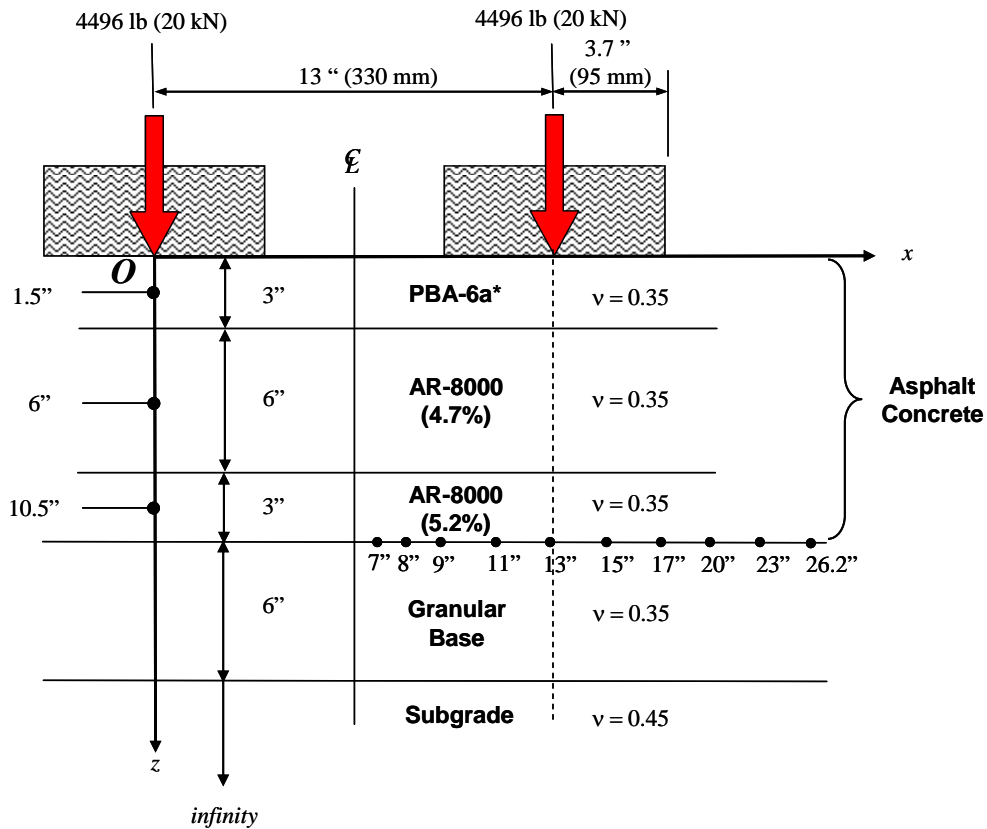


Figure E.2: ELSYMS input for pavement structure P2.

Table E.4: Pavement Structure P3

Layer	Thickness (mm)	Stiffness (MPa)	Poisson Ratio	AC (%)	AV (%)
PBA-6a*	76 (3")	Varied	0.35	5.0	6.0
AR-8000	102 (4")	Varied	0.35	4.7	6.0
AR-8000 (Rich Bottom)	76 (3")	Varied	0.35	5.2	3.0
Granular Base	152 (6")	130 (18,854 psi) or 400 (58,012 psi)	0.35		
Subgrade		65 (9,427 psi) or 100 (14,503 psi)	0.45		

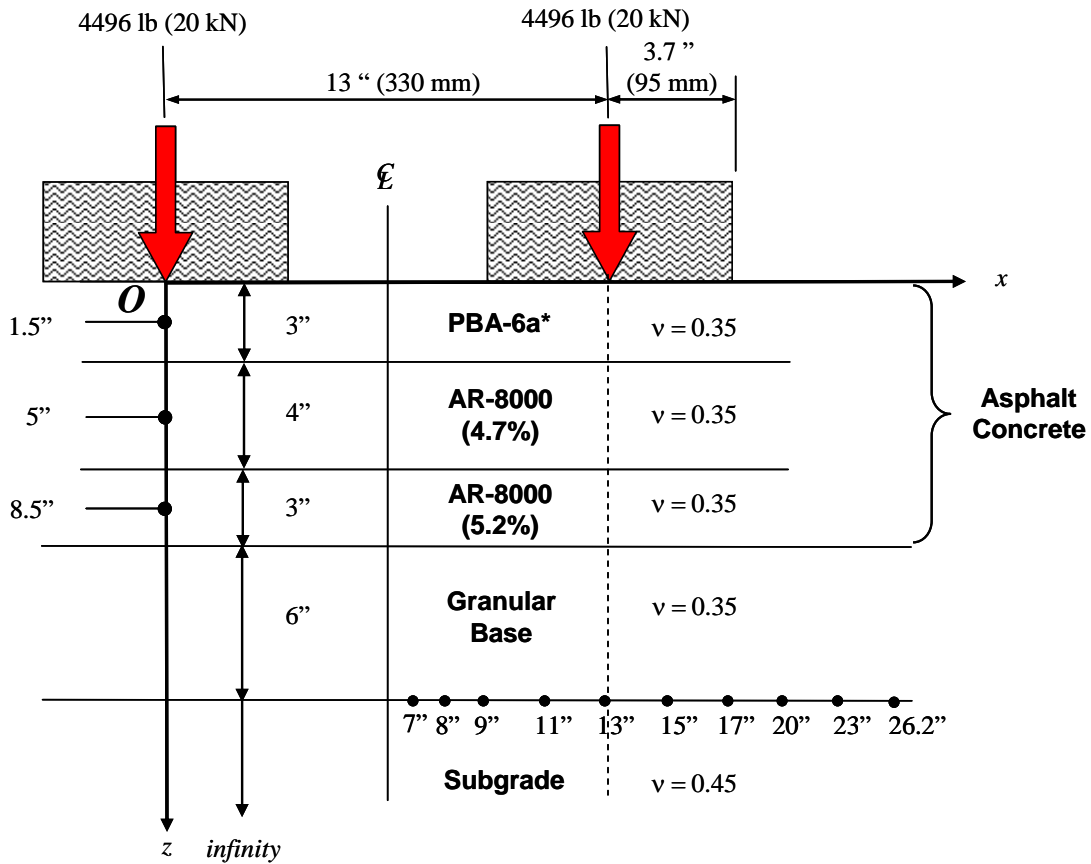


Figure E.3: ELSYM5 input for pavement structure P3.

The vertical compressive strains were calculated on top of the subgrade layer and at 10 positions along the x -axis as shown in Figure E.1 through Figure E.3 for various pavement structures. The maximum vertical compressive strain was selected for assessing the rutting performance for various pavement structures.

E.1.3 Temperature Distribution

The temperature data used in this calculation is based on the temperature data of Long Beach, California, which is embedded in the *EICM* program. For each of the pavement structures, the pavement temperature profiles, the temperature gradients, and the temperatures at bottom of asphalt concrete were calculated using the *EICM* program in an hourly base from 09/01/1996 to 01/31/2001. Temperature gradient is defined as $g\left(\frac{^{\circ}\text{C}}{\text{in.}}\right) = \frac{T_s(^{\circ}\text{C}) - T_b(^{\circ}\text{C})}{\text{AC thickness}}$, where T_s is the surface temperature and T_b the temperature at bottom of asphalt concrete layer. Figure E.4 displays the histograms and distribution functions of bottom AC temperatures (from 5:00 A.M. to 7:00 P.M.) for various pavement structures. Figure E.5 plots the histograms and distribution functions of temperature gradients (also from 5:00 A.M. to 7:00 P.M.) for various pavement structures.

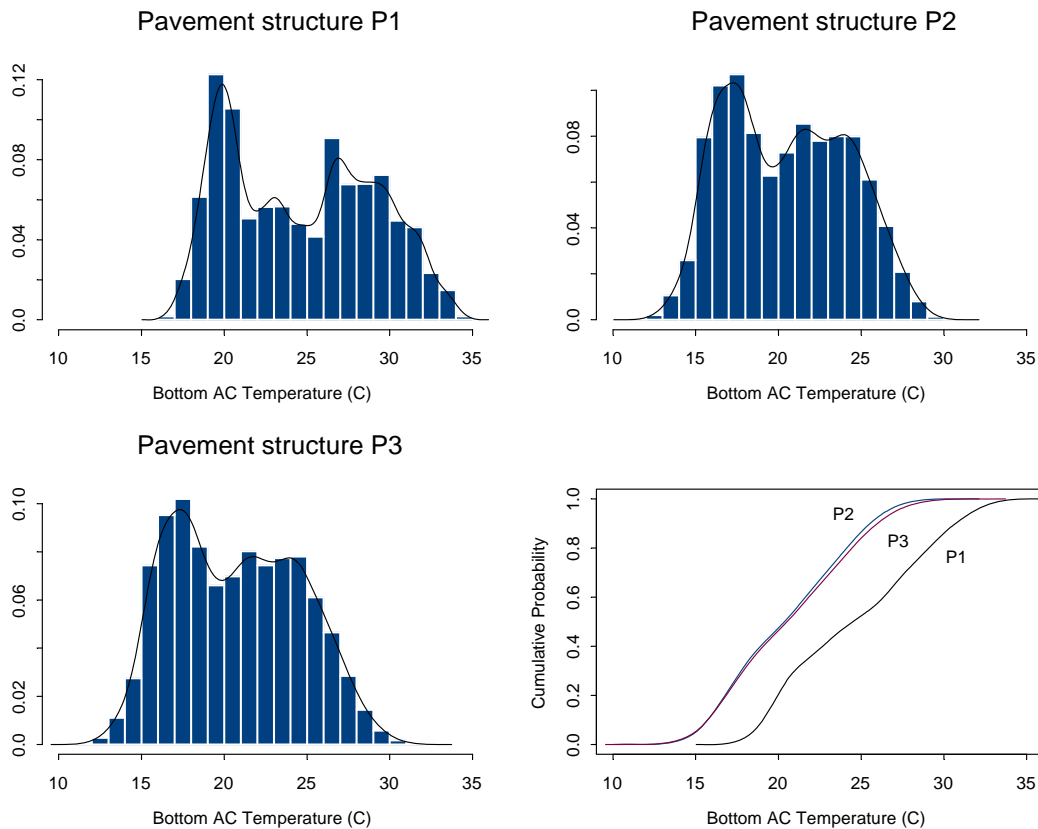


Figure E.4: The histograms and distribution functions of bottom AC temperatures for various pavement structures (from 5:00 A.M. to 7:00 P.M.).

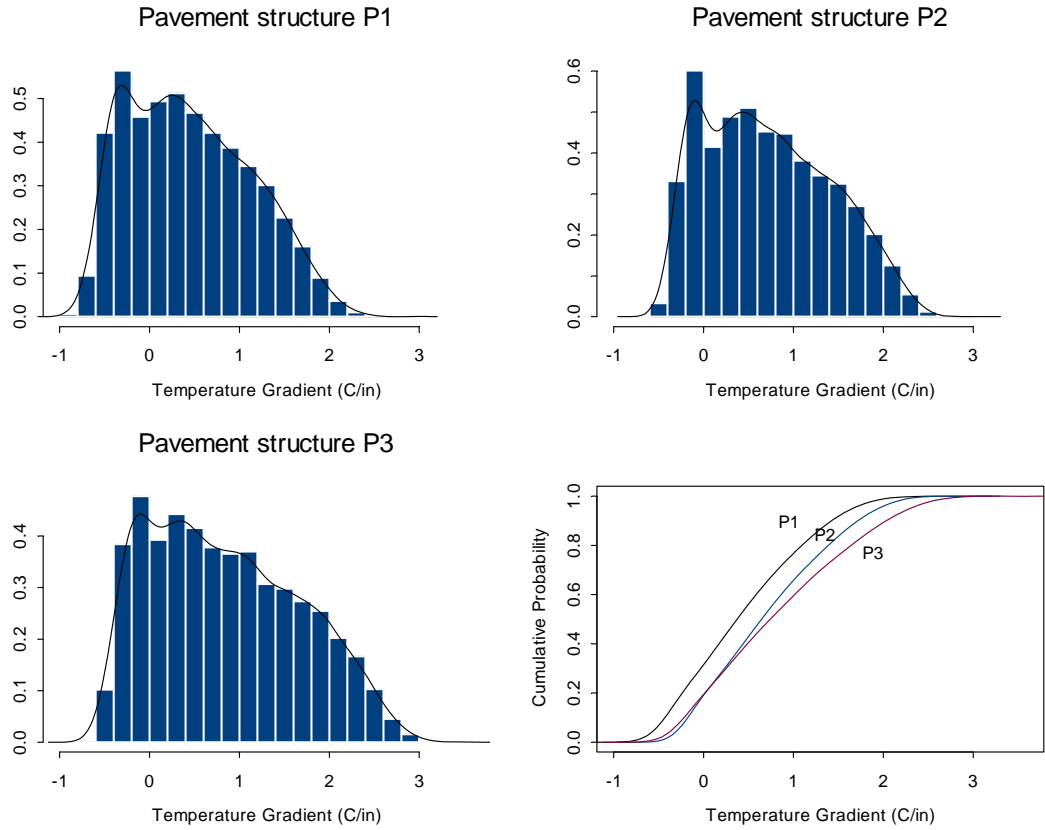


Figure E.5: The histograms and distribution functions of temperature gradients of asphalt concrete layer for various pavement structures (from 5:00 A.M. to 7:00 P.M.).

E.1.4 Traffic

A couple of assumptions are postulated in the calculation:

1. It is assumed that no-wander traffic was applied onto the specified pavement structures.
2. The trafficking was applied only from 5:00 A.M. to 7:00 P.M.

E.1.5 Variation of Subgrade Vertical Compressive Strain

The calculated vertical compressive strains on top of the subgrade layer for various pavement structures versus surface temperatures are plotted in Figure E.6 (pavement structures with 65 MPa subgrade or/and 130 MPa granular base) and Figure E.7 (pavement structures with 100 MPa subgrade or/and 400 MPa granular base) respectively.

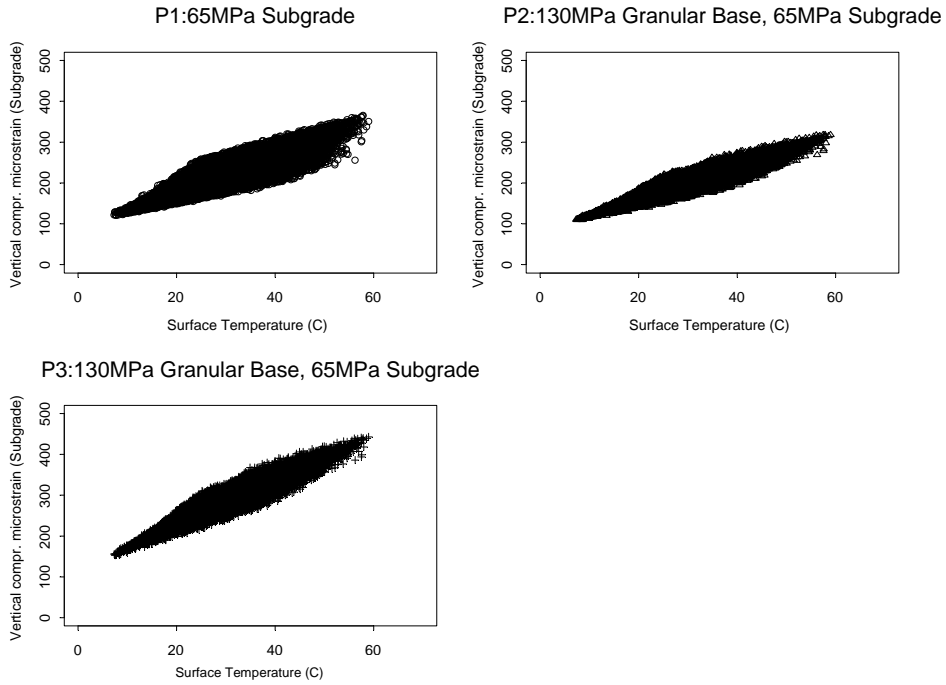


Figure E.6: Variations of subgrade vertical compressive strains versus surface temperatures for various pavement structures with 65 MPa subgrade or/and 130 MPa granular base.

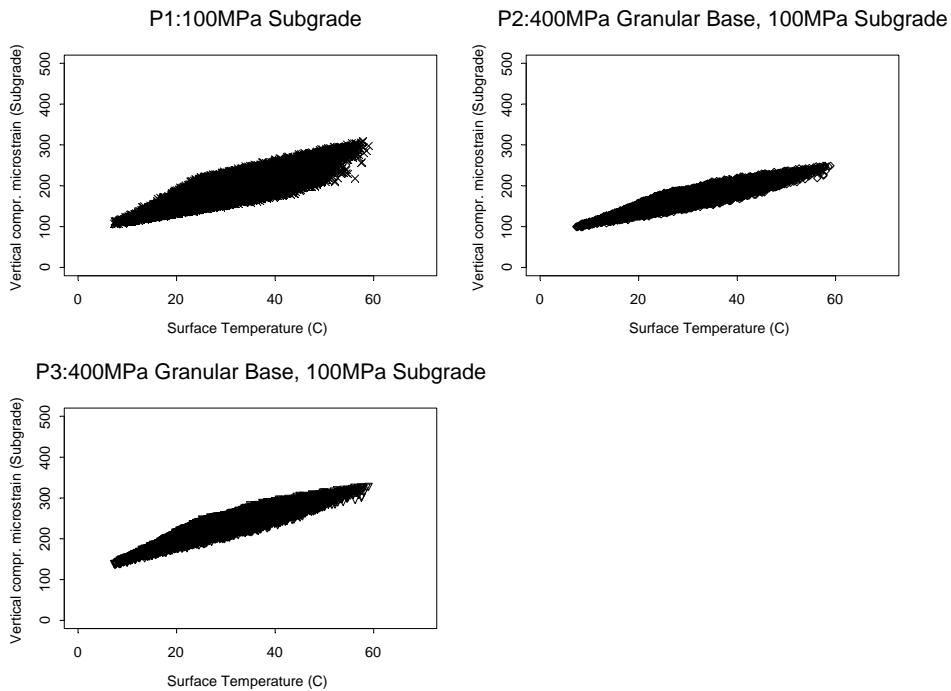


Figure E.7: Variations of subgrade vertical compressive strains versus surface temperatures for various pavement structures with 400 MPa granular base and/or 100 MPa subgrade.

E.1.6 Traffic

A couple of assumptions are postulated in the calculation:

1. It is assumed that no-wander traffic was applied onto the specified pavement structures.
2. The trafficking was applied only from 5:00 A.M. to 7:00 P.M.

E.2 Rutting Performance Estimation

Assumptions:

1. The surface permanent deformation is only attributed to the permanent deformation of the subgrade.
2. The Asphalt Institute Subgrade Strain Criteria formulation $N = 1.05 \times 10^{-9} \cdot \epsilon_v^{-4.484}$ (Figure E.8) is appropriate to relate the plastic deformation to the elastic vertical compressive strain of subgrade layer.
3. The permanent deformation accumulation is complied with the Miner's Law.
4. A cutoff point is set at 50×10^6 repetitions and 190.81 microstrain as shown in Figure E.8. In other words, there is no rutting damage if the vertical compressive strain is less than 190.81 microstrain.
5. Stiffness calculations based on the regression equations were deemed to be appropriate if extrapolation is necessary.

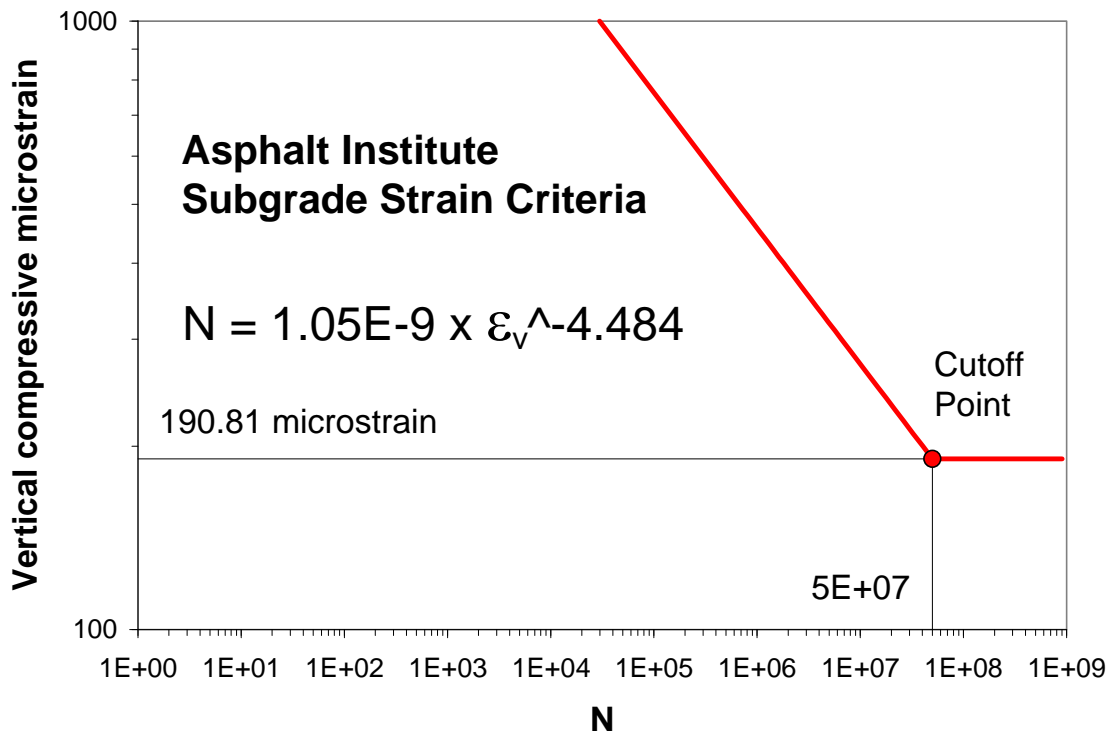


Figure E.8: Asphalt Institute subgrade strain criteria and cutoff point.

Miner's Law for Rutting Performance

The procedure to conduct the rutting performance estimation using Miner's Law is as follows:

1. Obtain the laboratory initial stiffness regression equations.
2. Run *EICM* to obtain the temperature profile of asphalt concrete layer.
3. Run *ELSYM5* to obtain the maximum vertical compressive strain on top of the subgrade layer in an hourly basis.
4. Summarize the frequencies (f_i) of maximum vertical compressive strains.

$$5. n_i = f_i \cdot ESAL_{Allowable}$$

$$6. N_i = 1.05 \times 10^{-9} \cdot (\epsilon_v)_i^{-4.484}$$

$$7. \sum_i \frac{n_i}{N_i} = \sum_i \frac{f_i \cdot ESAL_{Allowable}}{N_i} = ESAL_{Allowable} \cdot \sum_i \frac{f_i}{N_i} = 1$$

$$\Rightarrow ESAL_{Allowable} = \frac{1}{\sum_i \frac{f_i}{N_i}}$$

Table E.5 through Table E.7 list the calculations of $ESAL_{Allowable}$ for pavement structures with 65 MPa subgrade or/and 130 MPa granular base; Table E.8 through Table E.10 for pavement structures with 100 MPa subgrade or/and 400 MPa granular base. It should be noted that the P3 pavement structure consists of a thinner (4 in.) AR-8000 (AC=4.7%). The calculated $ESAL_{Allowable}$ s for various pavement structures can be summarized as follows:

Pavement Structure	65 MPa Subgrade (130 MPa granular base)	100 MPa Subgrade (400 MPa granular base)
P1	22,657,245	53,860,044
P2	40,175,466	155,464,730
P3	6,890,555	20,455,896

Note: Two additional pavement structures P4 and P5 were duplicated to have the same pavement structures as P1 and P2 respectively but with a 4-in. PBA-6a* layer. The pavement structure, *ELSYM5* input, temperature distribution, variation of vertical compressive strain versus surface temperature, and the summary table of Miner's Law are shown in Appendix C. The calculated $ESAL_{Allowable}$ s for pavement structures P4 and P5 are summarized in the following:

Pavement Structure	4" PBA-6a*, 65 MPa Subgrade (130 MPa granular base)
P4	30,524,262
P5	57,205,877

Table E.5: Allowable ESALs for Pavement Structure P1 (Traffic from 5:00 A.M. to 7:00 P.M.)

$\mathbf{\epsilon_v}$ range ($\mu\epsilon$)	$\mathbf{\epsilon_v}$ Frequency, f_i	Mean ($\mathbf{\epsilon_v}$) _{i} ($\mu\epsilon$)	N_i	f_i / N_i
95-105	0	NA	NA	NA
105-115	0	NA	NA	NA
115-125	0.000289	122.286	367617815	7.87002E-13
125-135	0.005828	130.575	273956013	2.12722E-11
135-145	0.028436	140.329	198329502	1.43376E-10
145-155	0.060756	149.746	148215316	4.09920E-10
155-165	0.071544	159.657	111196035	6.43402E-10
165-175	0.079769	169.608	84791938	9.40756E-10
175-185	0.076586	179.426	65881523	1.16248E-09
185-190.81	0.043728	187.503	54078236	8.08607E-10
190.81-195	0.028518	192.515	48045776	5.93565E-10
195-205	0.075677	199.723	40744980	1.85733E-09
205-215	0.067163	209.398	32957387	2.03786E-09
215-225	0.066749	219.444	26711244	2.49892E-09
225-235	0.059764	229.326	21923666	2.72602E-09
235-245	0.058400	239.600	18012304	3.24226E-09
245-255	0.054929	249.156	15115192	3.63401E-09
255-265	0.047654	259.374	12622477	3.77537E-09
265-275	0.043769	269.484	10633503	4.11618E-09
275-285	0.036950	279.279	9060600	4.07807E-09
285-295	0.030089	289.339	7731050	3.89195E-09
295-305	0.024013	299.296	6642821	3.61491E-09
305-315	0.016822	309.332	5729625	2.93591E-09
315-325	0.010870	319.091	4984652	2.18070E-09
325-335	0.006324	328.765	4359896	1.45041E-09
335-345	0.003430	339.036	3798099	9.03205E-10
345-355	0.001488	348.583	3353408	4.43701E-10
355-365	0.000413	358.800	2945988	1.40295E-10
365-375	0.000041	366.000	2694884	1.53368E-11
375-385	0	NA	NA	NA
385-395	0	NA	NA	NA
395-405	0	NA	NA	NA
405-415	0	NA	NA	NA
415-425	0	NA	NA	NA
425-435	0	NA	NA	NA
435-445	0	NA	NA	NA
445-455	0	NA	NA	NA
			Σ	4.4136E-08
			Allowable ESALs	22,657,245

Table E.6: Allowable ESALs for Pavement Structure P2 (Traffic from 5:00 A.M. to 7:00 P.M.)

ϵ_v range ($\mu\epsilon$)	ϵ_v Frequency, f_i	mean (ϵ_v) _i ($\mu\epsilon$)	N_i	f_i / N_i
95-105	0	NA	NA	NA
105-115	0.000951	112.348	537597579	1.76826E-12
115-125	0.006572	120.082	398854241	1.64762E-11
125-135	0.025501	130.499	274665339	9.28444E-11
135-145	0.058566	140.011	200352207	2.92314E-10
145-155	0.077743	149.580	148957776	5.21915E-10
155-165	0.087001	159.542	111557079	7.79883E-10
165-175	0.094441	169.495	85045272	1.11048E-09
175-185	0.093325	179.461	65824436	1.41779E-09
185-190.81	0.055507	187.448	54148774	1.02509E-09
190.81-195	0.037983	192.495	48067492	7.90203E-10
195-205	0.083943	199.365	41073363	2.04373E-09
205-215	0.073321	209.494	32889537	2.22931E-09
215-225	0.061831	219.302	26789155	2.30806E-09
225-235	0.054185	229.395	21894240	2.47484E-09
235-245	0.049721	239.493	18048487	2.75486E-09
245-255	0.043976	249.400	15048828	2.92222E-09
255-265	0.035255	259.470	12601485	2.79770E-09
265-275	0.028353	269.175	10688435	2.65268E-09
275-285	0.017318	279.033	9096343	1.90380E-09
285-295	0.009010	288.780	7798438	1.15538E-09
295-305	0.004092	298.687	6703787	6.10365E-10
305-315	0.001116	308.222	5822686	1.91653E-10
315-325	0.000289	316.571	5165045	5.60142E-11
325-335	0	NA	NA	NA
335-345	0	NA	NA	NA
345-355	0	NA	NA	NA
355-365	0	NA	NA	NA
365-375	0	NA	NA	NA
375-385	0	NA	NA	NA
385-395	0	NA	NA	NA
395-405	0	NA	NA	NA
405-415	0	NA	NA	NA
415-425	0	NA	NA	NA
425-435	0	NA	NA	NA
435-445	0	NA	NA	NA
445-455	0	NA	NA	NA
			Σ	2.48908E-08
			Allowable ESALs	40,175,466

Table E.7: Allowable ESALs for Pavement Structure P3 (Traffic from 5:00 A.M. to 7:00 P.M.)

ϵ_v range ($\mu\epsilon$)	ϵ_v Frequency, f_i	mean (ϵ_v) _{<i>i</i>} ($\mu\epsilon$)	N_i	f_i / N_i
95-105	0	NA	NA	NA
105-115	0	NA	NA	NA
115-125	0	NA	NA	NA
125-135	0	NA	NA	NA
135-145	0	NA	NA	NA
145-155	0.000083	153.500	132641469	6.23197E-13
155-165	0.001529	160.973	107178828	1.42681E-11
165-175	0.004216	170.343	83162896	5.06926E-11
175-185	0.009589	180.741	63759229	1.50390E-10
185-190.81	0.012523	187.749	53760725	2.32944E-10
190.81-195	0.010167	192.557	47998356	2.11828E-10
195-205	0.039306	199.725	40743202	9.64717E-10
205-215	0.050424	209.533	32862105	1.53440E-09
215-225	0.054185	219.545	26655957	2.03274E-09
225-235	0.060880	229.534	21834781	2.78823E-09
235-245	0.066915	239.643	17997868	3.71792E-09
245-255	0.066336	249.510	15019296	4.41672E-09
255-265	0.066667	259.513	12592076	5.29433E-09
265-275	0.067907	269.522	10626926	6.39005E-09
275-285	0.065923	279.495	9029132	7.30111E-09
285-295	0.057243	289.344	7730437	7.40492E-09
295-305	0.052945	299.427	6629802	7.98588E-09
305-315	0.047572	309.395	5724345	8.31044E-09
315-325	0.042447	319.528	4954192	8.56785E-09
325-335	0.037900	329.497	4316599	8.78015E-09
335-345	0.036702	339.469	3776458	9.71858E-09
345-355	0.035999	349.413	3317838	1.08502E-08
355-365	0.030089	359.473	2921355	1.02996E-08
365-375	0.026328	369.518	2581731	1.01977E-08
375-385	0.021947	379.301	2296273	9.55752E-09
385-395	0.014796	388.927	2052196	7.21005E-09
395-405	0.010043	398.910	1831761	5.48292E-09
405-415	0.005290	408.883	1639759	3.22630E-09
415-425	0.002769	419.090	1468133	1.88618E-09
425-435	0.000868	428.286	1331974	6.51625E-10
435-445	0.000413	438.300	1200842	3.44182E-10
445-455	0	NA	NA	NA
			Σ	1.45126E-07
			Allowable ESALs	6,890,555

Table E.8: Allowable ESALs for Pavement Structure P1 with 100 MPa Subgrade (Traffic from 5:00 A.M. to 7:00 P.M.)

ϵ_v range ($\mu\epsilon$)	ϵ_v Frequency, f_i	Mean (ϵ_v) _i ($\mu\epsilon$)	N_i	f_i / N_i
95-105	0	NA	NA	NA
105-115	0.002604	111.905	547207854	4.75842E-12
115-125	0.019054	121.215	382407642	4.98252E-11
125-135	0.063608	130.149	277990461	2.28814E-10
135-145	0.085968	139.696	202389944	4.24765E-10
145-155	0.097541	149.622	148767901	6.55658E-10
155-165	0.089895	159.472	111777820	8.04226E-10
165-175	0.088613	169.578	84858952	1.04424E-09
175-185	0.086795	179.283	66118269	1.31272E-09
185-190.81	0.049308	187.518	54058583	9.12116E-10
190.81-195	0.032403	192.500	48062005	6.74200E-10
195-205	0.071420	199.359	41078871	1.73860E-09
205-215	0.073900	209.418	32942707	2.24328E-09
215-225	0.058896	219.407	26731418	2.20327E-09
225-235	0.054433	229.436	21876821	2.48815E-09
235-245	0.042488	239.304	18112639	2.34577E-09
245-255	0.032197	249.228	15095420	2.13288E-09
255-265	0.023765	259.223	12655524	1.87786E-09
265-275	0.014548	269.136	10695304	1.36027E-09
275-285	0.007564	278.869	9120437	8.29296E-10
285-295	0.003596	288.805	7795438	4.61268E-10
295-305	0.001199	298.034	6769838	1.77049E-10
305-315	0.000207	306.800	5944699	3.47628E-11
315-325	0	NA	NA	NA
325-335	0	NA	NA	NA
335-345	0	NA	NA	NA
345-355	0	NA	NA	NA
355-365	0	NA	NA	NA
365-375	0	NA	NA	NA
375-385	0	NA	NA	NA
385-395	0	NA	NA	NA
395-405	0	NA	NA	NA
405-415	0	NA	NA	NA
415-425	0	NA	NA	NA
425-435	0	NA	NA	NA
435-445	0	NA	NA	NA
445-455	0	NA	NA	NA
			Σ	1.85666E-08
			Allowable ESALs	53,860,044

Table E.9: Allowable ESALs for Pavement Structure P2 with 400 MPa Granular Base and 100 MPa Subgrade (Traffic from 5:00 A.M. to 7:00 P.M.)

ϵ_v range ($\mu\epsilon$)	ϵ_v Frequency, f_i	Mean (ϵ_v) _i ($\mu\epsilon$)	N_i	f_i / N_i
95-105	0.001488	102.250	820085224	1.81434E-12
105-115	0.010663	110.686	574747175	1.85531E-11
115-125	0.049638	120.330	395181953	1.25609E-10
125-135	0.095061	129.685	282480460	3.36522E-10
135-145	0.112875	139.625	202849403	5.56445E-10
145-155	0.125811	149.457	149504605	8.41520E-10
155-165	0.128126	159.492	111714319	1.14690E-09
165-175	0.115602	169.303	85478917	1.35241E-09
175-185	0.097417	179.352	66004516	1.47591E-09
185-190.81	0.048646	187.506	54074744	8.99614E-10
190.81-195	0.029593	192.560	47994779	6.16586E-10
195-205	0.069684	199.445	40999999	1.69961E-09
205-215	0.055755	209.278	33041894	1.68741E-09
215-225	0.038355	218.952	26981689	1.42152E-09
225-235	0.016284	228.642	22219415	7.32889E-10
235-245	0.004505	238.000	18561720	2.42707E-10
245-255	0.000496	247.083	15692035	3.16065E-11
255-265	0	NA	NA	NA
265-275	0	NA	NA	NA
275-285	0	NA	NA	NA
285-295	0	NA	NA	NA
295-305	0	NA	NA	NA
305-315	0	NA	NA	NA
315-325	0	NA	NA	NA
325-335	0	NA	NA	NA
335-345	0	NA	NA	NA
345-355	0	NA	NA	NA
355-365	0	NA	NA	NA
365-375	0	NA	NA	NA
375-385	0	NA	NA	NA
385-395	0	NA	NA	NA
395-405	0	NA	NA	NA
405-415	0	NA	NA	NA
415-425	0	NA	NA	NA
425-435	0	NA	NA	NA
435-445	0	NA	NA	NA
445-455	0	NA	NA	NA
			Σ	6.43233E-09
			Allowable ESALs	155,464,730

Table E.10: Allowable ESALs for Pavement Structure P3 with 400 MPa Granular Base and 100 MPa Subgrade (Traffic from 5:00 A.M. to 7:00 P.M.)

ϵ_v range ($\mu\epsilon$)	ϵ_v Frequency, f_i	Mean (ϵ_v) _i ($\mu\epsilon$)	N_i	f_i / N_i
95-105	0	NA	NA	NA
105-115	0	NA	NA	NA
115-125	0	NA	NA	NA
125-135	0	NA	NA	NA
135-145	0.001447	141.400	191678829	7.54689E-12
145-155	0.005747	150.144	146463363	3.92247E-11
155-165	0.020707	160.597	108309118	1.91182E-10
165-175	0.046869	170.030	83851901	5.58952E-10
175-185	0.069436	179.544	65688067	1.05705E-09
185-190.81	0.046911	187.499	54083538	8.67371E-10
190.81-195	0.034925	192.557	47997797	7.27629E-10
195-205	0.092746	199.677	40786348	2.27396E-09
205-215	0.096301	209.494	32889704	2.92800E-09
215-225	0.100351	219.542	26657795	3.76443E-09
225-235	0.095433	229.421	21883183	4.36102E-09
235-245	0.080554	239.449	18063185	4.45956E-09
245-255	0.069932	249.342	15064739	4.64209E-09
255-265	0.061955	259.413	12613941	4.91163E-09
265-275	0.057822	269.526	10626133	5.44148E-09
275-285	0.048564	279.280	9060386	5.36001E-09
285-295	0.039016	289.195	7748371	5.03542E-09
295-305	0.020789	298.922	6680127	3.11213E-09
305-315	0.008308	308.483	5800682	1.43216E-09
315-325	0.001984	317.792	5076709	3.90781E-10
325-335	0.000207	325.600	4553155	4.53870E-11
335-345	0	NA	NA	NA
345-355	0	NA	NA	NA
355-365	0	NA	NA	NA
365-375	0	NA	NA	NA
375-385	0	NA	NA	NA
385-395	0	NA	NA	NA
395-405	0	NA	NA	NA
405-415	0	NA	NA	NA
415-425	0	NA	NA	NA
425-435	0	NA	NA	NA
435-445	0	NA	NA	NA
445-455	0	NA	NA	NA
			Σ	4.88857E-08
			Allowable ESALs	20,455,896

APPENDIX F: ASPHALT CONCRETE SHEAR AND FATIGUE PERFORMANCE TEST REQUIREMENTS

F.1 Permanent Deformation (Shear Test Requirements)

F.1.1 Assumptions

Assumptions associated with the derivation of minimum requirements of permanent deformation include the following:

1. The measurement of interest is the number of stress repetitions to reach a shear strain of 5 percent of the Repeated Simple Shear Test with Constant Height (RSST-CH).
2. The number of stress repetitions to 5 percent shear strain has a log-normal distribution.

F.1.2 Normal One-Sample Model

Let Y_1, \dots, Y_n be independent random variables having a common normal distribution with mean μ and variance σ^2 . This setup is recognized as the normal one-sample model. Under this model, the sample mean $\bar{Y} = (Y_1 + \dots + Y_n)/n$ is normally distributed with mean μ and variance σ^2/n . That is,

$$E(\bar{Y}) = E[(Y_1 + \dots + Y_n)/n] = \frac{E(Y_1) + \dots + E(Y_n)}{n} = \frac{n\mu}{n} = \mu$$

$$Var(\bar{Y}) = Var[(Y_1 + \dots + Y_n)/n] = \frac{Var(Y_1) + \dots + Var(Y_n)}{n^2} = \frac{n\sigma^2}{n^2} = \frac{\sigma^2}{n}$$

Under the assumptions of the normal one-sample model, if we know the mean μ and variance σ^2/n , then the 95% confidence interval of Ln(reps to 5% shear strain) with n tests is,

$$\left(\mu - 1.96 \cdot \frac{\sigma}{\sqrt{n}}, \mu + 1.96 \cdot \frac{\sigma}{\sqrt{n}} \right)$$

where μ is the mean,

n is the sample size,

σ is the standard deviation, and

1.96 is the quantile of normal distribution with probability 0.975.

In SHRP-A-415 Data included in *Permanent Deformation Response of Asphalt Aggregate Mixes* provide a value for a mean square error of 0.6, i.e., $\sigma = 0.7746$, of Ln(reps to 5% shear strain) for the

RSST-CH tests. Now, if three tests were conducted, then the 95% confidence interval of the mean should be

$$\left(\mu - 1.96 \cdot \frac{0.7746}{\sqrt{3}}, \mu + 1.96 \cdot \frac{0.7746}{\sqrt{3}} \right) = (\mu - 0.8765, \mu + 0.8765)$$

If we assume the means of stress repetitions to 5% shear strain are 660,000 for PBA-6a* and 132,000 for AR-8000, then the 95% confidence intervals for both PBA-6a* and AR-8000 mixes should have the intervals listed in Table F.1.

Table F.1: 95% Confidence Interval of Ln(reps to 5% shear strain)

Mix	Exp(μ)	μ	95% Confidence Interval of Ln(reps to 5% shear strain)	95% Confidence Interval of reps to 5% shear strain
PBA6A	660,000	13.4	(12.5235, 14.2765)	(274,718, 1,585,642)
AR8000	132,000	11.7906	(10.9141, 12.6671)	(54,946, 317,140)

Therefore, the mean of stress repetitions to 5% shear strain of three RSST-CH tests should be greater than, say, 275,000 for PBA-6a* and 55,000 for AR-8000.

F.2 Fatigue Cracking (Fatigue Test Requirements)

The following paragraphs regarding the confidence band are adapted from “Practical Biostatistical Methods” by S. Selvin.

For estimating a mean value from a regression line with the formulation of $y = a + bx$, an estimate of variance of \hat{y}_0 ($S_{\hat{y}_0}^2$) is

$$S_{\hat{y}_0}^2 = S_{y|x}^2 \left[\frac{1}{n} + \frac{(x_0 - \bar{x})^2}{\sum (x_i - \bar{x})^2} \right]$$

where $S_{y|x}^2 = \frac{\sum (y_i - \hat{y}_i)^2}{n - 2}$ is the square of residual standard error of the regression equation.

A $(1-\alpha)$ -confidence band, a band that has a probability of $1-\alpha$ of containing the true regression line, is not constructed from a series of confidence intervals based on \hat{y}_0 . The width of the geometric region at the point x_0 that has a probability of $1-\alpha$ of containing the true regression line is given by

Lower bound: $\hat{y}_0 - \sqrt{2F_{1-\alpha}} S_{\hat{y}_0}$

Upper bound: $\hat{y}_0 + \sqrt{2F_{1-\alpha}} S_{\hat{y}_0}$

Where $F_{1-\alpha}$ is the $(1-\alpha)$ -percentile of an F-distribution with 2 and $n-2$ degrees of freedom.

Notice that the number 2 of $n-2$ degrees of freedom comes from the fact that the regression equation has two parameters and has the formulation with $y = a + bx$.

In the following paragraphs, the 95% confidence bands are estimated respectively for (1) PBA-6a* mixes (pooled), (2) AR-8000 mixes with high air-void content (average AV = 5.9%), (3) AR-8000 mixes with low air-void content (average AV = 3.4%), and (4) AR-8000 mixes (pooled). The associated data are listed in Table F.5 through Table F.8 respectively. Figure F.1 through Figure F.4 display the corresponding 95% confidence bands of $\ln(N_f)$. Figure F.5 compares the lower bounds of $\ln(N_f)$ for various mixes. As shown in this figure, the percent air-void content does not have a significant impact on the lower bounds of AR-8000 mixes. It is suggested that the lower bound of AR-8000 mixes (pooled) should be utilized for fatigue specification.

The PBA-6a* mixes have a wide confidence band compared with the AR-8000 mixes. The sample size to derive the confidence band for PBA-6a* is 31.

For fatigue specification, it is suggested that the mean of natural logarithm of fatigue life, $\ln(N_f)$, of three fatigue tests at the specified strain level should be above the specified lower bound and the regression line obtained from specified strain levels should be in the range above the lower bound.

Table F.2 lists the estimated lower and upper bounds of 95% confidence bands of $\ln(N_f)$ of PBA-6a* and AR-8000 mixes.

Table F.2: Lower and upper bounds of 95% Confidence Bands for $\ln(N_f)$ of PBA-6a* and AR-8000 Mixes

Test Strain (microstrain)	95% Confidence Band							
	PBA-6a* (Pooled)		AR-8000 (High AV)		AR-8000 (Low AV)		AR-8000 (Pooled)	
	Lower Bound	Upper Bound	Lower Bound	Upper Bound	Lower Bound	Upper Bound	Lower Bound	Upper Bound
100	17.8220	24.3084	17.8784	19.1473	17.6605	21.1894	17.9027	19.2383
150	16.7025	21.7569	15.8570	16.6905	15.7475	18.4109	15.9086	16.8636
200	15.8896	19.9653	14.3836	14.9866	14.3717	16.4273	14.4734	15.1991
300	14.6823	17.5016	12.1523	12.7397	12.3624	13.7271	12.3727	12.9309
400	13.7184	15.8610	10.4542	11.2605	10.8077	11.9404	10.7890	11.4149
500	12.8334	14.7258	9.1082	10.1420	9.4739	10.6824	9.5167	10.2829
600	11.9808	13.9276	8.0000	9.2364	8.3101	9.7285	8.4612	9.3739
700	11.1734	13.3395	7.0598	8.4741	7.2929	8.9553	7.5623	8.6119
800	10.4261	12.8778	6.2437	7.8154	6.3965	8.3007	6.7805	7.9549

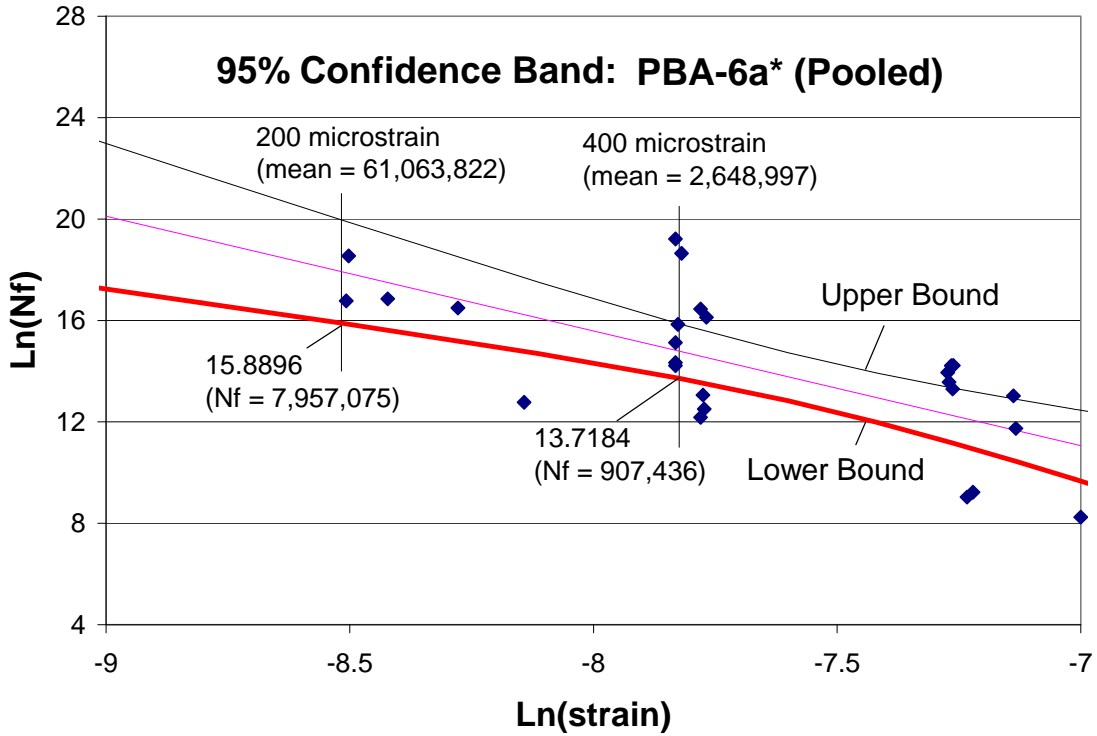


Figure F.1: 95% confidence band of PBA-6a* mixes (pooled).

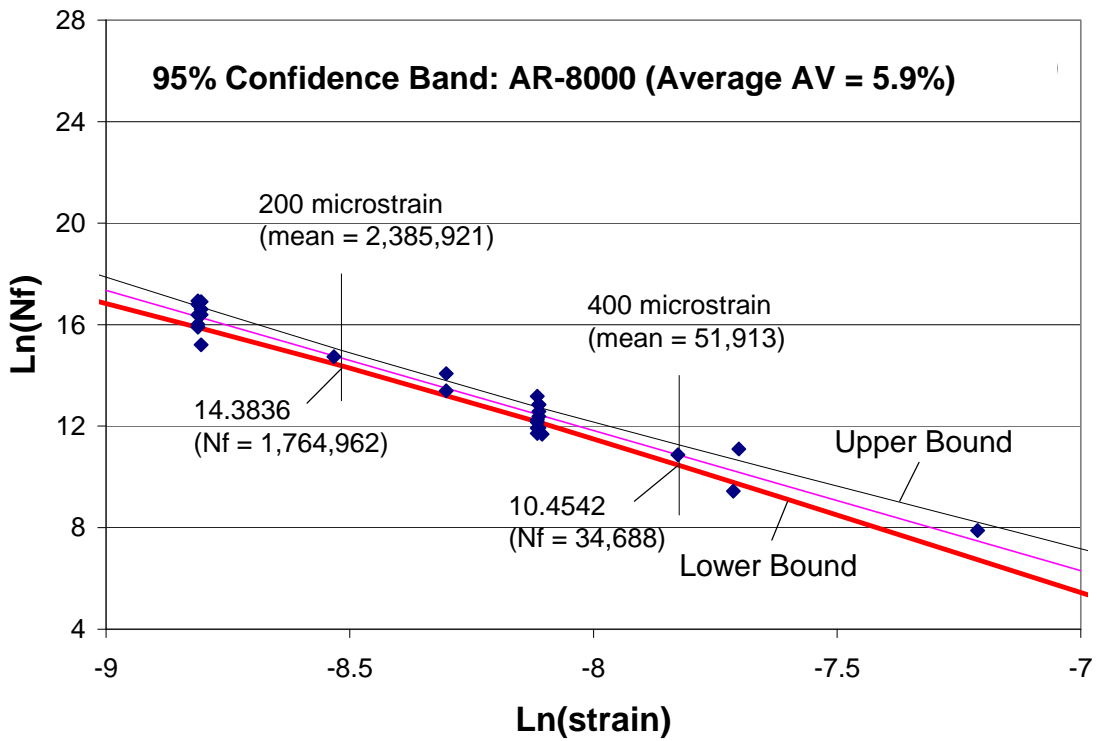


Figure F.2: 95% confidence band of AR-8000 mixes with high air-void content.

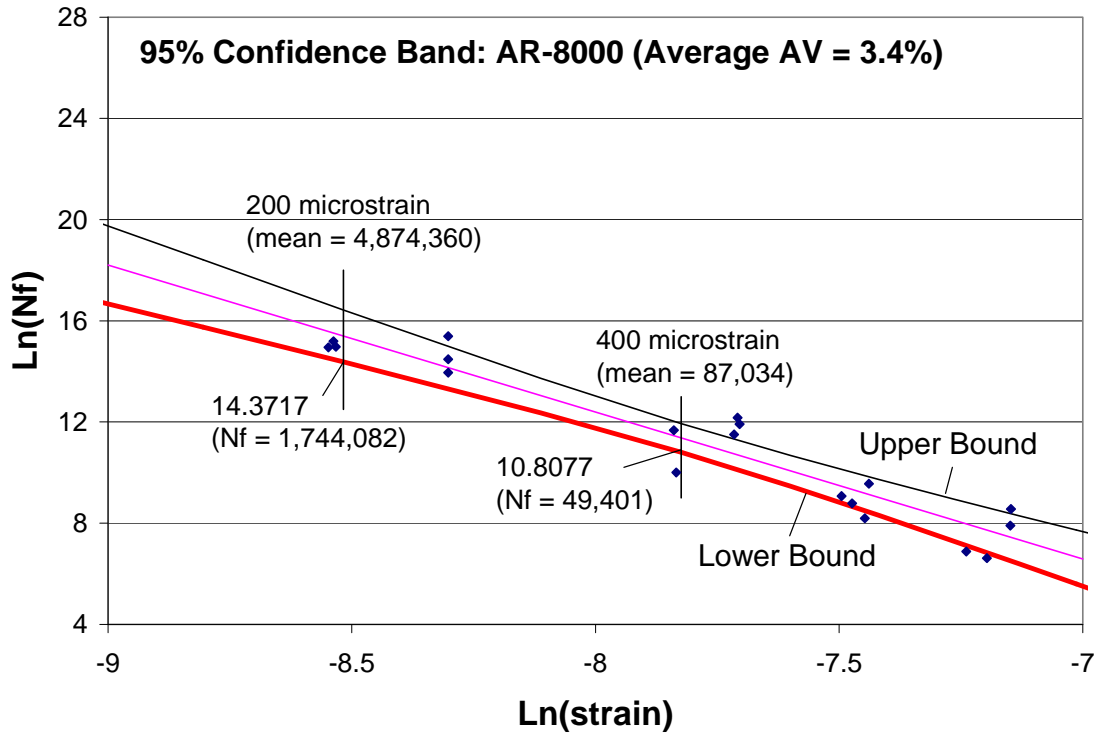


Figure F.3: 95% confidence band of AR-8000 mixes with low air-void content.

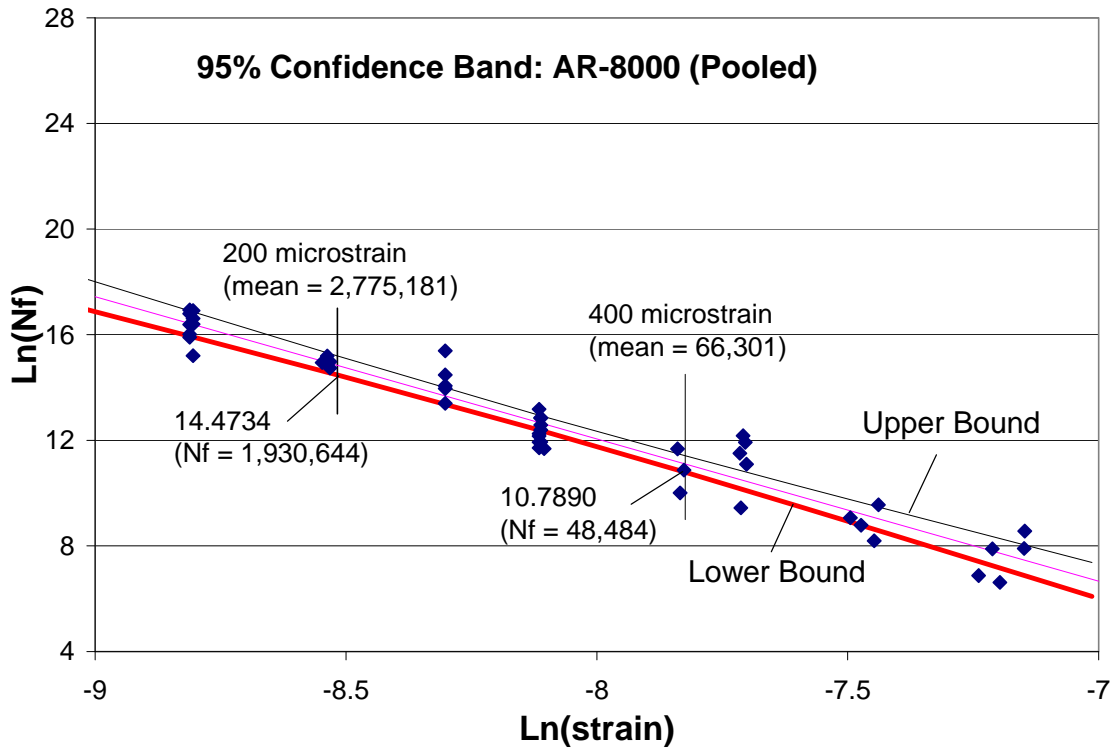


Figure F.4: 95% confidence band of AR-8000 mixes (pooled).

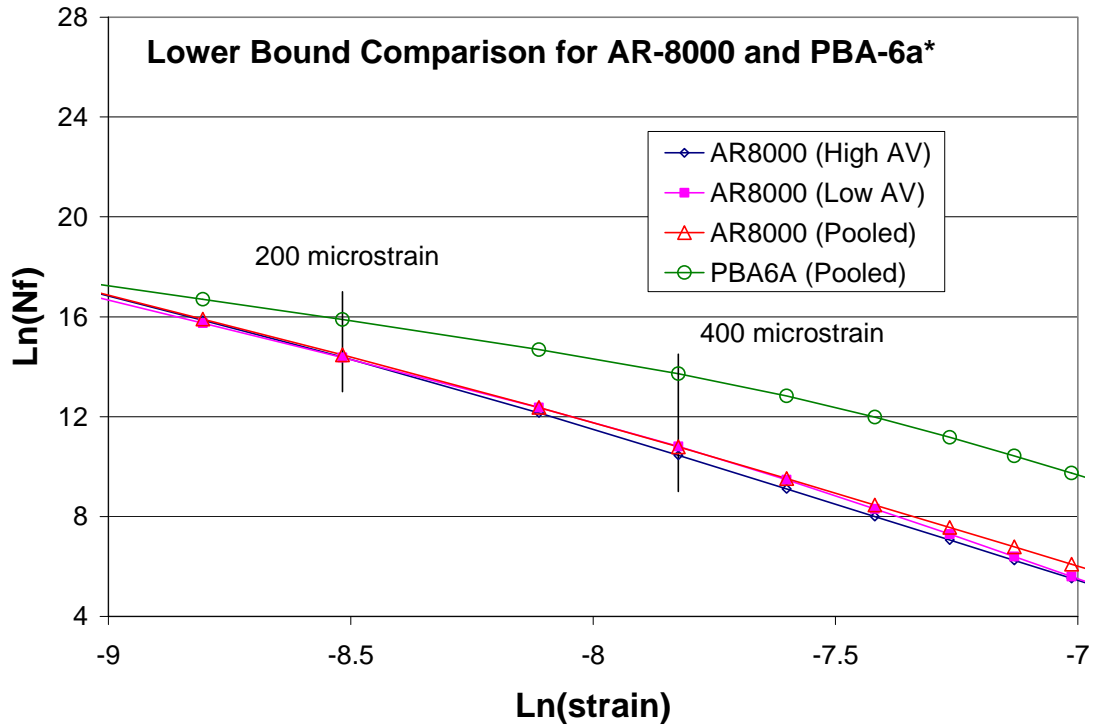


Figure F.5: Comparison of lower bound of 95% confidence band for AR-8000 and PBA-6a* mixes.

According to the lower bounds of 95% confidence bands of PBA-6a* and AR-8000 mixes as shown in Table F.3, we can specify the fatigue requirements as shown in following criteria:

1. The mean fatigue life of three fatigue tests at a specified test strain level should be satisfied the minimum requirements as listed in Table F.3.

Table F.3: Minimum Requirements of Fatigue Life

Strain Level (microstrain)	PBA-6a*	AR-8000
200	Nf > 7,957,075	Nf > 1,930,644
400	Nf > 907,436	Nf > 48,484

2. The regression line obtained from six fatigue tests (three replicates for each strain level) should be located above the specified lower bound as listed in Table F.4.

Table F.4: Lower Bounds of 95% Confidence Bands of Ln(Nf) of PBA-6a* and AR-8000 Mixes

Test Strain (microstrain)	95% Confidence Band	
	PBA-6a* (Pooled)	AR-8000 (Pooled)
	Lower Bound	Lower Bound
100	17.8220	17.9027
200	15.8896	14.4734
300	14.6823	12.3727
400	13.7184	10.7890
500	12.8334	9.5167
600	11.9808	8.4612
700	11.1734	7.5623
800	10.4261	6.7805

Table F.5: Fatigue Data of PBA-6a* Mixes (Pooled)

Specimen	Compaction	AV (%)	AC (%)	Temp. (C)	Test Strain	Initial Stiffness (MPa)	Fatigue Life
P47F21-CA	LMLC	5.5	4.7	20.0	0.000254	1098	14546777
P47F13-CA	LMLC	5.7	4.7	20.0	0.000397	1405	1680627
P47F22-CA	LMLC	5.1	4.7	20.0	0.000397	813	1487722
P47F22-CB	LMLC	5.0	4.7	20.0	0.000694	721	1139038
P47F13-CB	LMLC	5.3	4.7	20.0	0.000696	1242	783517
P47F21-CB	LMLC	4.4	4.7	20.0	0.000701	770	595154
P52F33-CA	LMLC	3.9	5.2	20.0	0.000399	1117	7615056
P52F32-CB	LMLC	3.4	5.2	20.0	0.000397	700	3695276
P52F33-CB	LMLC	3.6	5.2	20.0	0.000702	979	1499999
P52F32-CA	LMLC	2.9	5.2	20.0	0.000699	677	1486866
G601T	FMFC	6.7	5.0	20.6	0.000291	3381	350001
G606T	FMFC	6.2	5.0	19.8	0.000722	2678	8377
G604T	FMFC	6.1	5.0	19.5	0.000731	1738	10157
G605T	FMFC	4.9	5.0	19.2	0.000912	2947	3805
G603T	FMFC	5.6	5.0	19.4	0.000915	2886	3026
PB10A	FMLC	4.8	5.0	20.1	0.000418	1094	13984769
PB11A	FMLC	4.6	5.0	19.3	0.000423	1624	10091258
PB13A	FMLC	4.2	5.0	19.5	0.000397	1318	220439831
PB18B	FMLC	4.2	5.0	19.7	0.000402	1771	125217731
PB13B	FMLC	5.0	5.0	20.8	0.000798	1429	125744
PB06A	FMLC	5.2	5.0	19.8	0.000794	1426	455012
PB07A	FMLC	4.8	5.0	19.9	0.000982	1189	127259
PB04A	FMLC	4.8	5.0	20.3	0.000996	1169	73652
PB14B	FMLC	4.4	5.0	19.8	0.001192	1192	19791
PB01A	FMLC	5.1	5.0	19.8	0.001176	1390	14981
PG643413B	LMLC	6.2	5.0	19.5	0.000220	4434	20832465
PG643421A	LMLC	6.0	5.0	19.8	0.000203	2886	113499559
PG643423B	LMLC	6.1	5.0	20.9	0.000202	2782	19270127
PG643416B	LMLC	6.2	5.0	19.8	0.000421	3251	268926
PG64346B	LMLC	5.7	5.0	20.0	0.000418	3421	194881
PG643419A	LMLC	5.9	5.0	20.1	0.000420	3213	469028

Table F.6: Fatigue Data of AR-8000 Mixes with High Air-Void Content

Specimen	Compaction	AV (%)	AC (%)	Temp. (C)	Test Strain	Initial Stiffness (MPa)	Fatigue Life
C47F-2A	LMLC	6.0	4.7	20.0	0.000197	6684	2514516
C47F-1A	LMLC	6.7	4.7	20.0	0.000248	6085	1286696
C47F-2B	LMLC	5.4	4.7	20.0	0.000248	7279	656618
C47F-3B	LMLC	4.9	4.7	20.0	0.000452	6072	65950
C47F-3A	LMLC	4.5	4.7	20.0	0.000399	6660	52631
C47F-1B	LMLC	6.1	4.7	20.0	0.000447	5451	12600
710C47-7B	LMLC	5.7	4.7	20.0	0.000149	7695	22691381
710C47-3B	LMLC	6.0	4.7	20.0	0.000150	6877	13243391
710C47-6B	LMLC	6.3	4.7	20.0	0.000149	6817	13037942
710C47-5B	LMLC	5.9	4.7	20.0	0.000300	7490	290007
710C47-9B	LMLC	6.1	4.7	20.0	0.000300	7995	153181
710C47-4A	LMLC	6.2	4.7	20.0	0.000299	6459	151222
710C49-10B	LMLC	6.3	4.9	20.0	0.000150	6628	22049626
710C49-12B	LMLC	6.1	4.9	20.0	0.000149	5463	19626061
710C49-6B	LMLC	5.8	4.9	20.0	0.000150	6644	16415187
710C49-3A	LMLC	5.8	4.9	20.0	0.000300	6754	383186
710C49-14B	LMLC	5.9	4.9	20.0	0.000299	6534	527228
710C49-8B	LMLC	6.1	4.9	20.0	0.000300	7294	376403
710C49-13A	LMLC	6.3	4.9	20.0	0.000300	6058	240378
710CF-8A	FMLC	6.0	4.9	20.0	0.000149	4693	8999999
710CF-4A	FMLC	6.1	4.9	20.0	0.000149	5434	8016780
710CF-5B	FMLC	6.0	4.9	20.0	0.000150	5236	3999999
710CF-3A	FMLC	6.3	4.9	20.0	0.000299	5600	209264
710CF-10A	FMLC	5.9	4.9	20.0	0.000299	4619	189972
710CF-4B	FMLC	6.4	4.9	20.0	0.000299	5298	122129
710CF-5A	FMLC	5.9	4.9	20.0	0.000302	5455	118481
G608B	FMFC	4.8	5.2	19.7	0.000738	8264	2661

Table F.7: Fatigue Data of AR-8000 Mixes with Low Air-Void Content

Specimen	Compaction	AV (%)	AC (%)	Temp. (C)	Test Strain	Initial Stiffness (MPa)	Fatigue Life
C52F-1A	LMLC	3.6	5.2	20.0	0.000248	6319	4823471
C52F-2A	LMLC	3.2	5.2	20.0	0.000248	7091	1939332
C52F-3A	LMLC	3.0	5.2	20.0	0.000248	7933	1148394
C52F-2B	LMLC	3.4	5.2	20.0	0.000449	6358	193685
C52F-3B	LMLC	3.0	5.2	20.0	0.000451	5897	149999
C52F-1B	LMLC	2.7	5.2	20.0	0.000446	7789	99549
G609B	FMFC	4.1	5.2	20.3	0.000194	8242	3099997
G607B	FMFC	3.6	5.2	19.3	0.000556	7842	8689
G604B	FMFC	3.7	5.2	20.9	0.000568	8046	6548
G601B	FMFC	3.3	5.2	20.8	0.000718	7990	972
G603B	FMFC	3.1	5.2	20.7	0.000749	6815	750
AR32A	FMLC	3.7	5.2	19.9	0.000196	9993	3949978
AR31B	FMLC	3.4	5.2	20.1	0.000197	11545	3178281
AR05B	FMLC	3.6	5.2	20.2	0.000396	10770	22156
AR07A	FMLC	3.2	5.2	20.2	0.000394	10790	117543
AR24B	FMLC	3.9	5.2	20.6	0.000588	10643	14134
AR07B	FMLC	3.3	5.2	20.8	0.000583	10320	3619
AR20A	FMLC	3.7	5.2	20.5	0.000787	8861	5215
AR08B	FMLC	3.7	5.2	20.6	0.000786	9729	2706

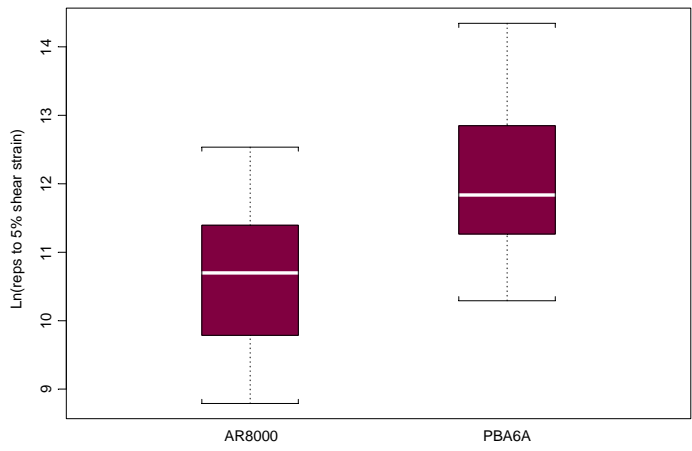
Table F.8: Fatigue Data of AR-8000 Mixes (Pooled)

Specimen	Compaction	AV (%)	AC (%)	Temp. (C)	Test Strain	Initial Stiffness (MPa)	Fatigue Life
C47F-2A	LMLC	6.0	4.7	20.0	0.000197	6684	2514516
C47F-1A	LMLC	6.7	4.7	20.0	0.000248	6085	1286696
C47F-2B	LMLC	5.4	4.7	20.0	0.000248	7279	656618
C47F-3B	LMLC	4.9	4.7	20.0	0.000452	6072	65950
C47F-3A	LMLC	4.5	4.7	20.0	0.000399	6660	52631
C47F-1B	LMLC	6.1	4.7	20.0	0.000447	5451	12600
710C47-7B	LMLC	5.7	4.7	20.0	0.000149	7695	22691381
710C47-3B	LMLC	6.0	4.7	20.0	0.000150	6877	13243391
710C47-6B	LMLC	6.3	4.7	20.0	0.000149	6817	13037942
710C47-5B	LMLC	5.9	4.7	20.0	0.000300	7490	290007
710C47-9B	LMLC	6.1	4.7	20.0	0.000300	7995	153181
710C47-4A	LMLC	6.2	4.7	20.0	0.000299	6459	151222
710C49-10B	LMLC	6.3	4.9	20.0	0.000150	6628	22049626
710C49-12B	LMLC	6.1	4.9	20.0	0.000149	5463	19626061
710C49-6B	LMLC	5.8	4.9	20.0	0.000150	6644	16415187
710C49-3A	LMLC	5.8	4.9	20.0	0.000300	6754	383186
710C49-14B	LMLC	5.9	4.9	20.0	0.000299	6534	527228
710C49-8B	LMLC	6.1	4.9	20.0	0.000300	7294	376403
710C49-13A	LMLC	6.3	4.9	20.0	0.000300	6058	240378
710CF-8A	FMLC	6.0	4.9	20.0	0.000149	4693	8999999
710CF-4A	FMLC	6.1	4.9	20.0	0.000149	5434	8016780
710CF-5B	FMLC	6.0	4.9	20.0	0.000150	5236	3999999
710CF-3A	FMLC	6.3	4.9	20.0	0.000299	5600	209264
710CF-10A	FMLC	5.9	4.9	20.0	0.000299	4619	189972
710CF-4B	FMLC	6.4	4.9	20.0	0.000299	5298	122129
710CF-5A	FMLC	5.9	4.9	20.0	0.000302	5455	118481
C52F-1A	LMLC	3.6	5.2	20.0	0.000248	6319	4823471
C52F-2A	LMLC	3.2	5.2	20.0	0.000248	7091	1939332
C52F-3A	LMLC	3.0	5.2	20.0	0.000248	7933	1148394
C52F-2B	LMLC	3.4	5.2	20.0	0.000449	6358	193685
C52F-3B	LMLC	3.0	5.2	20.0	0.000451	5897	149999
C52F-1B	LMLC	2.7	5.2	20.0	0.000446	7789	99549
G609B	FMFC	4.1	5.2	20.3	0.000194	8242	3099997
G607B	FMFC	3.6	5.2	19.3	0.000556	7842	8689
G604B	FMFC	3.7	5.2	20.9	0.000568	8046	6548
G601B	FMFC	3.3	5.2	20.8	0.000718	7990	972
G608B	FMFC	4.8	5.2	19.7	0.000738	8264	2661
G603B	FMFC	3.1	5.2	20.7	0.000749	6815	750
AR32A	FMLC	3.7	5.2	19.9	0.000196	9993	3949978
AR31B	FMLC	3.4	5.2	20.1	0.000197	11545	3178281
AR05B	FMLC	3.6	5.2	20.2	0.000396	10770	22156
AR07A	FMLC	3.2	5.2	20.2	0.000394	10790	117543
AR24B	FMLC	3.9	5.2	20.6	0.000588	10643	14134
AR07B	FMLC	3.3	5.2	20.8	0.000583	10320	3619
AR20A	FMLC	3.7	5.2	20.5	0.000787	8861	5215
AR08B	FMLC	3.7	5.2	20.6	0.000786	9729	2706

F.3 S-Plus Analysis

(The following analysis has been included for illustrative purposes; It is not necessary for detailed study since the results have been extracted and incorporated in the preceding discussion.)

```
=====
Permanent Deformation Specification
=====
> cshear<-i710shear[1:9,]
> pshear<-i710shear[10:22,]
> dim(cshear)
[1] 9 4
> dim(pshear)
[1] 13 4
>
> boxplot(log(cshear$rep5),log(pshear$rep5),names=c("AR8000","PBA6A"),ylab="Ln(reps to 5% shear strain)")
>
```



```
> cshear
  name av ac rep5
1 C52-11 2.7 5.2 17773
2 C52-12 2.9 5.2 10574
3 C52-21 3.4 5.2 44286
4 C47-11 4.8 4.7 150356
5 C47-21 3.4 4.7 88852
6 C47-22 2.5 4.7 277996
7 C42-12 5.1 4.2 6568
8 C42-22 4.8 4.2 34797
9 C42-23 4.7 4.2 66658
> pshear
  name av ac rep5
10 P52-33 1.9 5.2 29496
11 P52-31 2.4 5.2 306433
12 P52-22 4.2 5.2 379947
```

```

13 P52-12 6.7 5.2 138309
14 P52-13 6.9 5.2 78228
15 P47-12 1.8 4.7 75122
16 P47-22 3.5 4.7 1695614
17 P47-23 4.0 4.7 757464
18 P42-21 4.4 4.2 29965
19 P42-23 4.9 4.2 93071
20 P42-33 5.7 4.2 676348
21 P42-13 6.0 4.2 117248
22 P42-11 6.3 4.2 205525

```

```
>
```

```
=====
95% Confidence Interval
=====
```

```
>
```

```
> ### AR8000 Shear ###
```

```
>
```

```
> y<-log(cshear$rep5)
```

```
> meany<-mean(y)
```

```
> meany
```

```
[1] 10.66172
```

```
> s<-sqrt(var(y))
```

```
> s
```

```
[1] 1.229516
```

```
> se<-s/sqrt(length(y))
```

```
> se
```

```
[1] 0.4098386
```

```
>
```

```
> meany-qt(0.975,8)*se
```

```
[1] 9.716626
```

```
> meany+qt(0.975,8)*se
```

```
[1] 11.60681
```

```
>
```

```
> exp(9.716626)
```

```
[1] 16591.17
```

```
> exp(11.60681)
```

```
[1] 109843.3
```

```
> exp(10.66172)
```

```
[1] 42690
```

```
>
```

```
>
```

```
> ### PBA6A ###
```

```
>
```

```
> y<-log(pshear$rep5)
```

```
> meany<-mean(y)
```

```
> meany
```

```
[1] 12.08185
```

```
> s<-sqrt(var(y))
```

```
> s
```

```
[1] 1.236059
> se<-s/sqrt(length(y))
> se
[1] 0.3428211
>
> meany-qt(0.975,12)*se
[1] 11.33491
> meany+qt(0.975,12)*se
[1] 12.82879
>
> exp(11.33491)
[1] 83692.95
> exp(12.82879)
[1] 372797.3
>
> exp(12.08185)
[1] 176636.6
>
```


=====
Fatigue Specification
=====

```
> pba6a<-split(i710fat,i710fat$binder)$PBA6A  
> ar8000<-split(i710fat,i710fat$binder)$AR8000  
>
```

=====
Construct the 95% confidence band for PBA6A fatigue data (pooled)
=====

```
> pba6a  
      name binder comp av ac temp   lnstn   lns0   lnnf  
47 P47F21-CA PBA6A LMLC 5.5 4.7 20.0 -8.278176 7.001246 16.492880  
48 P47F13-CA PBA6A LMLC 5.7 4.7 20.0 -7.831574 7.247793 14.334678  
49 P47F22-CA PBA6A LMLC 5.1 4.7 20.0 -7.831574 6.700731 14.212757  
50 P47F22-CB PBA6A LMLC 5.0 4.7 20.0 -7.273039 6.580639 13.945695  
51 P47F13-CB PBA6A LMLC 5.3 4.7 20.0 -7.270161 7.124478 13.571548  
52 P47F21-CB PBA6A LMLC 4.4 4.7 20.0 -7.263003 6.646391 13.296575  
53 P52F33-CA PBA6A LMLC 3.9 5.2 20.0 -7.826549 7.018402 15.845638  
54 P52F32-CB PBA6A LMLC 3.4 5.2 20.0 -7.831574 6.551080 15.122566  
55 P52F33-CB PBA6A LMLC 3.6 5.2 20.0 -7.261577 6.886532 14.220975  
56 P52F32-CA PBA6A LMLC 2.9 5.2 20.0 -7.265860 6.517671 14.212181  
57 G601T PBA6A FMFC 6.7 5.0 20.6 -8.142187 8.125927 12.765691  
58 G606T PBA6A FMFC 6.2 5.0 19.8 -7.233485 7.892826 9.033245  
59 G604T PBA6A FMFC 6.1 5.0 19.5 -7.221097 7.460490 9.225918  
60 G605T PBA6A FMFC 4.9 5.0 19.2 -6.999871 7.988543 8.244071  
61 G603T PBA6A FMFC 5.6 5.0 19.4 -6.996586 7.967627 8.014997  
62 PB10A PBA6A FMLC 4.8 5.0 20.1 -7.780029 6.997596 16.453479  
63 PB11A PBA6A FMLC 4.6 5.0 19.3 -7.768138 7.392648 16.127180  
64 PB13A PBA6A FMLC 4.2 5.0 19.5 -7.831574 7.183871 19.211135  
65 PB18B PBA6A FMLC 4.2 5.0 19.7 -7.819058 7.479300 18.645565  
66 PB13B PBA6A FMLC 5.0 5.0 20.8 -7.133402 7.264730 11.742003  
67 PB06A PBA6A FMLC 5.2 5.0 19.8 -7.138427 7.262629 13.028079  
68 PB07A PBA6A FMLC 4.8 5.0 19.9 -6.925919 7.080868 11.753980  
69 PB04A PBA6A FMLC 4.8 5.0 20.3 -6.911763 7.063904 11.207107  
70 PB14B PBA6A FMLC 4.4 5.0 19.8 -6.732123 7.083388 9.892983  
71 PB01A PBA6A FMLC 5.1 5.0 19.8 -6.745636 7.237059 9.614538  
72 PG643413B PBA6A LMLC 6.2 5.0 19.5 -8.421883 8.397053 16.852023  
73 PG643421A PBA6A LMLC 6.0 5.0 19.8 -8.502305 7.967453 18.547310  
74 PG643423B PBA6A LMLC 6.1 5.0 20.9 -8.507243 7.931008 16.774067  
75 PG643416B PBA6A LMLC 6.2 5.0 19.8 -7.772878 8.086718 12.502192  
76 PG64346B PBA6A LMLC 5.7 5.0 20.0 -7.780029 8.137554 12.180144  
77 PG643419A PBA6A LMLC 5.9 5.0 20.1 -7.775256 8.049666 13.058418  
>  
> lnstn<-pba6a$lnstn  
> lnnf<-pba6a$lnnf  
> xxx.lm<-lm(lnnf~lnstn)  
> summary(xxx.lm)
```

```
Call: lm(formula = lnxf ~ lnstn)
```

```
Residuals:
```

```
   Min     1Q  Median     3Q    Max
-3.464 -1.31  0.07851  1.315  4.387
```

```
Coefficients:
```

```
                Value Std. Error  t value Pr(>|t|)
(Intercept) -20.6282    5.4850   -3.7608  0.0008
      lnstn   -4.5268    0.7248   -6.2455  0.0000
```

```
Residual standard error: 2.032 on 29 degrees of freedom
```

```
Multiple R-Squared: 0.5736
```

```
F-statistic: 39.01 on 1 and 29 degrees of freedom, the p-value is 8.14e-007
```

```
Correlation of Coefficients:
```

```
      (Intercept)
lnstn 0.9978
>
> xb<-mean(lnstn)
> xi<-lnstn
> x0<-log(seq(0.0001,0.001,length=10))
> y0h<--20.6282-4.5268*x0
> qf(0.95,2,29)
[1] 3.327654
> s2y0h<-2.032^2*(1/31+(x0-xb)^2/sum((xi-xb)^2))
>
> lowerbound<-y0h-sqrt(2*qf(0.95,2,29))*sqrt(s2y0h)
> upperbound<-y0h+sqrt(2*qf(0.95,2,29))*sqrt(s2y0h)
> lowerbound
[1] 17.821991 15.889572 14.682336 13.718378 12.833384 11.980837 11.173354 10.426089  9.741430
[10]  9.114729
> upperbound
[1] 24.30835 19.96529 17.50161 15.86101 14.72575 13.92763 13.33949 12.87782 12.49612 12.16892
>>
> #
> # 150 microstrain
> #
> 2.032^2*(1/31+(log(0.00015)-xb)^2/sum((xi-xb)^2))
[1] 0.9596584
> -20.6282-4.5268*log(0.00015)-sqrt(2*qf(0.95,2,29))*sqrt(0.9596584)
[1] 16.70249
> -20.6282-4.5268*log(0.00015)+sqrt(2*qf(0.95,2,29))*sqrt(0.9596584)
[1] 21.75693
>
=====
Construct the 95% confidence band for AR8000 fatigue data (av >= 4.5%)
=====
> ar80001<-ar8000[ar8000$av>=4.5,]
```

```

> ar80002<-ar8000[ar8000$av<4.5,]
> length(ar80001$av)
[1] 27
> length(ar80002$av)
[1] 19
>
> ar80001
      name binder comp  av  ac temp   lnstn   lns0   lnnf
1   C47F-2A AR8000 LMLC 6.0 4.7 20.0 -8.532307 8.807472 14.737591
2   C47F-1A AR8000 LMLC 6.7 4.7 20.0 -8.302082 8.713582 14.067588
3   C47F-2B AR8000 LMLC 5.4 4.7 20.0 -8.302082 8.892749 13.394858
4   C47F-3B AR8000 LMLC 4.9 4.7 20.0 -7.701828 8.711443 11.096652
5   C47F-3A AR8000 LMLC 4.5 4.7 20.0 -7.826549 8.803875 10.871061
6   C47F-1B AR8000 LMLC 6.1 4.7 20.0 -7.712952 8.603554  9.441452
7  710C47-7B AR8000 LMLC 5.7 4.7 20.0 -8.811564 8.948326 16.937496
8  710C47-3B AR8000 LMLC 6.0 4.7 20.0 -8.804875 8.835938 16.399009
9  710C47-6B AR8000 LMLC 6.3 4.7 20.0 -8.811564 8.827175 16.383374
10 710C47-5B AR8000 LMLC 5.9 4.7 20.0 -8.111728 8.921324 12.577660
11 710C47-9B AR8000 LMLC 6.1 4.7 20.0 -8.111728 8.986572 11.939376
12 710C47-4A AR8000 LMLC 6.2 4.7 20.0 -8.115067 8.773230 11.926504
13 710C49-10B AR8000 LMLC 6.3 4.9 20.0 -8.804875 8.799058 16.908806
14 710C49-12B AR8000 LMLC 6.1 4.9 20.0 -8.811564 8.605753 16.792369
15 710C49-6B AR8000 LMLC 5.8 4.9 20.0 -8.804875 8.801469 16.613718
16 710C49-3A AR8000 LMLC 5.8 4.9 20.0 -8.111728 8.817890 12.856276
17 710C49-14B AR8000 LMLC 5.9 4.9 20.0 -8.115067 8.784775 13.175388
18 710C49-8B AR8000 LMLC 6.1 4.9 20.0 -8.111728 8.894807 12.838416
19 710C49-13A AR8000 LMLC 6.3 4.9 20.0 -8.111728 8.709135 12.389968
20 710CF-8A AR8000 FMLC 6.0 4.9 20.0 -8.811564 8.509766 16.012735
21 710CF-4A AR8000 FMLC 6.1 4.9 20.0 -8.811564 8.600431 15.897047
22 710CF-5B AR8000 FMLC 6.0 4.9 20.0 -8.804875 8.563313 15.201805
23 710CF-3A AR8000 FMLC 6.3 4.9 20.0 -8.115067 8.630522 12.251352
24 710CF-10A AR8000 FMLC 5.9 4.9 20.0 -8.115067 8.437934 12.154632
25 710CF-4B AR8000 FMLC 6.4 4.9 20.0 -8.115067 8.575085 11.712833
26 710CF-5A AR8000 FMLC 5.9 4.9 20.0 -8.105084 8.604288 11.682508
37   G608B AR8000 FMFC 4.8 5.2 19.7 -7.211567 9.019664  7.886457
>
> range(ar80001$lnstn)
[1] -8.811564 -7.211567
> exp(range(ar80001$lnstn))
[1] 0.000149 0.000738
> range(ar80001$lnnf)
[1] 7.886457 16.937496
>
> lnstn<-ar80001$lnstn
> lnnf<-ar80001$lnnf
>
> ar80001.lm<-lm(lnnf~lnstn)
> summary(ar80001.lm)

```

Call: lm(formula = lnnf ~ lnstn)

Residuals:

Min	1Q	Median	3Q	Max
-1.072	-0.3618	-0.000147	0.4108	0.9142

Coefficients:

	Value	Std. Error	t value	Pr(> t)
(Intercept)	-32.3494	2.0175	-16.0346	0.0000
lnstn	-5.5223	0.2427	-22.7494	0.0000

Residual standard error: 0.5362 on 25 degrees of freedom

Multiple R-Squared: 0.9539

F-statistic: 517.5 on 1 and 25 degrees of freedom, the p-value is 0

Correlation of Coefficients:

```
(Intercept)
lnstn 0.9987
>
> xb<-mean(lnstn)
> xi<-lnstn
> x0<-log(seq(0.0001,0.001,length=10))
>
> y0h<--32.3494-5.5223*x0
> qf(0.95,2,25)
[1] 3.38519
> s2y0h<-0.5362^2*(1/27+(x0-xb)^2/sum((xi-xb)^2))
>
> lowerbound<-y0h-sqrt(2*qf(0.95,2,25))*sqrt(s2y0h)
> upperbound<-y0h+sqrt(2*qf(0.95,2,25))*sqrt(s2y0h)
> lowerbound
[1] 17.878408 14.383640 12.152284 10.454162 9.108169 8.000034 7.059804 6.243728 5.523003
[10] 4.877745
> upperbound
[1] 19.147317 14.986552 12.739708 11.260496 10.141959 9.236424 8.474122 7.815397 7.235256
[10] 6.716849
> exp(x0)
[1] 0.0001 0.0002 0.0003 0.0004 0.0005 0.0006 0.0007 0.0008 0.0009 0.0010
>
#
# 150 microstrain
#
> 0.5362^2*(1/27+(log(0.00015)-xb)^2/sum((xi-xb)^2))
[1] 0.02565487
> -32.3494-5.5223*log(0.00015)-sqrt(2*qf(0.95,2,25))*sqrt(0.02565487)
[1] 15.857
> -32.3494-5.5223*log(0.00015)+sqrt(2*qf(0.95,2,25))*sqrt(0.02565487)
[1] 16.69053
>
```

Construct the 95% confidence band for AR8000 fatigue data (av < 4.5%)

=====

```
> ar80002
      name binder comp av ac temp   lnstn   lns0   lnnf
27 C52F-1A AR8000 LMLC 3.6 5.2 20.0 -8.302082 8.751316 15.389004
28 C52F-2A AR8000 LMLC 3.2 5.2 20.0 -8.302082 8.866582 14.477854
29 C52F-3A AR8000 LMLC 3.0 5.2 20.0 -8.302082 8.978787 13.953875
30 C52F-2B AR8000 LMLC 3.4 5.2 20.0 -7.708488 8.757469 12.173988
31 C52F-3B AR8000 LMLC 3.0 5.2 20.0 -7.704043 8.682199 11.918384
32 C52F-1B AR8000 LMLC 2.7 5.2 20.0 -7.715192 8.960468 11.508405
33 G609B AR8000 FMFC 4.1 5.2 20.3 -8.547652 9.016998 14.946912
34 G607B AR8000 FMFC 3.6 5.2 19.3 -7.494742 8.967249 9.069813
35 G604B AR8000 FMFC 3.7 5.2 20.9 -7.473389 8.992930 8.786915
36 G601B AR8000 FMFC 3.3 5.2 20.8 -7.239041 8.985946 6.879356
38 G603B AR8000 FMFC 3.1 5.2 20.7 -7.196772 8.826881 6.620073
39 AR32A AR8000 FMLC 3.7 5.2 19.9 -8.537396 9.209640 15.189221
40 AR31B AR8000 FMLC 3.4 5.2 20.1 -8.532307 9.354008 14.971851
41 AR05B AR8000 FMLC 3.6 5.2 20.2 -7.834096 9.284520 10.005864
42 AR07A AR8000 FMLC 3.2 5.2 20.2 -7.839160 9.286375 11.674560
43 AR24B AR8000 FMLC 3.9 5.2 20.6 -7.438784 9.272658 9.556339
44 AR07B AR8000 FMLC 3.3 5.2 20.8 -7.447323 9.241839 8.193953
45 AR20A AR8000 FMLC 3.7 5.2 20.5 -7.147282 9.089415 8.559294
46 AR08B AR8000 FMLC 3.7 5.2 20.6 -7.148554 9.182866 7.903227
>
> range(ar80002$lnstn)
[1] -8.547652 -7.147282
> exp(range(ar80002$lnstn))
[1] 0.000194 0.000787
> range(ar80002$lnnf)
[1] 6.620073 15.389004
>
> lnstn<-ar80002$lnstn
> lnnf<-ar80002$lnnf
>
> ar80002.lm<-lm(lnnf~lnstn)
> summary(ar80002.lm)
```

Call: lm(formula = lnnf ~ lnstn)

Residuals:

Min	1Q	Median	3Q	Max
-1.427	-0.5905	-0.1967	0.609	1.471

Coefficients:

	Value	Std. Error	t value	Pr(> t)
(Intercept)	-34.0641	3.4127	-9.9815	0.0000
lnstn	-5.8075	0.4376	-13.2728	0.0000

Residual standard error: 0.918 on 17 degrees of freedom

Multiple R-Squared: 0.912

F-statistic: 176.2 on 1 and 17 degrees of freedom, the p-value is 2.121e-010

Correlation of Coefficients:

```
(Intercept)
lnstn 0.9981
>
> xb<-mean(lnstn)
> xi<-lnstn
> x0<-log(seq(0.0001,0.001,length=10))
>
> y0h<--34.0641-5.8075*x0
> qf(0.95,2,17)
[1] 3.591531
> s2y0h<-0.918^2*(1/19+(x0-xb)^2/sum((xi-xb)^2))
>
> lowerbound<-y0h-sqrt(2*qf(0.95,2,17))*sqrt(s2y0h)
> upperbound<-y0h+sqrt(2*qf(0.95,2,17))*sqrt(s2y0h)
> lowerbound
[1] 17.660517 14.371739 12.362406 10.807727 9.473921 8.310094 7.292872 6.396485 5.598082
[10] 4.879547
> upperbound
[1] 21.189387 16.427260 13.727115 11.940368 10.682361 9.728523 8.955285 8.300705 7.731058
[10] 7.225830
> exp(x0)
[1] 0.0001 0.0002 0.0003 0.0004 0.0005 0.0006 0.0007 0.0008 0.0009 0.0010
>
#
# 150 microstrain
#
> 0.918^2*(1/19+(log(0.00015)-xb)^2/sum((xi-xb)^2))
[1] 0.2435727
> -34.0641-5.8075*log(0.00015)-sqrt(2*qf(0.95,2,17))*sqrt(0.2435727)
[1] 15.74749
> -34.0461-5.8075*log(0.00015)+sqrt(2*qf(0.95,2,17))*sqrt(0.2435727)
[1] 18.41094
>
```

```
=====
Construct the 95% confidence band for AR8000 fatigue data (pooled with AR8000 richbottom)
=====
```

```
> lnstn<-ar8000$lnstn
> lnnf<-ar8000$ltnf
> ar8000.lm<-lm(lnnf~lnstn)
> summary(ar8000.lm)
```

```
Call: lm(formula = lnnf ~ lnstn)
Residuals:
    Min       1Q   Median       3Q      Max
```

```
-1.184 -0.4927 -0.01276 0.4786 1.712
```

Coefficients:

```
          Value Std. Error  t value Pr(>|t|)
(Intercept) -31.0493    1.7282  -17.9659  0.0000
          lnstn  -5.3874    0.2133  -25.2616  0.0000
```

Residual standard error: 0.7463 on 44 degrees of freedom

Multiple R-Squared: 0.9355

F-statistic: 638.1 on 1 and 44 degrees of freedom, the p-value is 0

Correlation of Coefficients:

```
(Intercept)
lnstn 0.998
```

```
>
```

```
> range(lnstn)
```

```
[1] -8.811564 -7.147282
```

```
> exp(range(lnstn))
```

```
[1] 0.000149 0.000787
```

```
> length(lnstn)
```

```
[1] 46
```

```
> xb<-mean(lnstn)
```

```
> xi<-lnstn
```

```
> x0<-log(seq(0.0001,0.001,length=10))
```

```
>
```

```
> s2yoh<-0.7463^2*(1/46+(x0-xb)^2/sum((xi-xb)^2))
```

```
> y0h<--31.0493-5.3874*x0
```

```
> qf(0.95,2,44)
```

```
[1] 3.209278
```

```
> s2y0h<-0.7463^2*(1/46+(x0-xb)^2/sum((xi-xb)^2))
```

```
>
```

```
> lowerbound<-y0h-sqrt(2*qf(0.95,2,44))*sqrt(s2y0h)
```

```
> upperbound<-y0h+sqrt(2*qf(0.95,2,44))*sqrt(s2y0h)
```

```
> lowerbound
```

```
[1] 17.902707 14.473364 12.372737 10.788996 9.516670 8.461188 7.562298 6.780529 6.089264
```

```
[10] 5.469891
```

```
> upperbound
```

```
[1] 19.238269 15.199089 12.930911 11.414935 10.282934 9.373937 8.611885 7.954879 7.377056
```

```
[10] 6.861191
```

```
> exp(x0)
```

```
[1] 0.0001 0.0002 0.0003 0.0004 0.0005 0.0006 0.0007 0.0008 0.0009 0.0010
```

```
>
```

```
> plot(lnstn,lnnf,type="n",xlab="Ln(stn)",ylab="Ln(Nf)",ylim=c(6,18),xlim=c(-9,-7),main="95% Confidence Band: AR8000 Mixes")
```

```
> points(lnstn,lnnf,pch="x")
```

```
> abline(ar8000.lm$coef)
```

```
> lines(x0,lowerbound)
```

```
> lines(x0,upperbound)

#
# 150 microstrain
#
> 0.7463^2*(1/46+(log(0.00015)-xb)^2/sum((xi-xb)^2))
[1] 0.03552893
> -31.0493-5.3874*log(0.00015)-sqrt(2*gf(0.95,2,44))*sqrt(0.03552893)
[1] 15.90855
> -31.0493-5.3874*log(0.00015)+sqrt(2*gf(0.95,2,44))*sqrt(0.03552893)
[1] 16.86362
>
```


F.4 Statistical Simulation

Given: A normal $N(\mu, \sigma)$ distribution with mean μ and variance σ^2 and a lower limit, usually is set up as $\mu - 1.960 \cdot \sigma$ (say, 95% of population).

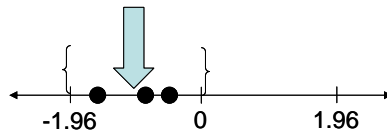
Objective: If three samples were selected from this population with replacement, then estimates of the probability indicate that the mean and lower limit of each sample complies with the following::

- (1) the mean should be in the range of $(\mu - 1.960 \cdot \sigma, \mu)$, and
- (2) For each sample x_i , $x_i \geq$ lower limit $(\mu - 1.960 \cdot \sigma)$.

F.4.1 Simulation Approach

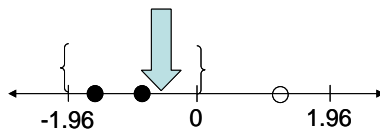
1. Standardize the normal $N(\mu, \sigma)$ distribution through the formulation $z = \frac{x - \mu}{\sigma}$; therefore, the above two conditions become:
 - (1) the mean should be in the range of $(-1.960, 0)$, and
 - (2) for each sample z_i , $z_i \geq$ lower limit (-1.960) .
2. Generate a standard normal distribution with population size n .
3. Randomly pick up three samples from the distribution with replacement.
4. For the three samples check if the conditions are met
 - (1) If the conditions are satisfied, then we cumulate the counts for the following three cases:
Case #1: all three z_i s are in the range of $(-1.960, 0)$

Average of three samples



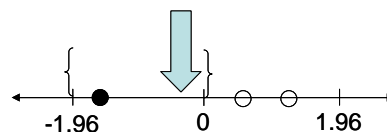
Case #2: two z_i s are in the range of $(-1.960, 0)$

Average of three samples



5. Case #3: only one z_i is in the range of $(-1.960, 0)$

Average of three samples



- (2) If the conditions are not satisfied, then we cumulate the counts and category this situation as the case #4.
6. Repeat steps 3 and 4 until reach the specified iterations.
 7. Report the result.

Simulation Results (S-Plus log not included)

Table F.9: Simulation Summary

	95 % (-1.96, 1.96)				90% (-1.645, 1.645)			
	Population = 1,000,000; iterations = 100,000				Population = 1,000,000; iterations = 100,000			
	Case #1	Case #2	Case #3	Case #4	Case #1	Case #2	Case #3	Case #4
1	10895	25609	6609	56887	9105	22284	5382	63229
2	10801	25734	6655	56810	9023	22353	5448	63176
3	10451	25789	6770	56990	9252	22421	5486	62841
4	10598	25658	6605	57139	8224	22328	5566	62882
5	10507	25800	6474	57219	9124	22422	5501	62953
6	10658	25935	6657	56750	9193	22237	5465	63105
7	10692	25795	6736	56777	9366	22406	5388	62840
8	10698	25675	6471	57156	9299	22374	5441	62886
9	10768	25817	6692	56723	8975	22498	5411	63116
10	10773	25608	6701	56918	9160	22156	5441	63243
Average	10684.1	25742.0	6637.0	56936.9	9172.1	22347.9	5452.9	63027.1
Std. Dev.	136.275	104.621	100.702	181.492	120.765	100.582	55.427	163.168
Prob.	0.107	0.257	0.066	0.569	0.092	0.223	0.055	0.630

APPENDIX G: ANALYSIS OF PHASE 2 PAVEMENT STRUCTURE USING REVISED SPECIFICATION REQUIREMENTS FOR FATIGUE

G.1 Initial Stiffness Equations and Fatigue Life Equations

Table G.1 lists the regression equations of initial stiffness and fatigue for PBA-6a* and AR-8000 respectively. The data to obtain the regression equations has been listed earlier in Appendix A: Laboratory Shear and Fatigue Test Data. The associated residual plots are listed in Appendix B: Initial Designs for Full-Depth Structural Sections.

Table G.1: Regression Equations of Initial Stiffness and Fatigue Life for PBA-6a* and AR-8000

PBA-6a*	
$E(\ln stif) = 9.1116 - 0.1137Temp$ <small>(0.1493) (0.0071)</small>	$R^2 = 0.93$
AR-8000	
$E(\ln stif) = 14.6459 - 0.1708AV - 0.8032AC - 0.0549Temp$ <small>(0.6701) (0.0235) (0.1221) (0.0058)</small>	$R^2 = 0.82$
$\ln nf = -30.819 - 5.3219 \ln stn$	NA

Where,

- $\ln stif$ is the natural logarithm of initial stiffness (MPa),
- $\ln nf$ is the natural logarithm of fatigue life,
- $\ln stn$ is the natural logarithm of tensile strain level,
- AV is the percent air-void content,
- AC is the percent asphalt content, and
- $Temp$ is the temperature in °C.

Note:

1. The stiffness of PBA-6a* depends only on the temperature.
2. The fatigue life equation of AR-8000 was obtained according to the fatigue specification at 200 and 400 microstrain.

Test strain level (microstrain)	Fatigue Life (Nf)
200	2,000,000
400	50,000

G.1.1 ELSYM5 Input and Pavement Structure

Figure G.1 illustrates the I-710 pavement structure used in phase 2 and the associated loading configuration. The tires of a dual-tire configuration were used at a 720 kPa (~104 psi) inflation pressure. The traffic loading on the pavement structure is 40 kN (~9 kips) on the dual tires.

The pavement structure consists of a four-layer system as follows:

Layer	Thickness (mm)	Stiffness (MPa)	Poisson Ratio	AC (%)	AV (%)
PBA-6a*	76 (3")	Varied	0.35	5.0	6.0
AR-8000	178 (7")	Varied	0.35	4.7	
AR-8000 (Rich Bottom)	76 (3")	Varied	0.35	5.2	3.0
Granular Base	152 (6")	130 (18,854 psi)	0.35		
Subgrade		65 (9,427 psi)	0.45		

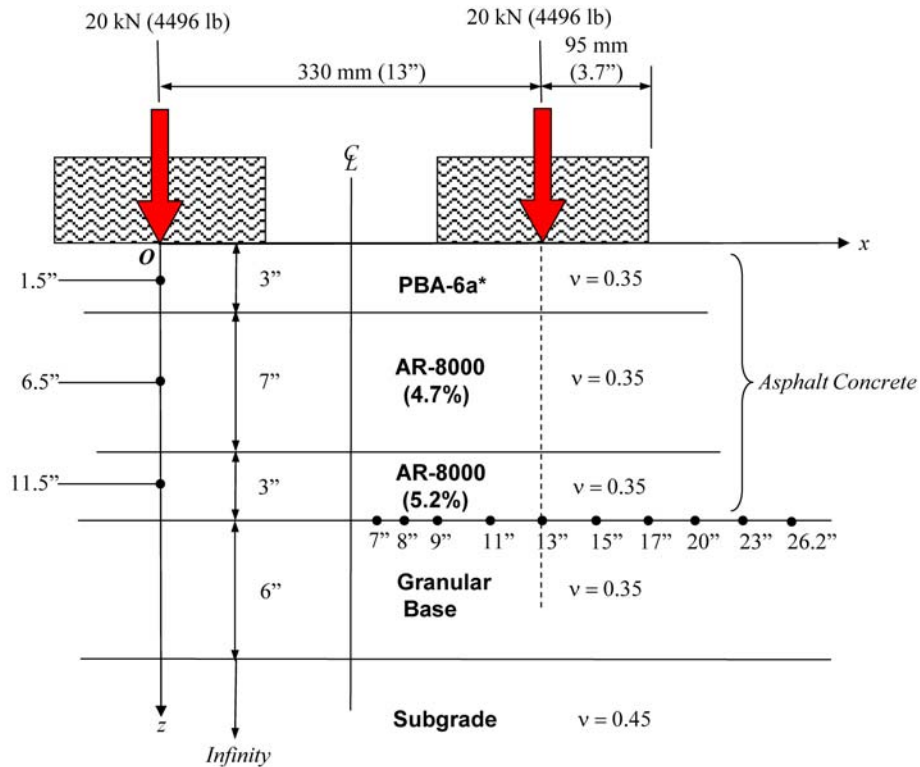


Figure G.1: Pavement structure and ELSYM5 input.

The tensile strains were calculated at depth of 330 mm (~13 in.) and at 10 positions along the x -axis as shown in Figure G.1. The maximum tensile strain was selected for the calculation of temperature equivalency factor (TEF) and temperature conversion factor (TCF).

G.1.2 Temperature Distribution

The temperature data used in this calculation is based on the temperature data of Long Beach, California, which is embedded in the $EICM$ program. The pavement temperature profiles, temperature gradients, temperatures at bottom of asphalt concrete were calculated using $EICM$ program in an hourly base from 09/01/1996 to 01/31/2001. Temperature gradient is defined as $g\left(\frac{^{\circ}C}{in.}\right) = \frac{T_s(^{\circ}C) - T_b(^{\circ}C)}{12"}$, where T_s is the surface temperature and T_b the temperature at bottom of asphalt concrete. Figure G.2 and Figure G.3 display the temperature histograms for surface temperatures and temperatures at bottom of AC layer respectively. Figure G.4 plots the corresponding temperature distribution curves. The distributions of temperatures extracted from 5:00AM to 7:00PM are also plotted in Figure G.5 through Figure G.7.

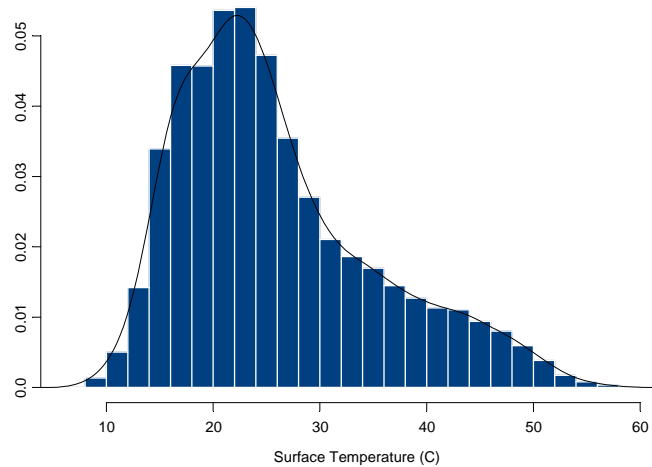


Figure G.2: Histogram of surface temperatures.

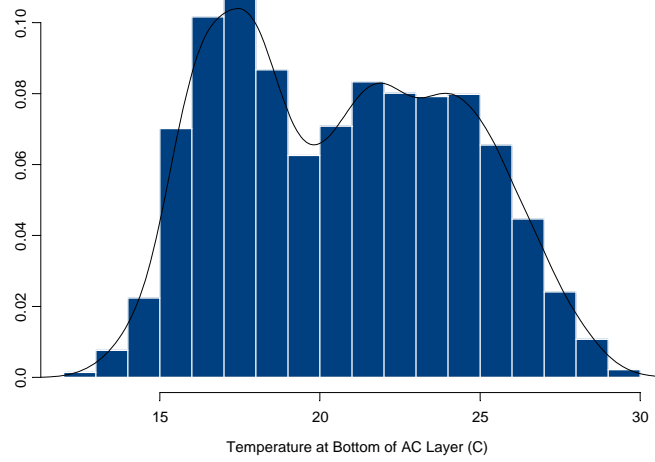


Figure G.3: Histogram of temperatures at bottom of AC layer.

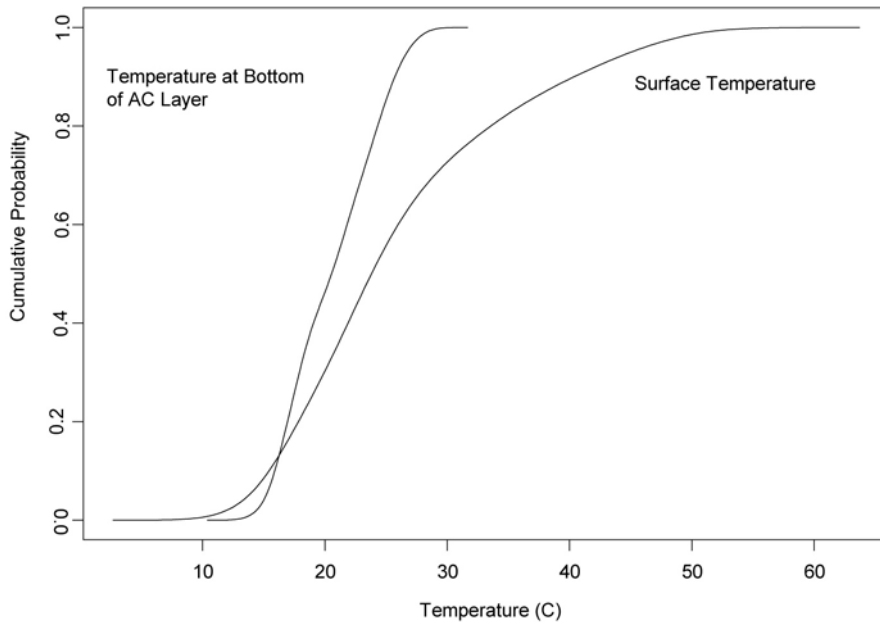


Figure G.4: Temperature distributions for surface temperature and temperature at bottom of AC layer.

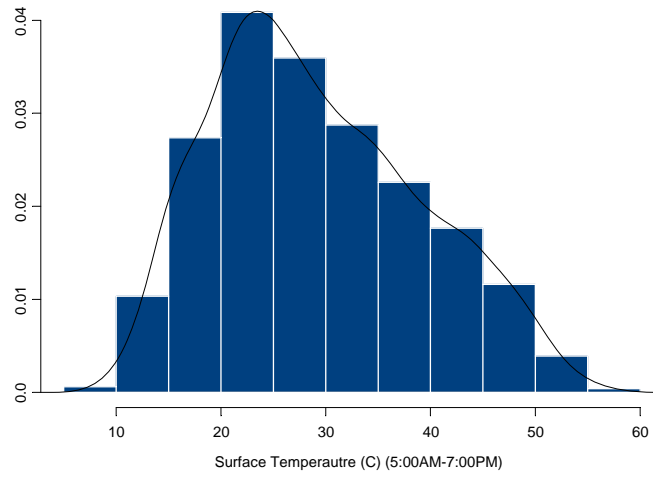


Figure G.5: Histogram of surface temperatures (5:00 A.M. to 7:00 P.M.).

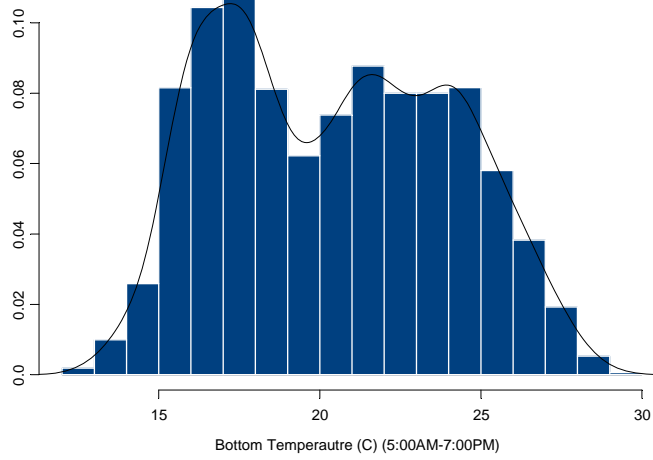


Figure G.6: Histogram of temperatures at bottom of AC layer (5:00 A.M. to 7:00 P.M.).

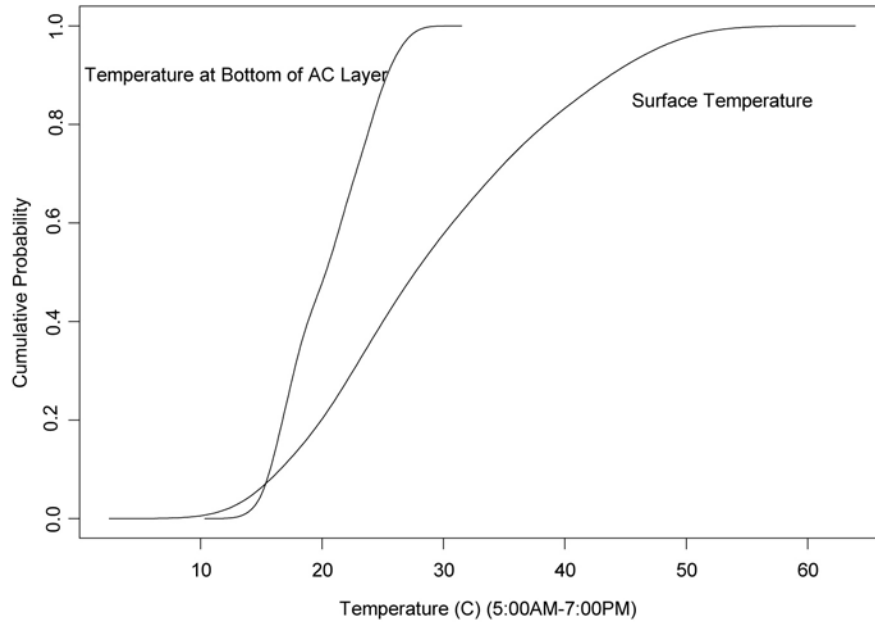


Figure G.7: Temperature distributions for surface temperature and temperature at bottom of AC layer (5:00 A.M. to 7:00 P.M.).

G.1.4 Traffic

Two assumptions are postulated in the calculation:

1. It is assumed that no wander traffic was applied onto the specified full-depth pavement structure.
2. The trafficking was applied only from 5:00 A.M. to 7:00 P.M.

G.2 Fatigue Performance Prediction and Comparison

TCF Calculation

The calculation of the temperature conversion factor is as follows:

1. Obtain the laboratory fatigue life and initial stiffness equations,
2. Run *ELSYM5* to obtain the maximum tensile strain and then calculate the fatigue life.

3. Calculate $TEF_i = \frac{Nf @ T_{ref} = 20C}{Nf @ T_i}$, and

4. $TCF = \sum_i^n f_i \cdot TEF_i$

Table G.2 lists the TCF calculation for temperatures at bottom of AC layer and Table G.3 presents the temperatures extracted from 5:00 A.M. to 7:00 P.M.

Table G.2: TCF Calculation

Temperature (C), <i>T_b</i>	Temperature Frequency, <i>f_i</i>	Temperature Equivalency Factor, <i>TEF_i</i>	<i>f_i · TEF_i</i>
12.5	0.005476	0.164279	0.000900
15.0	0.117664	0.290908	0.034229
17.5	0.252764	0.479901	0.121302
20.0	0.171575	1.000000	0.171575
22.5	0.202599	1.933574	0.391740
25.0	0.179066	3.502750	0.627223
27.5	0.067266	5.463488	0.367507
30.0	0.003591	7.545103	0.027092
<i>TCF</i>			1.741566

Table G.3: TCF Calculation (5:00 A.M. to 7:00 P.M.)

Temperature (C), <i>T_b</i>	Temperature Frequency, <i>f_i</i>	Temperature Equivalency Factor, <i>TEF_i</i>	<i>f_i · TEF_i</i>
12.5	0.007109	0.139388	0.000991
15.0	0.135317	0.259942	0.035175
17.5	0.250589	0.445474	0.111631
20.0	0.175532	1.000000	0.175532
22.5	0.204629	1.976370	0.404423
25.0	0.173631	3.706408	0.643547
27.5	0.051953	6.323180	0.328507
30.0	0.00124	8.399118	0.010414
<i>TCF</i>			1.71022

SF Calculation

The formulation for the shift factor calculation is $SF = 2.7639 \times 10^{-5} \cdot \varepsilon^{-1.3586}$, where ε is the tensile strain. In this calculation, the tensile strain occurred at bottom of AC layer at 20C while subjected to a zero temperature gradient is 55 micro strain. Thus, the shift factor is 16.93034.

M Calculation

The formulation of reliability multiplier M for a reliability level of 90 percent is shown in the following:

$$M = \exp(1.28\sqrt{0.22 + \text{Var}(\ln Nf)})$$

The regression analysis of *S-Plus* for the fatigue life of AR8000 is shown in the following:

	Value	Std. Error	t value	Pr(> t)
(Intercept)	-36.5184	4.0492	-9.0186	0.0000
av	-0.6470	0.2553	-2.5339	0.0164
log(stn)	-6.5315	0.5242	-12.4595	0.0000

Residual standard error: 1.414 on 32 degrees of freedom

Multiple R-Squared: 0.8291

Notice that the residual standard error is 1.414.

Let $x'_0 = (x_{00}, x_{01}, \dots, x_{0k})$ represent a set of values of the covariates in the regression equation, where $x_{00} = 1$ if an intercept is present. In this calculation, $x'_0 = (1, AV, \ln stn) = (1, 3.0, \ln(0.000055))$. Then, the predicted value of y , i.e., $\ln Nf$, at the point x_0 is $\hat{y}_0 = x'_0 b$. Hence, the variance $\text{Var}(\hat{y}_0) = \text{Var}(\ln Nf) = \sigma^2 [x'_0 (X'X)^{-1} x_0]$, where X is the design matrix and σ^2 the variance that is square of the residual standard error of the regression equation, in this case, $\sigma^2 = 1.999396$. Finally, we have $\text{Var}(\ln Nf) = 1.207278$.

Then, by substituting the value into the formulation, we have,

$$M = \exp(1.28\sqrt{0.22 + \text{Var}(\ln Nf)}) = 4.614483$$

Fatigue Performance Calculation

The allowable ESAL for this pavement design can be calculated according the formulation, $ESAL_{allowable} = \frac{Nf_{Lab} \cdot SF}{TCF \cdot M}$, where the Nf_{Lab} is the laboratory fatigue life of AR-8000 (Rich Bottom) at 20°C with the tensile strain 0.000055. The allowable ESAL calculated is then approximately 4.13×10^9 under the assumption that the trafficking is applied only from 5:00 A.M. to 7:00 P.M.

$$\begin{aligned} ESAL_{allowable} &= \frac{Nf_{Lab} \cdot SF}{TCF \cdot M} \\ &= \frac{1926824523 \cdot 16.93034}{1.71022 \cdot 4.614483} \\ &= 4,133,641,546 \\ &\cong 4.13 \times 10^9 \end{aligned}$$

G.3 S-Plus log

```
=====
# TCF calculation
=====
> range(tef710p7$tb)
[1] 12.05556 30.00000
> range(tef710p7$ts)
[1] 7.444444 58.944444
>
> cell<-function(x,a,b){
+   x1<-x[x[,1]<b,]
+   x2<-x1[x1[,1]>=a,]
+   mnf<-mean(x2[,2])
+   freq<-length(x2[,2])
+   return(mnf,freq)
+ }
> tcf<-function(x,rb,re,dd,tref,filename){
+   result<-NA
+   nfreq<-cell(x,tref-dd/2,tref+dd/2)
+   rn<-seq(rb,re,dd)
+   for(i in rn){
+     nfi<-cell(x,i-dd/2,i+dd/2)
+     tcfi<-nfreq$mnf/nfi$mnf
+     freqi<-nfi$freq
+     result<-rbind(result,c(i,tcfi,freqi))
+   }
+   result<-result[-1,]
+   write(t(as.matrix(result)),file=filename,ncol=3)
+ }
> data<-cbind(tef710p7$tb,tef710p7$nf)
> tcf(as.data.frame(data),10,35,2.5,20,"c:\\tcf710p7.txt")
>
>
> z_tef710p7[tef710p7$hour>=5,]
> zz_z[z$hour<=19,]
> length(zz$hour)
[1] 24195
> data1_cbind(zz$tb,zz$nf)
> tcf(as.data.frame(data1),10,35,2.5,20,"c:\\ntcf7107.txt")
>
>
=====
# Calculation of Shift Factor
=====
> 2.7639e-5*(0.000055)^-1.3586
[1] 16.93034
>
```

```

=====
# Calculation of Reliability multiplier M
=====

> mx<-ar8000[-c(14),]
> X<-cbind(1,mx$av,log(mx$stn))
> solve(t(X)%*%X)
      [,1]      [,2]      [,3]
[1,]  8.20275184 -0.01615483  1.03105302
[2,] -0.01615483  0.03261597  0.01351784
[3,]  1.03105302  0.01351784  0.13747839
> x<-c(1,3,log(0.000055))
> t(x)%*%solve(t(X)%*%X)%*%x
      [,1]
[1,] 0.6038212
>
> 0.6038212*1.999396
[1] 1.207278
>
> exp(1.28*sqrt(0.22+1.207278))
[1] 4.614483
>
> 1926824523*16.93034/1.71022/4.614483
[1] 4133641546
>
=====
# Temperature Distribution
=====

> hist(tef710p7$ts,prob=T,xlab="Surface Temperature (C)")
> ts.den_density(tef710p7$ts,n=200)
> lines(ts.den$x,ts.den$y)
>
> hist(tef710p7$tb,prob=T,xlab="Temperature at Bottom of AC Layer (C)")
> tb.den_density(tef710p7$tb,n=200)
> lines(tb.den$x,tb.den$y)
>
>
> plot(ts.den$x,cumsum(ts.den$y)/cumsum(ts.den$y)[200],type="n",xlab="Temperature
(C)",ylab="Cumulative Probability")
> lines(ts.den$x,cumsum(ts.den$y)/cumsum(ts.den$y)[200])
> lines(tb.den$x,cumsum(tb.den$y)/cumsum(tb.den$y)[200])
> text(locator(1),"Surface Temperatur")
> text(locator(1),"Temperatur at Bottom of AC Layer")
>
>
#
# 5:00AM - 7:00PM
#
> hist(zz$ts,prob=T,xlab="Surface Temperautre (C) (5:00AM-7:00PM)")

```

```
> xts.den_density(zz$ts,n=200)
> lines(xts.den$x,xts.den$y)
>
> hist(zz$tb,prob=T,xlab="Bottom Temperautre (C) (5:00AM-7:00PM)")
> xtb.den_density(zz$tb,n=200)
> lines(xtb.den$x,xtb.den$y)
>
> plot(xts.den$x,cumsum(xts.den$y)/cumsum(xts.den$y)[200],type="n",xlab="Temperature (C) (5:00AM-7:00PM)",ylab="Cumulative Probability")
> lines(xts.den$x,cumsum(xts.den$y)/cumsum(xts.den$y)[200])
> lines(xtb.den$x,cumsum(xtb.den$y)/cumsum(xtb.den$y)[200])
> text(locator(1),"Surface Temperatur")
> text(locator(1),"Temperatur at Bottom of AC Layer")
>
```

APPENDIX H: POSTCONSTRUCTION MEASUREMENTS AND ANALYSES

Table H.1: Backcalculated Siffness Moduli Based on 2003-2008 HWD Measurements

NB	From PCH toward 405	Full Depth (1)			Overlay (2)				Full Depth (3)			Overlay (4)				Full Depth (5)			
		Eac	Eab	Esg	Eac	Eb	Esb	Esg	Eac	Eab	Esg	Eac	Eb	Esb	Esg	Eac	Eab	Esg	
Lane 1	2003	Average	8636	3561	131	6730	12130	245.8	173.6	6837	3599	135	7213	12586	246.6	161.3	6484	3663	116
		StDev	2695	1980	23	1794	2029	23.1	22.51	959	1098	10	1227	2360	18.97	14.44	466	452	10
		20th %	7002	1492	112	5568	10811	225.5	156.7	6001	2712	126	5989	11428	230.2	151.4	5956	3416	106
	2004	Average	11027	4676	152	7602	13573	265.6	190.6	7556	4597	145	8113	14341	261.9	172.8	6959	3928	126
		StDev	3648	3973	142	3321	13240	209	152	3557	4218	156	4128	12735	239	164	4761	4046	152
		20th %	1037	1917	20	867	2561	24	18	695	1527	17	1023	2158	25	25	1276	623	16
	2006	Average	3064	2427	125	2771	11869	189	135	2987	2780	140	3475	10861	216	147	3714	3505	137
		StDev	4382	5308	159	3628	15416	217	168	4009	4867	169	4765	14312	261	174	6166	4398	167
		20th %	7066	7003	142	6015	11894	212	148	6153	4919	145	6749	14142	233	163	6812	5685	152
	2008	Average	1563	2942	20	976	1911	38	19	1060	2200	15	947	1659	14	18	1280	964	17
		StDev	5636	4231	124	5150	9504	170	133	5396	3267	134	5936	12825	222	151	5583	4904	133
		20th %	8115	9611	159	7004	13557	235	160	6485	6895	158	7495	15610	243	175	8034	6685	164
Lane 1	Average	6519	4816	127.7	5815	11213	250	142	7421	3687	164.4	6419	11431	223	135	7411	3576	171.6	
	StDev	1442	904	9.542	1149	1250	38	24	989.9	1048	20.42	1539	1508	44	39	888.1	700.8	37.02	
	20th %	5389	4310	119.4	4602	9958	215	116	6711	2832	148.8	5336	10108	185	106	6635	3034	148.4	
Lane 2	Average	8037	5067	134.2	6928	12330	285	163	8044	4194	174.9	7270	12635	257	170	8192	4063	192.2	
	StDev	6742	1287	110	5528	11169	249	177	6910	3302	124.7	6464	8108	199	182	5612	3337	126	
	20th %	1040	695	11	966	2348	27	17	754.2	1173	13.87	1324	1784	25	21	422	426	12	
Lane 2	Average	6084	762	106	4654	9633	227	163	6450	2527	116.2	5584	6641	181	169	5226	3067	115	
	StDev	7526	2143	119	6156	13125	272	190	7159	4824	141.1	7027	9433	221	197	5954	3434	137	
	20th %	5668	4931	127	6052	10500	221	153	5658	6931	158	6666	12973	247	165	6486	5027	150	
Lane 2	Average	915	2408	22	969	1873	24	21	565	3086	16	1482	2127	34	19	1044	1303	16	
	StDev	4949	3171	112	5340	9007	207	139	5284	4574	144	5842	11096	216	148	5728	4037	137	
	20th %	6570	7765	151	6736	12108	242	170	5878	7929	169	7173	14787	267	181	7452	5815	162	
Lane 2	Average	5529	5908	135	5035	10044	240	163	4691	6502	160	4948	12726	251	171	4602	5700	167	
	StDev	1067	3196	15	744	2496	37	19	645	1688	10	975	2726	40	18	503	2130	26	
	20th %	4876	3603	124	4375	8845	219	152	4216	5195	152	4461	9996	234	154	4145	4650	150	
Lane 2	Average	5853	6528	145	5606	11322	250	179	5010	8006	169	5246	14338	290	184	5026	6566	188	
	StDev	5768	4453	137	4769	10867	140	101	5428	4714	174	5270	11344	234	128	6283	3880	178	
	20th %	1434	1643	23	1178	1546	33	15	1377	776	22	1029	2822	86	50	744	697	40	
Lane 3	Average	4613	3326	122	3850	9818	116	105	4584	4174	156	4422	9654	173	70	5656	3239	144	
	StDev	7010	5488	155	5441	12596	175	105	5945	5245	193	6326	12976	251	173	6856	4668	198	
	20th %	5643	3652	124	6192	13105	242	169	6672	4762	136	7057	13837	236	182	6724	3096	123	
Lane 3	Average	645	678	9	765	2028	20	15	484	904	9	1746	2133	20	18	1368	1730	18	
	StDev	5313	3135	117	5559	11834	223	158	6251	4007	130	6075	12600	220	166	5830	2149	113	
	20th %	6160	4078	129	6786	14705	255	182	6872	5605	139	7895	15511	247	194	7432	3387	133	
Lane 3	Average	6418	2160	159	5865	10398	235	170	6913	4040	157	6095	11328	238	166	5081	3178	155	
	StDev	193	10	0	917	2063	30	24	1964	1351	26	1640	2789	38	25	996	566	12	
	20th %	6302	2154	159	4986	9250	216	154	5652	3218	132	4726	8612	211	148	4394	2802	142	
Lane 3	Average	6516	2166	159	6420	12036	255	187	8285	4752	181	7553	13395	272	189	5672	3669	166	
	StDev	7274	5084	129	6980	9445	361	149	5866	6742	161	6520	11865	279.4	162.4	6737	4429	101	
	20th %	1255	2411	20	1303	2825	174	26	519	2429	16	1248	2728	32.38	21.49	887	705	21	
Lane 3	Average	5947	3142	112	5723	7096	268	138	5435	5005	150	5381	9819	254	143.8	6053	4007	82	
	StDev	8352	6388	153	8347	12274	381	178	6167	8565	171	7704	14339	308.6	179.4	7521	4659	114	
	20th %	6770	7099	137	5449	9948	273	173	4955	7403	166	6283	8239	507	156	5264	5830	163	
Lane 3	Average	1582	3651	16	1016	1814	30	18	553	2665	12	1014	1831	156	17	989	1785	30	
	StDev	6509	4602	123	4786	9208	248	159	4607	5879	155	5686	6887	368	142	4545	4459	135	
	20th %	8069	7383	157	5903	10913	287	186	5373	9926	177	6880	9112	616	167	5745	6515	184	
Lane 3	Average	7877	3432	126	5672	8616	236	144	7933	3688	128	5659	11035	213	135	7436	3578	164	
	StDev	1385	976.5	21.25	1658	1328	69	41	1483	1040	24	1182	1676	57	43	1285	570	44	
	20th %	6979	2515	115.6	4304	7509	150	105	6606	2995	108	4686	9576	167	103	6676	3085	129	
Lane 3	Average	8937	4205	136.2	7318	9362	302	188	9262	4138	136	6380	12283	260	179	7965	4017	188	
	StDev																		
	20th %																		

SB

From 405 toward PCH		Full Depth (5)			Overlay (4)				Full Depth (3)			Overlay (2)				Full Depth (1)		
		Eac	Eab	Esg	Eac	Eb	Esb	Esg	Eac	Eab	Esg	Eac	Eb	Esb	Esg	Eac	Eab	Esg
Lane 1	2003	Average	6954	4135	161	6306	10837	228	169	5748	4357	136	5576	10172	198	159	6161	118
		StDev	1306	1596	25	1119	2690	53	17	877	1756	14	1404	3037	68	17	1316	14
		20th %	6141	2669	138	5300	9131	194	153	4927	3524	125	4432	7495	136	145	5257	110.3
		80th %	7703	4933	180	7337	13090	252	184	6397	5283	148	6357	13365	273	173	7555	126
Lane 1	2005	Average	6616	9384	163	6472	16408	240	177	6993	12576	155	5551	7615	227	175	11674	166.8
		StDev	1821	3919	24	1354	1541	15	11	1582	3080	16	983	1724	26	19	2802	23
		20th %	5269	5664	151	5463	15290	225	165	5425	10586	141	4670	6262	212	163	10426	149.9
		80th %	7803	12469	180	7218	17814	254	188	8357	14848	170	6272	8221	244	191	13098	186.2
Lane 1	2006	Average	5626	1640	107	9645	8372	287	157	6416	9770	156	8037	8467	194	158	11169	211.6
		StDev	351	1309	8	1835	3940	34	26	995	3411	15	861	1337	29	15	2287	31.5
		20th %	5432	791	101	8578	5563	276	142	5596	7444	145	7539	6762	168	148	9381	185.6
		80th %	5895	2617	113	10779	11855	311	181	7429	11869	167	8708	9455	231	163	13299	212.1
Lane 1	2008	Average	5175	9004	61	7071	7946	311	67	6426	9784	146	6765	9237	231	118	5988	114
		StDev	972	2511	13	1962	1705	94	8	1669	3175	12	1963	2742	106	35	1067	16
		20th %	4517	7041	59	5254	6544	241	66	5343	7368	135	5216	7275	98	93	5250	101
		80th %	5912	10091	60	8502	9501	402	70	6572	11487	154	8292	11153	308	151	6352	131
Lane 2	2003	Average	6387	1576	146	5464	8828	168	175	6106	3130	142	4992	12649	250	167	4482	109.6
		StDev	1182	1174	22	1302	2040	27	21	1327	1783	17	1064	3002	49	15	687	8
		20th %	5495	820	133	4569	7594	152	159	5118	1183	129	3983	10730	236	154	3857	102.7
		80th %	7334	1815	159	6063	10494	177	192	7609	4163	152	6007	14831	280	179	4941	114.4
Lane 2	2006	Average	3834	2639	87	4754	12912	236		4736	6106	132	5853	9227	141	162	14441	200.4
		StDev	1049	1486	14	886	2653	43		1222	1530	8	1079	1179	13	15	1986	26
		20th %	3489	1879	81	4163	10465	199		4217	5457	129	5261	8320	131	148	13458	180.1
		80th %	4464	3531	93	5600	15278	277		5254	6756	135	6799	10279	149	168	15831	222.9
Lane 2	2007	Average	4238	6839	185	4298	9249	159	174	4140	7165	151	4099	8949	133	173	3413	99
		StDev	948	1818	30	915	1403	12	18	807	3105	19	761	1358	12	16	645	8
		20th %	3493	5305	166	3474	8589	150	162	3832	4816	139	3422	8244	125	165	3034	95
		80th %	4929	7959	203	4863	9925	166	190	4376	8301	162	4799	9952	134	182	3945	105
Lane 2	2008	Average	6221	6552	111	5030	11642	183	151	4666	8044	79	4789	11399	195	164	4981	87
		StDev	1160	2165	18	1091	1105	30	26	536	1819	16	1035	1581	28	21	898	16
		20th %	5379	4561	91	4249	10719	170	139	4349	6494	70	4018	9918	167	148	4168	77
		80th %	6970	8553	129	5203	12560	206	170	4890	9056	98	5199	12442	212	177	5704	91
Lane 3	2003	Average								6493	4931	141	4497	15003	257	167	4630	109.3
		StDev								5289	2202	16	811	3894	58	16	785.3	13
		20th %								4692	3799	132	3789	13228	247	155	4032	100.6
		80th %								5722	6066	155	4935	17793	293	180	5157	116.9
Lane 3	2005	Average	6970	9507	151	5917	18093	258	183	6724	10261	163	6419	11779	141	115		
		StDev	1672	5718	31	720	1451	16	10	804	1316	9	1349	1337	8	6		
		20th %	5519	1805	115	5367	16696	246	178	5873	9198	159	5527	10868	134	111		
		80th %	8239	14989	180	6269	19025	275	187	7464	11397	170	7293	12575	149	120		
Lane 3	2006	Average	5401	3676	108	6896	6117	148	152	6028	6604	132	6147	8524	147	162	13475	202
		StDev	680	2037	23	1482	1414	36	15	1283	2696	13	1281	1203	12	16	1633	33
		20th %	4929	2792	96	5324	5081	126	137	4992	5131	121	5185	7393	138	148	12329	178
		80th %	6016	4155	106	8195	7064	150	164	6403	8049	145	7065	9652	155	172	14608	216
Lane 3	2007	Average	5172	6990	171	5280	8159	140	163	4836	5814	139	5099	9465	170	167	5146	100
		StDev	1366	1558	30	666	958	9	15	804	1909	13	2671	1517	10	23	1324	7
		20th %	4152	5630	150	4767	7469	133	151	4122	4240	130	3959	8274	163	150	3939	96
		80th %	5999	7542	185	5711	8995	145	176	5203	7126	149	5176	10588	175	180	6630	105
Lane 3	2008	Average	5854	8141	116	5608	9421	223	80	6075	6821	98	5665	9637	280	144	5715	96
		StDev	1395	1777	40	1022	1900	117	14	1120	2230	24	1196	2356	69	17	952	10
		20th %	4389	6683	104	4893	7439	111	70	5205	4921	74	4740	7603	247	138	4776	86
		80th %	6690	9467	138	6301	11133	278	88	6940	8687	114	6373	11583	329	151	6357	104

Table H.2: Layered Elastic Stress and Strain Calculations

	Section	VCS@TS	SSTS@2 in.	SSTR@2in.	TS@BAC
Northbound	1	-8.0014E-05	1.9843E-01	3.3901E-05	1.7516E-05
	2	-4.2404E-05	1.9047E-01	4.4394E-05	4.9596E-06
	3	-7.8043E-05	1.9811E-01	3.3597E-05	1.6716E-05
	4	-4.1277E-05	1.8864E-01	4.4012E-05	2.7171E-06
	5	-7.2095E-05	1.9828E-01	3.5747E-05	1.6488E-05
Southbound	1	-1.5055E-04	2.0803E-01	4.9139E-05	4.9164E-05
	2	-4.1898E-05	1.8972E-01	4.4204E-05	3.9398E-06
	3	-8.1657E-05	1.9382E-01	4.2814E-05	1.0741E-05
	4	-5.8835E-05	1.8818E-01	4.4731E-05	3.4035E-06
	5	-7.3245E-05	1.9332E-01	4.4161E-05	8.3789E-06

Note: (1) VCS@TC: Vertical compressive strain at top of subgrade

SSTS@2 in.: Shear stress at 2 in. depth

SSTR@2in.: Shear strain at 2 in. depth

TS@BAC: Tensile strain at the bottom of asphalt concrete

(2) Stresses are in MPa.

Table H.3 Shear Test Results on Specimens Prepared from Pavement Samples

I-710 Testing of Cores taken from the Wheelpath													
Stations 131 (1 core) and 133 (3 cores)					Tests executed July 14 - 22, 2005 at Caltrans TransLab								
Both cores from STA 131 (Specimens 5A and 5B) experienced problems during testing										Tested at 50°C			
Extrapolation from 1000 for a and b parameters													
										G* @ Rep 100			
										g= a*(N^b): {REP 1000}			
Station	Specimen	Material	AV	Reps	1%	2%	3%	4%	5%	(MPa)	a	b	
133	1 B	DGAC		45000	711	3,930	14,314	32,640	51,618	127.3	8.02E-04	0.381	
133	2 B	DGAC		45000	604	10,811	53,802	173,533	430,397	110.5	2.07E-03	0.246	
133	3 B	DGAC		35001	1160	9,027	21,975	56,722	107,027	128.4	8.54E-04	0.351	
131	5 B	DGAC		5000	670	44,920	540,257	3,154,899	12,400,514	94.9	3.49E-03	0.163	problematic test
Average of STA 133					825	7,923	30,030	87,631	196,348	122.0	1.24E-03	0.326	
133	1 A	PBA-6a*		45000	280	1,295	3,335	6,858	11,387	38.2	1.09E-03	0.408	
133	2 A	PBA-6a*		30001	232	2,204	10,440	33,486	75,407	31.5	2.28E-03	0.275	
133	3 A	PBA-6a*		30001	88	1,726	49,722	315,671	1,323,867	60.8	5.57E-03	0.156	
131	5 A	PBA-6a*		45000	1627	8,906	32,192	69,057	126,404	40.9	6.54E-04	0.369	problematic test
Average of STA 133					200	1,742	21,166	118,672	470,221	43.5	2.98E-03	0.279	

Table H.4: Summary of Fatigue Tests of I-710 QC/QA Project (Field-Mixed, Field-Compacted)

Specimen Designation	Mix Type	UCB AV (%)	Test Temp. (C)	Test Strain Level	Initial Phase Angle (Deg.)	Initial Stiffness (MPa)	Fatigue Life Nf
710QA-2L2C	PBA6A	2.9	19.96	0.000204	40.28	2040	45306762
710QA-1L2C		3.8	19.94	0.000208	34.39	1992	17086573
710QA-1L2D		4.7	19.62	0.000218	36.15	1774	17931162
Mean		3.8	19.84	0.000210	36.94	1935	26774832
Standard Deviation		0.9	0.19	0.000007	3.02	142	16054677
710QA-1L2A	PBA6A	3.9	19.92	0.000413	35.71	1888	147443
710QA-2L2B		2.7	19.96	0.000404	38.93	1966	757065
710QA-1L2B		3.7	19.68	0.000437	38.92	1878	76735
Mean		3.4	19.85	0.000418	37.85	1911	327081
Standard Deviation		0.6	0.15	0.000017	1.86	48	374052
Mean		3.62	19.85		37.40	1923	
Standard Deviation		0.73	0.15		2.30	96	
710QA-1L3A	AR8000	5.4	19.64	0.000212	16.12	11587	646485
710QA-2L3A		7.0	19.71	0.000212	21.00	8370	678690
710QA-2L3D		5.7	19.58	0.000211	18.95	9123	635790
Mean		6.0	19.64	0.000212	18.69	9693	653655
Standard Deviation		0.9	0.07	0.000001	2.45	1683	22331
710QA-1L3E	AR8000	7.9	19.49	0.000424	20.59	7550	26469
710QA-1L3H		8.2	19.76	0.000423	18.40	8421	19135
710QA-2L3C		6.3	19.71	0.000422	20.65	8420	45650
Mean		7.5	19.65	0.000423	19.88	8130	30418
Standard Deviation		1.0	0.14	0.000001	1.28	503	13692
Mean		6.75	19.65		19.29	8912	
Standard Deviation		1.15	0.10		1.87	1402	
710QA-2L4D	AR8000 Rich Bottom	8.4	19.69	0.000210	20.72	7626	85762
710QA-3L4B		5.8	19.64	0.000210	22.48	7140	618135
710QA-1L4D		4.7	19.63	0.000210	15.96	11422	627808
Mean		6.3	19.65	0.000210	19.72	8729	443902
Standard Deviation		1.9	0.03	0.000000	3.37	2345	310196
710QA-2L4A	AR8000 Rich Bottom	5.5	19.36	0.000418	22.74	7467	50332
710QA-1L4A		5.6	19.55	0.000422	20.17	9515	20770
710QA-3L4C		4.7	19.73	0.000418	23.06	7971	58555
Mean		5.3	19.55	0.000419	21.99	8318	43219
Standard Deviation		0.5	0.19	0.000002	1.58	1067	19871
Mean		5.78	19.60		20.86	8524	
Standard Deviation		1.36	0.13		2.66	1645	

**APPENDIX I: PAVEMENT ANALYSES OF FULL-DEPTH AND
OVERLAYS ON CRACKED AND SEATED PCC SECTIONS USING THE
CALME DESIGN/ANALYSIS PROGRAM**

by

**Dr. Rongzong Wu
Project Scientist
Pavement Research Center
University of California, Davis**

January 2009

Full-Depth Section

Project Location

On state highway I 710, between Pacific Coast Highway and I-405. PM (6.8 to 9.7).

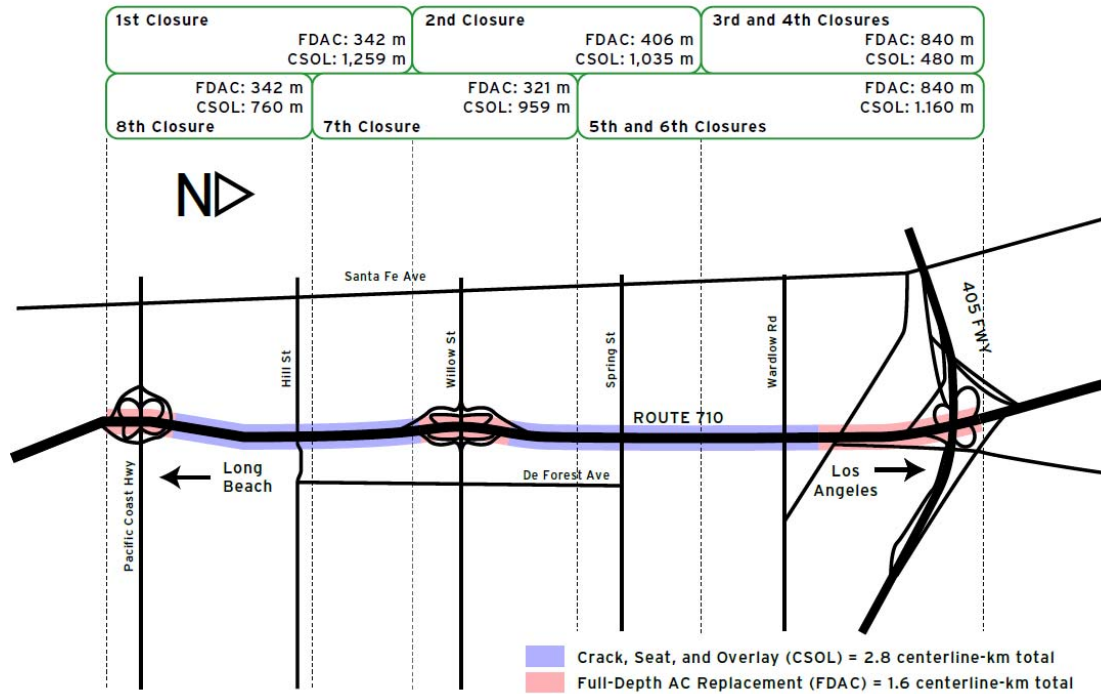


Figure 1: Map of Project.

Traffic

Traffic Spectrum: WIM Station No. 059060 S LA – 710 Los Angeles, Axles per truck = 4.16, axle per ESAL = 3.75, belongs to group 1a, 3-lane highway, directional factor 0.515, lane factor = 0.671 (0.513 to 0.874).

Traffic Volume: 30 year design TI of 17 (209 Million ESALs), yearly axle number 26,245,024, growth rate = 0%, this is equivalent of 7 million ESALs every year.

Using direction factor of 0.515, lane factor of 0.671, AADTT can be calculated as:

$$AADTT = \frac{26,245,024}{4.16 \times 0.515 \times [0.671, 0.513, 0.874] \times 365} = [50019, 65423, 38400]$$

Actual traffic volume based on Caltrans data are shown in Figures 2 and 3 for PM 6.9 and 10.8 respectively.

Table 1: Summary of Caltrans Traffic Volume

Observation Point	AADTT Exponential Fitting	2003 to 2032 ESALs	2003 to 2008 ESALs
PM 6.9	$21,525 \cdot (1 - 0.3\%)^{n-1992}$	92 Million	18.5 Million
PM 10.8	$24,275 \cdot (1 + 3.2\%)^{n-2001}$	178 Million	23.5 Million
Average		135 Million	21 Million

The design traffic volume is 1.5 times the actual values over the 30 years, and 2.0 times the actual value for the first 6 years (2003 to 2008).

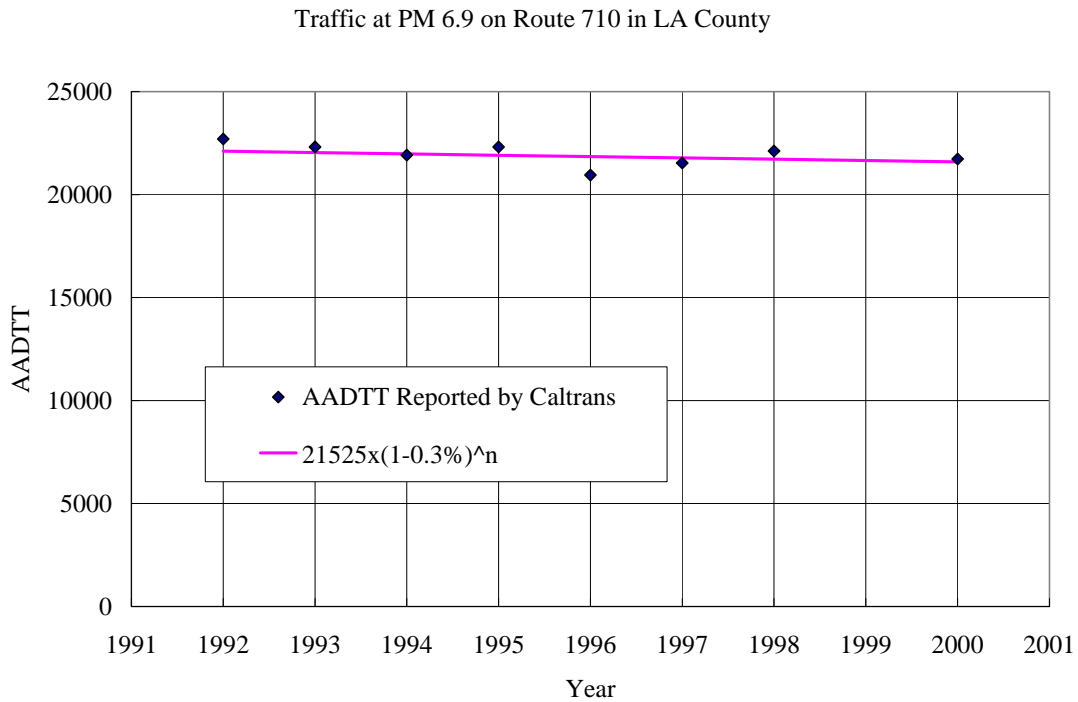


Figure 2. Traffic volume at PM 6.9 on Route 710 in LA County, between year 1992 and 2000

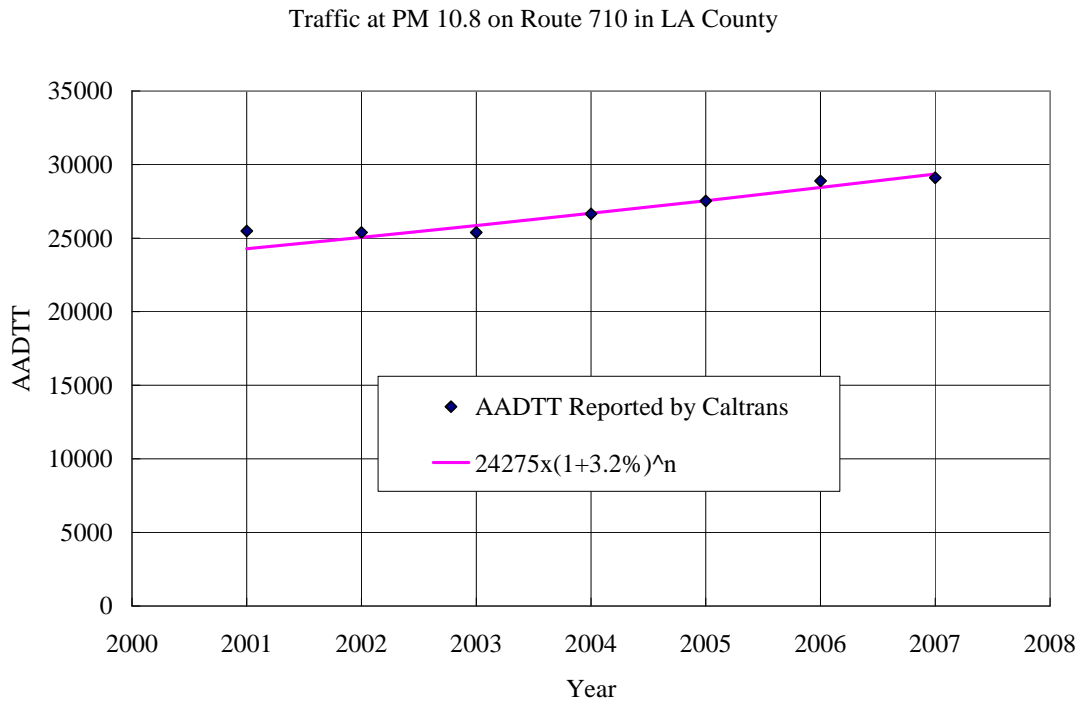


Figure 3. Traffic volume at PM 10.8 on Route 710 in LA County between 2001 and 2007

Temperature

South Coast, representative of Los Angeles, annual mean surface temperature 23°C, yearly range 12°C, daily range 16°C.

Structure

Thickness and Unbound Layer Stiffness

Table.2: Structure of full-depth sections

No.	Description	Thickness	Stiffness (MPa)
1	PBA-6a*	3" (75mm)	
2	AR-8000, 4.7% AC, 6% AV	6" (150mm)	
3	AR-8000, 5.2% AC, 3% AV	3" (75mm)	
4	Aggregate Base, recycled PCC	6" (150mm)	130
5	Subgrade	-	55~80, average 65

AC Stiffness (Master Curve)

Frequency sweep data are available from Rongzong Wu's dissertation study. Tests were conducted at three temperatures and two air void contents. The master curve parameters are listed below:

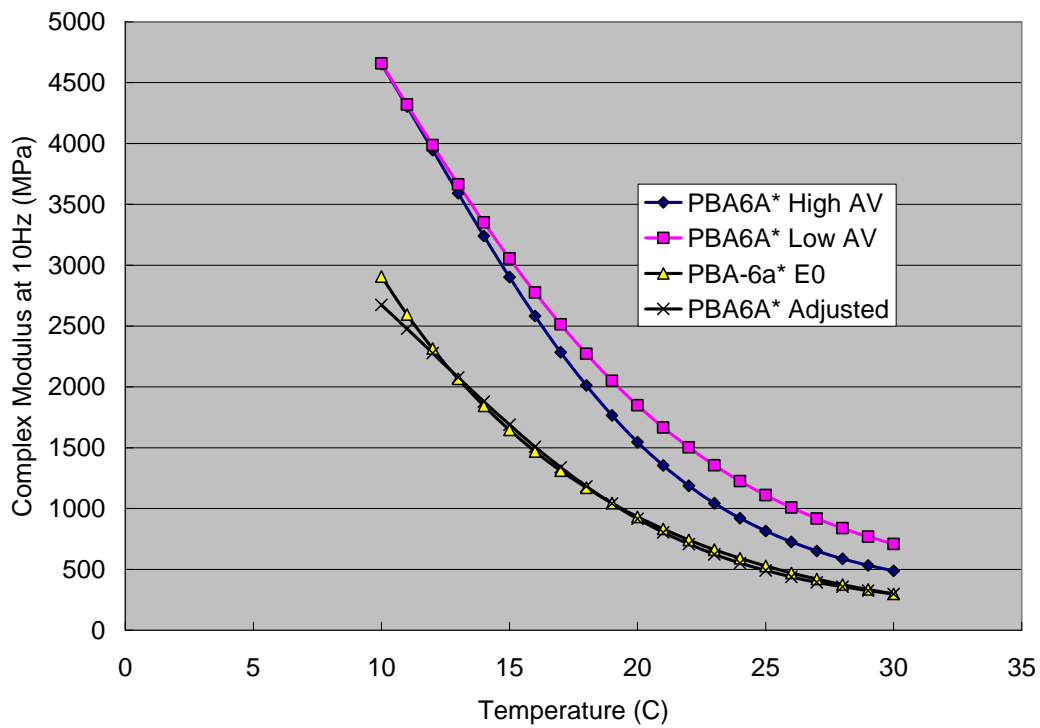
Description	δ	E_{ref}	β	γ	aT	α
PBA-6a* Low AV	2.301	1,885	1.123	0.807	1.196	1.662
PBA-6a* High AV	2.301	1,576	1.204	0.808	1.586	1.582
AR-8000 Low AV	2.301	10,511	-0.774	0.833	1.036	1.894
AR-8000 High AV	2.301	7,390	-0.321	0.709	1.480	1.880

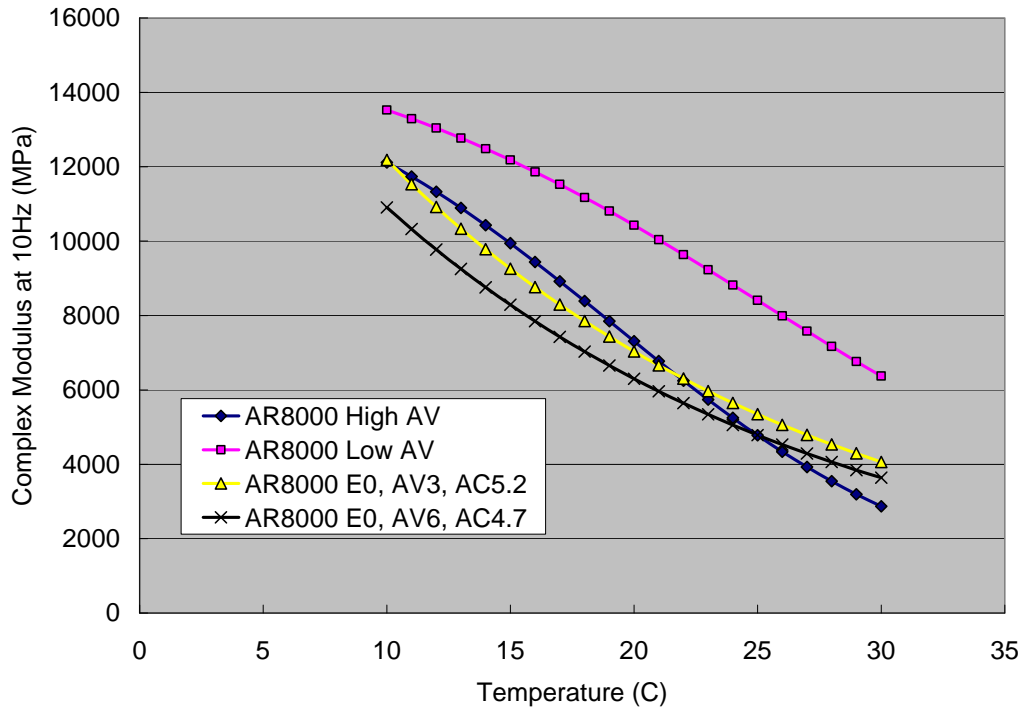
Note that reference stiffnesses are given for 20°C, 0.015s loading time (10Hz).

Initial stiffness data are also available from fatigue tests conducted in the design phase for the project. Regression equations are developed based on these initial stiffnesses to predict the effects of air-void content, binder content, and loading temperature on mix stiffness:

PBA-6a*: $\ln(E_0) = 9.1116 - 0.1137 * T$

AR-8000: $\ln(E_0) = 14.6459 - 0.1708 * AV - 0.8032 * AC - 0.0549 * T$.





The master curves for complex moduli at 10Hz loading frequency are shown above. Based on these two graphs, it was decided:

- For PBA-6a*: to use the adjusted master curve, which is essentially the master curve for a high AV content scaled down by a factor of 1.6.
- For the AR-8000 mixes, both the rich bottom and the regular mix, master curves for the low AV mixes will be used in the analyses.

The final master curves used in *CalME* are listed below:

Description	δ	E _{ref}	β	γ	aT
PBA-6a*	2.097	932	1.204	0.808	1.586
AR-8000	2.301	7,390	-0.321	0.709	1.480

Note that reference stiffnesses are given for 20°C, 0.015s loading time (10Hz).

Fatigue Parameters

Fatigue data were available from both the design phase of the I-710 project and from the Reflection Cracking Study conducted at the Richmond Field Station and referred to as Goal 6 (HVS Testing for I-710 Long Life Asphalt Concrete Mixes).

For the PBA-6a* mix, data used for design were complete include fatigue tests for mixes with both 4.7% and 5.2% AC, as well as temperature susceptibility tests conducted at 10, 25, and 30°C. These data are pooled together and extracted into the *Excel* workbook that comes with *CalME* to do the regression and get the fatigue model parameter.

For AR-8000 mix, tests under 20°C for mixes with 4.7% and 5.2% AC are available, but temperature susceptibility data are unavailable, so a set of beams tested under initial phase of Goal 6 project were used. These beams mostly have AV of 3%.

Name	α_0	A	$\mu\epsilon_{ref}$	β	E_{ref}	γ	δ
PBA-6a*	-1.65358	2906	200	-0.68862	3000	-0.34431	0
AR-8000	-0.12605	87.64	200	-4.80596	3000	-2.40298	0

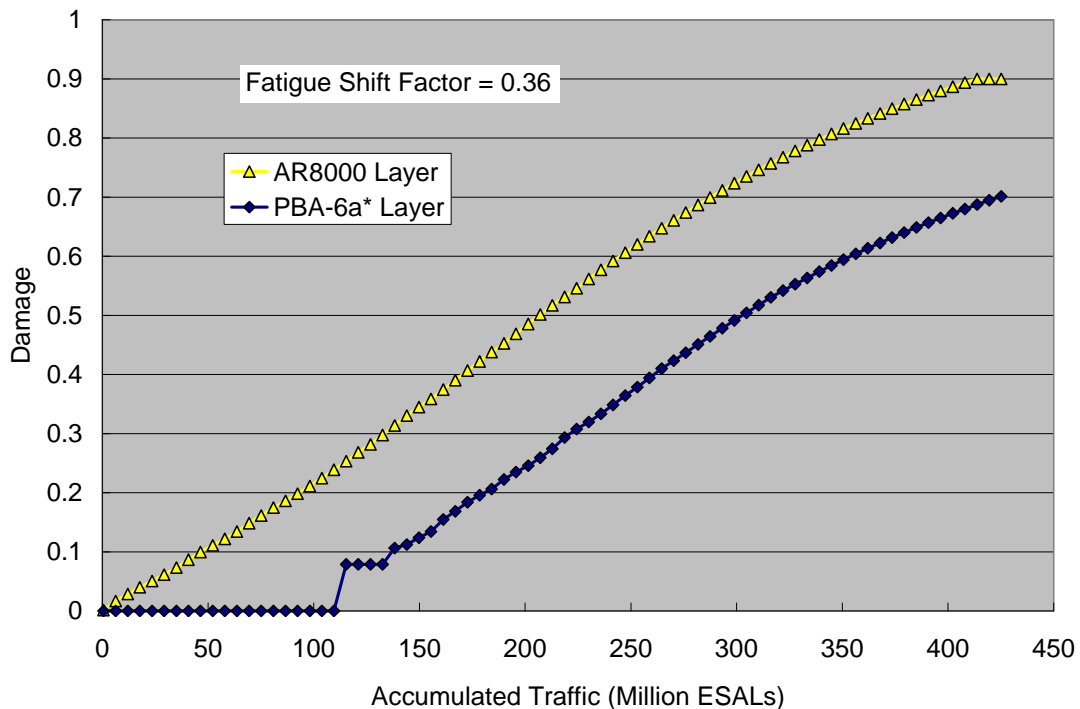
Note that we are not differentiating the two AR-8000 mixes because they have similar stiffness, and it is believed that the 0.5% difference in AC content does not cause significant difference in fatigue resistance of the AR-8000 mix.

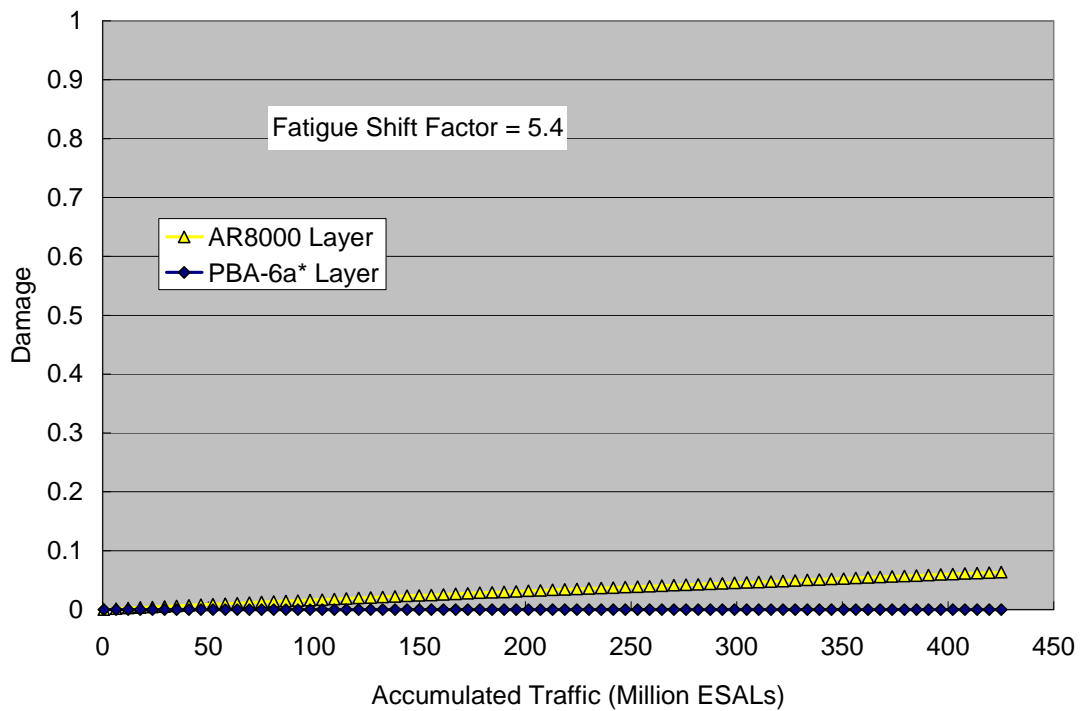
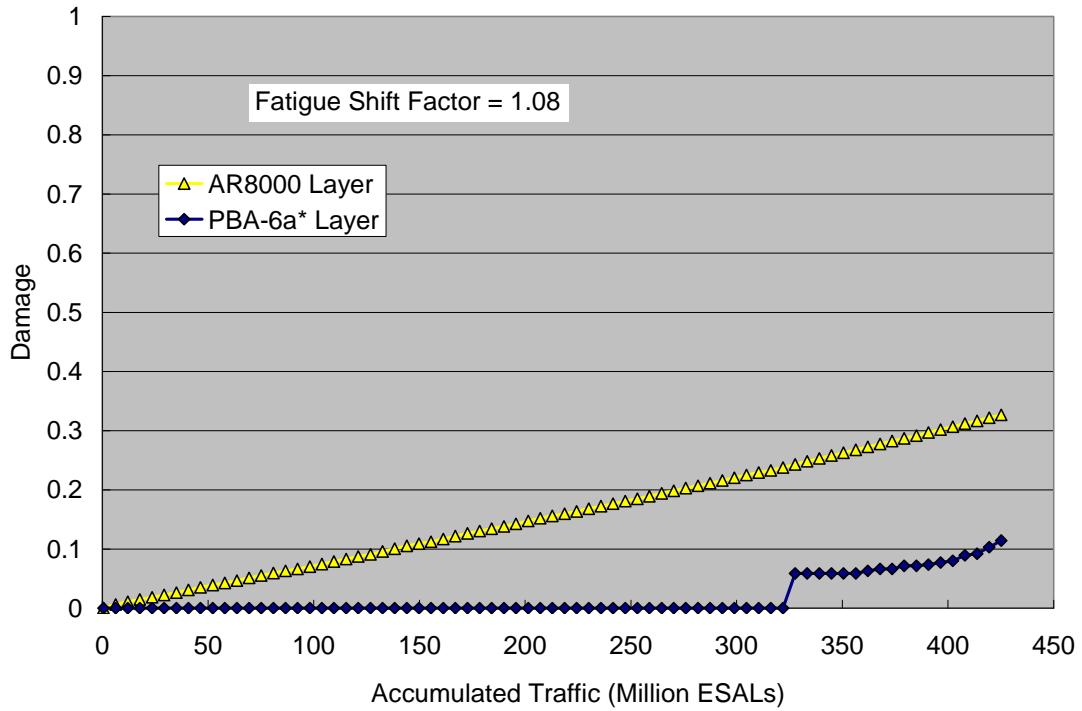
Based on calibration study using US 101 data, fatigue shift factors are listed below when using frequency sweep stiffness and assume no wander in the traffic:

- 0.36 for deterministic analysis
- 0.62 for probabilistic analysis

Based on HVS calibration study, the fatigue shift factor should be 0.6 or 3, with wander accounted for and using deterministic analysis. The actual shift factor for cases without wander should roughly be 1.8 times larger, which means it should be 1.08 or 5.4.

Simulation Results and Discussion





Shown above are the damage evolution history of the two HMA layers (note that the two AR-8000 layers are combined into one). *CalME* typically gives surface crack density based on HMA layer damage. Since there are two HMA layers the definition is ambiguous and therefore only damage histories are reported here.

According to the figures, damage does not increase dramatically. It is therefore decided to use residual stiffness ratio of 0.5 to define the fatigue life. In *CalME*, stiffness ratio (SR) is a function of damage ω :

$$SR = \frac{E}{E_i} = \left(\frac{E_{min}}{E_i} \right)^\omega \quad (1)$$

where E_i is the intact stiffness for the current loading condition (loading time and temperature) and $E_{min} = 10^\delta$ is the minimum stiffness, a constant as part of the HMA master curve, and ω is the damage. Assuming a loading time of 0.015s and temperature of 20°C, failure damage can be calculated as 0.19 for AR-8000 mix and 0.35 for PBA-6a* mix. Accordingly, fatigue life for each layer can be summarized below:

Table 3. Fatigue Life for Different Layer and Different Fatigue Shift Factors (in Million ESALs)

Fatigue Shift Factor	AR-8000 Layer	PBA-6a* Layer
0.36 (Based on US 101 Data)	92	242
1.08 (Goal 3 [1] Med Temp Underlying)	265	>425
5.40 (Goal 1, 3, 5, and 9 [1,2])	>425	>425

Effect of AB Stiffness

The following two tables summarize the backcalculated layer moduli for the full-depth sections of I-710 projects. There does not seem to be a consistent decreasing trend for AB stiffness and its values range from 2,160 to 10,261 MPa, which are much higher than the values used in the simulations (see Table 2).

Table 4: Elastic Modulus of all Northbound Sections for Lane 3 (MPa)

From PCH toward 405			Full Depth (1)			Full Depth (3)			Full Depth (5)		
Lane 3	2003 NB		Eac	Eab	Esg	Eac	Eab	Esg	Eac	Eab	Esg
	Average		5643	3652	124	6672	4762	136	6724	3096	123
	StDev		645	678	9	484	904	9	1368	1730	18
	20th %		5313	3135	117	6251	4007	130	5830	2149	113
	80th %		6160	4078	129	6872	5605	139	7432	3387	133
Lane 3	2004 NB		Eac	Eab	Esg	Eac	Eab	Esg	Eac	Eab	Esg
	Average		6418	2160	159	6913	4040	157	5081	3178	155
	StDev		193	10	0	1964	1351	26	996	566	12
	20th %		6302	2154	159	5652	3218	132	4394	2802	142
	80th %		6516	2166	159	8285	4752	181	5672	3669	166
Lane 3	2006 NB		Eac	Eab	Esg	Eac	Eab	Esg	Eac	Eab	Esg
	Average		7274	5084	129	5866	6742	161	6737	4429	101
	StDev		1255	2411	20	519	2429	16	887	705	21
	20th %		5947	3142	112	5435	5005	150	6053	4007	82
	80th %		8352	6388	153	6167	8565	171	7521	4659	114

Table 5: Elastic Modulus of all Southbound Sections for Lane 3 (MPa)

From 405 toward PCH			Full Depth (5)			Overlay (4)				Full Depth (3)			Overlay (2)				Full Depth (1)		
			Eac	Eab	Esg	Eac	Eb	Esb	Esg	Eac	Eab	Esg	Eac	Eb	Esb	Esg	Eac	Eab	Esg
Lane 3	2003 SB	Average								6493	4931	141	4497	15003	257	167	4630		109
		StDev								5289	2202	16	811	3894	58	16	785		13
		20th %								4692	3799	132	3789	13228	247	155	4032		101
		80th %								5722	6066	155	4935	17793	293	180	5157		117
Lane 3	2005 SB	Average	6970	9507	151	5917	18093	258	183	6724	10261	163	6419	11779	141	115			
		StDev	1672	5718	31	720	1451	16	10	804	1316	9	1349	1337	8	6			
		20th %	5519	1805	115	5367	16696	246	178	5873	9198	159	5527	10868	134	111			
		80th %	8239	14989	180	6269	19025	275	187	7464	11397	170	7293	12575	149	120			
Lane 3	2006 SB	Average	5401	3676	108	6896	6117	148	152	6028	6604	132	6147	8524	147	162	13475		202
		StDev	680	2037	23	1482	1414	36	15	1283	2696	13	1281	1203	12	16	1633		33
		20th %	4929	2792	96	5324	5081	126	137	4992	5131	121	5185	7393	138	148	12329		178
		80th %	6016	4155	106	8195	7064	150	164	6403	8049	145	7065	9652	155	172	14608		216

FSF = 0.36

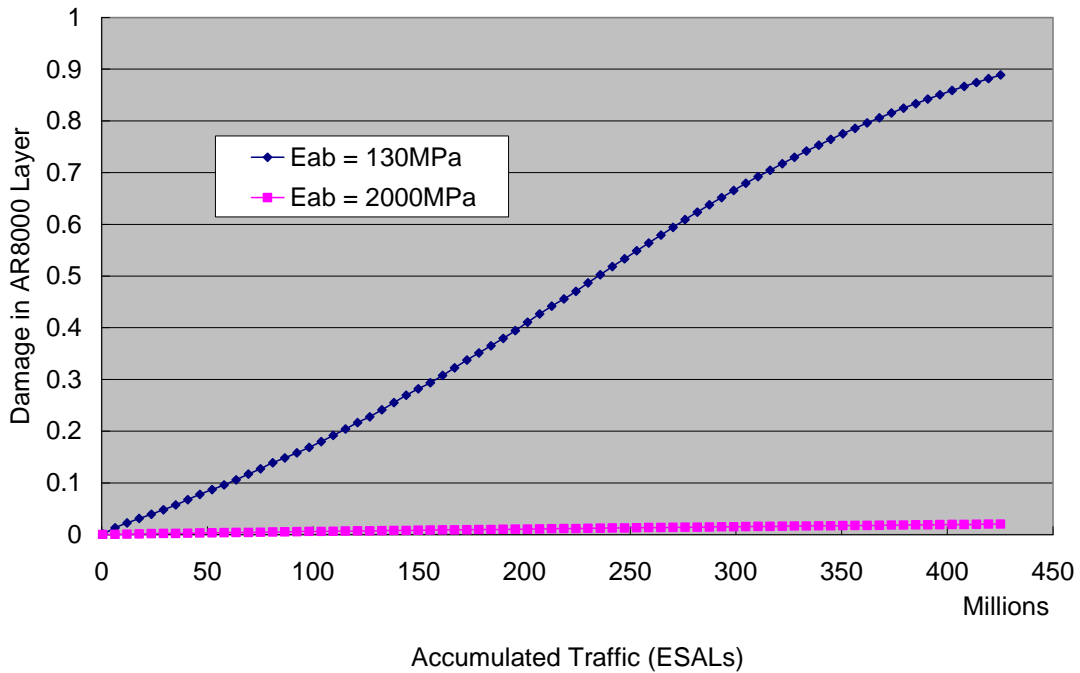


Figure 4: Effect of Eab on damage accumulation for AR-8000 layer.

Crack, Seat, and Overlay Sections

Introduction

CSOL sections have the same traffic, climate and material properties as the full-depth sections. The major difference is the structure type and failure mechanism. For full-depth sections, rutting and fatigue cracking is the dominant failure mode, while for CSOL sections rutting and reflective cracking are the dominant failure modes.

In *CalME*, there is a strain-based incremental recursive model for reflective cracking. In particular, average strain at the tip of a crack/joint, referred to as reflective cracking strain, is calculated based on pre-run finite element analyses as a function of the following quantities:

Table 6: Structural Parameters Used for Developing Statistical Strain Model for HMA on PCC Overlays

Name	Description	Unit
Ea	Overlay Stiffness	MPa
Ha	Overlay Thickness	mm
Hu	PCC Layer Thickness	mm
Ky	Subgrade Reaction Modulus	MPa/mm
Fx	Axle Load	kN
LS	Crack Spacing	mm

The average reflective cracking strain is used to calculate incremental damage of the HMA layer under traffic loading. Note that no thermal strain is accounted for in the current model.

In order to use this model, one needs to idealize the overlay system as a two-layer structure: HMA as the overlay, PCC underneath, and supported by a Winkler's foundation.

Structure

The materials for CSOL sections are the same as those for the full-depth sections, the only difference is the structure thickness and type.

Thickness and Unbound Layer Stiffness

No.	Description	Thickness	Stiffness (MPa)
1	OGFC	1" (25mm)	Same as PBA-6a* (Assumed)
2	PBA-6a*, 4.7% AC	3" (75mm)	
3	AR-8000, 4.7% AC, 6% AV	3.8" (97 mm)	
4	Fabric	0.1" (2.5mm)	
5	AR8000, 4.7% AC, 6% AV	1.2" (30mm)	
6	Cracked and Seated PCC	8" (200mm)	27,579
7	CTB	6" (150mm)	
8	Subgrade	-	55~80, average 65

The structure is simplified as below in order to conduct *CalME* simulation:

No.	Description	Thickness (mm)	Idealized Layer	Thickness (mm)
1	OGFC	25	PBA-6a*	100
2	PBA-6a*,	75		
3	AR8000	97	AR8000	130
4	Fabric	2.5		
5	AR-8000	30		
6	Cracked and Seated PCC	200	Old PCC	200
7	CTB	150	Winkler's foundation	-
8	Subgrade	-		

Note that after idealization, there are still two layers of HMA overlays. A two-stage simulation is adopted to incorporate the effect of the two lifts of HMA overlays.

In the first stage, PBA-6a* will be converted into an equivalent AR-8000 layer using the following equation:

$$H_e = H_{PBA} \left(\frac{E_{PBA}}{E_{AR8000}} \right)^{1/3}$$

Strictly speaking, the stiffness in the above equation should vary with traffic speed and loading temperature. As a simplification, the conversion is done using HMA stiffness at 20°C under 0.015 sec of loading time. This leads to:

$$He = 100 \times \left(\frac{932}{7390} \right)^{1/3} = 50 \text{ mm}$$

In other words, in the first stage, we are calculating the reflective cracking life of 50+130 = 180 mm of AR8000 overlay over 200mm of PCC layer.

In the second stage, we need to calculate the time it takes for crack to propagate from the top of the AR8000 layer to the surface through the PBA-6a* layer. Unlike the first stage, this is a HMA on HMA reflective cracking problem, which *CalME* uses a different set of equations to calculate the crack tip strain. The idealized pavement structure is shown below:

Layer	Material	Thick	Modulus	Poisson	R	GF	Cost/m3
1	I710 Phase I - PBA-6a*	100	636	0.35	0	1.46	114
2	I710 Phase I - AR8000	130	5819	0.35	0	1.46	114
3	Old-PCC	200	30000	0.2	0	1.7	80
4	CTB-A	150	130	0.2	0	1.7	80
5	Cal Subgrade Goal 1+3+5 SG	0	60	0.35	20	0	0

Figure 5: Structure for second-stage of *CalME* simulation for CSOL sections (HMA stiffness are given for 23°C, which is the MAAT for LA area.

The sum of reflective cracking lives obtained in the two stages is the total reflective cracking life.

Subgrade Reaction Modulus

In the memorandum from Caltrans (Shakir Shatnawi), the subgrade reaction moduli are backcalculated using FWD data collected at the center of slabs. Note that the CTB layer was combined with subgrade into a Winkler's foundation when conducting backcalculation. The values reported as listed below:

Segment Name	Post Mile Limits	Average psi/in (MPa/mm)
13S (SB)	6.81 to 12.97	107 (0.029)
20S (SB)	12.94 to 19.95	149 (0.0404)
26S (SB)	20.22 to 26.44	111 (0.0301)
7L (NB)	6.88 to 13.05	90 (0.0244)
13M (NB)	13.18 to 19.92	121 (0.0328)
20N (NB)	19.95 to 23.28	108 (0.0293)
23N (NB)	23.83 to 27.06	125 (0.0339)
Grand average		116 (0.0314)

The average value of 0.0314 MPa/mm will be used in *CalME*.

Selection of Fatigue Shift Factor

Based on a calibration study for the *CalME* HMA on PCC reflective cracking model, fatigue shift factors (FSF) are calculated for several CSOL sections from various California environmental regions, as listed in Table 7. As shown in the table, for cases with fabric, the value for FSF ranges from 0.85 to 20. If one excludes SJ-3, which has extremely thick overlay, then the average FSF is 4.8 with a range of 0.85 to 12.0.

Table 7: Calculated FSF Values for Various Crack, Seat, and Overlay Projects

Project	Structure Type	County	Overlay Thickness (mm)	Climate	FSF
SHA-1	C&S+HMA-OL	Shasta	175	MT*	0.7
SHA-2	C&S+HMA-OL	Shasta	119	MT	1.2
SHA-3	C&S+HMA-OL	Shasta	165	MT	0.03
SHA-4	C&S+HMA-OL	Shasta	119	MT	2.6
SB-2	C&S+Fabric+HMA-OL	Santa Barbra	140	SC	3.3
SB-3	C&S+Fabric+HMA-OL	Santa Barbra	145	SC	1.0
SB-4	C&S+Fabric+HMA-OL	Santa Barbra	152	SC	0.85
SB-5	C&S+Fabric+HMA-OL	Santa Barbra	119	SC	12.0
SJ-1	C&S+Fabric+HMA-OL	San Joaquin	175	CV	5.0
SJ-2	C&S+Fabric+HMA-OL	San Joaquin	157	CV	7.0
SJ-3	C&S+Fabric+HMA-OL	San Joaquin	279	CV	20.0

* Climate regions as shown in Figure 615.1 of Caltrans Highway Design Manual, September 1, 2006.

For the second stage simulation, a fatigue shift factor of 0.9 (when wander is ignored) is chosen based on the Reflective Cracking Study of RHMA mixes in HVS tests, i.e., Goal 9 (2). Note that FSF of 3.0 was used to match the performances of overlays in the HVS tests which has wander pattern accounted for, for simulations without wander, the HVS shift factor should be $3 \times 1.8 = 5.4$.

Results and Discussions

Fatigue damage history for the AR-8000 layer in the first stage simulation is shown below. Failure is again defined as residual stiffness ratio becomes 0.5. Results are also summarized in Table 8 which indicates that the total reflective cracking life is between 67 and 423 million ESALs, with an average estimate of 194 million ESALs.

The above results are obtained with a crack spacing of 1.2m (4ft), i.e., the typical crack spacing for designed CSOL sections. It is suspected that the actual crack spacing is however longer due to inadequate cracking practice. *CalME* reflective cracking model for HMA over PCC overlays predicts longer life when crack spacing increases, due to decrease in crack/joint tip strain. For longer crack spacing this might be over-predicting reflective cracking life because the omission of thermal-induced cracking. The effect of crack spacing on traffic-induced damage evolution is shown in Figure 7. Apparently, once crack spacing is more than (including) 2.0 m, the reflective cracking life of the first stage is more than 400 million ESALs.

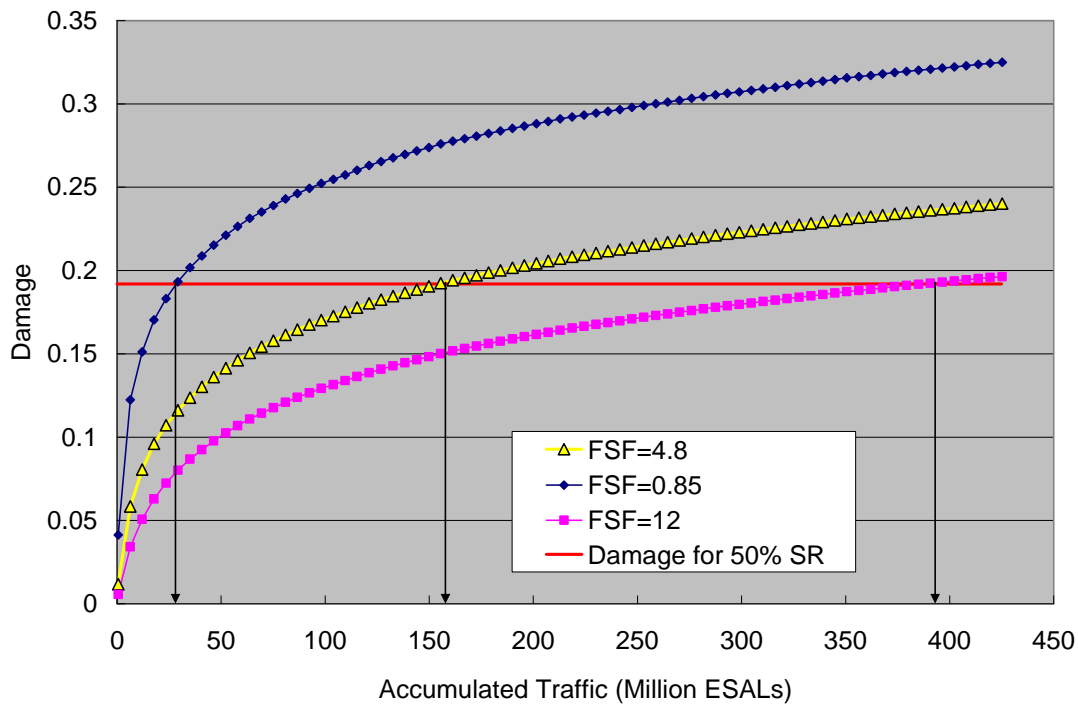


Figure 6: Damage evolution history for the AR8000 layer in the first stage simulation.

Table 8: Summary of Reflective Cracking Life for CSOL Sections

Stage	FSF	Reflective Cracking Life (Years)	Corresponding ESALs (Millions)
1	4.8/0.85/12 (Mean/min/max)	22/4.2/55	156/29/385
2	0.9	5.4	38
Combined		27.4/9.6/60.4	194/67/423

If the HVS FSF of 5.4 is used for the second stage instead, the reflective cracking life will increase from 5.4 to 32 years, which will increase the total traffic allowed by 186 million ESALs.

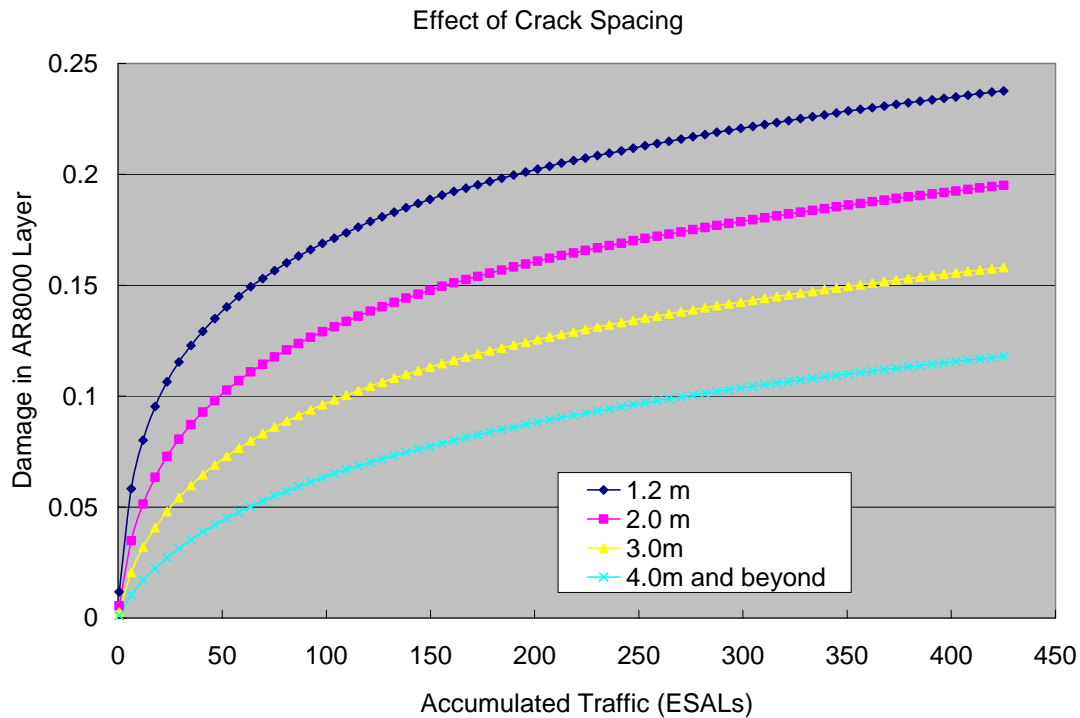


Figure 7: Effect of crack spacing on damage evolution for 1st stage simulation.

References

1. Harvey, J. T., J. Roesler, N. F. Coetzee, and C. L. Monismith. June 2000. *Caltrans Accelerated Pavement Test (CAL/APT) Program Summary Report Six Year Period: 1994-2000*. Report prepared for California Department of Transportation. Report No. FHWA/CA/RM-2000/15. Pavement Research Center, CAL/APT Program, Institute of Transportation Studies, University of California, Berkeley. UCPRC-RR-2000-08.
2. J. T. Harvey, C. L. Monismith, W. A. Nokes, and N. F. Coetzee. January 2007. *Caltrans Partnered Pavement Research Program (PPRC) Summary Report Four Year Period: 2000-2004*. Report prepared for Caltrans Division of Research and Innovation and Caltrans District 8 by the University of California Pavement Research Center, Davis and Berkeley. UCPRC-SR-2006-02.

Appendix

List of Additional Information:

1. Collect a list of available data: air voids, thickness, traffic, laboratory testing, FWD
 - a) The construction specification for the I-710 project required AC mixes to be compacted to 93 to 97 percent of Theoretical Maximum Density (TMD) for both Crack, Seat and Overlay sections and full depth sections. CT 308A was used to determine bulk specific gravity and AASHTO T209 (Method A) AASHTO T269 were used to determine percent of TMD. According to the QC/QA data collected during construction, air-void contents for AR-8000 mix were between 3.0 and 7.0 percent with an average of 4.9 percent, while air-void contents for PBA-6a* mix were between 2.4 and 7.0 percent with an average of 5.0 percent.
 - b) Several QC/QA beams were tested for fatigue, AVs are available
 - c) Several QC/QA cores were tested for rutting, AVs and thickness are not available
 - d) FWD (JS), AB stiffness at least 2000 MPa
 - e) Traffic AADTT 1992 to 2007, traffic volume for the first 6 years used in simulations are double the observed values, and 1.5 times over 30 years of service.
 - f) Thickness of the CSOL layer second stage is smaller compared to Stantec sections.